UNIVERSITÄT DES SAARLANDES

HEINRICH HEINE UNIVERSITÄT DÜSSELDORF

"Investigating the role of the iron dependent bHLH039 transcription factor in coordinating Fe homeostasis in Arabidopsis thaliana"

Dissertation

zur Erlangung des akademischen Grades

Doktor der Naturwissenschaften (Dr. rer. nat.) der

Naturwissenschaftlich-Technischen Fakultät der

Universität des Saarlandes

von Frau

Maria Augusta Naranjo Arcos

geboren am 03.05.1985 in Ambato-Ecuador

Saarbrücken Mai 2017

Tag des Kolloquiums:	12. Mai 2017
Dekan:	Prof. Guido Kickelbick
Berichterstatter:	Prof. Petra Bauer
	Prof. Katrin Philippar
Vorsitz:	Prof. Uli Müller
Akad. Mitarbeiter:	Dr. Gilles Gasparoni

Gold is for the mistress -- silver for the maid --
Copper for the craftsman cunning at his trade.
"Good!" said the Baron, sitting in his hall,
"But Iron -- Cold Iron -- is master of them all."

Rudyard Kipling

Acknowledgements

I would like to express my deepest thank to Prof. Dr. Petra for the financial support and for the experience of working in her lab during the diploma work and the PhD. For the financial support, I also thank the GradUS graduate school of the Saarland University and the Heinrich-Heine University Düsseldorf. I am thankful to Prof. Katrin Philippar for accepting the correction of the work. I thank the lab "Plant Development" in Golm/Potsdam, especially Dr. Kirsten Kaufmann and Dr. Wenhao Yan for the support during the ChIP experiments. Thanks to Prof. Jürgen Zeier and his group "Molekulare Ökophysiologie" for the supervision of the pathogen experiments.

Many thanks to all the members of the Institute of Botany for the nice coffee breaks, cakes, movie nights, BBQs, etc. A special thank goes to my best colleague Regina for the support, motivation, talks, beers, bus/train travels, through all these years. I thank our Postdocs Tzvetina and Rumen for the personal support and for showing me that happiness is at home after work. Thank you also Hansi and Andreas for answering all the questions and helping me with all my problems and doubts. Thanks to Angelika for the good mood in every situation and the "Fasching" atmosphere all the time. Thanks to Elke and Ginte for the technical support and the continuous organization with broken devices and roofs.

A very special thank to my parents Margarita and Augusto and to my siblings Ma. Margarita, Ma. Isabel and José Gabriel for supporting me and believing in me. To all my friends, especially Claudia for being on my side all the time, thank you. Last but not least, I want to thank Maël and his family for the constant help and support during this hard time. Thank you for bringing me laughter when only tears appeared.

Content

Abstract

Plants perceive and react to their environment. Upon iron deficiency, plants activate the iron-deficiency machinery which is controlled by the master regulator FIT and its four interaction partners the bHLH038, bHLH039, bHLH100 and bHLH101 from the subgroup Ib(2). This work reports the influence of bHLH039 overexpression (39Ox) in iron uptake and homeostasis as well as in pathogen and high iron responses. Physiological investigation of 39Ox plants revealed that they exhibit iron-deficiency responses and simultaneously iron overload and oxidative stress. Crosses of 39Ox with FIT knock-out and FIT overexpression plants confirmed that FIT is essential for the activation of the iron-uptake machinery. A Catma v6 microarray was performed with 39Ox plants at + Fe and at -Fe. More than 700 FIT and Fe-regulated genes have been identified. This data showed that the expression of genes coding for proteins involved not only in the absorption, internal transport and storage of iron, but also in the circadian clock, light response, pathogen response and oxidative stress were greatly increased. GUS experiments indicated that the *FIT* promoter was more active when bHLH039 was overexpressed. Consequently, the binding of bHLH039 to the promoter of Fe-related genes was investigated. However, ChIP experiments showed no direct binding of bHLH39 to the different promoter regions of the tested genes. This work shows the importance of bHLH039 in the regulation of iron homeostasis and the processes mentioned above.

Zusammenfassung

Pflanzen empfinden und reagieren auf Umweltveränderungen. Bei Eisenmangel aktivieren die Pflanzen die Eisenmangel-Maschinerie, die vom Masterregulator FIT und seinen vier Interaktionspartnern bHLH038, bHLH039, bHLH100 und bHLH101 aus der Untergruppe Ib (2) gesteuert wird. Diese Arbeit befasst sich mit dem Einfluss der bHLH039 Überexpression (39Ox) auf die Eisenaufnahme und -homöostase sowie die Auswirkungen auf die Pathogen- und Eisenüberflussantwort. Durch Kreuzungen der Linie 39Ox mit FIT knock-out und FIT Überexpressionslinien wurde bestätigt, dass FIT eine zentrale Rolle in diesen Prozessen spielt. Mit einem Catma v6 Microarray wurden die Transkripton von 39Ox Pflanzen unter + Fe und - Fe untersucht und verglichen. Mehr als 700 Gene wurden identifiziert, welche unabhängig von FIT und Eisenversorgung reguliert werden. Eine umfassende Analyse dieser Daten zeigte, dass in 39Ox Pflanzen nicht nur Gene mit Beteiligung an Eisenaufnahme, -transport und -lagerung stark hochreguliert waren, sondern auch Gene, die in der circadian *clock*, der Pathogenantwort und bei oxidativen Stress eine Rolle spielen. Promotor-GUS Experimente zeigten, dass der FIT Promotor in 39Ox Pflanzen stärker aktiviert sein könnte. Auf dieser Grundlage wurde die Bindung von bHLH039 an die Promotoren von bekannten stark eisenmangelregulierten Genen wie *FIT*, *IRT1*, *FRO2*, *AT3g12900*, *AT3g07720* und *AT3g58810* untersucht. ChIP-Experimente gaben jedoch keine Hinweise auf eine direkte Bindung von bHLH39 an verschiedene Promotorregionen der getesteten Gene. Diese Arbeit zeigt die Bedeutung von bHLH039 bei der Regulierung der Eisenhomöostase und der oben erwähnten Prozesse.

Abbreviations

39Ox	bHLH039 overexpression line
AA	Arvenic acid
AB	Antibody
AD-Primer	Arbitrary degenerate primer
AHA	H^+-ATPase
APC	Antigen presenting cells
APX	ASCORBATE PEROXIDASE
At	*Arabidopsis thaliana*
AzA	Azelaic acid
BABA	β-aminobutiric acid
BBX	B-BOX TYPE ZINC FINGER
BCB	BLUECOPPER-BINDING PROTEIN
BGLU	β-glucosidase
bHLH	Basic-helix-loop-helix motif
bHLH-TF	bHLH-transcription factors
bp	Base pairs
BTS	BRUTUS
CCA	CIRCADIAN CLOCK ASSOCIATED
Col-0	Columbia-0
CRISPR	Clustered Regularly Interspaced Short Palindromic Repeats
Ct (Cq)	cycle threshold (quantitation cycle)
DA	Diterpenoid dehydroabietinal
DW	Dry weight
Ef (g)	Elongation factor (genomic)
ETI	Effector-triggerd immunity
F6'H1	Feruloyl CoA ortho-hydroxylase 1
Fe	Iron
Fe^{2+}	Ferrous iron
Fe^{3+}	Ferric iron
-Fe	Iron deficient media (0 μM)
+Fe	Iron sufficient media (50 μM)

FER	FERRITIN
FIT	FER-LIKE IRON DEFICIENCY-INDUCED TRANSCRIPTION FACTOR
FLS	Flagellin-sensing
FRD	FERRIC REDUCTASE DEFECTIVE
FRO	FERRIC REDUCTASE OXIDASE
G3P	Glycerol-3-phosphate
GA	Gibberellin acid
GFP	Green fluorescent protein
GO	Gene ontology
GPX	Glutathione Peroxidase
GSH	Glutathione
GSSG	Glutathione disulfide
GUS	β-glucuronidase
H_2O_2	Hydrogen peroxide
HA	Hemagglutinin
HR	Hypersensitive Response
IAA	Auxin
IgG	Immunoglobulin G
IP	Immunoprecipitation
IREG1/FPN	IRON-REGULATED PROTEIN 1/FERROPORTIN
IRT	IRON-REGULATED TRANSPORTER
KO	Knock-out
LHY	LATE ELONGATED HYPOCOTYL
MA	Mugineic acid
MAMP/PAMP	Microbe/Pathogen –associated molecular patterns
MS	Murashige-Skoog Medium
MTPA	METAL TOLERANCE PROTEIN
MU	4-methylumbelliferone
MUG	4-methylumbelliferyl β-D-glucuronide
NA	Nicotianamin
NAS	NICOTIANAMIN SYNTASE
NO	Nitric oxide
NPR	NONEXPRESSOR OF PR GENES

NRAMP	NATURAL RESISTANCE-ASSOCIATED MACROPHAGE PROTEIN
OBP	OBF-BINDING PROTEIN
OPT	OLIGOPEPTIDE TRANSPORTER
$\cdot O_2^-$	Superoxide
·OH	hydroxyl radical
Os	*Oryza Sativa* (Reis)
PCD	Programmed cell death
PGPR	Plant growth-promoting rhizobacteria
PI	Promoter of interest
PIC1	PERMEASE IN CHLOROPLAST 1
PiP	Pipecoloc acid
Pox	PEROXIDASE GENE
PR	Pathogenesis-related
PRR	Pattern recognition receptors
PrxR	Peroxiredoxin
PS	phytosiderophores
PTI	PAMP-triggered immunity
PYE	POPEYE
qRT-PCR	Quantitative real time polymerase chain reaction
ROS	Reactive oxygen species
rpm	Rotations per minute
RPT	ROOT PHOTOTROPISM
RT	Room Temperature
S1-S3	Plasmid specific primers
SA	Salicylic acid
SAM	S-Adenosylmethionin
SAR	Systemic acquired resistance
SDS	Sodium dodecyl sulfate
SOD	Superoxide dismutase
T-DNA	Transfer DNA
TAIL-PCR	Thermal Asymmetric Interlaced Polymerase Chain Reaction
TF	Transcription factor
TGA	TGACG MOTIVE-BINDING PROTEIN

TGS/PTGS	Transcriptional/Post-transcriptional gene silence
Ti-plasmid	Tumor inducing plasmid
TLR	Toll-like receptors
TOC	TIMIG OF CAB EXPRESSION
TOM1	PHYTOSIDEROPHORE EFFLUX TRANSPORTER
TTSS	Type III secretion system
VIT	VACUOLAR IRON TRANSPORTER
VOC	Volatile organic compounds
WHO	World Health Organization
WT	Wild type
YS	YELLOW STRIPE
YSL	YELLOW STRIPE-LIKE

1 Introduction

The introduction of this work is a modification of the chapter "Iron Deficiency, Oxidative Stress, and Pathogen Defense" published in July 2016 in the Book "Nutritional Deficiency" [1].

Organisms have specific ways to assimilate necessary nutrients. Animals, including humans, have to ingest food and process it mechanically and chemically during the digestion. The principal nutrients needed by animals, such as carbohydrates, lipids, proteins, vitamins, and minerals, come from different sources [2]. A balanced alimentation is hence very important. A lack of essential vitamins or minerals in the diet affects immunity and healthy development. This condition of unproportioned alimentation is called undernourishment. Nutrition problems have always been an issue in third world or developing countries. Nowadays, about 104 million children worldwide are underweight (2010). The World Health Organisation (WHO) has a project to reduce by 40% the number of children that are stunted due to undernourishment until 2025. Currently, Central Africa , with over 60% of the population undernourished, followed by Southeastern Africa (~40%) and Southern Asia (~20%) are the regions the most affected by undernourishment [3, 4] (Figure 1).

A **B**

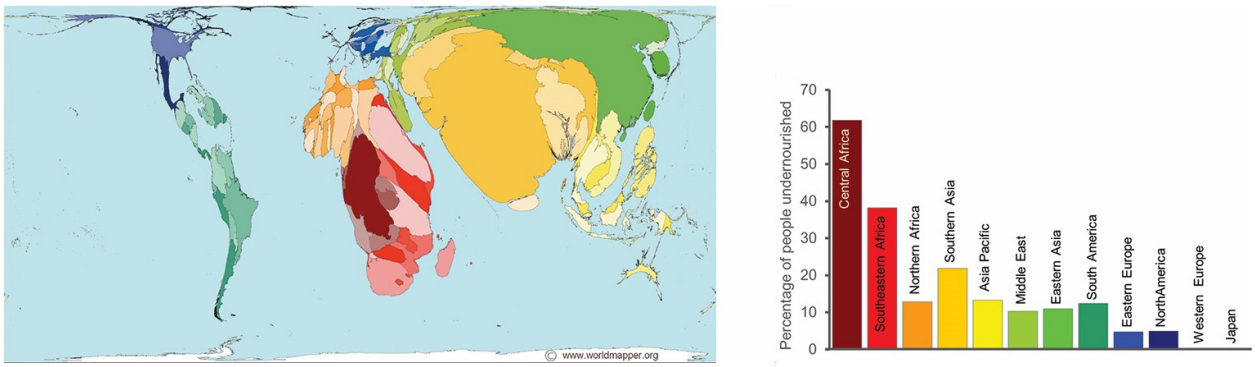

Figure 1: Worldwide map of undernourishment (2000). (A) The map illustrates the resized world corresponding to the number of under-nourished people living in the different regions. (B) The chart shows the percentage of undernourished people living in the different regions. Africa and southern Asia are the most affected regions with almost 50% of all undernourished people worldwide (adapted from [3], Map 178).

In regions with high undernourishment, many people do not have access to a varied diet and their main alimentation consists in only one specific sort of crop. In theory, crops can be fortified by increasing the level of nutrients or uptake-promoting substances in the soil. For example,

raising the supply of the essential micronutrient elements Zn, Ni, I, and Se increases their concentration in the grains of several plant products [5]. Unfortunately, for other micronutrients, such as Fe, the sole supplementation of the soil with Fe salts is not sufficient to step up the iron quantity in the crops. Foliar fertilization is the best way to increase Fe content in crops, but the costs and efforts are not economically interesting [6-8].

Fe deficiency in the form of anemia affects more than 2 billion people on the planet, being the most common nutritional problem in the world (WHO 2005), and regions with Fe deficiency anemia coincide with those of undernourishment, particularly Asia, Africa, and Latin America (compare Figure 1 and Figure 2).

A **B**

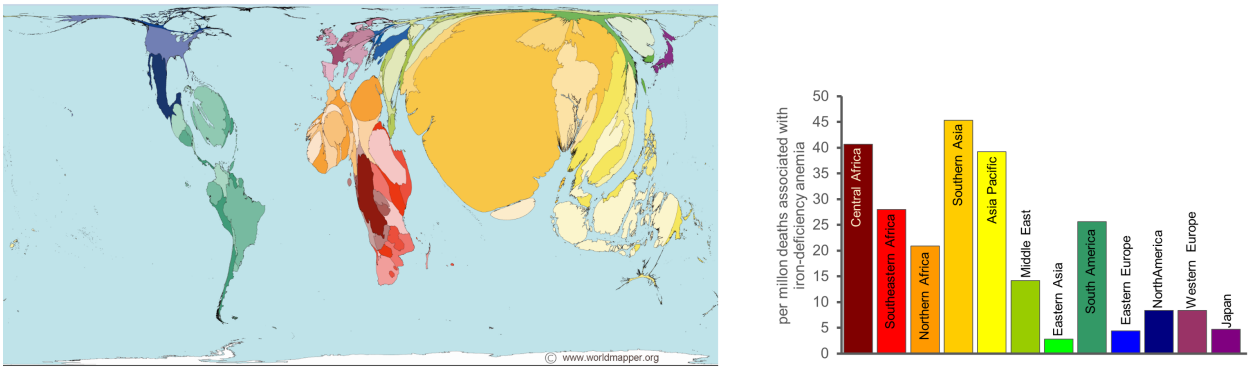

Figure 2: Iron deficiency anemia deaths. (A) The size of the regions corresponds to the number per million deaths associated with Fe deficiency anemia (2002). (B) The chart shows the number of per million deaths associated with iron-deficiency anemia depending on the regions. Africa, Asia, and South America are the most affected regions (adapted from [3], Map 414).

Due to the poor conditions and the lack of access to diverse nutritious food, it is challenging to counteract this problem by just supplementing the food with iron. Genetic engineering is a suitable approach to fortify plants with organic nutrients. In the case of Fe, it is crucial to not only find a way to increase the efficiency of the uptake into the plant but also the transport inside the crop, and more importantly to improve the bioavailability of Fe for assimilation in humans [9, 10]. An attractive source and plant crop have to be chosen. For instance, cassava (or manioc, *Manihot esculenta*) is extensively used by humans for food, livestock and extraction of starch. Manioc can be cultivated for over 30 years in the same field without fertilizer even in poor soil conditions [11, 12]. Besides, roots can be conveniently stored and remain in the soil for a long time. Although cassava is one of the basic foods for around 800 million people in the world, it is not a good source for iron and other nutrients [13]. Using genetic engineering [14], researchers were able to introduce a green algae gene (*FEA1*) in cassava and thus increase the storage

of iron in the roots from 10 to 36 ppm. This amount of iron would cover the daily requirements for an adult in a meal of 500 g.

Iron is an essential element for animals, bacteria, fungi, and plants so that they may be affected by similar iron related diseases. A competitive situation may arise between organisms when they live in close relationship. This is interesting in host–pathogen interaction systems, where a competition for nutrients between host and pathogen is a determinant for an effective immune system and can affect susceptibility and resistance to a pathogen [15].

1.1 Iron uptake in plants

Depending on the composition of soil particles, the soil can have different characteristics, some of which define it as fertile. The soil should provide a wide microorganism population, and for most crop plants, a soil pH around 5.5 and 7 is ideal due to the availability of nutrients. The texture of the soil is decisive for the aeration, irrigation, and adequate root proliferation. Its texture is characterized by the amount of sand, silt, and clay particles. High amount of clay particles is necessary to retain essential nutrients and for soil humidity [16]. Around 5.6% of the Earth's crust consists of iron (Fe), belonging to the five most abundant elements. However, the bioavailability of this metal is restricted and plants developed strategies for its mobilization [17]. Iron is a transition metal and its valence electrons are present in more than one shell so that atoms can be present in several oxidation states [18]. In nature, iron is present in two biologically important forms, the ferrous (Fe^{2+}) and ferric (Fe^{3+}) form. In acidic environment, iron acts as a reducing factor, whereas in basic medium, it acts as an oxidizing agent [19]. In soil, Fe^{3+} is predominant and attached to silicate structures and hydroxides. In order to take up the Fe ions, plants have strategies to dispatch iron from soil particles, chelate or reduce it and transport it into the plant root cells.

1.1.1 Strategies of iron uptake in plants

Regarding iron uptake, land plants can be separated into two main groups: Strategy I and Strategy II plants. All plants, except grasses, carry out Strategy I iron uptake. Among them are, tomato (*Lycopersicon esculentum*), tobacco (*Nicotiana tabacum*), potato (*Solanum tuberosum*),

and the model organism *Arabidopsis thaliana*. Strategy II plants are all sweet grasses including rice (*Oryza sativa*), maize (*Zea mays*), barley (*Hordeum vulgare*), and wheat (*Triticum* spp.). Studies demonstrated that iron uptake was more efficient in barley (*Hordeam vulgare*) than in cucumber (*Cucumis sativus*) especially at higher pH, which would give Strategy II plants an advantage over Strategy I plants [20].

In both strategies (Figure 3) the proteins required for iron uptake are located in the root epidermis cells [20]. Strategy I plants acidify the rhizosphere by pumping protons, carried out by a proton-ATPase (AHA2) [21]. FERRIC REDUCTASE OXIDASE (AtFRO2 in A*. thaliana*; LeFRO1 in tomato) is responsible for the reduction of Fe^{3+} to Fe^{2+}, which is a crucial step for the iron uptake in Strategy I plants [22-24]. In both strategies, roots enhance iron mobilization by secreting iron-chelating compounds [25]. Among these, many phenolic compounds and flavins are found in Strategy I plants. [26]. The investigation of the effect of phenolic compounds in red clover (*Trifolium pratense*) showed that the excretion of these molecules is important for the reutilization of apoplastic iron by decreasing the mobilization of iron from roots to shoots [27]. Studies in *A. thaliana, Brassica napus,* and *Medicago truncatula* demonstrated that these compounds can be related to coumarins such as scopoletin and other derivatives as well as flavins. They are produced under iron deficiency conditions, among others, via the action of the feruloylCoA 69-hydroxylase1 (F6'H1). Subsequently, the ABC transporter, called ABCG37, transports these compounds to the rhizosphere [28-31]. The response of grasses' roots of (Strategy II plants) to iron deficiency is to secrete phytosiderophores (PS) through the phytosiderophore efflux transporter TOM1 [32]. PS are high-affinity iron chelating compounds able to chelate and solubilize ferric iron (Fe^{3+}). The most well-known PS are members of the mugineic acid family (MA) and arvenic acid (AA) [33]. Nicotianamine synthase (NAS) is an important enzyme that catalyzes the fusion of three S-adenosyl methionine molecules (SAM) to form the MA precursor nicotianamine (NA), a non-proteinogenic amino acid [34].

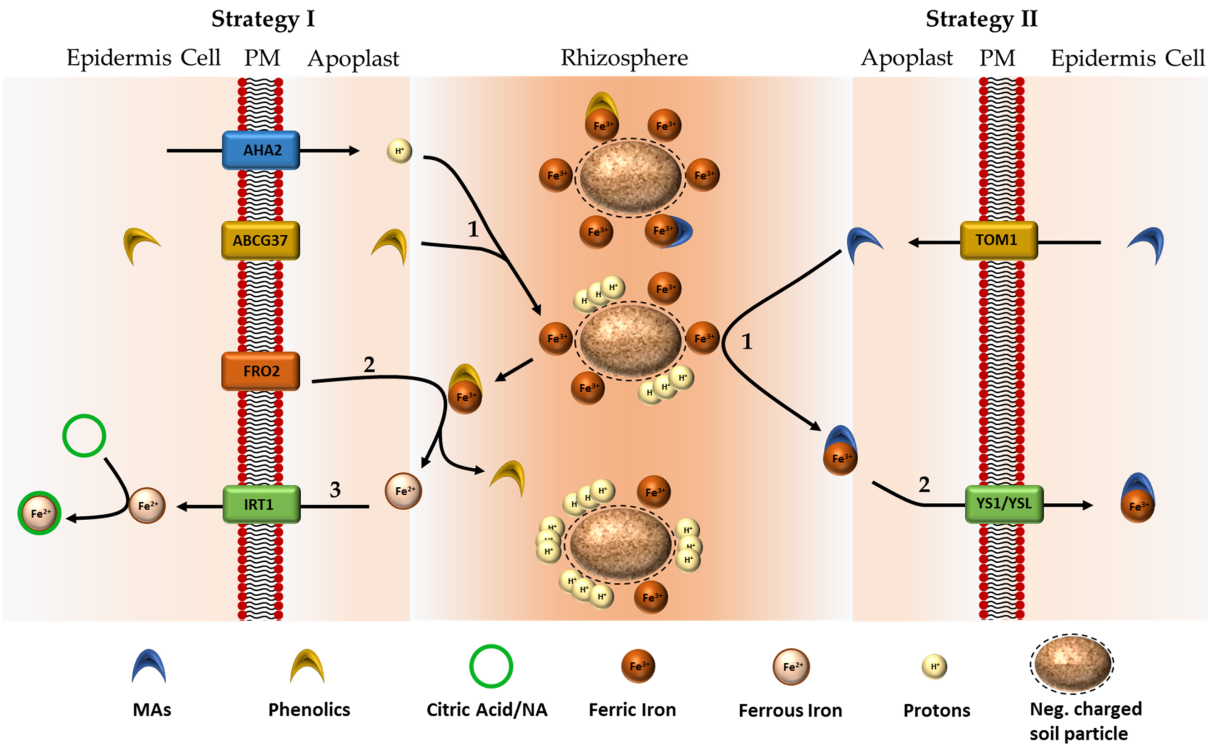

Figure 3: Strategy I and Strategy II iron acquisition in plants. Strategy I plants, exemplified by *Arabidopsis thaliana* (left side), take up iron in three steps: first, in order to liberate Fe^{3+} ions, the proton pump AHA2 acidifies the rhizosphere. The secretion of phenolic compounds through the ABCG37 transporter increases the solubilization of iron. Second, the iron reductase FRO2 reduces Fe^{3+} to Fe^{2+} that is finally transported into the epidermis cell by the iron transporter IRT1. Inside the plant, citric acid or nicotianamine chelates Fe^{3+}/Fe^{2+} for further transport it within the plant via xylem or phloem. The iron uptake in strategy II plants, exemplified by *Zea mays* and rice (right side) consists of two steps: first, TOM1 exports phytosiderophores into the rhizosphere to solubilize Fe^{3+} ions. The Fe^{3+}/PS complex is transported by the YS1 protein in maize and YSL in other grasses.

In maize, the first identified highly specific proton-coupled PS transporter was the yellow stripe 1 (YS1). It transports the Fe^{3+}/PS as well as Fe^{3+}/NA complex into the cells [35-37]. Further investigation revealed closely related transporters, yellow stripe 1-like (YSL), in barley and rice [38-40]. The last step of iron uptake in Strategy I plants is the transport of reduced/chelated Fe handled by the IRON-REGULATED TRANSPORTER 1 (IRT1) [41-43].

In contrast to the other Strategy II plants, rice represents a special case because this plant has the ability to take up both Fe^{3+}/PS and Fe^{2+} from the soil. Rice produces lower amounts of PS (2'-deoxymugineic acid DMA) than other grasses, but has two genes encoding for proteins similar to the *Arabidopsis* IRT1, OsIRT1, and OsIRT2. OsIRT proteins were found to be located in the root plasma membrane, and they are able to transport Fe^{2+}. However, rice plants are usually not forced to reduce iron before transport because they grow in submerged conditions where Fe^{2+} is more abundant than Fe^{3+} [44].

The IRON-REGULATED PROTEIN 1 (also known as ferroportin FPN1) IREG1/FPN1 loads Fe into the xylem [45]. The root-specific protein FERRIC REDUCTASE DEFECTIVE 3 (FRD3) mediates the efflux of citrate into the xylem. There, citrate chelates Fe and this complex is transported with the transpiration stream to the upper parts of the plants [46-48]. In order to reach developing organs where the xylem is not yet formed, for instance, meristem of young leaves or seeds [49], the Fe is loaded into the phloem and chelated with NA [50-52]. Potential transporters of iron between leaves and sinks are the OLIGOPEPTIDE TRANSPORTER 3 (OPT3) [53] and YSL proteins [54]. In Arabidopsis, NA-chelated Fe may be transported from the phloem to flowers and seeds via the AtYSL1 and AtYSL3 transporter [55, 56] and in rice, this is performed by OsYSL2 [57].

Immediately after reaching the tissue of destination, Fe has to be stored in cell compartments where utilization and storage need to be coordinated. The Fe-transporter FPN2 and VACUOLAR IRON TRANSPORTER 1 (VIT1) [58] are responsible for the import of iron into the vacuole, while NATURAL RESISTANCE-ASSOCIATED MACROPHAGE PROTEIN 3 and 4 (NRAMP3 and NRAMP4) mediate its export [59, 60]. In the vacuoles, iron is probably chelated with phytates.

Photosynthesis, the electron transport chain and synthesis of chlorophyll require an enormous amount of Fe. Therefore, the majority of iron is supplied to the chloroplasts [61]. The transport of Fe into the chloroplast requires first its reduction mediated by FRO7, followed by its transport performed by the transporter PERMEASE IN CHLOROPLAST 1 (PIC1) [62, 63]. In the chloroplast, Fe is sequestered in ferritin (FER), which is macroprotein complexes able to store up to 4500 iron atoms and present in animals, plants, fungi, and bacteria [64].

1.1.2 Regulation of the iron uptake in plants

Proteins that are able to bind DNA to regulate its transcription are called transcription factors (TF) [65] and have different structures. In the year 1989 a protein region was identified in immunoglobulin enhancer binding proteins in the mouse that was found conserved in different proteins from *Drosophila* and able to form dimers and simultaneously bind to a specific DNA sequence. This domain is highly conserved and comprises of around 60 amino acids with two functional regions. The so-called basic Helix-Loop-Helix (bHLH) TF. At the N-terminal are located

several amino acids with hydrophilic and basic residues. This positively charged region is responsible for the binding to the negatively charged DNA. Moreover, two amphipathic α-Helices are linked with a variable loop and function as a dimerization domain [66, 67].

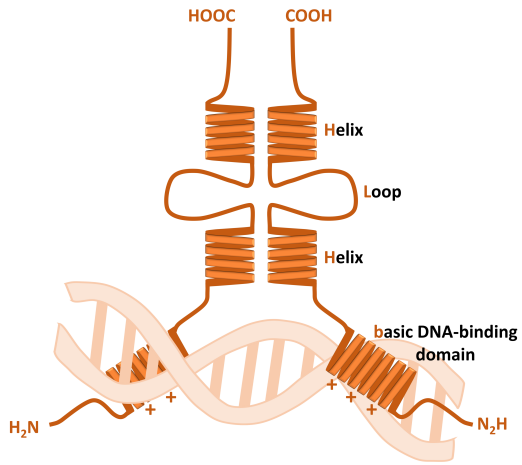

Figure 4: Structure of the bHLH transcription factors. The motive bHLH is composed at the N- terminal of around 15 basic charged amino acids. The positive charge of these amino acids allows the binding to the negatively charged DNA. Two aliphatic α-Helices separated by a Loop are responsible for the homo- or heterodimerization.

The DNA target-region of proteins with this motive is the so called E-Box motive with the sequence 5'-CANNTG-3' (N corresponds to any nucleotide) and its palindrome called G-boxes 5'-CACGTG-3' [66, 68]. bHLH transcription factors are present in all eukaryotes and are involved in countless processes including developmental events in animals such as muscle and heart development as well as neurogenic differentiation [69-71]. In yeast, genes involved in phosphate metabolism, phospholipid synthesis or regulation of methionine biosynthesis and chromatin stability are regulated by bHLH transcription factors [72-74]. In plants, they are the second most common transcription factor family (after Myb TF). Sequence analysis showed that a few BHLH genes present in the genome of chlorophytes and red algae are present in land plants as well [75].

The bHLH family in *A. thalian* comprises 161 members distributed in 26 subgroups [75, 76]. In the iron deficiency response, the main regulators in tomato and *A. thaliana* are LeFER (SlbHLH085) [77, 78] and FER-LIKE IRON DEFICIENCY-INDUCED TRANSCRIPTION FACTOR (AtFIT, AtbHLH029) [79-81]. LeFER belongs to the subgroup IV and AtFIT to the subgroup III of the bHLH family. They interact with the SlbHLH069 and with the bHLH proteins of the subgroup Ib(2) ,

respectively, to activate the transcription of the Fe reductase and the Fe transporter genes in roots [82-84].

The bHLH Ib(2) subgroup transcription factors comprise 6 genes from *O.sativa* and 12 genes of *A. thaliana*. The genes of *O.sativa* and *A. thaliana* that are regulated by iron are *OsbHLH56*, in rice, *AtbHLH038*, *AtbHLH039*, *AtbHLH100*, and *AtbHLH101* in Arabidopsis [75]. In rice, OsbHLH56 (OsIRO2) plays an important role in the positive regulation of the gene expression of the nicotianamin synthase (*NAS1*, *NAS2*, *NAS3*), the nicotianamin amino transferase (*OsNAAT1*), the deoxymuginein acid synthase (*OsDMAS1*) and the yellow stripe like (*OsYSL15*) [85].The four bHLH genes in Arabidopsis share partial redundant functions in iron homeostasis [86] and interact with the master regulator FIT for the regulation of the iron uptake [82, 83].

There is a large number of genes regulated by FIT and iron deficiency [79, 87, 88]. FIT- and Fe-dependent genes are for example *IRT1*, *FRO2,* [80] *KELCH REPEAT PROTEIN, MTPA2, CYP82C4,* among others [89]. In contrast, the four Ib subgroup *BHLH* genes are not regulated by FIT. Their high transcript levels in the *fit-3* mutant compared to the wild type are rather due to the iron deficiency [86]. These and other iron homeostasis genes such as *PYE, BTS, FRO3, NRAMP4,* and *NAS4* belong to a separate FIT-independent co-regulatory network [79, 90-92]. The regulation of the iron-uptake and the related proteins are summarized in the Figure 5.

POPEYE (PYE) and BRUTUS (BTS) are important iron-homeostasis regulatory components. Both genes are upregulated at –Fe conditions; however, they have opposite functions. PYE regulates positively the iron status of the plant, while BTS has repressing effects on the iron homeostasis [93-95]. PYE is a bHLH transcription factor which regulates the expression of genes involved in mitochondrial ferric reduction (*FRO3*) and internal storage such as the *FER1*, *FER4*, *NAS* [93]. *pye* mutants showed significant root growth inhibition upon iron deficiency conditions. This occurs because a decreased cell elongation compared to the WT. Additionally, these plants showed severe chlorotic cotyledons and leaves compared to the WT when grown in iron deficient media. Fe reductase and gene expression analysis suggested that these plants are more sensitive to iron deficiency [93]. PYE interact with three other bHLH transcription factors from the subgroup IV, namely bHLH104, bHLH105/ILR3 (IAA-LEUCINE RESISTANT3) and bHLH115. These PYE-like proteins (PYEL) are upregulated upon iron deficiency [93].

BTS encodes a protein with several conserved domains. These domains are three hemerythrin (HHE) cation-binding domains on the N-terminus, a CHY zinc-finger domain and a RING (Really

Interesting New Gene) domain on the C-terminus [96]. The HHE domains are able to bind Fe and Zn suggesting that BTS could act as an iron sensor in the plant [96]. Thanks its RING domain, BTS might have E3 ligase activity, which catalyzes the final step for the ubiquitination of its interaction partners for proteasomal degradation [94]. Unlike the *pye* mutant, *bts* mutants were more tolerant to iron deficiency. These plants displayed increased rhizosphere acidification, iron reductase activity and root elongation compared to WT plants. The iron content in shoots, roots and seeds were elevated in these mutants as well [94]. Additionally, BTS plays an important role in the embryonal development since some homozygous *bts* mutant alleles showed a lethal embryo phenotype [97, 98].

BTS interacts also with the PYEL proteins bHLH104, IL3 and bHLH115 for the regulation of the iron homeostasis. The interaction between BTS and PYE with the PYEL proteins might occur according to requirements to fine-tune iron homeostasis [93, 99]. Research showed that these elements are essential upstream regulators. Knockout mutants of the *PYEL* showed notably reduced tolerance to iron deficiency including low iron content in shoots and roots, reduced iron reductase activity and gene expression of iron homeostasis genes. On the other hand, compared to the WT, overexpression of these genes, caused at +Fe and –Fe, considerably increased the iron deficiency response [99, 100]. Chromatin immunoprecipitation experiments showed that the PYEL are able to bind the promoter of the Ib subgroup BHLHs activating its transcription [99, 100].

The transcription factors MYB10 and MYB72 are important players in the iron- deficiency response with probably redundant functions. *myb10myb72* double mutant displayed a lethal phenotype when grown in alkaline soil, but was comparable to the WT under normal growth conditions [101]. Microarray analysis of this mutant revealed that very few genes are regulated by MYB10/MYB72. One of these genes is the NICOTIANAMIN SYNTASE 4 (*NAS4*). The fact that the overexpression of NAS4 rescued the lethal phenotype of the *myb10myb72* double mutant and that the *NAS4* promotor has MYB binding sites, showed that *NAS4* is a target of these two transcription factors [101] (Figure 5).

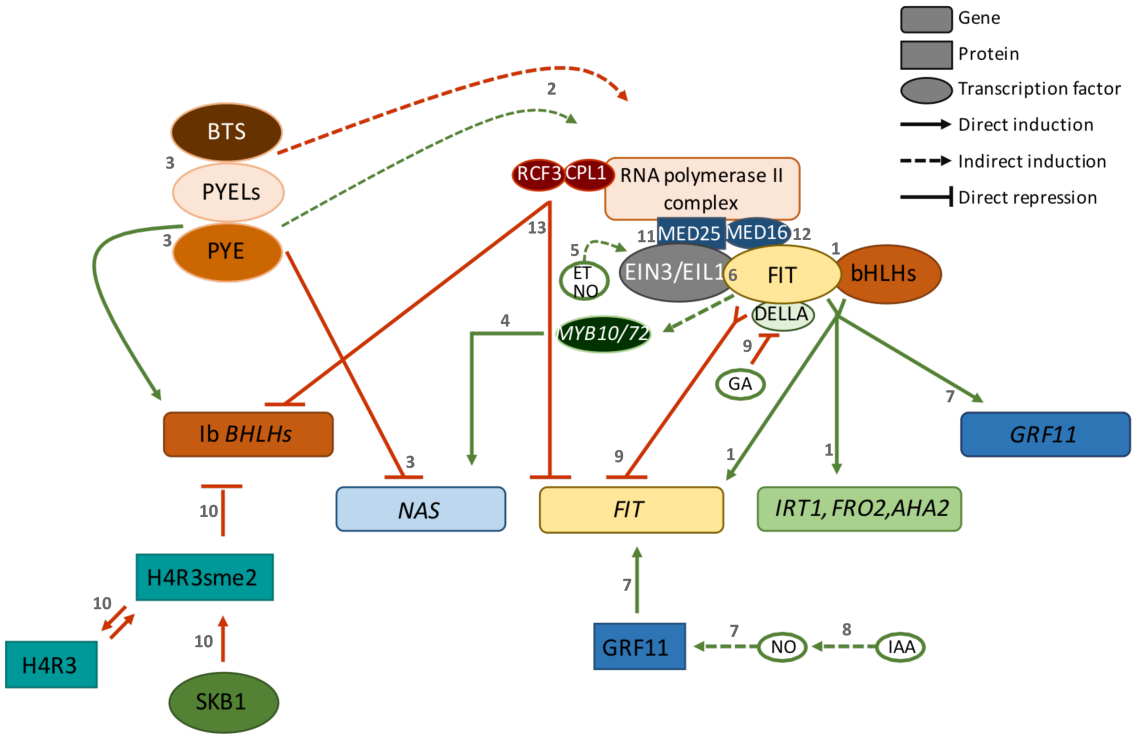

Figure 5: Regulatory network of the iron uptake in *A. thaliana*. The network was taken from [102] and some changes were implemented. The grey numbers refer to the publications in the reference list. Rectangles represent proteins, rounded corners rectangles represent genes and ovals represent transcription factors. Green arrows fight the evil point out direct induction. Red blunt lines mean direct repression. Broken green and red arrows point out positive or negative regulation, respectively. Ref. **1)** [79-83]; **2)** [93-95]; **3)** [93-95, 99, 100]; **4)** [101]; **5)** [103-105]; **6)** [106]; **7)** [107]; **8)** [108]; **9)** [109, 110]; **10)** [111]; **11)** [112]; **12)** [113]; **13)** [114, 115]

Hormones play an important role in the iron homeostasis. Ethylene (ET) is a positive regulator of the iron uptake genes. It was demonstrated that the gene expression of *FRO2*, *IRT1* and *FIT* was elevated after treatment with the ethylene precursor ACC [103]. This occurs because ethylene stabilized FIT protein through the interaction with EIN3/EIL1 proteins. These redundant proteins stabilized FIT preventing its proteosomal degradation and preserving it in an active state [105, 106]. Nitric oxide (NO) acts similar as ethylene. These two signal molecules are interconnected by a feedforward mechanism influencing the biosynthesis of each other for a more efficient regulation of the iron homeostasis [104]. Additionally, NO regulates the expression of the GENERAL REGULATORY FACTOR11 (*GRF11*) gene, which encodes a 14-3-3 protein. Previous analysis showed that GRF11 activates the transcription of *FIT*. In turn, FIT can regulate the transcription of *GRF11* by binding directly on the E-box motif of its promoter [107]. Upstream of the NO, for the activation of Fe-deficiency signal, acts auxin. Plants treated with external auxin increase the levels of NO and the Fe-deficiency responses [108]. Gibberellin acid

(GA) was reported to enhance the iron uptake in Arabidopsis plants. Treatment with GA activates the transcription of the iron uptake marker-genes [109]. Later investigations revealed that DELLA proteins interact with FIT and bHLH038 and bHLH039 preventing their interaction and activation of the iron reductase and transporter. The treatment with GA releases the interaction of FIT with DELLA proteins and allows the transcription of *IRT1* and *FRO2* [110] (Figure 5).

Epigenetic chromatin changes regulate also iron homeostasis. Chromatin immunoprecipitation experiment showed that the enzyme SHK1-BINDING PROTEIN 1 (SKB1) bind to the promoters of the four Ib subgroup bHLHs and symmetrically methylates the arginine 3 of histone H4R3. This methylation prevents the transcription of these genes. *skb1* mutants show higher expression of the bHLHs mentioned before, higher Fe accumulation and more tolerance to iron deficiency compared to the WT. This demonstrates that such chromatin modifications have an impact in the iron homeostasis [111] (Figure 5).

Mediator proteins play an essential role in the initiation of the transcription by linking transcription factors with the RNA polymerase II. Investigations identified a mutant that was hypersensitive to iron deficiency. The mutated gene was the *YID1,* which encodes for the MED16 protein. This protein interacts with MED25 for the activation of the transcription of Fe-homeostasis genes via interaction with the two ET-regulated EIN3/EIL1 [112]. Later studies showed that the MED16 interacts directly with FIT to improve the activation of, *IRT1*, *FRO2* and the subgroup Ib BHLHs genes [113]. Another subunit of this RNA polymerase complex that regulated iron homeostasis is the RNA POL II C-TERMINAL DOMAIN-LIKE PHOSPHATASE 1 (CPL1) which unlike other CPLs, has negative controlling features. It interacts with the REGULATOR OF CBF GENE EXPRESSION 3 (RCF3) affecting the mRNA availability of *FIT* and the Ib *BHLHs* [114, 115] (Figure 5).

1.2 Iron in relation to oxidative stress and pathogen response

1.2.1 Oxidative stress

The chemical transformation of vital substances in the normal metabolism generates free radicals, which can be any chemical species with one or more unpaired electrons. The free radicals candidates includes the hydrogen atom, as the simplest radical, most transition metals and the oxygen molecule. Oxygen radicals, the so-called reactive oxygen species (ROS), are the most

common radicals produced in an organism. Among these, the most relevant are the superoxide ($\cdot O_2^-$), hydrogen peroxide (H_2O_2) and hydroxyl radical ($\cdot OH$) [116, 117]. These radicals are produced under normal physiological, pathological, or stress conditions by specific reductase enzymes or in biochemical processes that involve an electron transport chain, for example photosynthesis, respiration or oxidative phosphorylation [118].

Cells use ROS as messenger molecules for specific responses. For example, H_2O_2 plays an important role in the signal transduction for the immune response of both humans and plants [119-122]. In humans, it induces the nuclear presence and the DNA-binding of the transcription factor NF-κB, which activates the transcription of genes involved in inflammatory and immune responses [119]. In plants, the immune response is also supported by the production of ROS. These molecules cross-link cell wall proteins to prevent pathogen entrance and induce the production of phytoalexins, which are small molecules that accumulate in the area of infection and prevent growth and spread of the bacteria. Likewise, ROS promote the induction of the hypersensitive response (HR), so that cells undergo programmed cell death to remove nutrient sources for the pathogen. ROS waves are also involved in systemic resistance responses [120, 123].

On the other hand, high production of ROS leads to oxidative stress. When Fe exists abundantly in a free state, it is able to catalyze the production of hydroxyl radicals in a two steps reaction called the Haber–Weiss reaction. Fe^{3+} first oxidizes the superoxide anion to oxygen and is reduced itself to Fe^{2+}. Then, Fe^{2+} is oxidized in a Fenton reaction, which catalyzes the split of H_2O_2 and the formation of a hydroxyl radical and a hydroxide ion [124-126].

In plants, ROS accumulate upon drought, salt stress, cold, heat, heavy metals, high light, ozone, mechanical stress, nutrient deprivation, and pathogen attack. Since plants are not able to escape stress, they developed mechanisms to adapt and control these circumstances. In high light conditions, for example, plant diminishes the leaf surface by curling, or upon drought, they close the stomata. If the plant is not able to counteract the production of ROS during the mentioned biotic and abiotic stresses, the cells undergo programed cell death and the plant may die [127].

Low molecular weight molecules and enzymatic proteins are responsible for keeping the balance between harmful and useful ROS. Most ROS are produced in the mitochondria, peroxisomes and, in plants, in chloroplasts [127, 128]. Hence, the majority of the ROS-scavenging en-

zymes are located there [129]. The most important enzymes for ROS-scavenging are the superoxide dismutases (SOD), which catalyze the dismutation of superoxide to form hydrogen peroxide and molecular oxygen. The hydrogen peroxide is further processed to water and oxygen by a glutathione peroxidase reaction. Glutathione (GSH) is a tripeptide consisting of glutamic acid, cysteine, and glycine. GSH plays a critical antioxidative role because it is produced in high amount in almost all cells in plants and mammals. It has the capacity of easily oxidizing to glutathione disulfide (GSSG). Subsequently, the glutathione reductase converts the GSSG back to GSH. Additionally, catalases are very potent enzymes to metabolize the hydrogen peroxide to water and oxygen [118, 127, 130, 131].

1.2.2 Pathogen defense

The principles of immune responses in plants and mammals differ in several aspects. Mammals have a circulatory system with specialized killing and memory cells as a part of the very effective adaptive immunity. Plants rely on an effective innate immunity.

The first protection against pathogens is generally to prevent pathogen entrance into the organisms using physical barriers. In plants, callose, lignin, and other phenolics reinforce the cell walls of wood and xylem vessels after pathogen attack or mechanical damage thereby preventing the spread of the pathogen and its toxins [132-135]. If these barriers fail, the innate immune system comes into place.

The first immediate (basal) immune defense in plants and animals is the innate immunity response. Specialized pattern recognition receptors (PRR) recognize microbe molecules, which are called microbe-associated or pathogen-associated molecular patterns (MAMPs/PAMPs) [136, 137]. The basic immune output responses are important mechanisms for the surviving of the plant during and after pathogen attack. The hypersensitive response (HR) is an emergency measure, which activates cell death (programmed cell death, PCD) of a limited number of surrounding cells to limit the nutrients and thereby avoid the spread of biotrophic pathogens [138]. Moreover, ETI and PTI activate the so-called systemic acquired resistance (SAR) and the corresponding pathogenesis-related (PR) genes. SAR is a long-distance and long-lasting immune response activated in the entire plant after a local infection [139, 140].

Pathogens gain from the host all required nutrients. Iron regulation is very important for pathogen survival during infection in plants. Iron plays dual roles for host and pathogen, either as nutrient or as essential cofactor constituent to initiate or avoid immune responses.

The genes *FER2* and *FER1* of a maize fungi *Ustilago maydis,* which encode a high-affinity iron permease and an iron multicopper oxidase respectively, are involved in the iron uptake in this microorganism. Deletion of these genes showed that the infection rate of the fungi in maize plants was impaired, concluding that these genes are crucial for its virulence as well [141]. NPS6 is a virulent gene conserved in many filamentous fungi, which is involved in siderophore biosynthesis and in tolerance to H_2O_2 [142].The requirement to sequestrate iron via siderophore production might be not only to take up iron but also to protect from reactive oxygen species [143].

In the host cells, iron exists mostly as a complex with ferritin, transferrin, hemoglobin, and other proteins. It was shown that, after a pathogen infection in plants, ferritin accumulates possibly to protect from ROS but also to deprive invaders from iron [144]. During a pathogen attack, iron accumulates in the apoplast to elevate the oxidative response, which in turn activates the expression of PR-genes. The translocation of iron to the apoplast causes intracellular iron deficiency activating iron-uptake genes and PR-genes [145]. Bacteria stimulate siderophore production, which may serve to solubilize iron inside the host and transport it into the microbial cells [15, 146]. The upregulation of ferritin may help to withstand siderophore action [144].

However, many bacteria can also act in a positive way on plants. In the plant's rhizosphere, many beneficial nonpathogenic rhizobacteria are present and protect the plants against pathogenic microorganisms by secreting antimicrobial components [147]. The content of plant growth-promoting rhizobacteria (PGPR), soil type and strategy of iron uptake plays a fundamental role for plants in the iron nutrition [148, 149]. In turn, the iron status of the plant influences the rhizobacteria community as well.

Plants may profit from siderophore production of the rhizobacteria for the activation of the induced systemic resistance (ISR), a SA-independent immunological pathogen response in plants [150, 151]. Iron deficiency and ISR are closely related. Transcriptome analysis in *A. thaliana* showed that a high number of genes upregulated upon iron deficiency conditions are also upregulated in plants treated with beneficial bacteria [152]. Similarly, treatment with synthetic

siderophores upregulated many gene encoding for WRKY transcription factors and genes required for the iron uptake, such as ferritin, the iron transporter (*IRT1*), the iron reductase (*FRO2*), and the NICOTIANAMINE SYNTHASE (*NAS*) [144, 153]. An overlap between these two processes is represented by the transcription factor MYB72. This transcription factor activates downstream an important component necessary for ISR called BGLU42 (β-glucosidase). BGLU42 is involved in the production and secretion of phenolic compounds from the root to the rhizosphere and is a key component for the activation of the ISR [154]. *MYB72* is strongly upregulated under iron deficiency conditions, and its regulation occurs in a FIT-dependent manner [101, 155]. Thus, mutants lacking MYB72, and its close homologue MYB10, were not able to survive in iron deficiency conditions. Finally, it was shown that MYB72 induces the expression of *NAS4* [101] [50] and *BHLH039* [154].

2 Aims

Nowadays, iron malnutrition is a critical challenge of our society. Since the resources are scarce in the affected regions, the necessity of nutrient richer crop is of primordial interest. The investigation of the mechanisms for iron mobilization, uptake and homeostasis within the plant is crucial. The iron homeostasis in *Arabidopsis thaliana* and other plants have been wide investigated; however, the regulation of this process needs to be further explored. Previous analysis in our lab [156] showed that the overexpression of bHLH039 enhances the iron uptake genes in iron sufficient medium leading to high iron amounts in roots and shoots.

These "features" gained from the overexpression of *BHLH039* opened the question if bHLH039 acts upstream of FIT in the iron homeostasis regulation. To address these question, following goals were established.

First, the iron-deficiency responses in 6-day old seedlings should be confirmed. Additional, the fact that the iron content in 39Ox plants is very high led us to suspect that bHLH039 might be able to activate the iron uptake in a stronger manner than FIT does. Therefore, 39Ox plants should be crossed with *fit-3* mutant and FIT-overexpression lines. Molecular and physiological experiments with these crosses should reveal whether bHLH039 activates the iron-deficiency machinery without FIT and if the overexpression of FIT changes the 39Ox phenotype.

Next, with the knowledge that 39Ox plants have an altered gene expression of iron uptake genes (*IRT1* and *FRO2*), a comparative transcriptome profiling of 6 days-old seedling should be performed. Genes that are not FIT- of Fe-regulated are particularly interesting because they would provide a hint which genes are direct or indirect targets of bHLH039. New processes and genes influenced by bHLH039 should be searched using this transcriptome data.

Finally, the activation of the *FIT* promoter by the bHLH039 TF should be investigated. To complete this objective, 39Ox plants should be crossed with *pFIT::GUS* plants and the expression of the GUS reporter gene verified using GUS assay. Furthermore, by means of chromatin immunoprecipitation the direct DNA binding of bHLH039 protein to *FIT* and other promoters should be analyzed.

3 Materials and Methods

3.1 Materials

3.1.1 Plant material

The following plant lines were used for physiological and molecular experiments as well as for crossing.

Table 1: Lines used as source material

Name	Stock number	Genotype	Source
WT	AA51.1, WE1	Col-0 Ecotype	
fit-3	AA9.1	T-DNA insertion 207 bp dowstream of ATG	[80]
39Ox	FM218, MN32/161/189/190	pAlligator 2*, p2xCaMV35S:3xHA-bHLH* (gDNA) in Col-0 background	[156]
HA_3-FIT	JM9	pAlligator 2*, p2xCaMV35S:3xHA-FIT* (cDNA)in Col-0 background	[105]
HA_7-FIT	JM8	pMDC32*, p2xCaMV35S:7xHA-FIT* (cDNA)in Col-0 background	[105]
3xbhlh	FM35, MN18, MN159, MN160	Crossing of single *bhlh39, bhlh100, bhlh101* mutants	[89]
pFIT::GUS	FP0415	Col-0 background	[80]

3.1.2 Oligonucleotides

Table 2: Genotyping Primers. Capital letters stand for a sequence within a gene region and small letters for untranslated regions

Primer Name	Sequence 5'-3'
FIT 5'	CCCTGTTTCATAGACGAGAACC
FIT 3'	CCGGAGAAGGAGACGTTAGG
BHLH38 LP	AGACACAAATGGGATCAAGTTG
BHLH38 RP	AAGGGTTAACTCGGTGTTCTTC
BHLH39 LP	GGAGGTCAACAAATAAATAAAATGC
BHLH39 RP	AAGGGTTAACTCGGTGTTC
BHLH100 LP	TTGTGGTAGAAAAATGTAATTGC
BHLH100 RP	TCAGTTTATGTTACTTGGGACCG
BHLH101 LP	TATGATTGGCGTAATCCCAAG
BHLH101 RP	TTTCCTACTTCATCCCATCAAAG
GABI T-DNA check	CCCATTTGGACGTGAATGTAGACAC
Salk LBb1	GCGTGGACCGCTTGCTGCACCT

Table 3: Primers for qPCR and standards. Capital letters stand for a sequence within a gene region and small letters for untranslated regions

Primer Name	Sequence 5'-3'
RT-Ef1Balpha2-5'	ACTTGTACCAGTTGGTTATGGG
RT-Ef1Balpha2-3'	CTGGATGTACTCGTTGTTAGGC
RT-FIT-5'(MN)	ATCCTTCATACGCCCTCTCC
RT-FIT-3'(MN)	ATCCTTCATACGCCCTCTCC
RT bHLH038	GGAGATAACCTAAATAACGGCA
RT3' bHLH038	GGTCCAGATCAGTGTTAGATTCA
RT bHLH039 (348)	GACGGTTTCTCGAAGCTTG
RT3' bHLH039 (459)	GGTGGCTGCTTAACGTAACAT
BHLH100-RT5'	AAGTCAGAGGAAGGGGTTACA
BHLH100-RT3' (479)	GATGCATAGAGTAAAAGAGTCGCT
BHLH101-RT (427)	CAGCTGAGAAACAAAGCAATG
BHLH101-RT3' (678)	CAGTCTCACTTTGCAATCTCC
STD-FIT-5'(MN)	AAGACATGACCAAAAATGTGTGT
STD-FIT-3'(MN)	TGCATCTCCAACAATGGATGC
STD-BHLH038-5'	GGAGATAACCTAAATAACGGCA
STD-BHLH038-3'	GGTCCAGATCAGTGTTAGATTCA
STD-BHLH039-5'	AACCAAAGCAGCTTCCAAG
STD-BHLH039-3'	CGAAGAGAAAAAGGACGACA
STD-BHLH100-5'	CCTCCCACCAATCAAACG
STD-BHLH100-3'	ATGACATCGGTGTGTAACCAC
STD-BHLH101-5'	CATCCCATCAAAGTCTCTCTAGC
STD-BHLH101-3'	CCTCCAGTCTCACTTTGCAAT
STD-EF1Balpha2-5'	GCTGCTAAGAAGGACACCAAG
STD-EF1Balpha2-3'	TGTTCTGTCCCTACTGGATCC

Table 4: Primers for Tail PCR. Capital letters stand for a sequence within a gene region and small letters for untranslated regions

Primer Name	Sequence 5'-3'	Tm °C	End conc. µM
pALLI2 RB1 (S1)s	GACCTGCAGGCATGCAAGCTA	60	20
pALLI2 RB2 (S2)	CCATCTTTGGGACCACTGTCG	51	20
pALLI2 RB3 (S3)	GACCTGCAGGCATGCAAGCTA	57	20
AD1	NGTCGASWGANAWGAA	43-48	24
AD2	TGWGNAGSANCASAGA	46-51	24
AD3	AGWGNAGWANCAWAGG	43-48	24
AD4	STTGNTASTNCTNTGC	43-51	32
AD5	NTCGASTWTSGWGTT	41-44	16
AD6	WGTGNAGWANCANAGA	40-48	32

Table 5: Primers for ChIP-qPCR. Capital letters stand for a sequence within a gene region and small letters for untranslated regions

Primer Name	Sequence 5'-3'	Fragment size
ChIP FITa 5'	tccaaatgtcaattagtgaaga	78 bp
ChIP FITa 3'	ttttgccacatgattatcttt	
ChIP FITb 5'	aacgaaataggaagaatttcag	54 bp
ChIPFIT-a-R	atttgatacatgtgaagctagcata	
ChIP FITc 5'	agcttgtgacaactaaaccag	60 bp
ChIP FITc 3'	attaatttgcaatcggctta	
ChIP FITd 5'	caagaatatatgtggatc	70 bp
ChIP FITd 3'	ctacgatattagacgtac	
ChIP FITe 5'	attccctccaccacaaaa	74 bp
ChIP FITe 3'	gcatgacaattatatttccaca	
ChIP FITa 5'	tccaaatgtcaattagtgaaga	78 bp
ChIP FITa 3'	ttttgccacatgattatcttt	
ChIP IRT1b 5'	atgccttaatcaagttttgaa	68 bp
ChIP IRT1b 3'	catttacaattgtcaggatgaa	
ChIP IRT1c 5'	gtcggtggagtatgagtttg	76 bp
ChIP IRT1c 3'	gagtggtttacctcccacgt	
ChIP IRT1d 5'	gctagatgtccctttttttagg	63 bp
ChIP IRT1d 3'	atgaaatcgggtatgaatgt	
ChIP IRT1e 5'	cgaataaaggaggaggaatc	75 bp
ChIP IRT1e 3'	ttgtgctcagtgtatggttg	
ChIP IRT1f 5'	gtagtgtttttggtgactgg	79 bp
ChIP IRT1f 3'	gtttatgctacgagcacaac	
ChIP FRO2a 5'	acgcgtgagatttcgtag	72 bp
ChIP FRO2a 3'	tgtgtaaaatacacgtgtcag	
ChIP FRO2b 5'	cggattttaattcatctttgat	64 bp
ChIP FRO2b 3'	cattattagtttgaaaactgatt	
ChIP FRO2c 5'	aatttttttttttggacaaatgc	127 bp
ChIP FRO2c 3'	aaagtacaccaccaataacctc	
ChIP FRO2d 5'	acaagatccatggggaaga	51 bp
ChIP FRO2-c-R 3'	agtaagctagttgcatgctccat	
STDChIPAt3g12900-5'	CCTCAAAACAAAGGTGATACTGT	64 bp
ChIPAt3g12900-a-3'	atctataaagctaggcaattg	
ChIPAt3g12900-b-5'	cgagacgcatgcaccacaa	56 bp
ChIPAt3g12900-b-3'	agggttttttctagctagtgtcttac	
ChIPAt3g12900-c-5'	tcgacgactagtttaccaagtga	80 bp
ChIPAt3g12900-c-3'	agagaagtttacgtacctgaga	
ChIPAt3g07720-a-5'	GCTCTAAGGCTCCTCAACTTC	79 bp
ChIPAt3g07720-a-3'	CGCTTGAGACGACACTGTTT	
ChIPAt3g07720-b-5'	CCTTCTCATTAGCCTCATTCTCCATATG	73 bp
ChIPAt3g07720-b-3'	GGCGACTCTTATGATGACAAATT	
ChIPAt3g07720-c-5'	GCCGTATGATTAAAGTTTACAATGC	89 bp
ChIPAt3g07720-c-3'	ccttccttttctttttttgtacc	
ChIPAt3g58810-a+b-5'	cagcagagtttcgtaaggtcag	75 bp
ChIPAt3g58810-a+b-3'	accacaacagacttagcggt	
ChIPAt3g58810-c-5'	gatagtcaatagtcatttcgtgtct	97 bp
STDChIPAt3g58810-3'	TGCCTCCCATCTAGTCTCTT	

Table 6: Primers to generate standards for ChIP-qPCR. Capital letters stand for a sequence within a gene region and small letters for untranslated regions

Primer Name	Sequence 5'-3'	Fragment size
ChIPFIT-a-F	agatgtgataggtacagcaaaattg	168
ChIPFIT-a-R	atttgatacatgtgaagctagcata	
ChIPFIT-b-F	gcttgtgacaactaaaccagttgac	191
ChIPFIT-b-R	atcgatcagaccgtattaaaaaggt	
ChIPFIT-c-F	ctcttgtttctaatctgcattccct	119
ChIPFIT-c-R	ttactcgaatgattaatttgtcgtgt	
ChIPIRT1-a-F	acacatgttttgattccatacacc	231
ChIPIRT1-a-R	ttacaattgtcaggatgaagtgtg	
ChIPIRT1-b-F	aatatggaaaatctccccaagttc	151
ChIPIRT1-b-R	agtggtttacctcccacgtttt	
ChIPIRT1-c-F	tgttcatgtaaaaatgcgtaagttc	185
ChIPIRT1-c-R	atcaattcaaaaatgaaaaatgact	
ChIPIRT1-d-F	tcatttttgaaaactagacatcaagc	159
ChIPIRT1-d-R	gtttatgctacgagcacaacatcac	
ChIPFRO2-a-F	atgatgatgaggaagaaagaagatg	161
ChIPFRO2-a-R	cgtgtgtaaaatacacgtgtcaga	
ChIPFRO2-b-F	ttttaacaaatgtcaatcagttttca	188
ChIPFRO2-b-R	aaagaggttattggtggtgtacttt	
ChIPFRO2-c-F	aaatgtattttgctaatcaaatcgt	157
ChIPFRO2-c-R	agtaagctagttgcatgctccat	
STDChIPAt3g07720-5'	TCCATTCACCGCTCAACTCT	908
STDChIPAt3g07720-3'	tctctgtctctatttaaggccca	
STDChIPAt3g58810-5'	ACGAGCTTGCAGTCTGATCA	903
STDChIPAt3g58810-3'	tgcctcccatctagtctctt	
STDChIPAt3g12900-5'	cctcaaaacaaaggtgatactgt	1283
STDChIPAt3g12900-3'	tgtctccacacttctgcttga	

3.1.3 Chemicals

Table 7: List of chemicals and their applications

Chemical	Company	End concentration
RNase inhibitor, recombinant ribolock	Fermentas	
EDTA	Fermentas	25 mM
Oligo (dt) $_{18}$	Fermentas	100 µM
5x M-MuLV buffer	Fermentas	
dNTP	Fermentas	10 mM each
m-MuLV RTase	Fermentas	
Saccharose	Roth	25 mg/ml
GUS substrate – x-Gluc	Sigma	2 mM
Plant Agar	Duchefa	
X-Gal	Sigma	70 ng/ml
Na_2HPO_4	Roth	100 mM pH7.2
NaH_2PO_4	Roth	100 mM pH7.2
$K_4[Fe(CN)_6]$ – (Fe^{2+})	Roth	2 mM
$K_3[Fe(CN)_6]$ – (Fe^{3+})	Roth	2 mM
Triton-X	Serva	0.2%
SDS	Roth	

3.1.4 Kits

Material	Company	Use
Spectrum Plant Total RNA Kit	Sigma-Aldrich	RNA isolation
DyNAmo ColorFlash SYBR Green	Thermo Fisher	qPCR
Amplex® Red Enzyme Assays	Thermo Fisher	H_2O_2 Assay

Stock solutions for the Amplex® Red Enzyme Assays

The reagents below are sufficient for 100 reactions with a volume of 100 µl.

10 mM Amplex® Red reagent stock solution: One vial of Amplex® Red reagent (Component A, blue cap) was dissolved in in 60 µl DMSO (Component B, green cap)

1X Reaction Buffer: 4 mL of 5X Reaction Buffer (Component C, white cap) were added to 16 mL of deionized water.

10 U/mL Horseradish Peroxidase (HRP) stock solution: The vial of HRP (Component D, yellow cap) was dissolved in 1.0 mL of 1X Reaction Buffer and aliquoted for storage at -20°C.

10 µM Hydrogen Peroxide (H_2O_2) working solution: 1µl of a 35% H_2O_2 (10 M) was dissolved in 1ml 1x reaction buffer to obtain a 1 mM stock solution. 1µl of the 10mM stock solution was dissolved in 1ml 1x reaction buffer to obtain a stock solution of 10 µM. This solution should be used within a few hours of preparation.

Working solution from stocks	5 ml for 100 assays	6 ml for 120 assays
10 mM Amplex Red reagent stock solution	50 µl	60 µl
of 10 U/mL HRP stock solution	100 µl	120 µl
1X Reaction Buffer	4.85 ml	5.82 ml

3.1.5 Antibodies

- Mouse HA tag monoclonal antibody (Diagenode, Cat. Nr. C15200190)
- Rabbit anti-actin monoclonal antibodies (Agrisera,Cat. Nr. AS13 2640)
- Goat anti-rabbit-HRP-coupled secondary antibody (Pierce)
- Rabit IgG polyclonal antibody (Diagenode, Cat. Nr. C15410206)

3.1.6 Media and buffer

Hoagland medium:

Macronutrients	Micronutrients	Iron
0.75 mM $MgSO_4$	50 µM KCL	50 µM FeNaEDTA (+Fe)
0.5 mM KH_2PO_4	50 µM H_3BO_4	0 µM FeNaEDTA (-Fe)
1.25 mM KNO_3	10 µM $MnSO_4$	
1.5 mM $Ca(NO_3)_2$	2 µM $ZnSO_4$	
	1.5 µM $CuSO_4$	
	0.075 µM $(NH4)_6Mo_7O_{24}$	
1% Saccharose		
0.8% plant agar		
pH 6.0		

Murashige-Skoog-Medium (MS):

4.4 g MS-Powder (full pack Duchefa)
7.5 g MES Monohydrat
5 g Sucrose (0.5%)
10 g Agar (1%)
pH 5.6-5.8

3.1.6.1 Immunoblot buffers

2x Laemmli buffer	
100 mM	Tris-HCL pH 6.8
4 %	SDS
20 %	Glycerol
0.2 %	Bromphenol blue
200 mM	DTT

TBS-T	
20 mM	Tris-HCl, pH 7.4
180 mM	NaCl
0.1 %	Tween 20

10x Running buffer	
250 mM	Tris
2.5 M	Glycin
1 %	SDS

1x transfer buffer	
10 %	Running buffer
20 %	Ethanol

3.1.6.2 GUS-assay Buffers

Table 8: Quantitative GUS-assay buffer. Prepare X-Gluc every time fresh.

Stock	Chemical	For 500 µl	End conc.
1 M	Na_2HPO_4	29 µl	100 mM
1 M	NaH_2PO_4	21 µl	pH 7.2
100 mM	$K_4[Fe(CN)_6]FeII$	10 µl	2 mM
100 mM	$K_3[Fe(CN)_6]FeIII$	10 µl	2 mM
20%	Triton-X	5 µl	0.2%
100 mM	X-Gluc	10 µl	2 mM
	H_2O	415 µl	

Table 9: Qualitative GUS extraction buffer

Stock	Chemical	For 1 ml	End conc.
1 M	Na_2HPO_4	29 µl	50 mM
1 M	NaH_2PO_4	21 µl	pH 7.2
0.5 M	Na-EDTA pH 8.0	2 µl	1 mM
20%	Triton-X	5 µl	0.1%
1 M	ß-mercaptoethanol	10 µl	10 mM
	complete protease inhibitor		
	H_2O	933 µl	

Table 10: 4-MUG Reaction buffer

Stock		For 250 ml	End conc.
	GUS extraction buffer	245 µl	
100 mM	MUG solved in DMSO (38.8 mg/ml)	5 µl	2 mM

MU (make fresh 100 mM in DMSO)

Stop reagent (1 M sodium carbonate)

3.1.6.3 Iron reductase assay buffers

Table 11: Plate reductase assay

Stock	Chemical	For 100 ml	End conc.
5 mM	CaSO4	10 ml	0.5 mM
	Agar	0.7 g	0.7% w/v
10 mM	FeNaEDTA	2.5 ml	0.25 mM
50 mM	Ferroxin	0.5 ml	0.25 mM

Table 12: Qualitative iron reductase assay

Stock	Washing solution	For 50 ml	End conc.
	$Ca_2(NO_3)*4H_2O$	1.18 g	100 mM
Stock	**reductase-assay solution**	**For 50 ml**	**End conc.**
10 mM	FeNaEDTA	500 µl	0.1 mM
50 mM	Ferrozin	500 µl	0.5 mM

3.1.6.4 Pearl stain

Table 13: Fixative and stain solution

Stock	Fixative : Methacarn	For 10 ml	End conc.
100%	Methanol	6 ml	6:3:1
100%	Chloroform	3 ml	
100%	Acetic acid	1 ml	
Stock	**Stain solution: Berliner blue**	**For 10 ml**	**End conc.**
	$K_4[Fe(Cn)_6]$	0.2 g	4%
37%	HCl	0.54 ml	4%

3.1.6.5 Chromatin Immunoprecipitation

Stock solutions. All stock solutions should be sterile-filtrated.

Conc.	Chemical	Mass	Volume	Comment	Store
5 M	NaCl	14,6 g	50 ml		RT
1 M	$MgCl_2$	4,8 g	50 ml		RT
1 M	NaH_2PO_4	6 g	50 ml		RT
1 M	Na_2HPO_4	7,1 g	50 ml		RT
1 M	2-Methyl 2,4-pentanediol	5,9 g	50 ml		RT
1.25 M	Glycine	4,7 g	50 ml		RT
0.5 M	HEPES	6 g	50 ml	pH 7.5	4°C
0.5 M	EDTA	7,3 g	50 ml		RT
100 mM	$ZnSO_4$	0,8 g	50 ml		RT
1 M	Tris Base	6 g	50 ml	pH 9	RT
3 M	Sodium acetate	2,5 g	10 ml		RT
10 %	SDS	1 g	10 ml		RT
20 %	Triton-X 100	2 ml	10 ml		RT
99 %	β-Mercaptoethanol				
100 %	Ethanol				
20 mg/ml	Proteinase K				
16%	Formaldehyde			Thermo fisher	
	Sarkosyl				
	Tween-20				
	Glycogen				
	Complete PI cocktail			Roche	
	Protein-A agarose beads			Santa Cruz	
	Low addition tubes			Eppendorf	

Working Solutions. All these buffers should be prepared fresh.

Sodium phosphate buffer pH 7 (1 M stock)		
Stock		Volume
1 M	Na_2HPO_4	57.7 ml
1 M	NaH_2PO_4	42.3 ml
	Total volume	100 ml
Sterile filtrate, Store RT		

MC buffer (fresh)			
Stock		Volume	End. Conc.
3.4 g	Sucrose		0.1 M
1 M	Sodium phosphate buffer	1 ml	10 mM
5 M	NaCl	1 ml	50 mM
	Total volume	100 ml	
	Store on ice		

M1 buffer (fresh)			
Stock		Volume	End. Conc.
1 M	Sodium phosphate buffer	250 µl	10 mM
5 M	NaCl	500 µl	0.1 M
1 M	2-methyl 2,4-pentanediol	3.2 ml	1 M
	β-mercaptoethanol	17.7 µl	10 mM
	protease inhibitor cocktail		½ tablet
	Total Volume	25 ml	

M2 buffer (fresh)			
Stock		Volume	End. Conc.
1 M	Sodium phosphate buffer	250 µl	10 mM
5 M	NaCl	500 µl	0.1 M
1 M	2-methyl 2,4-pentanediol	3.2 ml	1 M
1 M	$MgCl_2$	250 µl	10 mM
20%	Triton-X	625 µl	0.5 %
	β-mercaptoethanol	17.7 µl	10 mM
	protease inhibitor cocktail		½ tablet
	Total volume	25 ml	
	Store on ice		

M3 buffer (fresh)			
Stock		Volume	End. Conc.
1 M	Sodium phosphate buffer	250 µl	10 mM
5 M	NaCl	500 µl	0.1 M
	β-mercaptoethanol	17.7 µl	10 mM
	protease inhibitor cocktail		½ tablet
	Total volume	25 ml	
	Store on ice		

Sonic buffer (store frozen in aliquots at – 20 °C)			
Stock		Volume	End. Conc.
1 M	Sodium phosphate buffer	500 µl	10 mM
5 M	NaCl	1 ml	0.1 M
	Sarkosyl	250 mg	0.5 %
0.5 M	EDTA	1 ml	10 mM
	Total volume	50 ml	
Sterile filtrate make aliquots and add fresh the protein inhibitor cocktail from 25x stock			

IP buffer (store frozen in aliquots at – 20 °C)			
Stock		Volume	End. Conc.
0.5 M	HEPES	5 ml	50 mM
5 M	NaCl	1.5 ml	150 mM
1 M	$MgCl_2$	250 µl	5 mM
100 mM	$ZnSO_4$	5 µl	10 µl
20 %	Triton-X	2.5 ml	1 %
10 %	SDS	250 µl	0.05 %
	Total volume	50 ml	
Sterile filtrate make aliquots			

Elution buffer (store frozen in aliquots at – 20 °C)			
Stock		Volume	End. Conc.
1.25 M	Glycine	4 ml	0.1 M
5 M	NaCl	5 ml	0.5 M
	Tween-20	25 µl	0.05 %
	Total volume	50 ml	
Adjust the pH to 2.8 make aliquots and freeze.			

3.1.7 Other materials

Material	Company	Use
96 Fast PCR-Plate full skirt	Sarstedt	qPCR
GRE96ft_half_area	Greiner	Iron reductase assay
50 ml reaction tubes	Greiner	various
2 ml reaction tubes	Sarstedt	various
1.5 ml reaction tubes	Sarstedt	various
PCR strips	Sarstedt	various
DNA Low binding 1.5 ml	Eppendorf	ChIP
DNA Low binding 2 ml	Eppendorf	ChIP
Nitrocellulose membrane	GE Health Care	Immunoblot
ECL	GE Health Care	Immunoblot
Mini-PROTEAN precast gels	Biorad	Immunoblot

3.1.8 Devices

PRECELLYS® 24	Precellys
Infinite® 200 PRO series	TECAN
CFX96 Touch™ Real-Time PCR Detection System	Bio-Rad
Mini-PROTEAN Electrophoresis Chambers	Bio-Rad
Gel Doc2000	Bio-Rad
Bioruptor®	Diagenode
Vacuum pump	Vacuubrand
FluoChem Q system	Proteinsimple
Growth Chambers	Percival
PerfectBlue™ DNA Gelsystem	PeqLab
Thermocycler	PeqLab
Centrifuges and cool centrifuges	Thermo

3.1.9 Software

Primer design tool Primer3	http://primer3.ut.ee/
URI Genomics & Sequencing Center	http://cels.uri.edu/gsc/cndna.html
JMicro Vision	http://www.jmicrovision.com/
Virtual Plant	http://www.virtualplant.org
REVIGO	http://revigo.irb.hr/
TAIR	https://www.arabidopsis.org/
ATTED-II	http://atted.jp/
Venny 2.1.0	http://atted.jp/
NCBI	http://www.ncbi.nlm.nih.gov/geo/
MataCyc	https://metacyc.org/

3.2 Methods

3.2.1 Plant growth

Seeds were surface sterilized for 8 minutes (6% NaOCl, 0.1% Triton X), washed four times with dest. sterile water and then stratified for 2 days at 4°C in 1% plant agar. The seeds were placed in Hoagland agar plates under iron sufficient (50 µM Fe-EDTA) or iron deficient (0 µM Fe-EDTA) medium and grown vertically in the Percival growth chamber with a 110-150 $\mu mol.m^{-2}s^{-1}$ light intensity. The plant growth time is described in each experiment.

3.2.2 Plant screening

Using phenotypical analysis, GUS-assay (see 3.2.7) and genotyping homozygote transgenic plants were selected. 39Ox [156] plants were selected first by the phenotype. Then, these plants as well as HA_3-FIT and HA_7-FIT [105] plants were genotyped using the forward primer 35S and the gene specific primer. Primer names are shown in the gen map of Figure 6.

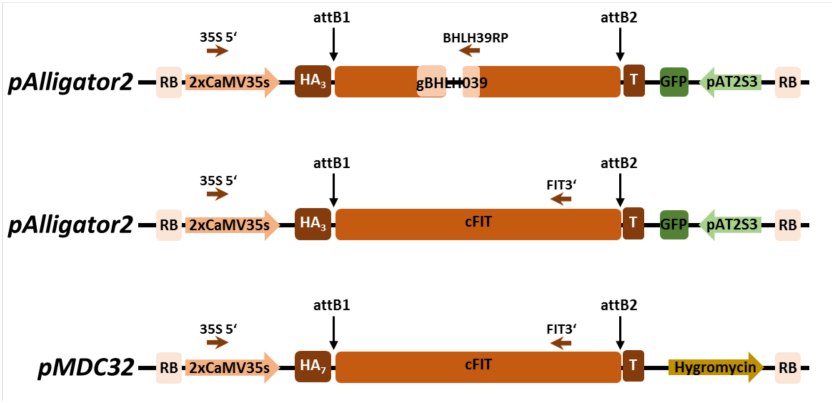

Figure 6: Gene map *BHLH039* and *FIT* overexpression lines. The gDNA of BHLH039 and the cDNA of FIT were used for the generation of the overexpression lines 39Ox [156] and the HA_3-FIT and the HA_7-FIT [105]

The PCR for the selection of KO the *fit* [80] and the *3xbhlh* [89] mutants was performed using primers combination against the endogenous gen (for WT gene) as well as T-DNA specific forward primer and the gene specific reverse primer (for T-DNA insertion)

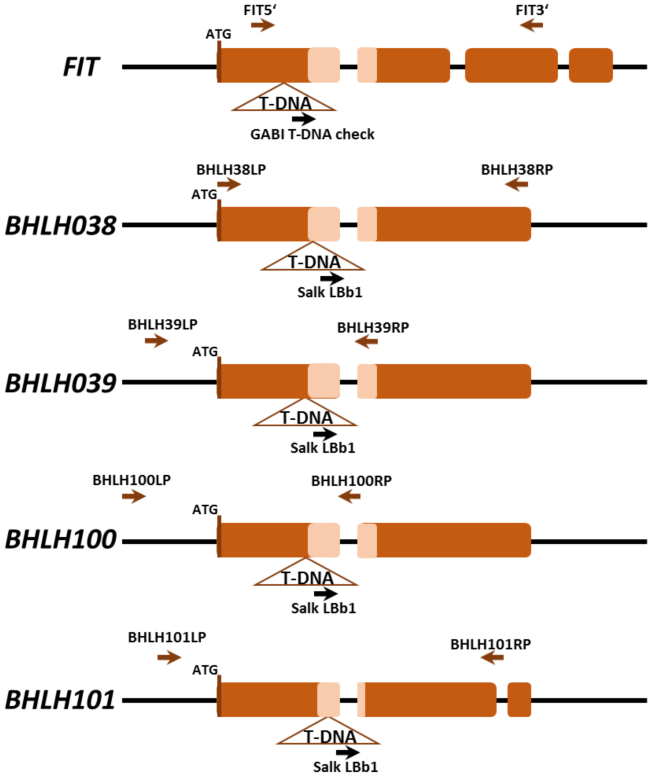

Figure 7: Gene map of FIT, bHLH038/39/100/101 with T-DNA insertion. Schematic representation of the WT genes with the T-DNA and the primers used for genotyping.

PCR program used for the genotyping:

First denaturation	94°C	3 min	
Denaturation	94°C	30 s	
Annealing	64°C – 1°C/cycle	30 s	6x
Elongation	72°C	60 s	
Denaturation	94°C	30 s	
Annealing	58°C	30 s	34x
Elongation	72°C	60 s	
Final elongation	72°C	7 min	
Store	12°C		

3.2.3 Crossings

The open and very young flowers as well as the inflorescence apex were removed. The sepals, petals and anthers of closed flower buds from parent 1 were removed to let the pistil free. Three ripe flowers from the parent 2 were used to pollinize the free pistil of parent 1. Table 14 shows the crossed lines.

Table 14: F1 generation of crossed plants

Name	Parent 1	Parent 2	F1
39Ox/*fit*	MN32	MN34	MN52-54
fit/39Ox	MN34	MN32	MN49
39Ox /pFIT::GUS	MN33	MN32	MN47-48
HA_3-FIT/39Ox	JM9	FM218	MN132-134
39Ox/HA_3-FIT	FM218	JM9	MN135-138
HA_7-FIT/39Ox	FM218	JM8	MN122-126
39Ox/HA_7-FIT	JM8	FM218	MN127-131

The lines were multiplied and selected by genotyping (see 3.2.2) until they were homozygote. The final lines with the corresponding name and number are listed in Table 15. These lines were used for biological and molecular analysis.

Table 15: Final lines from crossings

Name	Stock number	Generation
39Ox/*fit*	MN85	F4
39Ox/*fit*	MN188	F5
39Ox/*fit*	MN191	F6
pFIT::GUS/39Ox	MN183	F3
39Ox/HA_3-FIT	MN187	F6

3.2.4 Immunoblot analysis

Around 40 six day-old seedlings were harvested, frozen in liquid nitrogen and grinded using the Precellys. 1 µl 2x Laemmli buffer was added per mg plant powder. The samples were centrifuged at 10.000 x g for 5 min at 4°C. 10 µg heat-denatured, total protein was loaded on a 12 % SDS-polyacrylamide gel and protein separated by electrophoresis. Proteins were electro-transferred to a nitrocellulose membrane with transfer buffer. The membrane was blocked 10 min with 5 % milk-TBS-T solution. HA3-bHLH039 protein was detected with anti-HA-horseradish peroxidase (HRP)-coupled high-affinity monoclonal rat antibody e, 1:1.000 dilution in 2.5 % milk-TBS-T, 1 h incubation at RT). The membrane was washed three times with TBS-T and signals detected with the ECL Chemiluminescence reagents (ECL) and the FluoChem Q (Biozym) device. The membrane was stripped 10 min with citric acid (4% w/v) and re-blocked. For the detection of actin protein, the membrane was incubated for 1 h at RT with anti-actin antibodies (1:5000 dilution in 2.5 % milk-TBS-T), washed three times with TBS-T and then incubated 1 h at RT with a goat anti-rabbit-HRP-coupled secondary antibody (1:1000 dilution in 2.5 % milk-TBS-T). After three washes, the membrane was detected as described above. The intensity of the bands were determined using the AlphaView (FluorChem Q) software. The bands were selected and the local backgrounds were subtracted. HA signal intensity was normalized to that of actin.

3.2.5 TAIL-PCR for the localization of the inserts in the transgenic overexpressing lines.

The thermal asymmetric interlaced PCR (TAIL-PCR) [157] is a suitable method for the identification of the exact position of a T-DNA insertion in a transgenic organism. Using plasmid specific (S1- S3) and unspecific primers (low TM arbitrary degenerate primer AD1 – AD6), it is possible to amplify a fragment by a series of three PCRs. For the first PCR was used the genomic DNA of

the transgenic line. For the second PCR, the first PCR was diluted and used as a template and so was the third PCR with the second PCR. The third PCR was run on a gel, the DNA was isolated and the DNA was sent for sequencing. Figure 8 shows a scheme of the three steps in the TAIL-PCR.

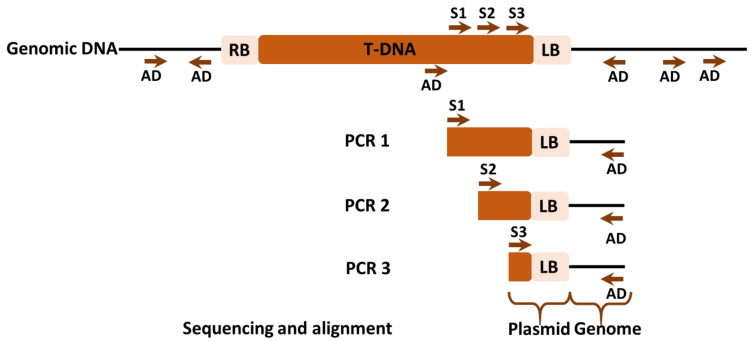

Figure 8: Scheme of the TAIL-PCR. The first PCR uses transgenic genomic DNA as a template. For the second PCR was used of PCR 1 and for PCR 3 a diluted sample of PCR 2. The PCR 3 was run on a gel and after purification sequenced. The sequence of the T-DNA-LB was proven and the rest sequence aligned to the genomic DNA using the blasting tool of NBCI. S are the specific primers and AD the unspecific.

A part of the sequence was aligned to the corresponding vector and the remaining sequence was blasted using the tool NBCI. This alignment gives the exactly position of the T-DNA in the genome of the transgenic line.

Set up and program for TAIL-PCR

PCR 1:

Master Mix:	**1 rxn**	**6 rxn (+1 reserve)**
2 x Ready Jump Start Red TAQ Mix	10 µl	70 µl
Plant genomic DNA	2.5 µl	17.5 µl
Primer S1	0.2 µl	1.4 µl
H2O	4.8 µl	33.6 µl
Total	17.5 µl	122.5 µl

Add per single rxn:

Master mix	17.5 µl
AD primer	2.5 µl
Final rxn volume	20 µl

PCR 1 program:

1 min	93 °C		initial denaturation
1 min	95 °C		
1 min	94 °C		cycles of high stringency amplifications
1 min	TmS1 + 2 °C	5 cycles	
2:30 min	72 °C		
1 min	94 °C		low stringency cycle
3 min	25 °C		
3 min ramp to	72 °C		
2:30 min	72 °C		
1 min	94 °C		supercycles of two high stringency
1 min	TmS1+2°C		cycles and one reduced stringency
cycle			
2:30 min	72 °C		
1 min	94 °C C	15 supercycles	
1 min	TmS1+2°		
2:30 min	72 °C		
1 min	94 °C		
1 min	40 °C		
2:30 min	72 °C		
5 min	72 °C		final elongation
Store	12 °C		

PCR 2:

Master Mix:	**1 rxn**	**6 rxn**
Primer S2	0.2 µl	1.4 µl
2 x Ready Jump Start Red TAQ Mix	10 µl	70 µl
H2O	6.9 µl	48.3 µl
Total	17.1 µl	119.7 µl

Add per single rxn:

Master mix	17.1 µl
1:50 PCR 1	1 µl
AD primer	1.9 µl
Final rxn volume:	20 µl

PCR 2 program:

1 min	93 °C		initial denaturation
1 min	95 °C		
0:30 min	94 °C		supercycles of two high stringency cycles and one reduced stringency cycle
1 min	TmS2+2 °C		
2:30 min	72 °C		
0:30 min	94 °C		
1 min	TmS2 + 2 °C	15 supercycles	
2:30 min	72 °C		
0:30 min	94 °C		
1 min	44 °C		
2:30 min	72 °C		
5 min	72 °C		final elongation
Store	12 °C		

PCR 3

Master Mix:	1 rxn	6 rxn
Primer S3	0.5 µl	3.5 µl
2 x Ready Jump Start Red TAQ Mix	25 µl	175 µl
H2O	18.75 µl	131.25 µl
Total	44.25 µl	309.75 µl

Add per single rxn:

Master mix	44.25 µl
1:20 PCR 2	1 µl
AD primer	4.75 µl
Final rxn volume:	50 µl

1 min	93 °C		initial denaturation
1 min	95 °C		
1 min	94 °C		reduced stringency cycles
1 min	44 °C	20 cycles	
2:30 min	72 °C		
5 min	72 °C		final elongation
Store	12 °C		

After sequencing and alignment, we could find the exact location of the *2xCAMV35S::HA$_3$-gBHLH039* insert (Figure 9), which was in chromosome 4 at the position 6039161, 544 bp up-stream from the gene *GIP1A* (GCP3-INTERACTING PROTEIN 1, AT4G09550).

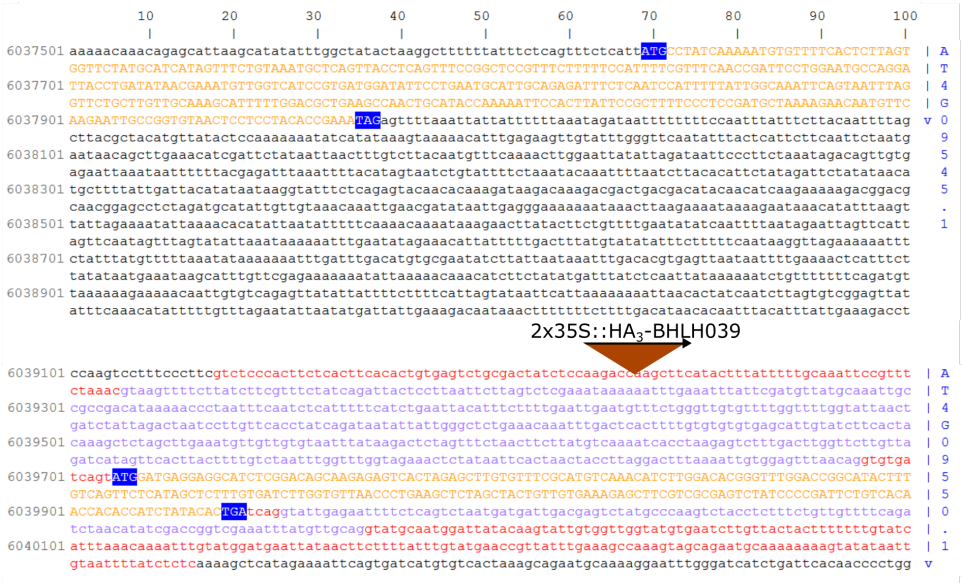

Figure 9: Position in genome of *2xCAMV35S::HA$_3$-BHLH039*. Using the method TAIL-PCR with specific primers against the right border of the pAlligator2, the exact position of the insert was determined. The insert is located between the genes AT4G09545 and AT4G09550. Primers for the PCR are listed in the materials part.

Using specific primers against the vector pMDC32 and the unspecific primers (AD), it was possible to find the position of the insert in HA$_7$-FIT genome. T-DNA with the insert *2xCAMV35S::HA$_7$-FIT* is located at the position 25620334 in the chromosome 5 between the genes AT5G64010 and AT5G64020.

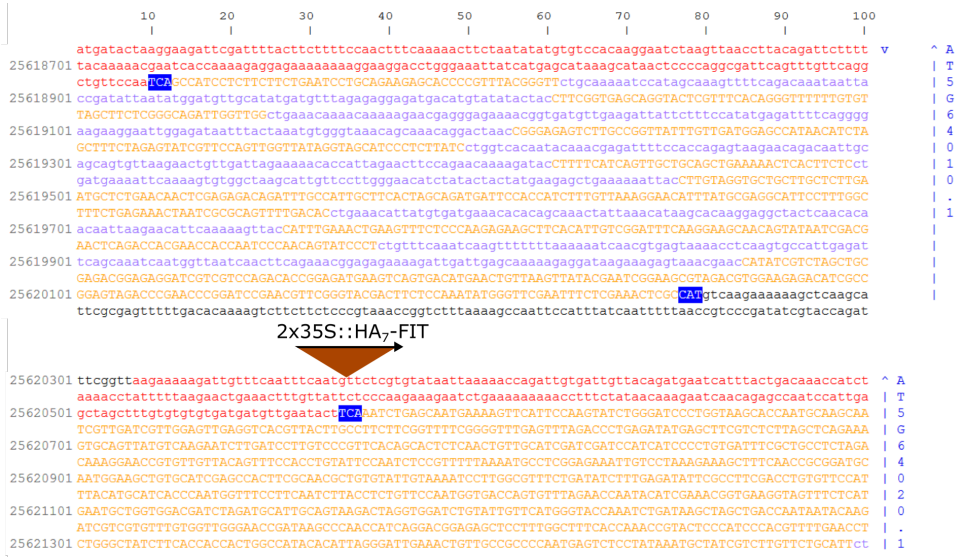

Figure 10: Position in genome of *2xCAMV35S::HA$_7$-FIT*. Using the method TAIL-PCR with specific primers against the left border of the pMDC32, the exact position of the insert was determined. The insert is located in between the genes AT5G64010 and AT5G64020. Primers for the PCR are listed in the materials part.

3.2.6 RNA isolation, cDNA synthesis and qRT-PCR

The gene expression analysis including the RNA isolation, cDNA synthesis and the qRT-PCR analysis were based on the protocol of Klatte et al. (2009) [158] with some changes.

mRNA isolation

Around 60 seedlings per line per replicate were harvested in liquid nitrogen and grinded with the PRECELLYS® 24. The total RNA was isolated with the Kit Spectrum™ Plant Total RNA from Sigma-Aldrich according to the manufacturer's instructions.

cDNA-Synthesis

The total RNA concentration was measured using the NanoQuant Plate of the TECAN reader Infinite® 200 PRO series. The absorbance of the RNA was measured at 260 nm and its quality determined by the ratio of A260/A280.This ratio should be between 1.8 and 2, otherwise it may indicate the presence of proteins or other impurities.

1 µg of total RNA was used for the cDNA synthesis previous DNase treatment. This was performed as follows:

DNase treatment

RNA+H_2O (1 µg)	7.0 µl
10x DNaseI buffer	1.0 µl
RNase inhibitor	0.5 µl
DNaseI	1.0 µl
H_2O	0.5 µl
Total volume	10.0 µl

30 min by 37°C, then 4°C

Deactivation of DNase and primer annealing

25 mM EDTA	1.0 µl
100 µM (0.5 µg/µl) oligo $(dT)_{18}$	1.0 µl
Total volume	12.0 µl

10 min by 65°C, then 4°C (deactivate Dnase and denature RNA)

cDNA synthesis

5x M-MuLV buffer	4.0 µl
H_2O	1.0 µl
RNase inhibitor	0.5 µl
dNTP 10 mM each	2.0 µL
m-MuLV RTase	0.5 µl
Total volume	20.0 µl

2 h by 42°C, 10 min by 70°C (to deactivate enzyme), then 4°C

The cDNA was filled up to 200 µl with PCR water and stored at -20°C. For the qRT-PCR, the samples were diluted 1:10 with PCR-water and distributed in PCR-strips (each 30 µl). For more details see [158].

Quantitative Real-Time PCR

This method of DNA quantification is based on a polymerase chain reaction on cDNA, which monitors the amplification of a specific cDNA fragment. This allows the comparison of gene expression between different organisms or treatments.

The qPCR in this study was performed using the 2x DyNAmo Flash SYBR Green qPCR Kits. This master mix contains a hot-start version of a modified *Thermus brockianus* DNA polymerase, which gives additional stability to the polymerase-DNA complex. It is activated during the initial DNA denaturation step in the PCR avoiding nonspecifically primer bound during reaction setup.

The design of primers is a critical step for a successful qPCR. It is important that the primers yield a 100-150 bp cDNA fragment with an annealing temperature of ~60°C. The concentrations of the primers were optimized by titration of each primer pair. Concentrations combinations of 100:200, 100:100 and 200:100 nM were verified by qPCR and the combination with the lowest Ct was chosen as the most efficient [158].

Mass standards allow the absolute quantification of the cDNA. For this purpose, a 1 kb fragment of the gene of interest was amplified with a regular PCR from a control cDNA sample (e.g. WT or *fit-3*). After separation on an agarose gel, the fragment was isolated and its concentration determined. Using the DNA concentration and the length of the fragment the copy number of the purified DNA was calculated with the formula from http://cels.uri.edu/gsc/cndna.html. The stock standard DNA was diluted to obtain dilution series from 10^7 to 10^2 molecules/10µl and distributed 30 µl in PCR strips.

The qPCR was set up in a 96 well qPCR plate with three biological replicates two technical replicates for the samples, the standards and the water control [158, 159]

cDNA/standard/H_2O control	10 µl
2x DyNAmo ColorFlash SYBR Green	9.6 µl
Primer (15 µM)	0.2 µl
Primer (15 µM)	0.2 µl
Total volume	20 µl

The device used was the CFX96 Touch™ Real-Time PCR Detection System from Bio-Rad with the following program:

First denaturation	95°C	3 min	
Denaturation	95°C	10 s	x40
Annealing	60 °C	15 s	
Elongation	72 °C	20 s	
Melting curve analysis	65 °C -95 °C, 0.5 °C increment		

The qPCR device reads the fluorescence after every cycle and creates curves. At a certain point, the signal increases exponentially with each cycle until it reaches a certain number of PCR cycles and the signal turns linear. The section where all the curves are straight and parallel to each another is called threshold. The number of cycles (Ct) needed to reach this threshold is proportional to the amount of mRNA molecules in a certain sample. The standards, which have a known number of molecules (10^7-10^2), serve as the reference point to convert the Ct values to absolute expression values.

After the qPCR, the quality of the curves needs to be verify. It is essential that the curves of the technical replicates coincide (to exclude pipetting mistakes). The melt curve indicates if the primers amplify only one fragment and the purity of the sample.

The data was analyzed with the program Bio-Rad CFX Manager 3.0 following the instructions of Klatte and Bauer (2009) [158]. For each sample value, a genomic DNA control gene (intron region from EF2Bα2) is subtracted and then normalized to the amount of total cDNA (exon region from EF2Bα2). The average and standard deviation of the three biological replicates were calculated and a bar diagram generated.

3.2.7 Histochemical GUS-Assay

Using this method, the line pFIT::GUS/39Ox was screened. For that, the root tip of ~3 weeks-old plants grown at +Fe Hoagland agar plates was cut and incubated at 37°C for 30 min-2h in 50 µl GUS-assay buffer in a 96 well plate. The blue color pointed out the presence of the transgene. The corresponding plant was used for the 39Ox screening (see 3.2.2) and the plants were further multiplied.

For the qualitative GUS assay five 6 days-old seedlings were incubated in 50 µl GUS-assay buffer in a 96 well plate at 37°C for 30 min-2h and then pictured using a binocular. For the quantitative GUS-assay, around 20 seedlings were harvested in liquid nitrogen and grinded to a fine powder.

200 µl of GUS extraction buffer were added and mixed. The samples were centrifuged at 15000 rpm for 1 minute at 4°C. The extracts were then transferred to a new tube (always on ice). A MU (fluorescent) dilution series (1-10 mM) was prepared. 10 µl sample and MU standard were pipetted in a 96 well plate and filled up to 200 µl (sample) or 250 µl (standard) with GUS-extraction buffer. 40 µl of the 4-MUG reaction buffer (non-fluorescent) were added to the samples and incubated 1h at 37°C. 200 µl stop reagent were added to the samples and the formation of the fluorescent methylumbeliferone was measured. The values were normalized to the protein concentration using a BSA standard curve with the Bradford-assay.

3.2.8 Iron reductase assay

Qualitative plate iron reductase assay

The agar plates should be prepared fresh. For this purpose, water was boiled in the microwave with 0.5 mM CaSO4 and 0.7% (w/v) agar until the agar is completely dissolved. When medium cooled down to approx. 50˚C, 0.25 mM FeNaEDTA and 0.25 mM ferrozine were added, and finally the plates poured. Around 10 seedlings were transferred using plastic forceps to the agar plates and incubated in the dark for 2 h. Then the plates were pictured.

Quantitative iron reductase assay

Before the assay, the seedlings were pictured and the roots length was measured using the software JMicro Vision. Using plastic forceps 10-15 6-day-old seedlings/replicate were washed with 1 ml 100 mM $Ca_2(NO_3)$ solution, then with 1 ml water and finally incubated 1 h with 500- 1000 µl reductase-assay solution. 170 µl of each sample and one for the blind value were transfered to a GRE96ft_half_area and measured in the Tecan at 562 nm. For the calculation, the OD of the blind was subtracted from the OD of the samples, then divided by the molar extinction coefficient of Fe^{2+} complex (28.6 $nM^{-1}cm^{-1}$) and finally normalized to the volume of the measured sample and the sum of the all root lengths.

3.2.9 Pearl stain for iron visualization

The visualization of Fe in the plant is possible using the Perl's Prussian blue stain assay. This consists of a solution of potassium ferrocyanide that reacts with Fe^{3+} and form an insoluble blue

precipitate. This precipitate cannot diffuse from the tissue and reflects the iron content of living tissue.

6 days-old 39Ox and WT seedlings were incubated in 1 ml fixation solution under vacuum (500 mbar) for 1.5 h. The fixation solution was removed and the seedlings were washed 3x with des. H_2O. The seedlings were the incubated with 1 ml pre-warmed (37°C) stain solution for 15 min-1 h under vacuum (checking every 15 min for the blue staining). The stain solution was removed and the seedlings were washed again 3x with H_2O. For storage, the stained seedlings were dehydrated with an EtOH dilution series 10%, 30 %, 50% and 70% (15 min each).

3.2.10 Hydrogen peroxide Assay

To detect the production of H_2O_2 in the roots of 6-day old seedlings, we used the Amplex® Red Enzyme Assays kit. The Amplex® Red reagent (10-acetyl-3, 7-dihydroxyphenoxazine) reacts stoichiometrically 1:1 with H_2O_2 (catalyzed by the horseradish peroxidase) to produce a highly fluorescent resorufin (excitation/emission maxima=570/585 nm). This method allows the detection of very low levels of H_2O_2 of around 50 nM.

The protocol used here was from Brumbarova (2016) [160]. Briefly, The roots of about 30-100 plants (WT-39Ox respectively) per replicate were cut and grinded to a fine powder. 200 µl phosphate buffer (20 mM K2HPO4, pH 6.5) per 30 mg root powder were added and the samples well mixed. The samples were centrifuged for 3 min at 13000 rpm and the supernatant transfered to PCR strips. Using the multichannel pipette, 50 µl of the sample were transfered to a 96 well UV Star plate, 50 µl working solution (two technical replicates) were added and the samples were incubated in the dark at room temperature for 30 minutes. The samples were measured at an excitation/fluorescence of 545/590 respectively.

For the analysis, the values of the controls (A), (B) and (C) were subtracted from the sample values, calculated by the mean of the technical replicates and then normalized to the volume and root weight.

3.2.11 UV detection of phenolic compounds

For the visualization of phenolic compounds, 39Ox and WT plants were directly grown of +Fe and –Fe agar medium. After 14 days they were pictured under UV light (362 nm).

For the quantification, around 30 39Ox and WT plants were grown for 10 days directly on ½ liquid Hoagland (no sugar) supplied with or without Fe. 170 µl growth medium were transferred to a half-area UV-Star and measured using the Tecan Infinite 200. The excitation and emission of phenolic compounds have their maximum between 260- 330 and 360-426 respectively [161]. An emission spectrum between 325 and 600 nm with a fixed excitation of 280 was generated. The highest emission was 400 nm. Next, an excitation spectrum between 250 and 400 was generated with a fixed emission of 400 nm. The highest excitation was 300 nm. At last, once again the emission between 360 and 500 was measured with fixed excitation of 300 nm. The data was normalized to the number of plants. It was not possible to measure the plant weight or root length because of the small size of the plants.

3.2.12 Transcriptome analysis

In this work, the CATMA v6 microarrays was been used for comparative expression analysis. This method allows the comparison of the transcriptome between two samples and yields gene expression ratios instead of absolute expression values. The CATMA v6.2 contains 30834 probes that include mitochondrial and chloroplast genes, EUGENE software predictions, repeat elements, miRNA/MIR, other RNAs (rRNA, tRNA, snRNA, soRNA), duplicates and controls.

For the analysis of the transcriptome, 4 µg of total RNA (see 3.2.6) from 6 days-old WT and 39Ox seedlings grown at 50 µM iron (+Fe) or 0 µM iron (-Fe) were processed by Stephanie Pateyron and José Caius at The Transcriptomic Platform at INRA/CNRS - URGV, Evry, France. cDNA synthesis, microarray hybridization, readout and data normalization have been performed according to their protocols. Validation of the results was performed via RT-qPCR with the same RNA (see 3.2.6).

For the Table 17, the differentially regulated genes in 39Ox +Fe vs. WT +Fe and 39Ox -Fe vs. WT –Fe were compared to the robust Fe-regulated genes from [162] (without considering the fold change). For Figure 21, the up and downregulated genes in 39Ox +Fe vs. WT +Fe and 39Ox –Fe

vs. WT –Fe were compared in a Venn Diagram (Venny 2.1 online tool) to find the genes differentially regulated irrespectively of the iron supply in the growth medium. These 485 upregulated and 321 downregulated genes were then compared to the robust Fe-deficiency regulated genes from [162]. The 397 upregulated and 298 downregulated genes that were not Fe-deficiency regulated were used for the analysis with the microarray data from *3xbhlh* [89]. The 19 contrary regulated genes in 39Ox vs. WT +/-Fe (downregulated) and *3xbhlh* (upregulated) were used for the generation of a co-expression network (with the tool ATTED II).

GO analysis of the data of 39Ox +Fe vs. WT at +Fe (Figure 26 and Figure 29) was performed with VirtualPlant and then represented with the REVIGO tool [163]. For the Table 20, genes from five different expression data of plants treated with different stresses [164] were compared to the regulation in WT –Fe vs. WT +Fe, *fit* +Fe vs. WT +Fe, *fit* –Fe vs. WT –Fe and 39Ox +Fe vs. WT +Fe. This table serves only as a qualitative investigation because the data are from different experiments. For each gene in each line, the percentages of the frequency in the five different stresses were calculated. Genes that were not differentially regulated in one of the stresses were not taken in account for the calculation. For the Figure 30, the differentially regulated genes in 39Ox +Fe vs. WT +Fe were compared to the up and down regulated genes of plants treated with *P. simiae* WCS417 [152].

3.2.13 Chromatin immunoprecipitation (ChIP)

This method consists in the detection of specific DNA, which is associated with specific proteins. These proteins can be, for instance, transcription factors or histone proteins. The detection of this DNA is important to determine direct target genes of certain transcription factors, or histone interaction for chromatin structure modifications [165]. The protocol used in this work was taken from Kaufmann et al. (2010) [166] with some changes. A schematic overview of the method is shown in Figure 11.

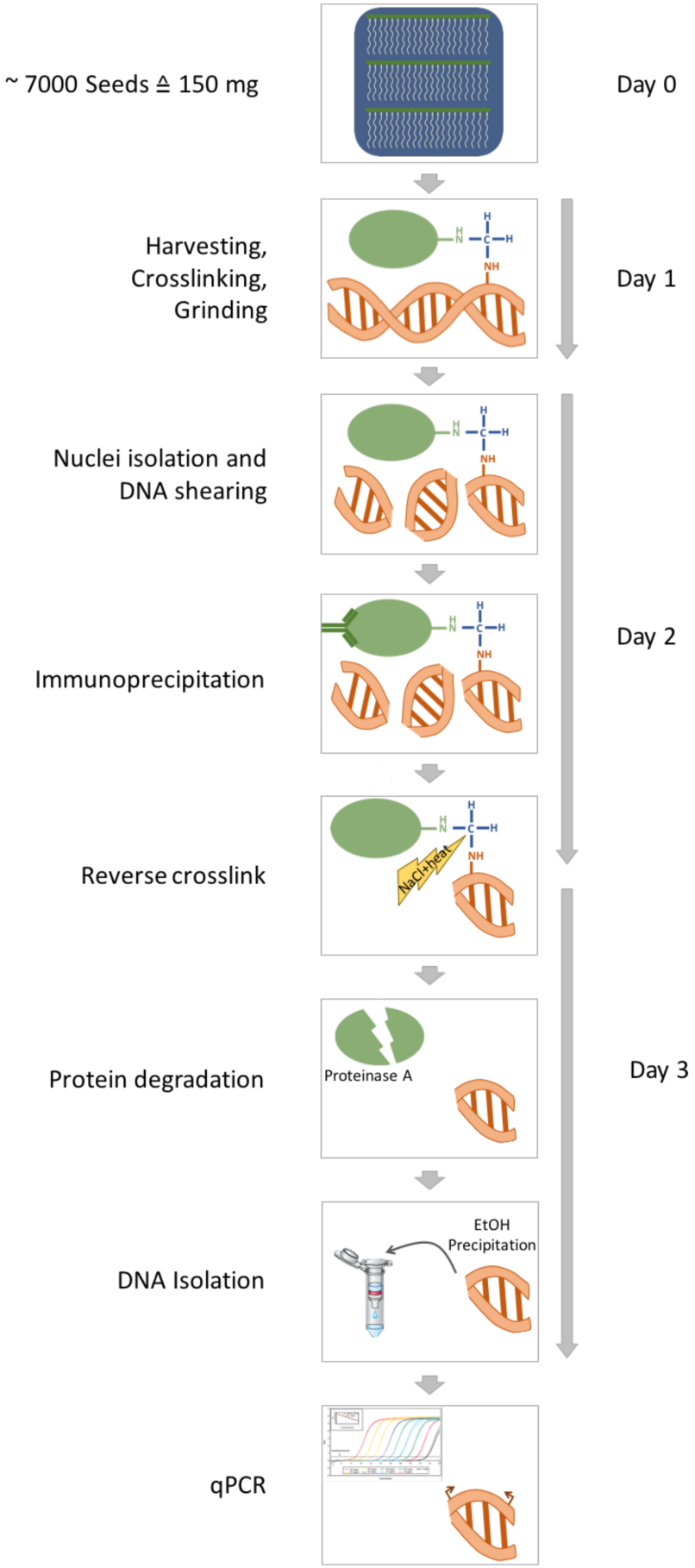

Figure 11: Schematic representation of the ChIP. Around 5000 39Ox seeds (100 mg) were sown on +Fe plates and grown for 14 days. The plant material is first crosslinked, then the nuclei are isolated and the chromatin sheared. With antibodies against the specific protein, the protein-DNA complex is imunoprecipitated. The protein-DNA complex is destroyed by high NaCl concentration and incubation overnight at 65°C. The proteins are then removed and the DNA precipitated with EtOH/NaAc/Glycogen for 2h by -80°C. For an especially clean DNA the samples are then purified with a DNA purification kit and eluted with 30 µl. The ChIP-DNA serves as a templated for qPCR analysis with specific primers against the protein target-DNA.

Protocol

Day 1: Harvesting, crosslinking, grinding.

Around 5000 (~100 mg) 39Ox seeds were sown close together on Hoagland agar plates with iron supply and grown for 14 days. The roots (0.9 g) and the shoots (4.5 g) were harvested separately in ~ 23.5 ml cold MC buffer. The harvesting took no longer than 40 min (avoiding degradation).

1.5 ml of 16% formaldehyde were added to the samples to a final concentration of 1%. The tissue was crosslinked under vacuum (~20 mbar) for 2x10 min. To stop the crosslinking, 2.5 ml glycine stock solution were added and vacuum was applied for 2 more minutes.

The tissue was rinsed three times with each 25 ml MC buffer and subsequently dried in paper towels (it is important to get out as much water as possible).

The tissue was shock frozen in liquid nitrogen and grinded with a mortar to a fine powder. It was then transfer to a new 50 ml tube and stored at -80 °C.

Day 2: Lysis and nuclei isolation, chromatin shearing, immunoprecipitation, reverse crosslinking.

All solutions were kept on ice. 20 ml of M1 buffer were added to the tissue powder. Then, it was filtered through two layers of miracloth using a funnel into a new 50 ml tube. The previous tube was rinsed with additional 5 ml M1 buffer to collect all the nuclei. The filtrate was centrifuged 20 min at 1000 G and 4°C.

The pellet was washed five times with 5 ml M2 buffer by centrifuging 10 min at 4°C and 1000 g between washes (no shaking or vortexing). Then the pellet was washed once with M3 buffer.

After the washes, the pellet was resuspended in 1 ml MC puffer. The 1 ml sample was distributed in three 1.5 ml tubes.

Using the Bioruptor® of Diagenode the samples were sonicated three times 5 min (cooling the water bath with some ice after every cycle). All the fractions were merged again to a one sample in 1.5 ml tubes.

The sample was centrifuged at top speed for 10 min at 4°C and the supernatant was transferred to a 2 ml tube. The centrifugation was repeated twice more.

Using the pipette, the total volume of the sample was determined and diluted with equal amounts of IP buffer. 1:20 of the total volume was taken as an Input DNA and checked for sonication efficiency (see later).

For each sample (IgG control and HA-sample) 160 µl protein-A agarose beads were transferred to a 1.5 ml low-adhesion tube and washed twice with 1 ml IP buffer (spin at 3.8000 g for 3 min). The beads were resuspended with IP buffer in the initial volume (+50 µl).

80 µl of the beads were added to the sample and incubated for 1h at 4°C on a rotating wheel. Subsequently the samples were centrifuged at 3.8000 g for 5 min at 4°C.

The supernatant was carefully transferred to a new 2 ml tube and spun again at 4°C for 10 min at maximum speed.

The sample was divided in two equal parts into two 1.5 ml low-adhesion tubes. One served as the non-specific antibody (IgG) and the other for the anti HA-antibody (specific).

3 µl antibody (~4 µg) antibody (IgG or anti HA) was added to each sample and incubated for 2h. Then the samples were centrifuged at 160000 g for 5 min at 4°C and the supernatant was transferred to a new 1.5 ml tube.

40 µl of the washed beads were added to the each sample and incubated for 1h at 4°C on a rotating wheel.

The samples were centrifuged for 5 min at 3800 g at 4°C. The supernatant was removed and discarded without disturbing the beads pellet.

The beads were washed five times with 1 ml IP buffer for 8 min on a rotating wheel at room temperature. Between the washes, the beads were pelleted by 2 min centrifugation at 3800 g at room temperature.

The protein-DNA complex was eluted from the beads by adding 100 µl cold elution buffer and incubated 5 min at 37°C and 1 min additionally with vigorous shaking. The elution was repeated twice and 50 µl of 1M Tris pH 9 were added after every elution (end volume 450 µl per sample) to neutralize the solution.

The samples were centrifuged and transferred to a new 2 ml tube to remove the remaining beads.

The Input DNA was filled up to 450 µl with TE buffer. 20 µl of a 5 M NaCl stock solution were added to the samples and Input DNA and incubated overnight at 65°C.

Day 3: DNA precipitation, DNA isolation, qPCR.

56.25 µl of a 4 mg/ml Proteinase K stock solution were added to the samples and Input DNA. Then the samples were incubated 1h at 65°C.

The DNA was precipitated by adding 2.5 vol of 100% ethanol, 1/10 vol 3M NaAC and 1 µl glycogen and incubated 2h at -80°C.

The samples were centrifuged for 30 min at maximum speed at 4°C. The supernatant was removed and resuspended in 100 µl miliQ water after the DNA was dried.

The DNA was further purified using Qiagen PCR purification columns and eluted with 35 µl (low adhesion tubes).

The DNA of the samples were diluted 1:10 and the DNA of the Input 1:100. 10 µl of diluted DNA was used for qPCR. The program used was the same as in 3.2.6 (Quantitative Real-Time PCR). However, the first denaturation was extended to 7 min and the annealing temperature adjusted to 52°C. Additionally, the primer concentration was increased from 0.15 µM to 0.5 µM end concentration.

3.2.13.1 Primer design for ChIP

Transcription factors bind to specific DNA motives on the promoter region. bHLH TF bind to the E-boxes (5'-CANNTG-3') and the palindromic G-boxes (5'-CACGTG-3') [67]. First, the E- and G-boxes have to be determined. The primers for the qPCR were designed surrounding these regions and they yielded a fragment of around 50-80 bp.
Figure 12 shows a schematic representation of the promoters of interest (PI) *FIT, FRO2, IRT1, At3g12900, At3g07720 and At3g58810* 2000 bp upstream from the start codon. Below every representation are found the qPCR products with the corresponding E- and G-boxes.
Additionally, the amplification of a negative control gene is necessary for the calculation. Here were used primers for the genomic sequence of the elongation factor Ef1Balpha2 (Efg), which is not supposed to be targeted of the investigated protein.

Moreover, both the target and the control gene regions were verified in the sample with the HA-antibodies and in the control sample with IgG-antibodies.

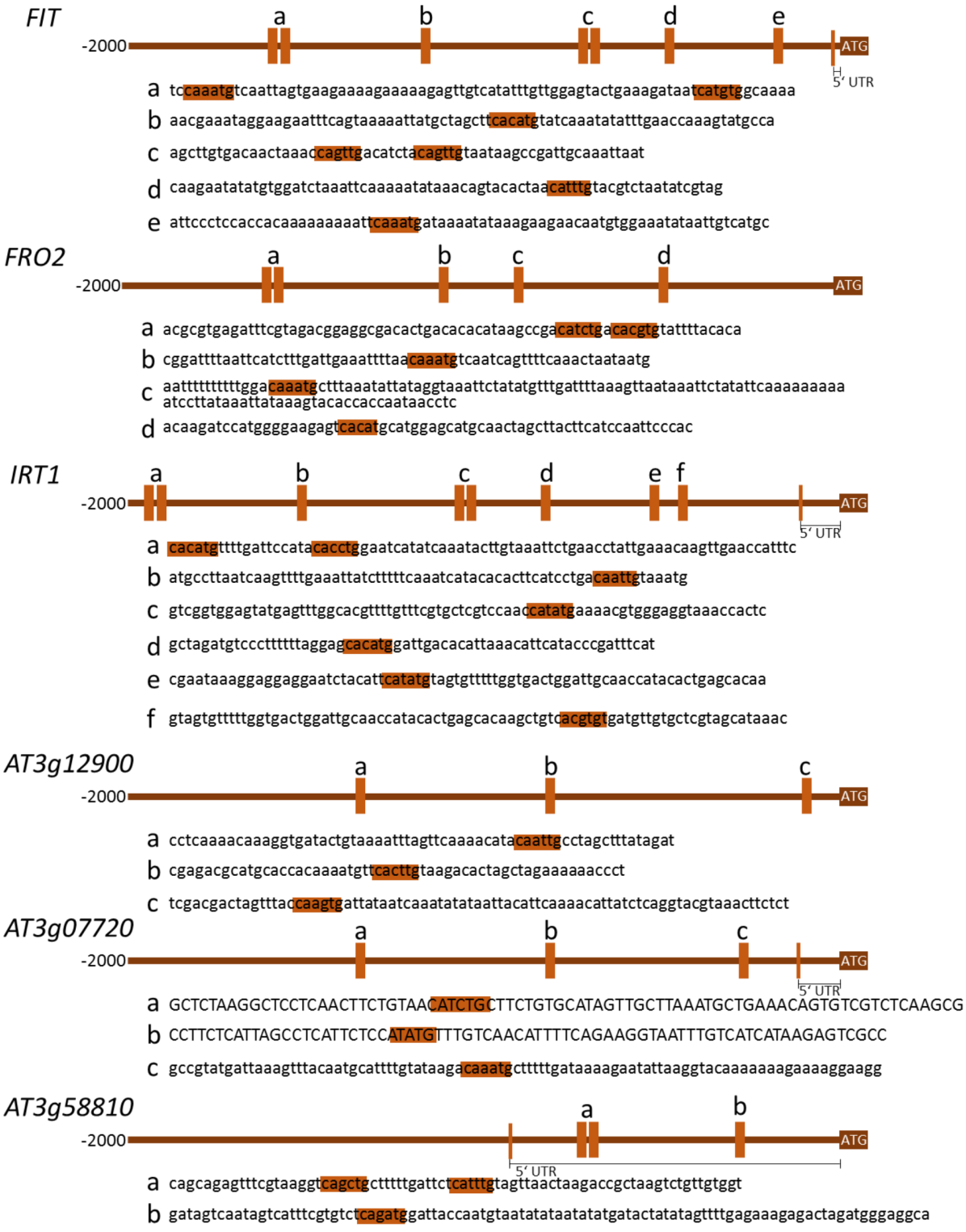

Figure 12: Promoter region of *FIT, FRO2, IRT1, At3g12900, At3g07720 and At3g58810*. The dark orange line represents 2000 bp upstream from start codon. Light orange perpendicular lines are the E- and G-boxes with the corresponding identifier (a-f). Below every promoter are the sequences of the qPCR product. Capital letters in the fragments mean coding sequences (of the adjacent gene) and small letters represent non-coding sequences. The UTR regions are marked with a thin orange line.

3.2.13.2 Analysis of ChIP-qPCR

The analysis was performed using the ΔΔCt method. To this end, the Ct values of the Efg control gene was subtracted from the Ct of each specific promoter of interest (PI). This correspond to the ΔCt value. Subsequently, the ΔCt of the anti-HA sample was subtracted from the ΔCt value of the IgG-sample, which correspond to the ΔΔCt value. The negative ΔΔCt value was set to the power of 2 (primer efficiency). The last value is the ChIP fold enrichment (example in Table 16). The ChIP fold enrichment of all the PIs were represented in a bar diagram (see 4.3). It is important to compare the Ct value of all PIs from the Input to ensure that the primers worked well. They should have a difference of no more than +/- 2 cycle.

Table 16: Calculation of the $2^{-\Delta\Delta Ct}$. First, the Ct values of PI and Efg are subtracted (ΔCt). The ΔCt values of the HA-sample and the IgG-control are subtracted as well (ΔΔCt). The fold enrichment is calculated by the 2 to the power of –ΔΔCt. PI= Promoter of interest, HA= Hemagglutinin tag, Ef= Elongation factor

	Ct	ΔCt $Ct_{PI} - Ct_{Efg}$	ΔΔCt $\Delta Ct_{HA} - \Delta Ct_{IgG}$	$2^{-\Delta\Delta Ct}$ Fold enrichment
HA-PI	31	31-34 = -3	-3-(-1) = -2	$2^{-(-2)} = \underline{4}$
HA-Ef	34			
IgG-PI	35	35-36 = -1		
IgG-Ef	36			

3.2.14 Inoculation of 39Ox and WT plants with *Pseudomonas syringae* pv. maculicola

This experiment was performed in the lab of Prof. Dr. Jürgen Zeier (Düsseldorf University). 39Ox and WT plants were grown for 6 weeks on mixture of soil, vermiculite and sand (3:1:1) with a 9h day/15h night with 70µmol$m^{-2}s^{-1}$ light intensity. Three leaves of 6 Plants in three biological replicates (18 plants per biological replicate) were inoculated with *Pseudomonas syringae* pv. maculicola of the strain ES4326 (*Psm*). This strain contains a photorhabdus luminescens luxCDABE operon under the control of a constitutive kanamycin promoter, which allows the monitoring of the bacterial vitality. The bacteria were grown overnight in Kings B medium containing the appropriate antibiotics. The culture was pelleted and washed three times with 10 mM $MgCl_2$ solution and diluted to a 0.01 OD for inoculation. Using a needleless syringe the bacterial and a $MgCl_2$ solution (mock control) were pressure-infiltrated to the abaxial side of the leaves (Prof. Jürgen Zeier, unpublished, [167]). After 2 days of inoculation, a leave disc was punched out and using the Sirius L Tube Luminometer the fluorescence was measured. The background (mock treatment) was subtracted and normalized to the surface of the leave disc. Then the mean of the 6 biological and the tree leaves was calculated and represented in a bar diagram. The vitality of the bacteria is inversely proportional to the resistance of the plant.

4 Results

4.1 The iron-uptake regulation in 39Ox plants

Stable transgenic lines overexpressing the transcription factor bHLH039 were previously generated in our group by cloning the genomic BHLH039 gene behind the 2xCAMV35S promotor and tagged with 3xhemagglutinin (HA) [156]. Four independent lines were selected, which showed stronger activation of the Fe-deficiency responses than the WT at +Fe conditions [156]. This was a promising line for further investigation of the regulation of the iron homeostasis. The line JM78-5 was then selected for further physiological and molecular analysis with 6 days-old 39Ox seedling. This line was named 39Ox.

Root length and reductase activity were investigated. As expected, the 6 days-old 39Ox seedlings showed significantly shorter roots at both +Fe and –Fe compared to the WT (Figure 13 A, B). The Fe reductase activity in the WT increased when grown on iron deficient media (Figure 13 C, D). In 39Ox seedlings, the activity was eightfold higher at +Fe compared to the WT. However, at –Fe the reductase activity of 39Ox seedlings was comparable to that of WT (Figure 13 C, D).

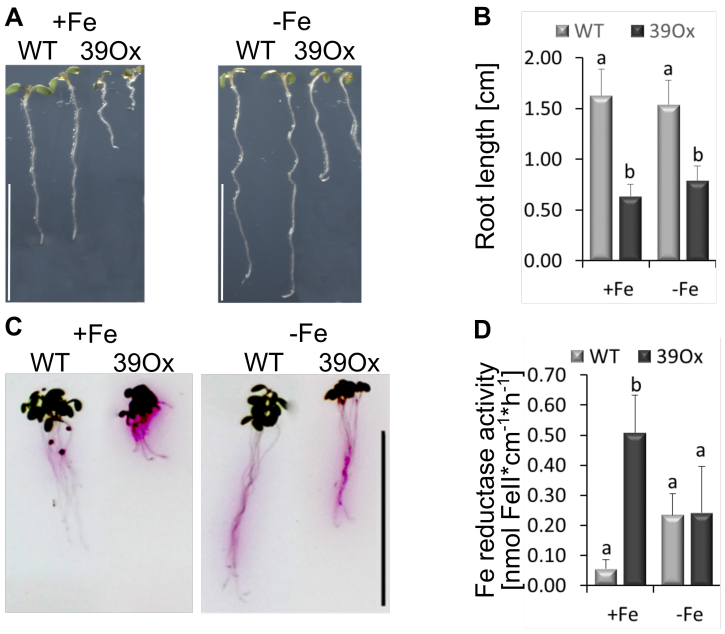

Figure 13: Phenotype of 39Ox plants compared to the WT. Plants were grown for 6 days in Hoagland agar plates at +Fe and -Fe media. The statistical significance was calculated with the Anova test and Tukey correction. Different letters indicate statistically significant differences ($p < 0.05$). (A) The plants were pictured and (B) the root length was determined using Jmicrovision (n=20). (C) Qualitative Fe reductase activity of all five plants on agar plates. (D) Quantification of the iron reductase activity (n=4).

We know that 39Ox shoots and roots contain high amounts of Fe [156]. Hence, the iron in these plants was visualized using the Pearl stain. Figure 14 shows the distribution of iron in 6 days-old 39Ox (A) and WT (B) seedlings grown at +Fe conditions. In WT seedlings, Fe accumulates only in

the upper part of the root; the content in the rest of the root is probably too low for the detection. In 39Ox seedlings, the iron accumulates along the whole root and in substantially higher amounts. In the cotyledons of the WT, the Fe is poorly visible whereas in those of 39Ox, it formed a strong dark coloration, which confirms the high Fe content shown before.

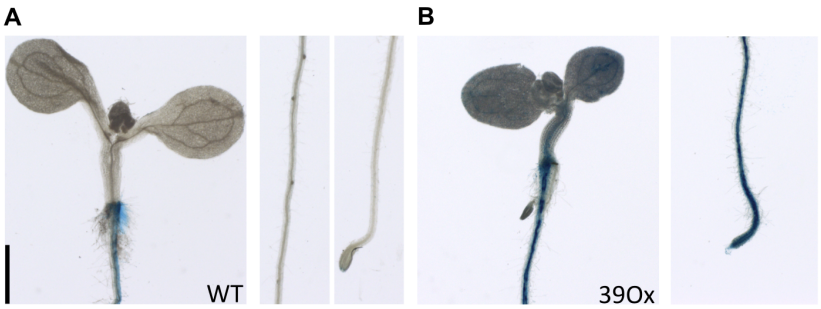

Figure 14: Perl's Prussian blue stain for the localization of Fe in 39Ox seedlings. 6 days-old seedlings were grown at +Fe conditions. The plants were incubated for 1.5h under vacuum (500mbar) in 1ml fixation solution. Subsequently, the seedlings were washed and incubated in 1 ml pre-warmed stain solution for 30 min under vacuum. Finally, the seedlings were dehydrated with an ethanol dilution series.

These analyses showed increased iron content and physiological response of 39Ox seedlings to iron deficiency. Next, the gene expression of the Fe-uptake genes was verified. In the WT, the gene expression of the master regulator (*FIT),* the Fe transporter (*IRT1*) the Fe reductase (*FRO2*) and the *BHLH039* were typically increased at –Fe conditions compared to +Fe conditions. However, Fe-deficiency did not affect the expression of these genes in 39Ox seedlings. By comparing the expression in the two lines, it is clearly visible that all these genes are strong upregulated at +Fe and –Fe in 39Ox seedling. Nevertheless, the levels at –Fe in both lines are more or less the same (Figure 15).

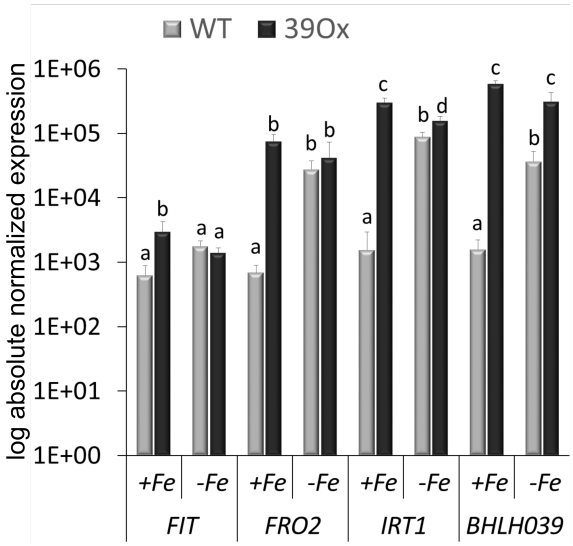

Figure 15: Gene expression analysis of iron marker genes in WT and 39Ox seedlings. Seeds were germinated and grown for 6 days directly on +Fe of -Fe Hoagland medium. Whole seedlings were harvested and processed for RT-qPCR. The statistical significance was calculated with the Anova test and Tukey correction. Different letters indicate statistically significant differences ($p < 0.05$, n=3)

Fe is a necessary element for the surviving of the organisms. However, when it over accumulates, it can trigger oxidative stress causing damages in tissues [124-126]. Roots and cotyledons of 39Ox seedlings contain high amounts of iron that most probably leads to a high production of reactive oxygen species. Fe is able to catalyze the production of hydroxyl radicals in a two steps reaction called the Haber–Weiss reaction. Fe^{3+} first oxidizes the superoxide anion to oxygen and is reduced itself to Fe^{2+}. Then, Fe^{2+} is oxidized back to Fe^{3+} in a Fenton reaction, which catalyzes the split of H_2O_2 and the formation of a hydroxyl radical and a hydroxide ion [124-126].

39Ox plants showed indeed indication of an oxidative stress. Figure 16 A shows clearly the violet coloration (black arrowheads) of the 39Ox hypocotyl at both +Fe and –Fe while in the WT this coloration is almost not visible. Violet coloration is a sight of high anthocyanin content. Anthocyanin accumulates in plants exposed to environmental stress such as high light, drought, high metals etc. Quantification of the anthocyanin content in 39Ox and WT seedlings showed almost threefold higher content in 39Ox seedlings grown at +Fe. WT seedlings grown at +Fe and –Fe as well as 39Ox grown at –Fe had lower levels of anthocyanin (Figure 16 B). These indications were confirmed by the measurement of the hydrogen peroxide H_2O_2 content in 39Ox and WT seedlings. The H_2O_2 concentration sank in 39Ox and WT seedlings grown in –Fe media compared to +Fe. However, 39Ox seedlings showed around twofold and fivefold more H_2O_2 at +Fe and –Fe respectively, compared to the WT (Figure 16 C).

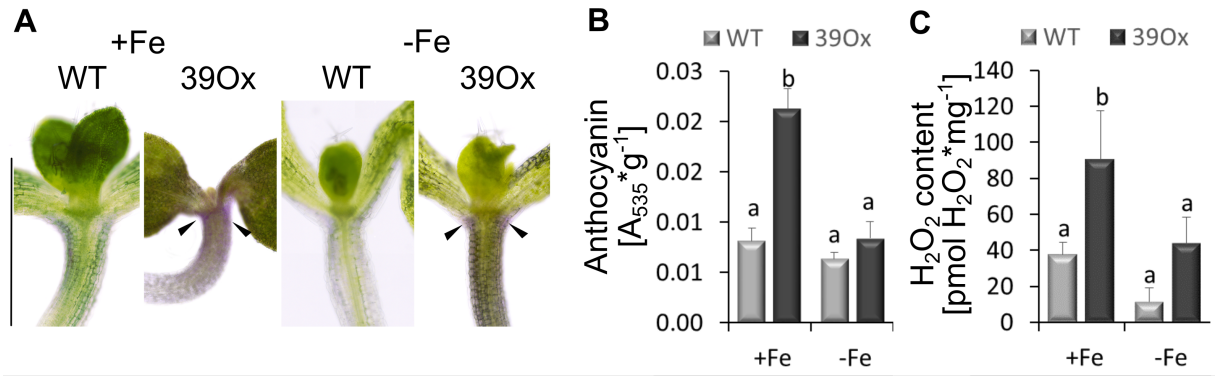

Figure 16: Anthocyanin and hydrogen peroxide content in 39Ox and WT seedlings. Seeds were sterilized and grown for 6 days directly at +Fe or –Fe on Hoagland agar plates. (A) Localization of the anthocyanin in the hypocotyl (Bar = 1 mm). (B) Photometric measurement of the anthocyanin content. (C) Hydrogen peroxide content in seedlings. The statistical significance was calculated with the Anova test and Tukey correction. Different letters indicate statistically significant differences ($p < 0.05$, n=3)

Previous works [82] showed that the overexpression of the single *BHLH038* and *BHLH039* did not show similar phenotype and physiological response as 39Ox plants from our lab. The reason might be that DNA is present either as tightly or as lightly packed chromatin and is called heterochromatin and euchromatin respectively. In heterochromatin, DNA is hardly accessible and an insert located there could be silenced. On the other hand, when the insert is in the transcription active euchromatin, the expression of this gene might be stronger. The *BHLH039* insert is located near to the *GIP1* genes, which encodes a small (71 amino acids) gamma-tubulin complex protein. It is constitutively expressed and is involved in gamma-tubulin complex localization, spindle stability and chromosomal segregation. *GIP1* shares 72% homology with the *GIP2* gene. Single mutants of this GIPs showed the same phenotype as the WT, suggesting a functional redundancy [168]. We can conclude that the insertion of *2xCAMV35S::HA$_3$-gBHLH039* has no impact on the spindle stability. Additionally, one can say that *GIP1* counts as a housekeeping gene and the chromatin in this region is probably very accessible for transcription. This might be the reason why 39Ox plants showed this kind of phenotype, and physiological response compared to the overexpressed *BHLH039* of other works [82].

Taken together, these experiments confirmed that the Fe-uptake in 6 days-old seedlings was strongly activated at the gene expression and physiological level causing high Fe accumulation in shoots and roots. This high Fe accumulation leads to oxidative stress in 39Ox seedlings, which is displayed in the violet coloration of anthocyanin.

4.1.1 The overexpression of bHLH039 has no impact without FIT

The appropriate Fe-uptake regulation is of great importance for plants. The interplay of transcriptions factors, protein regulation and gene expression is crucial for the proper regulation. FIT is the master regulator of the iron uptake. It interacts with the four bHLH proteins of the subgroup Ib to activate the gene expression of *IRT1* and *FRO2* [82]. *FIT* is expressed in lower amounts compared to its interactors and its downstream genes. On the one hand, the absence of FIT in the *fit* mutants leads to chlorosis and lethality [80]. On the other hand, its overexpression alone does not lead to an intensification of the Fe-uptake [80, 82]. As shown before, the overexpression of bHLH039 leads to the activation of the iron uptake genes *FIT, IRT1* and *FRO2* at Fe sufficient conditions. To verify whether bHLH039 is able to activate these genes without

the presence of FIT, 39Ox plants were crossed with *fit* mutant plants. 39Ox plants carrying this mutation in the background had the same phenotype as *fit* mutants. They were chlorotic (Figure 17 A), had longer roots (Figure 17 B) and the Fe reductase activity was reduced (Figure 17 C) compared to single 39Ox seedlings.

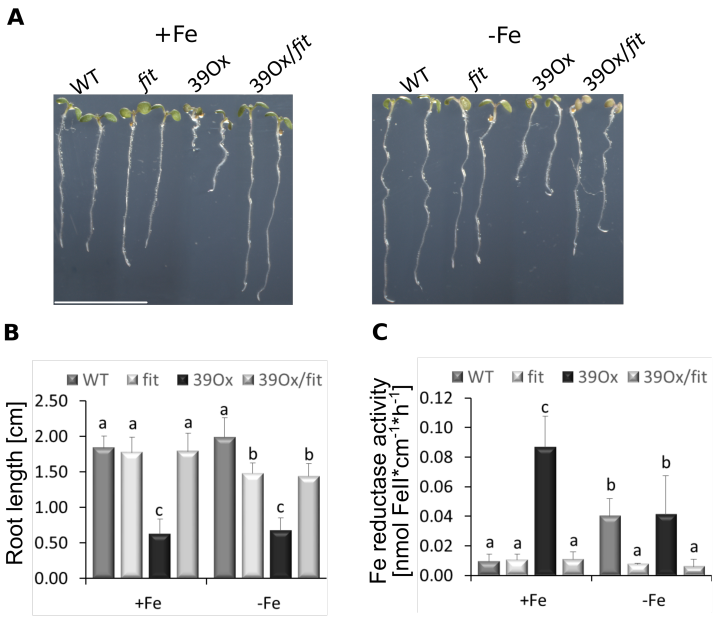

Figure 17: Physiological analysis of WT, *fit-3* 39Ox/*fit* and 39Ox plants. Plants were grown for 6 days in Hoagland agar plates at +Fe or –Fe. (A) The plants were pictured and (B) the root length was determined using Jmicrovision (n=20). (C) Iron reductase activity (n=4). The statistical significance was calculated with the Anova test and Tukey correction. Different letters indicate statistically significant differences ($p < 0.05$)

In 39Ox/*fit* seedlings, the genes *FIT*, *FRO2* and *IRT1* had the same response as *fit,* even though bHLH039 is expressed just as in 39Ox. This means that these genes were not upregulated upon Fe deficiency and the gene expression level were significantly lower compared to the WT and 39Ox (**Figure 18** A). We were concerned if the bHLH039 protein stability was affected by the absence of FIT. Therefore, we verified by immunoblot whether the protein amount in 39Ox/*fit* is reduced compared to 39Ox. Figure 18 B and C shows that in 39Ox plant the protein amount did not change under +Fe nor –Fe condition. The same occurred by 39Ox/*fit* seedlings. The bHLH039 protein stability was not affected either by the *fit* background. These results suggest that 39Ox phenotype is dependent of the FIT protein activity.

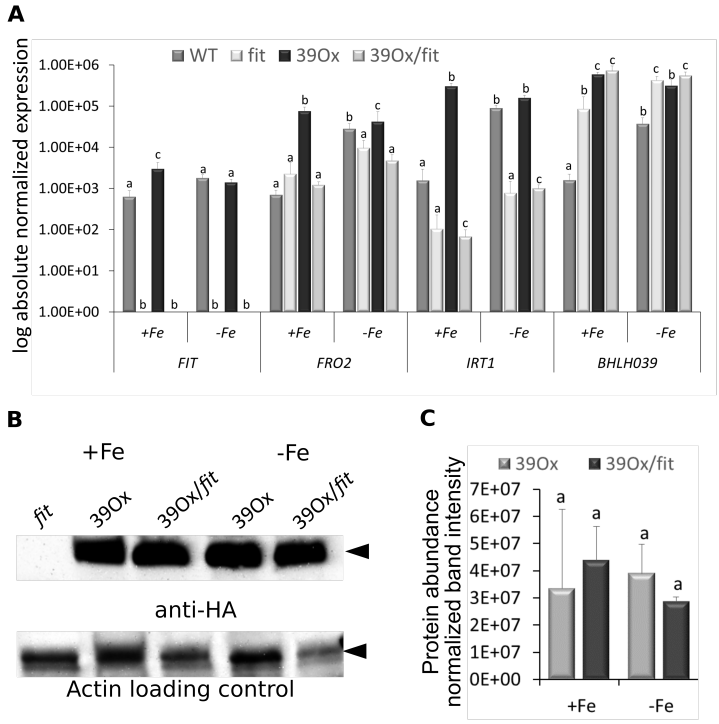

Figure 18: Gene expression and protein analysis of WT, 39Ox and 39Ox/*fit* seedlings. Seeds were germinated and grown for 6 days directly on +Fe of -Fe Hoagland medium. Whole seedlings were harvested and processed for (A) RT-qPCR of *FIT*, *FRO2*, *IRT1* and *BHLH039*. (B) Immunoblot with anti-HA antibodies and anti-Actin for the background control. Arrowheads indicate the HA_3-bHLH039 (36 kDa) and actin (45 kDa) protein (C) Quantification of the bands from the immunoblot in (B). The statistical significance was calculated with the Anova test and Tukey correction. Different letters indicate statistically significant differences ($p < 0.05$, n=3)

Yuan et al. 2008 [82] showed that the overexpression of *FIT* together with *BHLH038* or *BHLH039* leads to an enhanced expression of *IRT1* and *FRO2* as well as a Fe reductase activity. To verify whether the overexpression of *FIT* in 39Ox plants changes the iron deficiency responses compared to single 39Ox, 39Ox plants were crossed with HA_3-FIT and HA_7-FIT plants from Meiser et al. 2011 [105]. HA_3-FIT plants showed a substantially lower *FIT*, *IRT1* and *FRO2* gene expression as HA_7-FIT plants at +Fe and at -Fe [169]. This is because the HA_3-FIT insertion might be located in an inactive DNA region. On the other hand, the HA_7-FIT insert is located upstream of the TRICHOME BIREFRINGENCE-LIKE 14 (*TBL14, AT5G64020*). This protein belongs to the TBL gene family that is involved in the biosynthesis of cellulose, thus it is probably expressed constantly. Since the insert with the construct *2xCAMV35S::HA_7-FIT* is directly behind these genes, it is most likely more strongly expressed.

The overexpression of *HA_3-FIT* in 39Ox plants (39Ox/HA_3-FIT) caused different phenotype, physiological response and gene expression compared to the single 39Ox and HA_3-FIT plants. Compared to 39Ox plants, they showed longer roots (Figure 19 A, B), slight (but not statistical significant) reduction of the Fe reductase activity (Figure 19 C) and *IRT1* and *FRO2* gene expression (Figure 19 D) at +Fe and at –Fe. On the other hand, these responses are enhanced compared to the WT and single HA_3-FIT.

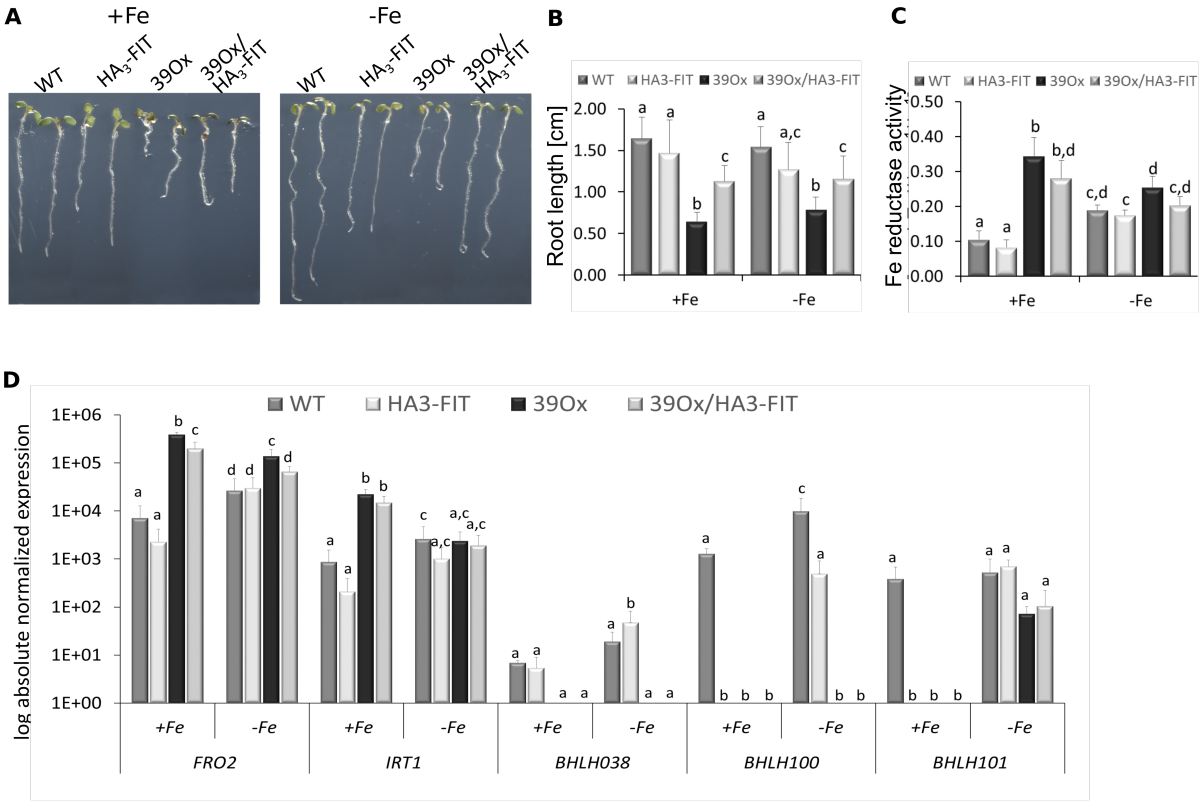

Figure 19: Genetic and physiological analysis of 39Ox/HA$_3$-FIT, 39Ox, HA$_3$-FIT and WT plants. Plants were grown for 6 days in Hoagland agar plates at +Fe or –Fe. (A) The plants were pictured and (B) the root length was determined using Jmicrovision (n=20). (C) Iron reductase activity (n=4). (D) Gene expression of FIT, FRO2 and IRT1 (n=3). The statistical significance was calculated with the Anova test and Tukey correction. Different letters indicate statistically significant differences ($p < 0.05$)

Furthermore, the crossing 39Ox/HA$_7$-FIT showed a lethal phenotype at both +Fe and –Fe conditions. It was not possible to grow the plants for further physiological and molecular investigations. Attempts to rescue the plants by adding less iron or Ferrozin were not successful either (not shown). These plants might be intoxicated to such extent that they are not able to survive.

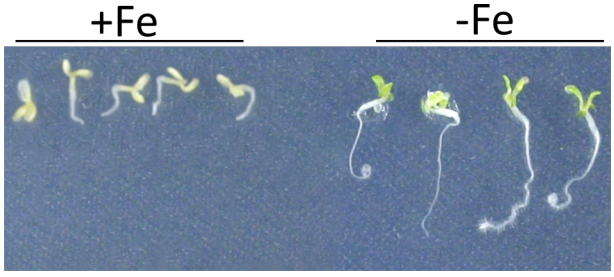

Figure 20: Crossing of 39Ox plants with the strong overexpressing HA$_7$-FIT line. Plants were grown for 14 days on agar medium with and without Fe. The plants germinated but were not able to survive.

These results showed that, without FIT, the iron uptake was not switched on, although bHLH039 is excessively expressed. Consequently, the plants suffered on iron deficiency as *fit* plants did. The moderated overexpression of FIT did not lead to any enhancing of the iron deficiency response compared to the single 39Ox. This could mean that the amount of FIT in 39Ox plants is

sufficient in these responses. On the other hand, strong overexpression of *FIT* in 39Ox plants probably activates and stabilizes the iron uptake to such an extent that IRT1 protein uptakes high amounts of other metals. It is known that IRT1 is a divalent metal transporter as well as a heavy metal transporter and is able to uptake metals such as zinc, manganese, cobalt, and cadmium [170]. In this case, the plants would be poisoned with the amount of toxic metals and are not able to develop normally.

4.2 Transcriptome analysis of 39Ox seedlings.

4.2.1 FIT- and Fe-dependent response in 39Ox seedling

bHLH039 is a FIT-independent Fe-deficiency responsive gene [86]. It is co-regulated together with other FIT-independent genes such as *PYE, BTS,* and *NAS4* [90-92]. To observe eventual changes in this co-regulatory network by the overexpression of bHLH039, a complete *Arabidopsis* Transcriptome MicroArray v6 (CATMA) analysis was performed. This method was chosen due to the direct comparison of the gene expression between too samples, here 39Ox vs. WT, which yields ratios between the two samples and no absolute values. The plant material selected was 6 days-old seedlings grown directly at +Fe and –Fe because several microarrays were available with this grow conditions [89, 162].

A total of 3745 genes were differentially regulated compared to the WT at +Fe conditions. From those, 1959 were upregulated and 1786 downregulated. At –Fe conditions 1466 were regulated, 814 were upregulated and 652 downregulated. Previous studies defined 34 robust FIT-regulated genes [79, 162]. 32 of these genes appeared to be positively (red cells) regulated by FIT and two negatively (green cells) regulated. These robust FIT-regulated genes were regulated in a similar manner in 39Ox plants compared to WT at +Fe and -Fe conditions (Table 17).

Table 17: List of the 34 FIT-regulated genes [79, 162] in 39Ox. Comparison of the FIT-regulated genes with 39Ox +Fe vs. WT +Fe and 39Ox -Fe vs. WT –Fe.

Annotation	AGI	FIT-Regulated	39Ox +Fe vs. WT +Fe	39Ox -Fe vs. WT -Fe
FERRIC REDUCTION OXIDASE 2 (FRO2)	AT1G01580			
GERMIN-LIKE PROTEIN 5 (GLP5)	AT1G09560			
COBRA-LIKE PROTEIN 6 PRECURSOR (COBL6)	AT1G09790			
SCR-LIKE 28 (SCRL28)	AT1G14182			
Glucose-methanol-choline (GMC) oxidoreductase family protein	AT1G14185			
PHOSPHORIBOSYL PYROPHOSPHATE (PRPP) SYNTHASE 2 (PRS2)	AT1G32380			
GENERAL REGULATORY FACTOR 11 (GRF11)	AT1G34760			
unknown protein	AT1G53635			
unknown protein	AT1G73120			
PURPLE ACID PHOSPHATASE 7 (PAP7)	AT2G01880			
RING/U-box superfamily protein	AT2G20030			
unknown protein	AT2G35850			
unknown protein	AT3G06890			
Galactose oxidase/kelch repeat superfamily protein	AT3G07720			
2-oxoglutarate (2OG) and Fe(II)-dependent oxygenase superfamily protein	AT3G12900			
COPPER TRANSPORTER 2 (COPT2)	AT3G46900			
UDP-GLUCOSYL TRANSFERASE 72E1 (UGT72E1)	AT3G50740			
ATP-BINDING CASSETTE G37 (ABCG37)	AT3G53480			
Cation efflux family protein	AT3G58060			
METAL TOLERANCE PROTEIN A2 (MTPA2)	AT3G58810			
unknown protein	AT3G61410			
unknown protein	AT3G61930			
RING/U-box superfamily protein	AT4G09110			
SBP (S-ribonuclease binding protein) family protein	AT4G17680			
IRON REGULATED TRANSPORTER 2 (IRT2)	AT4G19680			
IRON-REGULATED TRANSPORTER 1 (IRT1)	AT4G19690			
IRON REGULATED 2 (IREG2)	AT5G03570			
Encodes a putative amino acid transporter	AT5G38820			
ZINC TRANSPORTER 8 PRECURSOR (ZIP8)	AT5G45105			
Protein of unknown function. DUF599	AT5G46060			
IAA CARBOXYLMETHYLTRANSFERASE 1 (IAMT1)	AT5G55250			
NAD(P)-linked oxidoreductase superfamily protein	AT5G62420			
ZRT/IRT-LIKE PROTEIN 2 (ZIP2)	AT5G59520			
SERINE CARBOXYPEPTIDASE-LIKE 31 (scpl31)	AT1G11080			

Some genes showed no differential expression (grey cells) or downregulation at –Fe. The reason is that the difference between the gene expression in the WT and 39Ox plants is less significant at –Fe than at +Fe. At +Fe, almost all the Fe-robust genes were regulated in the same manner. The two exceptions were *AT5G55250* and *AT5G62420*. The first gene is a carboxyl methyltransferase that is able to methylate indole-3-acetic acid (IAA) to methyl-IAA. The second gene is predicted to have oxidoreductase activity but is not well characterized. These genes are not reported to be Fe- or FIT-regulated [162]. Unfortunately, they were not further characterized and a further functionality analysis was not possible.

An analysis of arrays from 14 different iron-response experiments led to the identification of 598 robust Fe-regulated genes (437 upregulated, 161 downregulated) [162]. To identify genes that are differentially regulated in 39Ox vs. WT, irrespectively of the Fe-supply in the experimental setup, a pairwise comparison with the genes of 39Ox vs. WT at +Fe and –Fe was performed. The Venn diagram in Figure 21 shows the intersections of the differentially regulated genes in 39Ox vs. WT at +Fe and –Fe conditions. 806 genes (485 upregulated and 321 downregulated) were differentially expressed in 39Ox at both +Fe and –Fe. 44 genes were upregulated at +Fe but downregulated at –Fe and 48 genes were upregulated at –Fe and downregulated at +Fe (Figure 21).

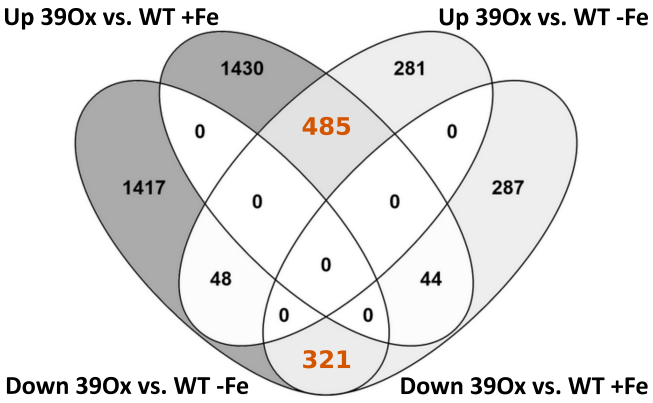

Figure 21: Venn diagram of the differentially regulated genes in 39Ox vs. WT at +Fe and –Fe conditions. Upregulated and downregulated genes of 39Ox at +Fe were compared to the –Fe. 485 genes were upregulated, 321 downregulated and 92 oppositely regulated in both Fe conditions.

As expected, among the 485 upregulated genes, were involved genes that take part in the Fe uptake into the roots such *IRT1* and *FRO2* but also genes coding for the *YSL1* and *YSL3*. Since, these two proteins are homologous to the maize phytosiderophore transporter (YS1), they are predicted to transport metal-nicotianamine complexes into cells and are induced by Fe [35, 51]. These transporters mediate the transport of Fe-NA from the vascular tissues to the seeds. Previous analysis in *ysl1ysl3* double mutant showed that the seed accumulate lower levels of Fe, Zn and Cu than WT seeds [54]. We verified whether the high expression of the *YSL1* and *YSL3* genes in 39Ox seedling led to a discrepancy in the metal content of 39Ox seeds. For that purpose, we measured the content of Fe, Zn, Mn and Cu in WT, *fit* and 39Ox seeds. *fit* mutant seeds has a lower Fe, Mn and Cu content compared to WT seeds. However, the Fe content in 39Ox seeds is twice higher than in WT seeds (Figure 22). The content of Mn, but not Zn and Cu, was slightly higher in 39Ox seeds than in WT seeds as well. These results confirm that YSL1 and YSL3 are

capable to load Fe into the seeds and that the higher expression of these genes increases the efficiency.

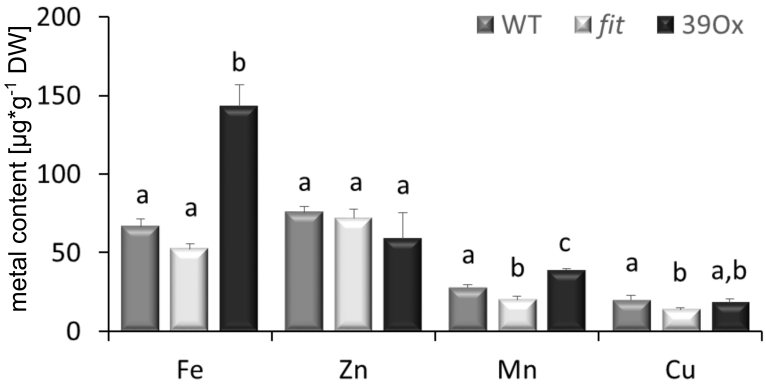

Figure 22: Metal content in WT, *fit* and 39Ox seeds. The statistical significance was calculated with the Anova test and Tukey correction. Different letters indicate statistically significant differences ($p < 0.05$, n=3).

The 806 genes (red highlighted in Figure 21) regulated in 39Ox vs. WT at +/-Fe, were used to compare to the robust Fe-deficiency regulated genes from [162]. A total of 112 robust Fe-deficiency regulated genes were regulated in 39Ox seedling. 84 of these genes were regulated in the same manner as in the WT and 28 genes oppositely. The remaining 695 genes are probably regulated due to the overexpression of *BHLH039* rather than to the iron condition. These genes were analyzed later.

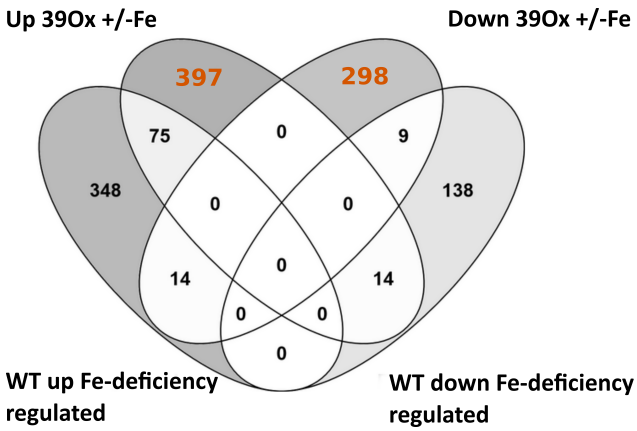

Figure 23: Venn diagram of the up and downregulated genes from Figure 21 compared to the robust Fe-deficiency up and down regulated genes. The 806 differentially regulated genes in 39Ox +/-Fe were compared to the robust Fe-deficiency regulated genes from [162]. 75 genes are upregulated, 9 genes downregulated and 28 oppositely regulated.

Among the 75 genes upregulated in 39Ox +/-Fe and in the WT, were typical Fe-deficiency response genes such as the *AT3g07720*, *MTPA2*, *IRT1*, *F6´H1* and *CYP82C4*. 14 of the genes downregulated in the WT were upregulated in 39Ox +/-Fe. These genes were *FER1*, *FER4*, *ASCORBATE PEROXIDASE1* (*APX1*), two genes involved in pathogen response (*MEE14* and *APRR5*), two genes coding for heat shock proteins (AT5G23240 and AT1G56300) and seven genes with unknown

function (Table 18 A). It is not surprising that genes for ferritin and ascorbate peroxidase were upregulated in 39Ox seedlings because the Fe content in these plants is elevated and ferritin binds the excess of Fe while the ascorbate peroxidase scavenges the hydrogen peroxide. 14 genes were downregulated in 39Ox but upregulated in the WT. Among them were included two oligopeptide transporters (*OPT3* and *AT3G01350*), the *NAS4* gene, two genes with metal binding properties (*AT5G45340* and *AT1G43800*), one gene involved in the regulation of light responses as well as eight unknown proteins (Table 18 B).

Table 18: Oppositely regulated genes in 39Ox +/-Fe and WT-Fe. (A) List of genes upregulated in 39Ox+/-Fe and downregulated in WT. (B) List of genes downregulated in 39Ox upregulated in WT-Fe.

A

Up 39Ox+/-Fe – Down WT-Fe	
AGI	**Annotation**
AT5G01600	ATFER1
AT2G40300	ATFER4
AT1G07890	APX1
AT2G15890	MEE14
AT5G24470	APRR5
AT5G23240	DNAJ heat shock protein
AT1G56300	DNAJ heat shock protein
AT3G26740	CCL (CCR-LIKE)
AT3G49160	Pyruvate kinase family protein
AT2G39920	Subfamily IIIB acid phosphatase
AT3G62550	USP family protein
AT5G40510	Unknown protein
AT5G45410	Unknown protein
AT3G10020	Unknown protein

B

Down 39Ox+/-Fe - Up WT-Fe	
AGI	**Annotation**
AT4G16370	ATOPT3 (OLIGOPEPTIDE TRANSPORTER);
AT3G01350	Oliogopeptide transport
AT1G56430	NAS4
AT5G45340	CYP707A3
AT1G43800	FLORAL TRANSITION AT THE MERISTEM1
AT3G22840	ELIP1 (EARLY LIGHT-INDUCABLE PROTEIN)
AT2G43620	Chitinase
AT4G36700	Cupin family protein
AT5G05250	Unknown protein
AT5G67370	Unknown protein
AT2G27402	Unknown protein
AT1G47400	Unknown protein
AT3G56360	Unknown protein
AT1G48300	Unknown protein

The remaining 695 (397 upregulated and 298 downregulated Figure 23) genes were used to determine direct putative genes downstream of the transcription factor bHLH039.

4.2.2 Quest of bHLH039-dependent genes

The triple mutant *3xbhlh* (*bhlh039*, *bhlh100*, *bhlh101*) expresses only one of the bHLH TF of the subgroup Ib, namely the *BHLH038*. *3xbhlh* triple mutant plants did not show any iron-deficiency phenotype when grown at +Fe conditions. However, at –Fe conditions the plants suffered stronger leaf chlorosis than the WT [89]. Microarray analysis of this triple mutant revealed that only 29 Fe-regulated genes were differentially expressed compared to the WT. 24 of these genes

were less strongly expressed than in the WT and five genes were oppositely regulated. These five genes were the genes encoding for a putative Kelch-repeat protein (At3g07720), an oxidoreductase gene (*At3g12900*), the *CYP82C4* (*At4g31940*) the MTPA2 (*At3g58810*) and the *PPC1* (*At1g53310*). [89].

The 695 genes differentially regulated in the 39Ox +/-Fe from the previous analysis (Figure 23) were then compared with the differentially regulated genes in the *3xbhlh* vs. WT at –Fe (group I and III from [89]). The 29 genes of the intersection are represented in Table 19.

Table 19: Genes differentially regulated in 39Ox and *3xbhlh* mutant seedlings. Red means upregulated, green downregulated. Genes marked with (*) cluster together in a co-regulatory network and genes marked with (**) have common GO terms.

Annotation	AGI	39Ox +/-Fe	*3xbhlh* vs. WT -Fe		
cytochrome b6f complex subunit	AT2G26500				
ATNRT2.6; nitrate transporter	AT3G45060				
QQS, QUA-QUINE STARCH	AT3G30720				
meprin and TRAF homology domain-containing protein	AT4G01390				
S-adenosyl-L-methionine:carboxyl methyltransferase family protein	AT1G15125				
unknown protein	AT1G21670				
GRP17	AT5G07530				
copper amine oxidase	AT3G43670				
unknown protein	AT5G03545				
zinc finger (B-box Type) family protein	AT5G482 50				
dynein light chain	AT4G27360				
zinc finger (B-box Type) family protein	AT4G38960			*	**
unknown protein	AT4G15430			*	
LHY (LATE ELONGATED HYPOCOTYL)	AT1G01060			*	**
Dof-Type zinc finger domain-containing protein	AT1G69570			*	**
unknown protein	AT3G54500			*	
unknown protein	AT2G37720				
RPT2 (ROOT PHOTOTROPISM 2)	AT2G30520			*	**
CCA1 (CIRCADIAN CLOCK ASSOCIATED 1)	AT2G46830			*	**
zinc finger (B-box Type) family protein	AT2G21320			*	**
STH (salt tolerance homologue), zinc ion binding	AT2G31380			*	**
THI2 (THIONIN 2); Toxin receptor binding	AT5G36910				
zinc finger (B-box Type) family protein	AT3G21890			*	**
glutaredoxin family protein	AT1G64500			*	
DNA binding , zinc ion bindig	AT4G15248				
ATTIP2; water channel	AT5G47450				
unknown protein	AT4G24700			*	
unknown protein	AT2G15020			*	
2S albumin storage protein / NWMU2-2S albumin 2	AT4G27150				

The differential regulated genes in 39Ox at +Fe and –Fe from Figure 23 were compared to the genes differentially regulated at –Fe in th3 *3xbhlh* mutant (group I and III of [89]).

The first three genes are downregulated in *3xbhlh* mutants as well as in the 39Ox. The cytochrome b6f complex (AT2G26500) and the nitrate transporter (AT3G45060) are specifically located in the chloroplast, and the QQS (AT3G30720) is found, in general, in the over ground parts

of the plant. bHLH100 and bHLH101 are probably positive regulators of these genes. The *BHLH100* and *BHLH101* genes were strongly downregulated in roots and shoots of 39Ox plants compared to the WT (Figure 24) and knocked out in the *3xbhlh* [89].

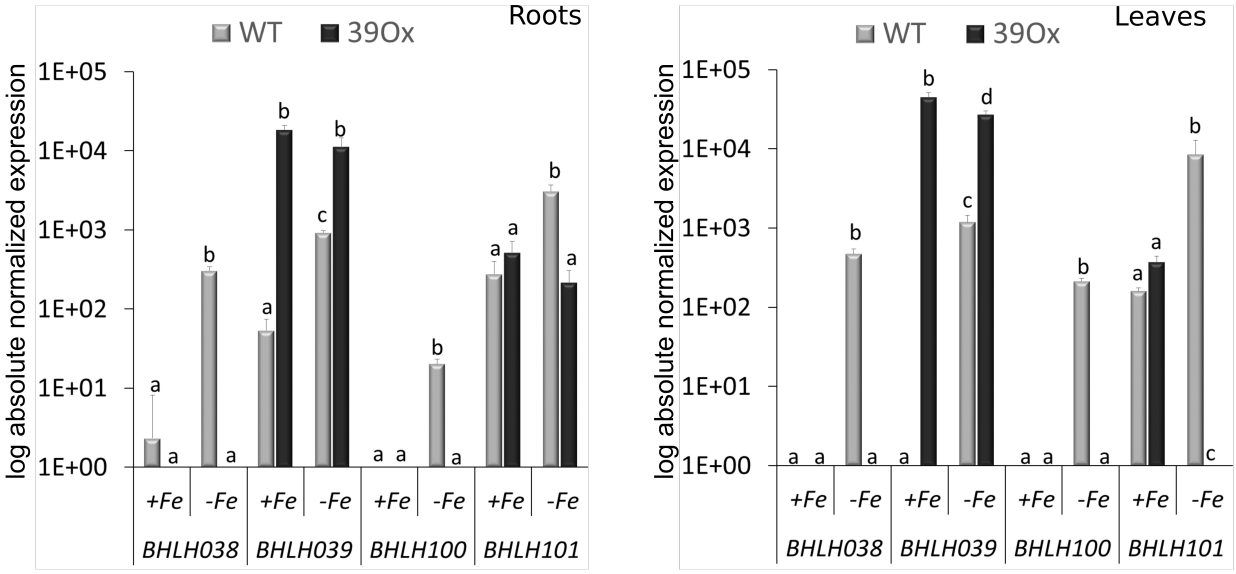

Figure 24: Gene expression analysis of the Ib subgroup bHLH TF in WT and 39Ox seedlings. Seeds were germinated and grown for 14 days on +Fe then transferred for 3 days to +Fe or -Fe Hoagland agar medium. Roots and shoots were harvested separately and processed for RT-qPCR. The statistical significance was calculated with the Anova test and Tukey correction. Different letters indicate statistically significant differences ($p < 0.05$, n=3)

Seven of the 29 genes were upregulated in the 39Ox and downregulated in the *3xbhlh.* These genes are most probably activated by bHLH039. The remaining 19 genes are downregulated in the 39Ox and upregulated in the *3xbhlh*, which means that they might be repressed by bHLH039.

The most bHLH039-repressed genes were found together in a co-regulatory network (* in Table 19). Eight of the genes of this network (** in Table 19) have common functions (GO terms), which are listed in Figure 25. There are six genes coding for transcription factors (octagon), one with transcription factor activity (STH) and one signal transduction gene (RPT2).

A

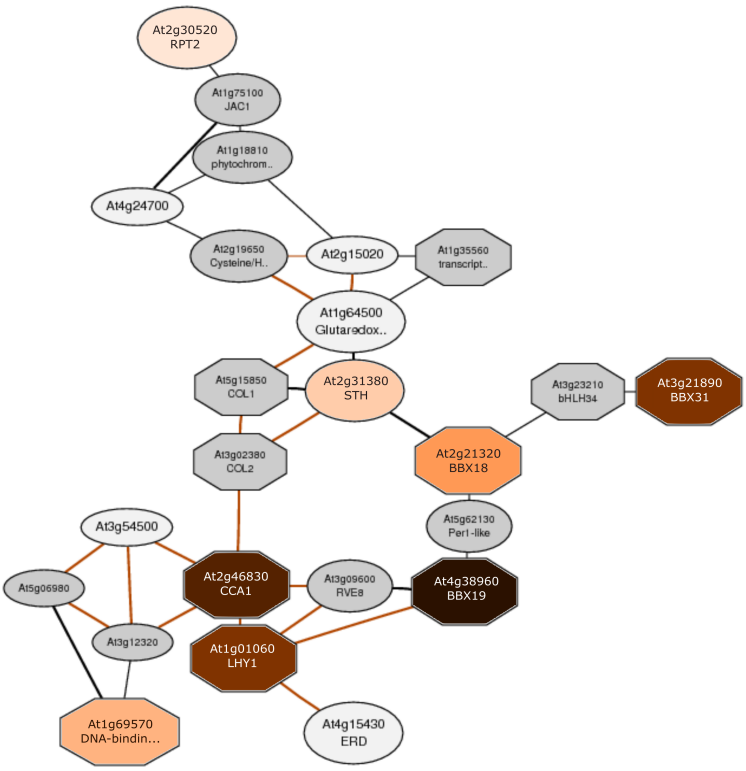

B

AGI	Gene ontology
AT2G31380	Transcription factor activity Transcription regulatory activity DNA binding Regulation of transcription
AT1G69570	
AT2G21320	
AT1G01060	
AT3G21890	
AT2G46830	
AT4G38960	
AT1G01060	Long-day photoperiodism Circadian rhythm Vegetative to reproductive phase transition
AT2G46830	
AT2G31380	Zinc ion bindig Transition metal ion bindig Zinc finger Bbox
AT1G69570	
AT2G21320	
AT4G15248	
AT3G21890	
AT4G38960	
AT2G30520	Response to light stimulus Response to radiation Response to abiotic stimulus
AT1G01060	
AT3G21890	
AT2G46830	

Figure 25: Putative bHLH039-repressed genes. (A) Co-expression network of the genes downregulated in 39Ox seedlings and upregulated in *3xbhlh* seedlings represented with the tool ATTED-II. Octahedrons are TF, light grey color means the gene was in the query and dark grey the genes were added by the tool. The different orange colors correspond to the genes listed in (B) with the corresponding GO annotations. (B) The GO was determined with the tool Virtual Plant. The different GO are listed (right) and genes from the network (left) are assigned to the GO. Each gene might have several GOs and appear more than once.

These genes formed four main groups with similar functions. In the first group are mostly TF related to the transcription activity and regulation. The second group comprises only two genes associated with the changes of rhythm and the clock. The third group consists in five zinc-finger proteins and one related with salt tolerance. The last group contains genes involved in the response to light and abiotic stimulus.

In the first and second group are the *LATE ELONGATED HYPOCOTYL* (*LHY*) and *CIRCADIAN CLOCK ASSOCIATED 1* (*CCA1*), which are redundant morning expressed Myb transcription factors. They play a very important role in the regulation of the circadian clock [171]. They bind directly to the promoter and regulate negatively the evening component so-called oscillator gene *TIMING OF CAB EXPRESSION 1* (*TOC1*) [171, 172]. In turn, TOC1 binds to the promoters of *CCA1* and *LHY* and regulates them positively, thus forming a regulatory loop mechanism [172, 173]. Studies showed that deficiency of iron, but not of any other nutrient, prolongs the circadian period of the oscillating genes. Additionally, they showed that the *irt1* and *fit1-2* mutant had longer periods, which

could be regularized with the supplementation of Fe [174, 175]. Moreover, in 39Ox plants, *TOC1* is 1.6-fold upregulated while LHY/CCA1 2.7/2.2 fold downregulated. Research also indicated that the simple overexpression of *TOC1* does not cause an upregulation of the *CCA1* and *LHY* genes [172, 173]. This would mean that bHLH039, when overexpressed, might interplay with all these three genes or proteins to change rhythm periods in seedlings.

In the third group are five genes coding for B-box type zinc finger (BBX) family proteins (*AT2G31380, AT2G21320, AT4G15248, AT3G21890*, and *AT4G38960*) and for one Dof-type zinc finger DNA-binding family protein (*AT1G69570*). Zinc finger proteins are a large family of proteins involved in many developmental processes. They are divided in three major groups depending on their ability to bind DNA, as in the case of Dof zinc-finger transcription factors, RNA like microRNA processing factors, and protein such as the B-box zinc finger proteins [176]. BBX19 (*AT4G38960*) is reported to be important for the controlling of the flowering time. Downregulation of BBX19 leads to an acceleration of the flowering in *Arabidopsis* [177]. BBX25 (*AT2G31380*) regulates the seedlings photomorphogenesis negatively and the deetiolation process positively. The other four genes are not well described but they are also related to phototropism, flowering and circadian rhythm (Tair.org).

The last group contains four genes, two are *LHY* and *CCA,* which were in the third group, one of the *BBX* genes (*AT3G21890*) and one gene called ROOT PHOTOTROPISM2 (*RPT2, AT2G30520*). RPT2 together with NPH3 are photoreceptors, which induce the phototropic response [178, 179]. The gene coding for NPH3 is not differentially regulated in 39Ox plants but is around two-fold downregulated at +Fe and –Fe for *RPT2*. Downregulation of this gene causes retarded and reduced responses to phototropism [178, 180].

Interestingly, one of the co-regulated genes included in the ATTED-II tool was the gene *AT3g23210* coding for the bHLH034 (subgroup IVc) transcription factor. Previous reports indicated that the interaction of this protein with bHLH104 (subgroup IVc) activates directly the gene expression of the four bHLHs subgroup Ib *BHLH038/039/100/101*. Single *bhlh034, bhlh104* mutants and the double mutants showed strong sensitivity in –Fe conditions and a down regulation of additional iron homeostasis genes. In contrast, overexpression of either *BHLH034* or *BHLH104* positively regulated the gene expression of the iron uptake genes *IRT1* and *FRO2* as well as *FIT,* the four *BHLHs, NAS2, NAS4, FRD3, OPT3 and PYE.* The overexpression of these genes led to a high Fe concentration in shoots and a visible phenotype, which is similar to 39Ox plants

[100]. Further investigations suggested that these two proteins are able to form homodimers and heterodimers with each other and with a third player bHLH105 (ILR3, subgroup IVc) to regulate iron homeostasis [99, 100]. These results confirm that bHLH039 acts downstream of these other bHLH transcription factors in the regulation of iron homeostasis.

With these analyses, we concluded that the overexpression of bHLH039 might lead to a disorder in the transcription of the circadian clock and light responsive genes causing disturbance in the daily rhythm of the plants.

4.2.3 Stress responses are induced in 39Ox plants

The processes in which the products of genes are involved are of great importance for the investigation of misregulation of regulatory pathways in a certain plant line or growth condition. Toward this end, the Gene Ontology (GO) can be determined. A GO analysis was hence performed with the online tool VirtualPlant using the differentially expressed genes in 39Ox +Fe vs. WT +Fe. The GO terms were then represented with the tool REVIGO. Figure 26 shows the GOs clustered according to their semantic space This semantic similarity-based calculations remove redundant GOs and summarize them in a scatterplot [163].

The upregulated genes of the 39Ox +Fe vs. WT +Fe conditions were used to determine the GOs and generate a scatterplot (Figure 26 A). The most enriched GOs are highlighted in Figure 26 B.

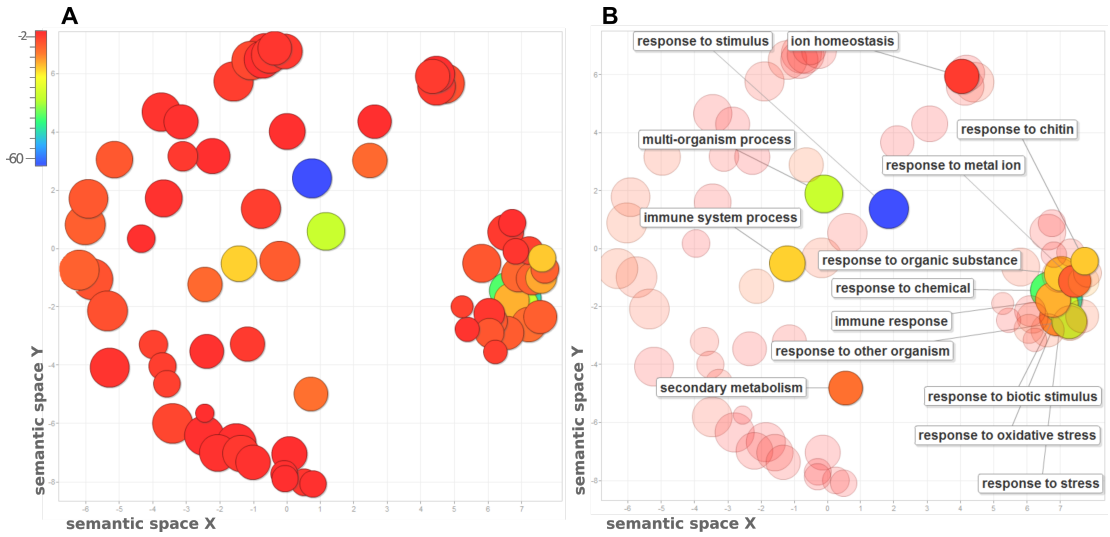

Figure 26: REVIGO representation of GOs from gens upregulated in 39Ox +Fe vs. WT +Fe. The GOs of the differentially regulated genes from the microarray (39Ox +Fe vs. WT +Fe) were analyzed using the tool virtual plant. The GO numbers and the corresponding p-Value were used to generate the scatterplot. The GOs are summarized and the redundant terms are removed. The remaining terms are visualized in semantic similarity-based scatterplots. The size indicates the frequency of the GO term. The colors indicate the log 10 of the p-Value. A) Scatterplot showing all the GOs corresponding to the upregulated genes at +Fe conditions. B) Scatterplot of A with highlighted GO terms with the highest p-Values.

It is clearly visible that stress responses are upregulated in 39Ox compared to the WT. Several GOs involved in the immune response are strongly enriched. Several *WRKY*, genes for disease resistant proteins and *PR* genes but also iron homeostasis genes like *IRT1*, *AT1G07720*, MTPA2 and *FER* are included. It is known that pathogen response and Fe-homeostasis are tightly co-regulated [152], thus it was not surprising to find GO of both biological functions.

Genes involved in the secondary metabolic processes are upregulated in 39Ox seedlings. It is known that the excretion of phenolic compounds, for example scopoletin, enhances the iron mobilization from the rhizosphere to the roots [30]. Scopoletin and scopolin, among other, are products of the phenylpropanoid metabolism. This pathway starts with phenylalanine, passes over ρ-Coumaroyl-CoA to Caffeoyl-CoA catalyzed by the enzyme C3'H (ρ-coumaroylshikimate/quinate 30-Hydrolxylase). This is followed by the synthesis of Feruloyl-CoA by the enzyme CCoAOMT (CAFFEOYL COENZYME A ESTER O-METHYLTRANSFERASE). From Feruloyl-CoA are then synthetized lignin, scopoletin or scopolin, etc. [181]. This step is catalyzed by the 2-oxoglutarate-dependent dioxygenase (F6'H1) [182].

In 39Ox plants at +Fe, some of the phenylpropanoid synthesis enzymes such as PAL1 (*AT2G37040*), 4CL1 and 4CL2 (*AT1G51680*, *AT3G21240*), CCoAOMT1 (*AT4G34050*) as well as the F6'H1 (*AT3G13610*) are upregulated. Additionally, three genes of the shikimate pathway are upregulated in 39Ox plant, which are *DSH1* (AT4G39980), *ADT4* and *ADT5* (AT3G44720, AT5G22630). Apparently, the overexpression of BHLH039 leads to the overexpression of genes necessary for the metabolism of these phenolic compounds; this leads to higher iron availability for the plants. The mobilized Fe is then taken up by IRT1. To confirm that 39Ox produces and secretes more phenolic compounds than the WT, the concentration of phenolic compounds secreted into the growth medium was quantified. 39Ox and WT plants were grown for 10 days in liquid ½ Hoagland medium with (25 µM) and without (0 µM) iron supply. An emission spectrum at 300 nm excitation was generated (Figure 27 A). The emission at 400 nm is represented in a bar diagram with three biological replicates (Figure 27 B). WT seedlings exposed to –Fe conditions extruded more phenolic compounds that at +Fe, but not in a statistically significant manner. As expected, 39Ox plants at iron sufficient conditions secrete around four times more phenolic compounds to the medium as the same plants at iron deficient conditions or the WT in both conditions (Figure 27 B).

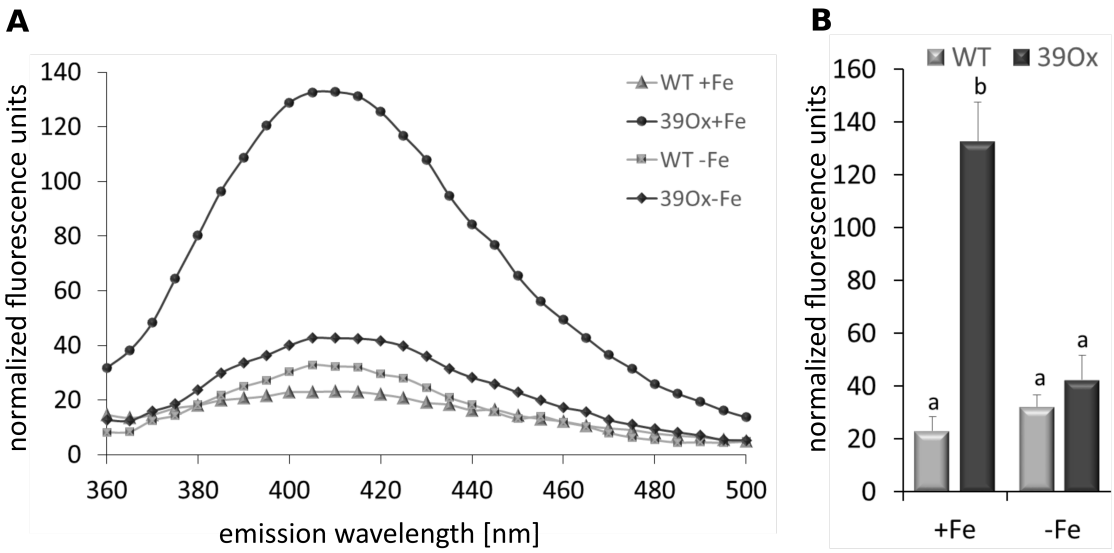

Figure 27: Phenolic compounds content of WT and 39Ox plants. The plants were grown for 10 days in liquid ½ Hoagland medium at +Fe and –Fe. 170 µl of the growth medium was transferred to a UV Star half area plate and the spectrum (A) was measured. (B) Diagram of the maximum emission at 410 nm with an excitation of 300 nm. Bars represent the standard deviation. The statistical significance was calculated with the Anova test and Tukey correction. Different letters indicate statistically significant differences ($p < 0.05$, $n=3$).

For the visualization of the phenolic compounds, plants were grown for 14 days. The WT was grown directly at +Fe or –Fe in Hoagland agar medium whereas 39Ox plants were grown only at +Fe. The plants on the agar medium were pictured under UV light (365 nm).

Figure 28: Phenolic compound secretion of 39Ox and WT plants. WT plants were grown for 14 days directly at +Fe or –Fe agar medium and 39Ox only at +Fe agar medium. The plants on the plate were pictured on the UV table at 365 nm. For better visualization, the colors of the picture were inverted.

It is noteworthy that WT plants accumulate large amounts of phenolic compounds in the roots under –Fe deficient conditions, but not under +Fe conditions. 39Ox plants showed strong accumulation of the phenolic compound at +Fe conditions (Figure 28). These results coincided with the gene expression investigation. Genes that are involved in the phenolic compounds biosynthesis are upregulated as well as the ABCG37 coumarin transporter, which is around fourfold upregulated in 39Ox seedlings at +Fe.

When plants are confronted with stresses, high amounts of H_2O_2 are produced. Hence, they are forced to handle these toxic molecules; this process is mediated by NADPH oxidases and NADPH oxidases-like. Mittler et al. [164] summarized data plants treated with different stresses and showed that the ROS-gene network consist in an interplay of ROS-scavenging and ROS-producing proteins to ensure an adequate defense response (Table 20).

We already demonstrated that 39Ox plants have high amounts of H_2O_2 (Figure 16 C). Therefore, the differentially regulated genes WT-Fe vs. WT +Fe, *fit* +Fe vs. WT +Fe and *fit* -Fe vs. WT-Fe from [162] as well as 39Ox +Fe vs. WT +Fe were compared with those of plants exposed to many other stresses such as heat, drought, salt, cold and high light [164].

As expected, several enzymes from this network were upregulated in 39Ox seedling. The gene *AT5G47910,* which encodes for a NADPH oxidase called RBOHD, is related with the production of H_2O_2 during salt stress. Higher amounts of H_2O_2 and upregulation of RBOHD leads to the upregulation of delta1-pyrroline-5-carboxylate synthetase, which is a key enzyme for the synthesis of proline. Proline can chelate metals with antioxidant effect in osmotic and salt stress due to its property as osmolyte [183]. The gene encoding for the enzyme delta1-pyrroline-5-carboxylate synthetase was 1.43-fold upregulated in 39Ox and was not considered as differentially expressed, but probably sufficiently overexpressed to raise the levels of proline in the plant. The three genes coding for NADPH oxidase-like proteins simultaneously have Fe reductase activity. FRO8 (*AT5G50160*), FRO6 (*AT5G49730*) and FRO7 (*AT5G49740*) are expressed in the shoots and are involved in the compartmentation of iron. However, they are not further described [184].

Table 20: List of genes differentially regulated in WT, *fit* and 39Ox seedlings compared to differently stressed plants summarized by Mittler et al. [164].

Enzymatic activity	Gene Name	Gene ID	WT –Fe vs. WT +Fe	*fit* +Fe vs. WT +Fe	*fit* –Fe vs. WT –Fe	39Ox +Fe vs. WT +Fe	Heat vs. Mock	Drought vs. Mock	Salt vs. Mock	Cold vs. Mock	High Light vs. Mock
NADPH oxidase NADPH + e- + O_2 → NADP- + O_2- + H+	NADPH oxidase (RbohD)	AT5G47910	80%	80%	0%	20%					
NADPH oxidase-like NADPH + e- + O_2 → NADP- + O_2- + H+	FRO8 (NADPH oxidase like)	AT5G50160	60%	60%	60%	40%					
	FRO6 (NADPH oxidase like)	AT5G49730	0%	100%	0%	100%					
	FRO7	AT5G49740	0%	0%	0%	100%					
Ferritin Fe + P → P-Fe	Ferritin 1	AT5G01600	40%	40%	0%	60%					
	Ferritin 2	AT3G56090	40%	40%	60%	60%					
	Ferritin 3	AT2G40300	40%	40%	0%	60%					
	Phospholipid GPX6	AT4G11600	0%	0%	0%	80%					
Alternative Oxidase (AOX) 2e- + 2H+ + O_2 → H_2O	AOX1A	AT3G22370	0%	0%	0%	100%					
	APX1	AT1G07890	20%	20%	20%	80%					
	APX4	AT4G09010	0%	0%	0%	100%					
Blue copper protein Cu + P → P-Cu	Blue copper binding protein	AT5G20230	60%	40%	60%	40%					
	Blue copper protein	AT1G72230	50%	50%	0%	50%					
Dehydroascorbate Reductase (DHAR) DHA + 2 GSH → Asc + GSSG	MDAR5	AT5G03630	0%	0%	0%	40%					
Glutaredoxin (GLR) DHA + 2 GSH → Asc + GSSG	Glutaredoxin putative	AT5G63030	0%	0%	0%	40%					
	Glutaredoxin family	AT4G33040	33%	33%	0%	67%					
	Glutaredoxin family	AT1G28480	40%	40%	40%	60%					
	Glutaredoxin family	AT2G47880	0%	0%	0%	33%					
	Glutaredoxin family	AT4G15690	0%	0%	0%	80%					
	Glutaredoxin family	AT4G15700	0%	0%	0%	80%					
	Glutaredoxin family	AT2G30540	33%	33%	0%	67%					
	Glutaredoxin family	AT2G20270	0%	0%	0%	60%					
	Glutaredoxin family	AT3G62950	0%	0%	0%	75%					
	Thioredoxin x	AT1G50320	0%	0%	0%	80%					
	Glutaredoxin family	AT5G14070	50%	50%	50%	50%					
	Glutaredoxin family	AT4G15680	0%	0%	0%	100%					
	Glutaredoxin family	AT4G15660	0%	0%	0%	100%					
	Glutaredoxin family	AT5G18600	0%	0%	0%	100%					
	Glutaredoxin family	AT3G62930	0%	0%	0%	100%					
Glutathione Peroxidase (GPX) H_2O_2 + 2 GSH → 2H_2O + GSSG	Cat3	AT1G20620	80%	80%	0%	20%					
	GPX1	AT2G25080	0%	0%	0%	60%					
	GPX7	AT4G31870	0%	0%	0%	60%					
Monodehydroascorbate Reductase (MDAR) MDA + NAD(P)H + H+ → Asc + NAD(P)-	MDAR4	AT3G52880	40%	40%	0%	60%					
	thylakoid-APX	AT1G77490	0%	0%	0%	80%					
Peroxiredoxin (PrxR) 2P-SH + H_2O_2 → P-S-S-P + 2H_2O	Type 2 PrxR C	AT1G65970	50%	50%	50%	50%					
	Type 2 PrxR D	AT1G60740	50%	50%	50%	50%					
	PrxR Q	AT3G26060	0%	0%	0%	40%					
	2-cys PrxR B	AT5G06290	0%	0%	0%	80%					
	2-cys PrxR A	AT3G11630	0%	0%	0%	80%					
Superoxide Dismutase (SOD) O_2- + O_2- + 2H+ → H_2O_2 + O_2	FeSOD (FSD1)	AT4G25100	60%	40%	60%	60%					
	Cu/ZnSOD (CSD2)	AT2G28190	0%	0%	0%	60%					
Thioredoxins (Trx) P-S-S-P + 2H+ → 2P-SH	similar to thioredoxin	AT1G43560	0%	0%	0%	80%					
	Thioredoxin reductase	AT2G41680	0%	0%	0%	80%					

The data of WT-Fe vs. WT +Fe, *fit* +Fe vs. WT +Fe and *fit* -Fe vs. WT-Fe from [162] as well as 39Ox +Fe vs WT +Fe were compared to the data of Mittler et al. 2004 [164]. Red means upregulation, green downregulation and grey no differential regulation. The percentages represent, for each gene and for each line, the overlap between the way the line is regulated and the way the WT is regulated upon the different stresses. When a gene is not differentially regulated, it is not included in the calculation. Values above 75% are considered meaningful and marked in black. The data of Mittler et al. 2004 is a summary of different experiments and reflects only a qualitative analysis. They should not be used for statistical analysis.

In WT and fit, the majority of the genes listed in were not differentially regulated and not meaningfully regulated in contrast to the genes in 39Ox. Around half of the genes of 39Ox were at least 75% regulated (marked in black) in the same manner as the WT upon the different stresses.

The fact that the gene expression of stress responsive genes in 39Ox was regulated in a similar manner as plants exposed to different stresses suggests an activation of the stress defense response. This explains and confirms the dwarf phenotype and the high anthocyanin content. The overexpression of bHLH039 is connected to the strong activation of iron-uptake genes. This led to high iron content in these plants. Moreover, bHLH039 might activate the synthesis of phenolic compounds, which facilitates even more the iron uptake in 39Ox plants. This leads to oxidative stress in the plants via the Fenton reaction and high hydrogen peroxide content in plants.

In plant cells, plastids are the major sink of iron. It is stored in the vacuoles as a complex with Ferritin or in the chloroplast for the synthesis of chlorophyll and the electronic transport chain. During photosynthesis, iron plays a special role as a complex with the cytochrome b6/f complex in the transport of electrons from photosystem II (PS II) to photosystem I (PS I) and further in the Fe-S protein Fx, FB and FA in the way to $NADP^+$ [185].

In 39Ox plants many genes involved in pigment metabolism, photosynthesis and electron transport chain were downregulated. Figure 29 shows the most enriched GO of the downregulated genes in 39Ox +Fe vs. WT +Fe.

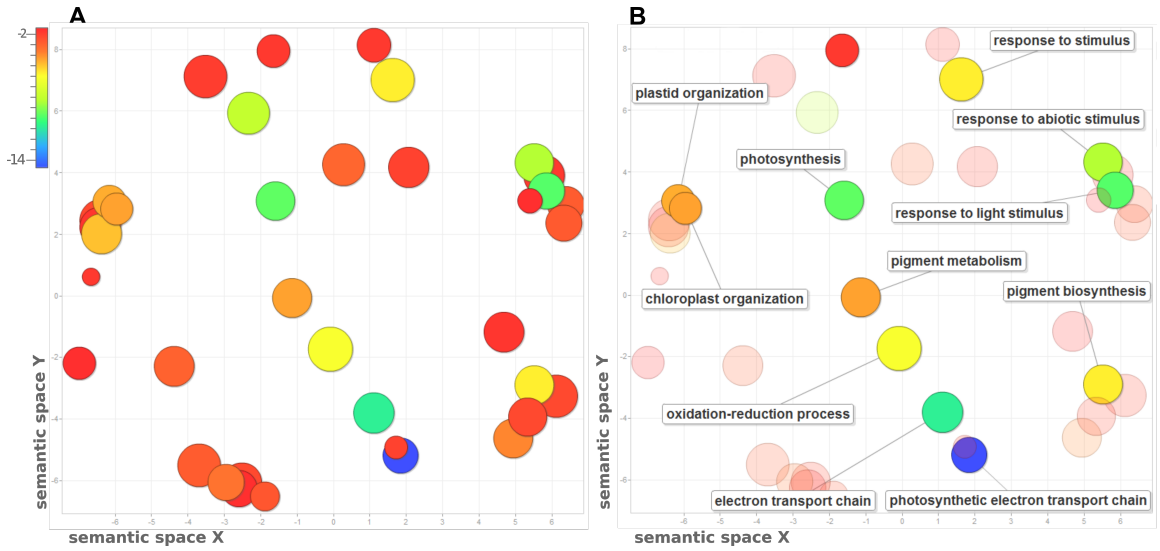

Figure 29: REVIGO representation of GOs from gens downregulated in 39Ox +Fe vs. WT +Fe. The GOs of the differentially regulated genes from the microarray (39Ox +Fe vs. WT +Fe) were analyzed using the tool virtual plant. The GO numbers and the corresponding p-Value were used to generate the scatterplot. The GOs are summarized and the redundant terms are removed. The remaining terms are visualized in semantic similarity-based scatterplots. The size indicated indicates the frequency of the GO term. The colors indicate the log 10 of the p-Value. A) Scatterplot showing all the GOs corresponding to the upregulated genes at +Fe conditions. B) Scatterplot of A with highlighted GO terms with the highest p-Values.

Carotenoid are pigments essential for the photoprotection by high light stress. They protect antenna pigments by non-photochemical quenching of chlorophyll fluorescence and de-excite

chlorophyll singlets, triplets and O_2 [186, 187]. In 39Ox seedling grown at +Fe conditions, genes responsible for the carotenoid biosynthesis are downregulated (Table 21).

The biosynthesis of chlorophyll comprises a high number of pathways and enzymes. It starts with the synthesis of the protoporphyrin ring, followed by the incorporation of the phytol chain, then the insertion of the magnesium, synthesis of the protochlorophyllide and finally the reduction to chlorophyllide and phytylation [188]. Several genes involved in the pigment biosynthesis and metabolism were downregulated. Table 21 shows the downregulated genes, which encode for enzymes responsible for the chlorophyll synthesis. Bonfig et al. 2006 [189] showed that after pathogen attack the levels of chlorophyll and the photosynthesis activity decreased in the infected zones. The high iron content of the plants produces high amounts of ROS. This high concentration of oxygen species switches in turn down the photosynthesis to avoid further production of ROS by the electron transport chain. This might be the explanation for the downregulation of photosynthesis, pigment metabolism, plastid organization and electron transport chain in 39Ox seedlings.

Table 21: List of downregulated genes in 39Ox +Fe vs. WT +Fe classified in the GO:0046148 and GO:0042440 (pigment biosynthetic process and pigment metabolic process)

Gene	Protein	Pathway
AT3G53130	LUT1; carotene ε-monooxygenase	carotene synthesis
AT1G31800	LUT5; ß-ring hydroxylase	
AT4G25700	BETA-OHASE 1; ß-zeacaronene hydroxylase	
AT5G52570	BETA-OHASE 2; ß-ring hydroxylase	
AT3G10230	LYC; lycopene ß cyclase	
AT3G25660	glutamyl-tRNA(Gln) amidotransferase, putative	chlorophyll synthesis
AT1G58290	HEMA1; glutamyl-tRNA reductase	
AT2G40490	HEME2; uroporphyrinogen decarboxylase	
AT3G14930	HEME1; uroporphyrinogen decarboxylase	
AT4G18480	CHLI1; magnesium chelatase	
AT5G13630	GUN5; genomes uncoupled 5	
AT4G25080	CHLM; magnesium-protoporphyrin IX methyltransferase	
AT3G56940	AT103; dicarboxylate diiron 1	
AT5G18660	DVR; 3,8-divinyl protochlorophyllide a 8-vinyl reductase	
AT5G08280	HEMC; hydroxymethylbilane synthase	
AT3G51820	CHLG; chlorophyll synthetase	
AT1G44446	CH1; chlorophyll a oxygenase	

4.2.4 The response to beneficial pathogen might be increased in 39Ox plants

In the microarray data of 39Ox vs. WT, many upregulated pathogen-related genes stand out. The FIT-dependent gene, root-specific transcription factor *MYB72* is involved on the onset of the rhizobacteria-ISR and simultaneously related to the plant Fe-deficiency response [152].

The exposure of WT plants to *P. simiae* WCS417 results in a high expression of *MYB72* as well as the iron-marker genes *FIT*, *BHLH039*, *BHLH039*, *IRT1* and *FRO2*. For that reason, we compared the gene expression data of 39Ox +Fe vs. WT +Fe with WT plants treated with the *P. simiae* WCS417 from Zamioudis et al. 2015 [152]. An intersection of 282 upregulated and 159 downregulated genes was found (Figure 30).

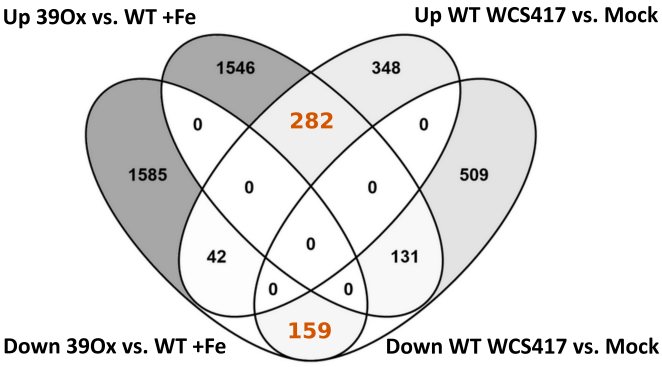

Figure 30: Venn diagram of the pair-wise comparisons 39Ox +Fe vs. WT +Fe with WT- WCS417 vs. WT-Mock. Microarray of Zamioudis et al 2015 [152] of WCS417 inoculated two-week-old Arabidopsis Col-0 seedlings was used for the comparison. Upregulated and downregulated genes in 39Ox +Fe and WT +WCS417 were compared to each other. An intersection of 282 common upregulated and 159 common downregulated genes in 39Ox +Fe vs. WT +Fe and WCS417 vs. Mock were found.

Included in the 282 common upregulated genes in 39Ox +Fe vs. WT +Fe and WT WCS417 vs. Mock were 41 robust Fe-deficiency regulated and 17 robust FIT-regulated (from [162]). These were genes like *MYB72/10, CYP82C4, GRF11, AT3G07720, AT3G12900, MTPA2* and *IRT1* among others.

Among the 159 commonly downregulated genes in 39Ox +Fe vs. WT +Fe and WT WCS417 vs. Mock, were genes involved in photosynthesis, light response and pigment biosynthesis. As mentioned in the previous section (4.2.3), the pathogen attack interferes with the production of chlorophyll. Although plants are not infected by any pathogen, the defense responses are strongly upregulated in 39Ox seedlings and this might be a signal for the downregulation of the photosynthesis. This gene regulation suggests that 39Ox might be strongly involved in the regulation of the pathogen defense, or that the upregulation of *MYB72* is sufficient for the activation of this response.

To verify whether the large amount of high upregulated pathogen response genes in 39Ox plants leads to a pathogen resistance, 6 weeks-old WT, *cpr5* mutant and 39Ox plants were inoculated with *P. syringae*. The *cpr5* mutant was used as a reference of pathogen resistance. These plants are constitutively resistant against *Pseudomonas*. They show an enhanced expression of *PR*-1 and have higher levels of salicylic acid (SA). Consequently, the hypersensitive response (HR) is strongly activated and the plants show areas of dead cells, which indicates an activation of the HR without being treated [190]. CPR5 acts as a negative regulator of *NPR1,* which is responsible to activate WRKY TF and PR-genes [190-193] .

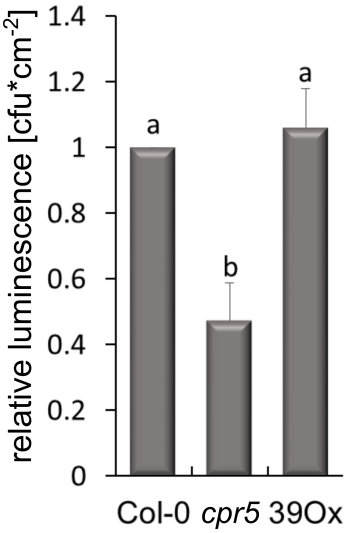

Figure 31: Luminescence measurement of plants inoculated with *P. syringae*. 6 weeks-old plants were inoculated with the bacterial strain *P. syringae* caring the photorhabdus luminescens luxCDABE operon. After two days, a leaf disk of 1 cm diameter was cut and the fluorescence of the bacteria was measured. The resistance of the plants is inversely proportional to the luminescence of the the bacteria. The statistical significance was calculated with the Anova test and Tukey correction. Different letters indicate statistically significant differences ($p < 0.05$, n=3)

The fluorescence, which is inversely proportional to the resistance of the plant to the bacteria, was measured after 2 days of inoculation. As expected, the *cpr5* mutant was significantly more resistant as the WT. On the other hand, the fluorescence in 39Ox plants was almost at the same level as the WT, which means that these plants are as susceptible for pathogen as the WT (Figure 31).

All this data suggests that bHLH039, when overexpressed, activates strongly the iron uptake machinery via activation of genes responsible for the solubilization of iron and the upregulation of the iron-uptake master regulator FIT. This activation triggers the Fe-reductase and transporter leading to high iron content. Obviously, the high iron amount within the plant correlates with the upregulation of the Ferritin genes and the downregulation of the nicotianamin synthases to avoid intoxication of the plant. High iron concentration generates high amounts of ROS via the

Fenton reaction. This ROS and probably the overexpression of bHLH39 inhibit the photosynthesis and pigment biosynthesis to avoid further production of ROS. Simultaneously, the produced ROS activates pathogen response genes.

4.3 Investigation of putative promoter activation by bHLH039

Jakoby et al. [80] studied the *FIT* promoter activity in different tissues and iron conditions in *Arabidopsis* WT plants. For that purpose, pFIT::GUS reporter lines were created. Quantitative GUS activity measurements showed that the *FIT* promoter was activated in roots in a stronger extent than in leaves. Under –Fe, the promoter activity increased fourfold compared to +Fe. Histochemical analysis showed that the activation of the *FIT* promoter is located in the epidermis of developing roots (elongation zone) [80].

Gene expression analysis revealed that *FIT* is more strongly expressed in 39Ox plants compared to the WT at +Fe condition. We suggested that bHLH039 is able to activate *FIT* promoter and that the overexpression of bHLH039 activates it much more strongly as in WT plants.39Ox plants were hence crossed with the pFIT::GUS/WT reporter line. Figure 32 shows the quantitative and qualitative GUS expression in pFIT::GUS/WT and /pFIT::GUS/39Ox plants. In WT background, the activation of the FIT promoter occurs only at –Fe conditions and only in the elongation zone (Figure 32 middle square). On the other hand, it can be clearly seen that the *FIT* promoter activity was substantially stronger in pFIT::GUS with 39Ox background as with a WT background upon both +Fe and –Fe. Quantification of this activity confirmed that the *FIT* promoter is more strongly activated in seedling with 39Ox background than with WT background at +Fe conditions. Surprisingly, the GUS activity at –Fe conditions in pFIT::GUS/39Ox plants was comparable to pFIT::GUS/WT (Figure 32 B).

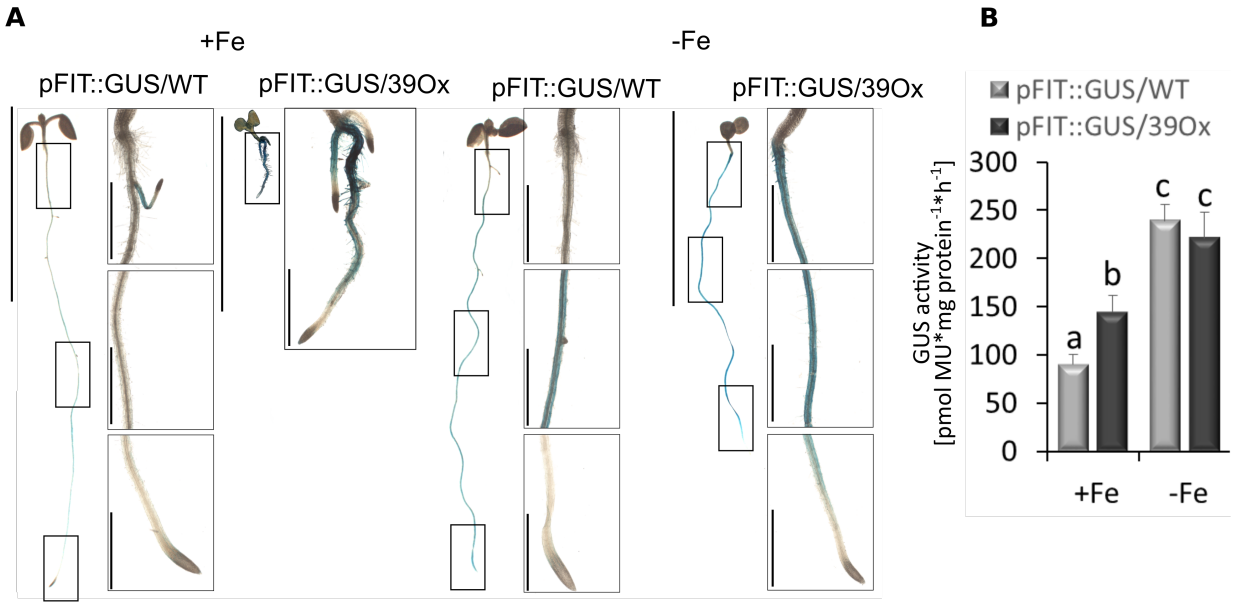

Figure 32: Qualitative and quantitative analysis of the analysis of the FIT promoter activity via GUS-expression assay. pFIT::GUS seedlings with wild type (pFIT::GUS/WT) and 39Ox mutant background (pFIT::GUS/39Ox) were grown under Fe sufficiency (+Fe) or deficiency (-Fe) in the six-days agar plate assay. (A) Qualitative GUS activity assay on the left, whole plant (bar 1 cm) with squares representing close-ups on the right (bar 1 mm). The three squares represent the transition from hypocotyl to upper root zone (top), middle zone of the root (middle), and root tips (bottom). (B) Quantitative GUS activity assay (n=3). Different letters indicate significant differences between samples ($p < 0.05$).

Not only is the quantity of this activity important but also its localization. In both +Fe and –Fe, the activation of the *FIT* promoter in pFIT::GUS/39Ox was visible along the roots, while upon –Fe in the pFIT::GUS/WT only in the elongation zone was visible (Figure 32 A). No GUS activity was found in the leaves neither at +Fe nor at –Fe (data not shown). Taken together, these promoter activation analyses demonstrated that the overexpression of bHLH039 leads to an ectopic activation of the *FIT* promoter, and in turn the FIT-target genes.

The data of the microarray and of the GUS-activity assay point out the possible activation of several promoters by bHLH039. To verify this hypothesis, a chromatin immunoprecipitation (ChIP) with 39Ox plants was performed. It was very important to establish and adapt the protocol for the analyzed proteins, tissues and antibodies used for the experiment. It took several attempts to find the best crosslinking and chromatin shearing time as well as the right antibody and beads for the immunoprecipitation. Several protocols were tested and the protocol of Kaufmann et al. (2016) [166] was adapted (see 3.1.6.5).

After crosslinking, chromatin shearing, immunoprecipitation and reverse crosslinking the DNA was purified and analyzed by qPCR. The data of the qPCR was normalized to the no-antibody

sample and to the control gene (Elongation Factor). Figure 33 shows the fold change of the different promoter regions of the putative bHLH039 target genes. The investigated regions (see 3.2.13.1) were from the promoters of *FIT, IRT1, FRO2*, *AT3G12900*, *AT3G07720* and *AT3G58810*. *FIT* was tested because the GUS and expression analyses showed that the promoter is more activated when *BHLH039* is overexpressed. *IRT1* and *FRO2* were shown by Yuan et al. 2008 [82] to be targets of the TF complex of bHLH039 and FIT *in vitro*. Finally, the genes *AT3G12900*, *AT3G07720* and *AT3G58810* are known to be FIT-targets [162] and they were respectively 7.8, 5.8 and 15.3 fold upregulated in 39Ox seedlings at +Fe conditions.

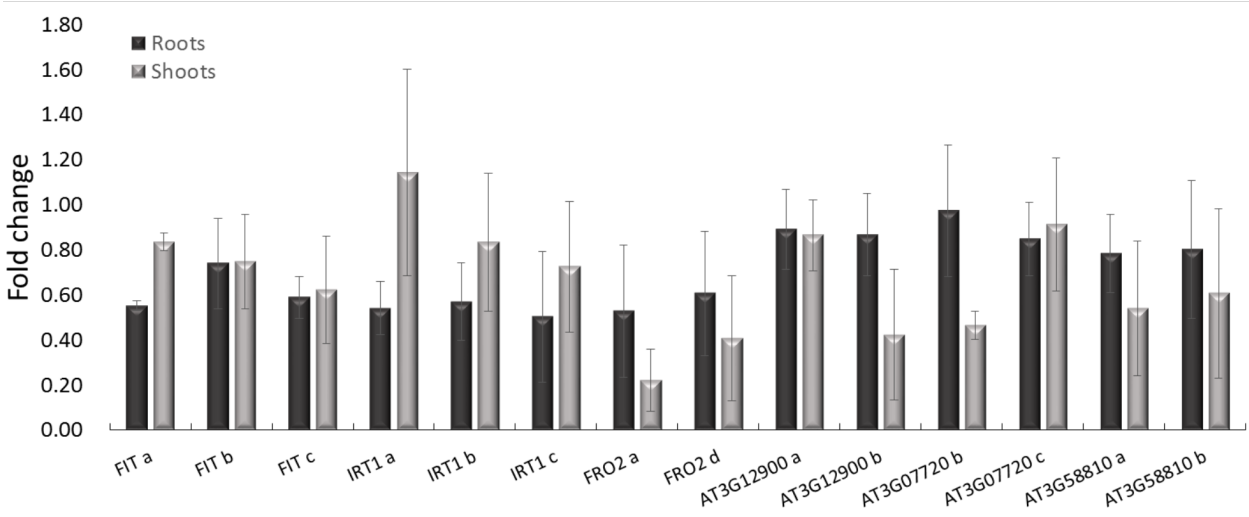

Figure 33: Chromatin immunoprecipitation of putative bHLH039 targets. 14 days-old 39Ox plants grown at +Fe were used to calculated chromatin immunoprecipitation. Roots and shoots were separately harvested and crosslinked for 2x10 min. The nuclei were isolated and the chromatin sheared for 15min. The shared chromatin was divided in two samples and one was used for immunoprecipitation using protein-A agarose beads with anti-HA antibodies and the other as a negative control with anti-IgG. After washing, the Protein-DNA complex was eluted from the antibodies and then overnight reverse crosslinked. The DNA was isolated by ethanol precipitation and further purified with the Qiagen PCR purification columns. The DNA fragments were analyzed by qPCR using specific primers for the different promoter regions of the genes. The data was normalized against the control gene ELONGATION FACTOR (Ef) and the negative control IgG to obtain the fold change over the background. Bars represent the standard deviation, n=2-3

The fold change represents the enrichment of the fragments over the background. This means that the unspecific DNA binding is subtracted from the actual values. The input is not included in the calculation, but it is an indication of the efficiency of the primers and the starting DNA quantity before immunoprecipitation. Therefore, the Ct number of all the tested fragments should be similar in the input. In the qPCR, the number of cycles is inversely proportional to the amount of DNA in the sample. The protocol used [166] recommends an input Ct value of around 14 and the HA-PI sample of around 27. The Ct of the input DNA in the 39Ox was around 21-23

that means around thousand times less DNA as expected (3 Ct = tenfold). The graphic above shows clearly that none of the fragments on the putative target genes yielded an enrichment. Usually, an enrichment higher than 4 counts as significant. It is most probable that the starting DNA in the input was too low to be enriched.

With the collaboration of Kaufman's group, I performed the procedure in their laboratory, with their conditions and devices. The plant material used was 1 g and 2 g of 39Ox seedlings. During the procedure, two control samples (each 0.7 g fresh inflorescence samples) were included. The shearing of the DNA in an adequate size is important for the immunoprecipitation. Usually, the desired size was about 200 bp. Figure 34 shows that most of the DNA of the control samples corresponded to the correct size. However, in the 39Ox seedlings samples, almost no DNA was present.

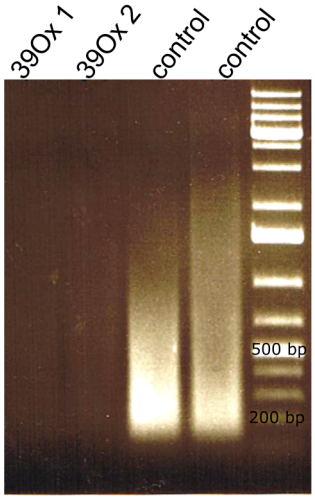

Figure 34: DNA agarose gel after DNA-shearing and reverse crosslinking. To determine the size of the sheared chromatin, a DNA sample was run on an agarose gel. One (39Ox 1) and two (39Ox 2) grams fresh seedlings were used for the procedure. As a control for the method, two samples (each 0.7 g fresh material) from the Kauman's lab were included in the procedure.

An explanation to this issue is that the inflorescence samples contain much more cells per weight, because they are smaller compared to roots or shoots cells. Additionally, the protocol might not be adequate for this type of samples and amount of DNA. It is extremely important to find better conditions for the DNA extraction and find direct targets of bHLH039 that might be involved in so many processes.

5 Discussion

5.1 Iron deficiency and accumulation responses are activated in 39Ox plants

In the scope of this work, we demonstrated that the single overexpression of *BHLH039* in *Arabidopsis* led to a different phenotype and a different physiological response as shown in the literature [82, 194]. 39Ox seedlings exhibited strong expression of the master regulator *FIT*, the iron reductase (*FRO2*) and the iron transporter (*IRT1*) that in turn resulted in a higher Fe reductase activity and iron content in shoots and roots. However, this effect could be observed only in the presence of FIT (Figure 17). The generated 39Ox plants in *fit-3* background confirmed that the iron uptake machinery could be activated only if these two proteins were present.

Yuan et al. [82] showed that plants co-overexpressing *FIT* and *BHLH038* or *BHLH039* were more tolerant to iron deficiency than the WT and plants with single overexpression. Here, we demonstrated that plants overexpressing *BHLH039* and *FIT* in a strong manner were not able to survive in any conditions. Unfortunately, these plants had a lethal phenotype and further investigations of this strong double transgenic line was not possible (Figure 20). On the other hand, moderate overexpression of *FIT* (HA_3-FIT) even led to a reduction of the iron deficiency response compared to the single 39Ox. If we compare the gene expression of *FIT* in the single 39Ox and in 39Ox/HA_3-FIT, we can suggest that *FIT* is not only strongly expressed but also that the stabilization of the transcript might be enhanced in 39Ox plants, especially at +Fe conditions. Post-transcriptional regulation is an important mechanism for the control of many processes, including iron uptake. Experiments in overexpression lines showed that the protein accumulation of FIT (and its tomato homolog *FER*), IRT1 and FRO2 occur only at iron deficient media although high amounts of transcript are available. Hormones as well as protein interactions stabilize the transcript and its product [23, 80, 105, 106, 195]. The experiments in this work showed that the gene expression of the Fe-uptake genes, the Fe-reductase activity and the iron transport are activated at +Fe conditions. In the WT, this activity is present only at –Fe conditions. Meiser et al., Lingam et al. and Sivitzt et al. demonstrated in 2011 that the FIT protein undergoes a turnover upon Fe deficiency. They suggested that FIT is found in two different pools, an active and an inactive form. This regulation is independent of the transcriptional level. In FIT-overexpression lines, the transcript level at +Fe and –Fe iron is equal, but the protein amount is reduced at –Fe conditions. Hence, FIT should undergo a constant degradation and new synthesis. FIT might be ubiquitinated and

proteasomal degraded [105, 106, 196]. It was also suggested that a repressor might prevent the FIT gene expression and that the –Fe signal removed this repressor [105]. It might be that bHLH039 is able to activate the transcription of proteins that act as stabilizing factors for the FIT protein or inhibit the repressors of FIT at +Fe conditions.

To prove if FIT and bHLH039 protein regulate each other posttranscriptional, it is necessary to detect the amounts of FIT and bHLH039 proteins in the double 39Ox/HA_3-FIT and single transgenic lines using specific antibodies against the endogenous proteins. It is not possible to use a tag-directed antibody because both proteins have the 3xHA-tag. Another double transgenic line was generated in parallel by crossing 39Ox plants with FIT-GFP plants (data not shown). However, the gene might have been silenced because we could not detect the protein despite the presence of the gene. Transcriptional and post-transcriptional gene silencing (TGS and PTGS) can be caused by the disabling of transcription initiation, triggered by methylation as well as chromatin condensation [197].

39Ox have similar phenotype, gene expression of the iron homeostasis genes and physiological response as plants overexpressing *BHLH034*, *BHLH104* and *BHLH0105* [99, 100]. Interestingly, the *BHLH034* gene was twofold downregulated at +Fe and 1.5 fold at –Fe in 39Ox vs. WT seedlings, while the other two genes are not differentially downregulated. This confirmed that the regulation of *BHLH039* is downstream of these three other bHLHs of the subgroup IVc. According to the results of Zhang et al. (2015) [99] and Li et al. (2016) [100], the homo and heterodimerisation of these three proteins activate directly the transcription of the four Ib *BHLHs* and *PYE,* regulating positively the iron uptake and homeostasis. It could be interesting to prove if the crossing of 39Ox plants with the double mutant *bhlh034/104* and triple mutant *bhlh034/104/105* rescues its chlorotic phenotype.

WRKY46 is one of the genes that was strongly upregulated in 39Ox seedlings (8.31 +Fe and 3.17 –Fe). Early investigations showed that WRKY46 is upregulated upon –Fe treatment and further investigation revealed that mutation in this gene causes more sensitivity to iron deficiency. The reason to iron deficiency in *wrky46* mutants is that this protein is involved in the translocation of Fe from roots to shoots under Fe deficiency conditions. The authors argued that WRKY46 regulates the transcription of *VIT1* by directly binding on its promoter [198].

VIT1 is the vacuolar iron transporter important for the seed and seedling development, its gene is repressed under iron deficiency conditions [58]. In 39Ox vs. WT seedlings this gene is not differentially regulated, although Yan et al. (2016) [198] confirmed that WRKY46 directly regulates the transcription of *VIT1*. The reason could be that the regulation of *VIT1* is Fe-dependent and not only influenced by the high expression of WRKY46 and the iron deficiency response. WRKY46 is also known to be induced in response to pathogens, drought, salt and oxidative stresses [199, 200]. It is evident that this gene is upregulated in 39Ox seedlings because of the high hydrogen peroxide level.

The reporter gene GUS experiments showed that the overexpression of bHLH039 enhanced the activity of the FIT promoter. This in turn was probably the reason of the upregulation of robust FIT-regulated genes including *IRT1* and *FRO2*. Using chromatin immunoprecipitation, we wanted to confirm the promotor activation of these and other FIT-regulated genes by the binding of FIT/bHLH039 heterodimer *in vivo*. Additionally, we wanted to determine new bHLH039 target genes by sequencing the precipitated DNA. In this work, the investigation of bHLH039 promoter binding to several Fe-deficiency related genes did not bring any indication concerning the interaction with the examined DNA regions.

The chromatin immunoprecipitation method had to be developed especially for our model. It was important to determine the required mass of tissue, the time of crosslinking, an adequate antibody and the proper solutions of the extraction buffers as well as the IP buffer. Curiously, the qPCR analysis showed no specific binding of HA_3-bHLH039 to the analyzed DNA regions. The reliability of the method was confirmed with the inflorescence sample included in the procedure, which yielded enough input DNA (Figure 34). An explanation for this result could be that this protocol is not suitable for the amount of DNA in the samples and it is probable that a large amount of the DNA is lost. Another possibility could be that bHLH039 does not bind directly to these promoters and that other TF or proteins are needed for this activation.

5.2 bHLH039 might be involved in many more other processes than in the iron uptake

The iron uptake is strictly regulated by innumerable proteins. FIT, being the master regulator, plays the major role in the iron uptake [80]. However, other proteins and processes are important for a proper Fe-homeostasis. It seems that the function of bHLH039 goes over being only the FIT interaction partner for the activation of the iron uptake genes *FRO2* and *IRT1*, starting with the solubilizing of Fe before reduction and uptake. Iron is solubilized by the extrusion of protons for the acidification and phenolic compounds for the chelation. Many genes are involved in the synthesis and excretion of phenolic compounds. Coumarins such as scopoletin and scopolin are synthetized via the shikimate and phenylpropanoid pathways. Studies showed that iron deficiency leads to a strong expression of the genes important for the synthesis and transport (ABCG37) of these organic compounds [30, 154]. 39Ox plants have a strong expression of many of these genes including the transporter. Additionally, to the gene expression analysis, the concrete secretion of these compounds was investigated and resulted in high amounts of phenolic compounds in the growth medium of 39Ox seedlings at +Fe. This and the increased expression of the iron reductase and transporter led to strong iron availability and enhanced uptake.

After iron reduction and uptake, it has to be chelated, to be transported to the upper parts of the plants and stored. Once iron enters the plant, it is chelated by nicotianamin (NA) and citrate in the xylem for the transport from roots to shoots. The genes responsible for the synthesis of NA are the nicotianamin synthases (NAS1-4). These four proteins are essential for the iron homeostasis, since the quadruple mutant shows a sterile phenotype [52, 201]. The upregulation of these genes might increase the NA synthesis, in turn enhancing the iron transport to the shoots.

Following the iron uptake and its transport to the shoots, the different organs need to be loaded with iron. Many NA-dependent Fe transporters are surrounding the vasculature [202]. The OPT3 and YSL1-3 proteins transport Fe-loaded NA into the young leaves, the inflorescence, and seeds as well as between xylem and phloem. In 39Ox plants, this transport is probably enhanced due to the upregulation of *YSL1* and *YSL3* in both +Fe and -Fe. Although OPT3 is downregulated in these plants, the seeds are loaded with high amounts of iron (Figure 22). It is probable that the

upregulation of the genes coding for the YSL proteins is sufficient for the iron transport into the seeds.

The increase of all these processes leads to a high iron content in the plant and this in turn to a high production of reactive oxygen species (ROS), probably via the Fenton reaction. In the process of ROS production and scavenging, many enzymes are involved and they are tightly regulated. The principal ROS scavenging enzymes are the superoxide dismutase (SOD), glutathione peroxidase (GPX), peroxiredoxin (PrxR) and ascorbate peroxidase (APX) [203]. The SOD are the first defense against ROS. They dismutase O_2^- to O_2 and H_2O_2 [204, 205] followed by the elimination of H_2O_2 by APX and GPX [206] as a result, the levels of ROS in plants can be measured by the amount of hydrogen peroxide. The H_2O_2 content in 39Ox seedling increased at iron sufficient compared to iron deficient conditions (Figure 16 C). Moreover, these levels are two- and four-fold higher as the WT at +Fe and –Fe respectively. This means that regardless the iron condition, the plants suffers oxidative stress. The high Fe and H_2O_2 at –Fe might be explained by the high amount of iron loaded into the seeds (Figure 22). This quantity of iron is probably sufficiently high to produce elevated H_2O_2 amounts in young seedlings.

Additionally, to deal with the high iron in 39Ox plants the ferritin genes were upregulated at +Fe and –Fe whereas these genes are in the WT downregulated under Fe-deficient conditions. Ferritin counts as a Fe-regulated gene [162]. Ferritins are able to bind Fe^{3+} and keep it in a bioavailable form [207]

Hydrogen peroxide, besides causing oxidative stress in plants, serves also as a signal molecule for many important processes. One of the most predominant is the answer to pathogens. After a pathogen attack, the level of H_2O_2 raises rapidly (within minutes) followed by a second burst after a few hours [138]. In standard cases, a pathogen attack triggers the MAPK cascade, which after prolonged activation leads to the generation of ROS. This ROS activates in turn the hypersensitive response (HR) which leads to the local cell death and to the activation of the *PR* genes in other parts of the plants [208]. With this knowledge, one could expect that 39Ox plants are resistant to a pathogen attack because many genes of the pathogen response are upregulated. Besides, the high level of hydrogen peroxide in the plants serves as a signal of stress. However, as shown in Figure 31, the plants did not show any resistance against leave inoculation with *P. syringae*. The age of the plants and the growth conditions probably play an important role for the pathogen response in 39Ox plants. For this experiment, the plants were grown 6 weeks in

short day conditions. All the other physiological and molecular analyses in this work were performed with 6-days old seedlings. Additionally, we observed that the phenotype of 39Ox plants on soil did not show the strong phenotype as in 6 days-old seedlings. For this reason, it is first necessary to investigate how the gene expression and physiological response behave in older plants. Another option would be to inoculate 2-weeks old plants with a bacterial suspension as described in the literature [209]. Then, the hypersensivity response (HR) can be measured by trypan blue staining which is an azo compound that cannot enter living cells [209].

In 39Ox seedlings, genes coding for many processes are upregulated; however, the photosynthesis and response to light are downregulated compared to WT, especially at +Fe conditions. Adaptation to light is an important signal in the growth and development of plants. The so-called phototropism enables the plants to grow in the direction of the light. There are three main highly sensitive photoreceptors: phytochrome A (phyA), cryptochrome2 (cry2) and phototropin1 (phot1), which mediate photo sensory adaptation [178, 180]. Although the genes for these receptors were not differentially regulated in 39Ox seedlings, many other genes responsible for light perception are downregulated. For instance, around 80 genes belonging to the response to light stimulus (GO:0009416) are downregulated. The photosynthesis is also repressed in these plants. Genes involved in the electron transport chain (GO:0022900, 30 genes; GO:0009767, 24 genes), photosynthesis (GO:0015979, 30 genes), pigment biosynthetic process (GO:0046148, 23 genes), photosystem II assembly (GO:0010207, 10 genes), among others, are downregulated. Figure 25 shows eight putative bHLH039-repressed co-regulated genes that are related to light stimulus and clock. These genes are upregulated in the *3xbhlh* (*bhlh39/100/101*) mutant which probably means that these genes are directly or indirectly repressed by bHLH039. Because independent of the iron supply in the growth medium (Figure 21 and Table 19) these gene are downregulated in 39Ox plants.

6 Conclusion

The main conclusion of this work is that the overexpression of bHLH039 unleashes a vast number of processes that are interconnected. Because of the overexpression of bHLH039, responses such as Fe-deficiency, Fe-overload and stress signaling were strongly induced or repressed. In 39Ox plants, the gene expression of BHLH039 and its protein are strongly upregulated independently of the iron status in the growth medium. This could mean that the overexpression of bHLH039 suppresses negative regulators, which in WT prevent the activation of the iron-uptake genes. This causes the high amount of iron in roots, shoots and seeds that in turn triggers other signaling pathways.

To sum up, the overexpression of *BHLH039* might repress as many processes as it enhances. An overview is shown in Figure 35.

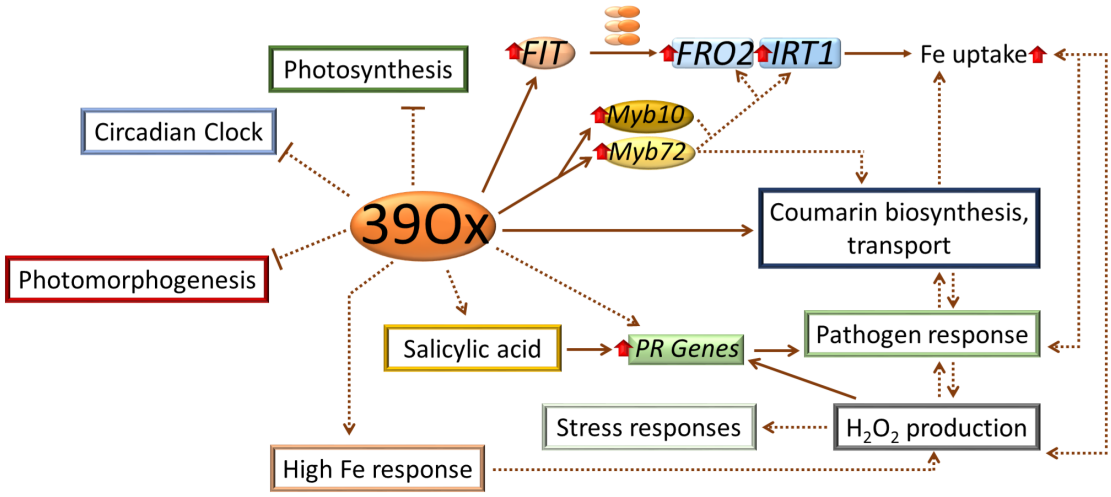

Figure 35: Model of the influences and activation when *BHLH039* is overexpressed. The overexpression of *BHLH039* leads to activation of different genes and responses as well as the repression of many others. Continuous lines mean direct association with the genes and dashed lines influence of the process. Arrows mean an intensification and blunt ends mean repression of a process.

The overexpression of 39Ox leads to the strong activation of the iron homeostasis genes. Including genes involved in the biosynthesis and transport of the Fe-chelating coumarins. These genes can be activated directly by the overexpression of bHLH039 or via the MYB72 and MYB10 transcription factors. The strong Fe uptake causes high hydrogen peroxide accumulation; this rises the expression of PR genes. Activation of these genes and the hydrogen peroxide activates pathogen defense and stress responses. On the other hand, processes in light response such as photosynthesis, including electron transport chain, photomorphogenesis and rhythm are inhibited.

7 Perspectives

This work supports the importance of bHLH039 in iron homeostasis as the interaction partner of FIT and the putative function in additional processes. To investigate more deeply the regulating role of bHLH039 the following goals are suggested.

Firstly, there are only *in vitro* evidences of the *FRO2* and *IRT1* promoter activation by FIT and bHLH039 but no concrete reports about activation in *A. thaliana* plants. Using the chromatin immunoprecipitation, the DNA binding sites of bHLH039 should be further analyzed. A more adapted protocol specific for these seedlings is needed to obtain more starting DNA from the plants, and sequence the ChIPed DNA to find all targets of bHLH039.

Additionally, this DNA should be cloned to create a plasmid library and find a novel binding site for other proteins [210]. Using this library, it would be possible to perform an activation assay. For that, these plasmids would be co-transformed with putative activators of these promoters. The proteins bHLH034, bHLH105 and bHLH115 for instance but also other iron homeostasis proteins such as PYE, BTS, the other four Ib bHLHs, and of course FIT can be used for the assay. FIT phosphorylation-site mutants (Regina Gratz) are being currently analyzed in our lab to find out if the phosphorylation plays a role in the binding of FIT to these specific promoters.

Next, observations showed that older 39Ox plants loses its characteristic phenotype. There might be two reasons for the missing of the characteristic 39Ox phenotype in older plant. Either the overexpression of bHLH039 is post-transcriptionally regulated and the iron homeostasis genes are expressed in a comparable manner as the WT; or the line develops a mechanism to store big amounts of Fe to avoid intoxication. If the Fe content in older 39Ox plants is remarkably higher that the WT, it would mean that the overexpression of bHLH039 could be considered as a suitable method to increase the amounts of this metal in other plants including crops. To test this hypothesis, a time curse experiment should be performed. The iron reductase activity, gene expression and iron content should be determined in shoot and roots of the plants grown in different time points.

Last, the evolution of flowering plants demanded a flexibility of their genome for better and faster adaptation to the environment. This involves, among others, the doubling of the genome that caused one or several duplication of the genes. These duplications can be disperse within the genome, or they can be in tandem [211]. Three different processes are responsible for these

duplications. The first is the silencing through mutations in the duplicated gene. The second is that one copy of the genes becomes a novel favorable function for the plants and the other copy preserves the original function. And in the third, both genes share the same functions in a certain process [212], which might cause functional redundancy. This is the case of the bHLHs of the subgroup Ib(2), which includes the four FIT interactors. *bHLH038* and *bHLH039* are in tandem in chromosome 3, they share 79% of the same sequence and in total 89% similarity. *bHLH100* and *bHLH101* are more distant form each other, they are located in chromosome 2 and 5 respectively. They share only 39% identity and in total 69% similarity [155, 213]. In *Arabidopsis,* many genes are a product of duplications and hence redundant. Usually, it is difficult to investigate knock out mutants, since there are other genes coding for proteins that compensate this function. To reach a complete knock out of the protein function, it is necessary to knock out all the genes coding for the redundant proteins. To reach this goal one possibility is to cross the single mutants and multiply the progeny until homozygosity of all the genes is reached. Unfortunately, when two genes are in tandem they are passed on together to the progeny. To date, it is possible to generate only a triple knock out mutant with the four bHLHs. In our lab, the *3xbhlh* (*bhlh039, bhlh100, bhlh101*) was characterized by Maurer et al. [89]. However, the generation of a quadruple mutant is of extremal importance for the entire understanding of the function these bHLHs in the iron homeostasis and other processes.

Maurer et al. [89] previously attempted to generate the quadruple mutant by posttranscriptional deactivation of the *BHLH038* gene via RNA Interference [156]. *3xbhlh* plants were transformed with miR319a, which binds to a specific mRNA and is degraded. After selection, the T2 generation showed strong chlorosis as well as retarded leaf and root growth. Analysis of these plants showed a strong decrease (but not totally) of the *BHLH038* gene expression but not of the iron-uptake marker genes *FIT*, *IRT1* and *FRO2*. Unfortunately, in the third generation the plants showed the WT phenotype, probably because the miRNA was repressed and the effect was no longer present [156].

Nowadays, a better method can be used for the targeted deactivation of a specific gene. This method is called CRISPR-Cas9 and is based in the editing of DNA using an RNA-guide bacterial DNA endonuclease. The CRISPR (Clustered Regularly Interspaced Short Palindromic Repeats) are DNA repeats in the genome of prokaryotes used as a defense mechanism against invading DNA from e.g. phages [214]. The mechanism consists of a 20 bp CRISPR RNA (crRNA) that recognizes

the target DNA, a second RNA that binds the crRNA (transactivating crRNA, tracrRNA) and the nuclease Cas9 that recognizes the crRNA, binding it and cutting the sequence near to the tracrRNA. The crRNA and tracrRNA are nowadays fused to a single guide RNA (sgRNA) that is transformed in the plants. Due to the small size of the sgDNA, it is possible to edit several genes in one procedure; this is called multiple gene editing. Compared to methods such as EMS treatment of seeds or T-DNA insertions that take a long time and several generations of selections, this method has the advantage of a relatively fast and targeted edition of genes.

Altogether, this work could emphasize the importance of bHLH039 in the regulation of the iron homeostasis. When this protein is overexpressed, it causes a strong upregulation of the iron uptake genes including genes for the secretion of phenolic compounds. This upregulation leads in turn to a high iron content in the roots, the shoots and in the seeds. Although this high iron concentration is dangerous for the plant, due to the generation of reactive oxygen species, the overexpression of bHLH039 could be an alternative for the increment of the iron content in the edible parts of crops and hence for the reduction of iron deficiency anemia.

8 Literature

[1] Naranjo Arcos MA, Bauer P. Iron Deficiency, Oxidative Stress, and Pathogen Defense; Nutritional Deficiency 2016, Erkekoglu P, ed, 978-953-51-2437-5

[2] Gropper SS, Smith JL. Advanced Nutrition and Human Metabolism. Cengage Learning. 2013;6th Edition(2).

[3] Dorling D, Barford A, Newman M. WORLDMAPPER: the world as you've never seen it before. Visualization and Computer Graphics, IEEE Transactions on. 2006;12(5):757-64.

[4] Dorling D, Newman M, Allsopp G, Barford A, Wheeler B, Pritchard J, et al. Worldmapper.org 2006. Available from: http://www.worldmapper.org.

[5] Bouis HE, Welch RM. Biofortification-A Sustainable Agricultural Strategy for Reducing Micronutrient Malnutrition in the Global South. Crop Science. 2010;50(Supplement 1):S-20-S-32.

[6] Mortvedt JJ. Correcting iron deficiency in annual and perennial plants: Present technologies and future prospects. Plant and Soil. 1991;130:273-9.

[7] Marschner H, Römheld V. Strategies of plants for acquisition of iron. Plant and Soil. 1994;165:261-74.

[8] Frossard E, Bucher M, Mächler F, Mozafar A, Hurrell R. Potential for increasing the content and bioavailability of Fe, Zn and Ca in plants for human nutrition. Journal of the Science of Food and Agriculture. 2000;80:861-79.

[9] Perez-Massot E, Banakar R, Gomez-Galera S, Zorrilla-Lopez U, Sanahuja G, Arjo G, et al. The contribution of transgenic plants to better health through improved nutrition: opportunities and constraints. Genes Nutr. 2013;8(1):29-41.

[10] Zhu C, Naqvi S, Gomez-Galera S, Pelacho AM, Capell T, Christou P. Transgenic strategies for the nutritional enhancement of plants. Trends Plant Sci. 2007;12(12):548-55.

[11] Tracy SM. Cassava. US Department of Agriculture, . 1903;167:1-32.

[12] Nweke F, Steven H, Zulu B. Recent growth in African cassava, building on successes in African Agriculture. International Food Policy Research Institute (IFPRI). 2004;Focus 12(Brief3).

[13] Sautter C, Poletti S, Zhang P, Gruissem W. Biofortification of essential nutritional compounds and trace elements in rice and cassava. Proceedings of the Nutrition Society. 2007;65(02):153-9.

[14] Ihemere UE, Narayanan NN, Sayre RT. Iron Biofortification and Homeostasis in Transgenic Cassava Roots Expressing the Algal Iron Assimilatory Gene, FEA1. Front Plant Sci. 2012;3:171.

[15] Payne SM. Iron acquisition in microbial pathogenesis. Trends in microbiology. 1993;1(2):66-9.

[16] Jones JB, Plant Nutrition and Soil Fertility Manual (2nd Edition), CRC Press. Boca Raton, FL, USA. 2012, p. 9781439816103.

[17] Guerinot ML, Yi Y. Iron: Nutritious, Noxious, and Not Readily Available. Plant Physiol. 1994;104(3):815-20.

[18] McNaught AD, Wilkinson A. IUPAC. Compendium of Chemical Terminology, 2nd ed. (the "Gold Book"). Blackwell Scientific Publications, Oxford. 1997.

[19] Pauling L. General Chemistry, 3rd ed. Dover Publication, INC, New York. 1988;3:578-89; 678-93.

[20] Marschner H, Romheld V, Kissel M. Different strategies in higher plants in mobilization and uptake of iron. Journal of Plant Nutrition. 1986;9(3):695-713.

[21] Santi S, Schmidt W. Dissecting iron deficiency-induced proton extrusion in Arabidopsis roots. New Phytol. 2009;183(4):1072-84.

[22] Robinson NJ, Procter CM, Connolly EL, Guerinot ML. A ferric-chelate reductase for iron uptake from soils. Nature. 1999;397(6721):694-7.

[23] Connolly EL, Campbell NH, Grotz N, Prichard CL, Guerinot ML. Overexpression of the FRO2 ferric chelate reductase confers tolerance to growth on low iron and uncovers posttranscriptional control. Plant Physiol. 2003;133(3):1102-10.

[24] Li L, Cheng X, Ling H-Q. Isolation and characterization of Fe (III)-chelate reductase gene LeFRO1 in tomato. Plant molecular biology. 2004;54(1):125-36.

[25] RSmheld V, Marschner H. Mechanism of iron uptake by peanut plants. Plant Physiol. 1983;71:949-54.

[26] Yoshino M, Murakami K. Interaction of iron with polyphenolic compounds: application to antioxidant characterization. Analytical biochemistry. 1998;257(1):40-4.

[27] Jin CW, You GY, He YF, Tang C, Wu P, Zheng SJ. Iron deficiency-induced secretion of phenolics facilitates the reutilization of root apoplastic iron in red clover. Plant Physiol. 2007;144(1):278-85.

[28] Mladenka P, Macakova K, Zatloukalova L, Rehakova Z, Singh BK, Prasad AK, et al. In vitro interactions of coumarins with iron. Biochimie. 2010;92(9):1108-14.

[29] Rodriguez-Celma J, Pan IC, Li W, Lan P, Buckhout TJ, Schmidt W. The transcriptional response of Arabidopsis leaves to Fe deficiency. Front Plant Sci. 2013;4:276.

[30] Fourcroy P, Siso-Terraza P, Sudre D, Saviron M, Reyt G, Gaymard F, et al. Involvement of the ABCG37 transporter in secretion of scopoletin and derivatives by Arabidopsis roots in response to iron deficiency. New Phytol. 2014;201(1):155-67.

[31] Schmid NB, Giehl RF, Doll S, Mock HP, Strehmel N, Scheel D, et al. Feruloyl-CoA 6'-Hydroxylase1-dependent coumarins mediate iron acquisition from alkaline substrates in Arabidopsis. Plant Physiol. 2014;164(1):160-72.

[32] Nozoye T, Nagasaka S, Kobayashi T, Takahashi M, Sato Y, Sato Y, et al. Phytosiderophore efflux transporters are crucial for iron acquisition in graminaceous plants. J Biol Chem. 2011;286(7):5446-54.

[33] Römheld V. Different strategies for iron acquisition in higher plants. Physiologia Plantarum. 1987;70(2):231-4.

[34] Higuchi K, Nakanishi H, Suzuki K, Nishizawa NK, Mori S. Presence of nicotianamine synthase isozymes and their homologues in the root of graminaceous plants. Soil science and plant nutrition. 1999;45(3):681-91.

[35] Curie C, Panaviene Z, Loulergue C, Dellaporta SL, Briat JF, Walker EL. Maize yellow stripe1 encodes a membrane protein directly involved in Fe(III) uptake. Nature. 2001;409(6818):346-9.

[36] Roberts LA, Pierson AJ, Panaviene Z, Walker EL. Yellow stripe1. Expanded roles for the maize iron-phytosiderophore transporter. Plant Physiol. 2004;135(1):112-20.

[37] Schaaf G, Ludewig U, Erenoglu BE, Mori S, Kitahara T, von Wiren N. ZmYS1 functions as a proton-coupled symporter for phytosiderophore- and nicotianamine-chelated metals. J Biol Chem. 2004;279(10):9091-6.

[38] Murata Y, Ma JF, Yamaji N, Ueno D, Nomoto K, Iwashita T. A specific transporter for iron(III)-phytosiderophore in barley roots. Plant J. 2006;46(4):563-72.

[39] Inoue H, Kobayashi T, Nozoye T, Takahashi M, Kakei Y, Suzuki K, et al. Rice OsYSL15 is an iron-regulated iron(III)-deoxymugineic acid transporter expressed in the roots and is essential for iron uptake in early growth of the seedlings. J Biol Chem. 2009;284(6):3470-9.

[40] Araki R, Murata J, Murata Y. A novel barley yellow stripe 1-like transporter (HvYSL2) localized to the root endodermis transports metal-phytosiderophore complexes. Plant Cell Physiol. 2011;52(11):1931-40.

[41] Eide D, Broderius M, Fett J, Guerinot ML. A novel iron-regulated metal transporter from plants identified by functional expression in yeast. Proc Natl Acad Sci U S A. 1996;93(11):5624-8.

[42] Cohen CK, Fox TC, Garvin DF, Kochian LV. The role of iron-deficiency stress responses in stimulating heavy-metal transport in plants. Plant Physiology. 1998;116(3):1063-72.

[43] Eckhardt U, Marques AM, Buckhout TJ. Two iron-regulated cation transporters from tomato complement metal uptake-deficient yeast mutants. Plant molecular biology. 2001;45(4):437-48.

[44] Ishimaru Y, Suzuki M, Tsukamoto T, Suzuki K, Nakazono M, Kobayashi T, et al. Rice plants take up iron as an Fe3+-phytosiderophore and as Fe2+. Plant J. 2006;45(3):335-46.

[45] Morrissey J, Baxter IR, Lee J, Li L, Lahner B, Grotz N, et al. The ferroportin metal efflux proteins function in iron and cobalt homeostasis in Arabidopsis. Plant Cell. 2009;21(10):3326-38.

[46] Green LS, Rogers EE. FRD3 controls iron localization in Arabidopsis. Plant Physiol. 2004;136(1):2523-31.

[47] Durrett TP, Gassmann W, Rogers EE. The FRD3-mediated efflux of citrate into the root vasculature is necessary for efficient iron translocation. Plant Physiol. 2007;144(1):197-205.

[48] Rogers EE. FRD3, a Member of the Multidrug and Toxin Efflux Family, Controls Iron Deficiency Responses in Arabidopsis. The Plant Cell Online. 2002;14(8):1787-99.

[49] Grusak MA. Iron Transport to Developing Ovules of Pisum sativum (I. Seed Import Characteristics and Phloem Iron-Loading Capacity of Source Regions). Plant Physiol. 1994;104(2):649-55.

[50] von Wirén N, Klair S, Bansal S, Briat J-F, Khodr H, Shioiri T, et al. Nicotianamine chelates both FeIII and FeII. Implications for metal transport in plants. Plant Physiology. 1999;119(3):1107-14.

[51] Curie C, Cassin G, Couch D, Divol F, Higuchi K, Le Jean M, et al. Metal movement within the plant: contribution of nicotianamine and yellow stripe 1-like transporters. Ann Bot. 2009;103(1):1-11.

[52] Schuler M, Rellan-Alvarez R, Fink-Straube C, Abadia J, Bauer P. Nicotianamine functions in the Phloem-based transport of iron to sink organs, in pollen development and pollen tube growth in Arabidopsis. Plant Cell. 2012;24(6):2380-400.

[53] Stacey MG, Patel A, McClain WE, Mathieu M, Remley M, Rogers EE, et al. The Arabidopsis AtOPT3 protein functions in metal homeostasis and movement of iron to developing seeds. Plant Physiol. 2008;146(2):589-601.

[54] Chu HH, Chiecko J, Punshon T, Lanzirotti A, Lahner B, Salt DE, et al. Successful reproduction requires the function of Arabidopsis Yellow Stripe-Like1 and Yellow Stripe-Like3 metal-nicotianamine transporters in both vegetative and reproductive structures. Plant Physiol. 2010;154(1):197-210.

[55] Le Jean M, Schikora A, Mari S, Briat JF, Curie C. A loss-of-function mutation in AtYSL1 reveals its role in iron and nicotianamine seed loading. Plant J. 2005;44(5):769-82.

[56] Waters BM, Chu HH, Didonato RJ, Roberts LA, Eisley RB, Lahner B, et al. Mutations in Arabidopsis yellow stripe-like1 and yellow stripe-like3 reveal their roles in metal ion homeostasis and loading of metal ions in seeds. Plant Physiol. 2006;141(4):1446-58.

[57] Ishimaru Y, Masuda H, Bashir K, Inoue H, Tsukamoto T, Takahashi M, et al. Rice metal-nicotianamine transporter, OsYSL2, is required for the long-distance transport of iron and manganese. Plant J. 2010;62(3):379-90.

[58] Kim SA, Punshon T, Lanzirotti A, Li L, Alonso JM, Ecker JR, et al. Localization of iron in Arabidopsis seed requires the vacuolar membrane transporter VIT1. Science (New York, NY). 2006;314(5803):1295-8.

[59] Thomine S, Lelièvre F, Debarbieux E, Schroeder JI, Barbier-Brygoo H. AtNRAMP3, a multispecific vacuolar metal transporter involved in plant responses to iron deficiency. The Plant Journal. 2003;34(5):685-95.

[60] Lanquar V, Lelievre F, Bolte S, Hames C, Alcon C, Neumann D, et al. Mobilization of vacuolar iron by AtNRAMP3 and AtNRAMP4 is essential for seed germination on low iron. EMBO J. 2005;24(23):4041-51.

[61] Kim SA, Guerinot ML. Mining iron: iron uptake and transport in plants. FEBS Lett. 2007;581(12):2273-80.

[62] Duy D, Wanner G, Meda AR, von Wiren N, Soll J, Philippar K. PIC1, an ancient permease in Arabidopsis chloroplasts, mediates iron transport. Plant Cell. 2007;19(3):986-1006.

[63] Duy D, Stube R, Wanner G, Philippar K. The chloroplast permease PIC1 regulates plant growth and development by directing homeostasis and transport of iron. Plant Physiol. 2011;155(4):1709-22.

[64] Briat J-F, Lobréaux S. Iron transport and storage in plants. Trends in plant science. 1997;2(5):187-93.

[65] Lenardo M, Pierce JW, Baltimore D. Protein-binding sites in Ig gene enhancers determine transcriptional activity and inducibility. Science (New York, NY). 1987;236(4808):1573-7.

[66] Murre C, McCaw PS, Baltimore D. A new DNA binding and dimerization motif in immunoglobulin enhancer binding, daughterless, MyoD, and myc proteins. Cell. 1989;56(5):777-83.

[67] Toledo-Ortiz G. The Arabidopsis Basic/Helix-Loop-Helix Transcription Factor Family. The Plant Cell Online. 2003;15(8):1749-70.

[68] Bachhawat N, Ouyang Q, Henry SA. Functional Characterization of an Inositol-sensitive Upstream Activation Sequence in Yeast A cis-REGULATORY ELEMENT RESPONSIBLE FOR INOSITOL-CHOLINE MEDIATED REGULATION OF PHOSPHOLIPID BIOSYNTHESIS. Journal of Biological Chemistry. 1995;270(42):25087-95.

[69] Weintraub H, Dwarki V, Verma I, Davis R, Hollenberg S, Snider L, et al. Muscle-specific transcriptional activation by MyoD. Genes & development. 1991;5(8):1377-86.

[70] Srivastava D, Cserjesi P, Olson EN. A subclass of bHLH proteins required for cardiac morphogenesis. Science (New York, NY). 1995;270(5244).

[71] Lee JE, Hollenberg SM, Snider L, Turner DL, Lipnick N, Weintraub H. Conversion of Xenopus ectoderm into neurons by NeuroD, a basic helix-loop-helix protein. Science (New York, NY). 1995;268(5212):836-44.

[72] Berben G, Legrain M, Gilliquet V, Hilger F. The yeast regulatory gene PHO4 encodes a helix-loop-helix motif. Yeast. 1990;6(5):451-4.

[73] Nikoloff DM, McGraw P, Henry SA. The INO2 gene of Saccharomyces cerevisiae encodes a helix-loop-helix protein that is required for activation of phospholipid synthesis. Nucleic acids research. 1992;20(12):3253.

[74] Cai M, Davis RW. Yeast centromere binding protein CBF1, of the helix-loop-helix protein family, is required for chromosome stability and methionine prototrophy. Cell. 1990;61(3):437-46.

[75] Pires N, Dolan L. Origin and diversification of basic-helix-loop-helix proteins in plants. Mol Biol Evol. 2010;27(4):862-74.

[76] Feller A, Machemer K, Braun EL, Grotewold E. Evolutionary and comparative analysis of MYB and bHLH plant transcription factors. Plant J. 2011;66(1):94-116.

[77] Ling HQ, Bauer P, Bereczky Z, Keller B, Ganal M. The tomato fer gene encoding a bHLH protein controls iron-uptake responses in roots. Proc Natl Acad Sci U S A. 2002;99(21):13938-43.

[78] Brumbarova T, Bauer P. Iron-mediated control of the basic helix-loop-helix protein FER, a regulator of iron uptake in tomato. Plant Physiol. 2005;137(3):1018-26.

[79] Colangelo EP, Guerinot ML. The essential basic helix-loop-helix protein FIT1 is required for the iron deficiency response. Plant Cell. 2004;16(12):3400-12.

[80] Jakoby M, Wang HY, Reidt W, Weisshaar B, Bauer P. FRU (BHLH029) is required for induction of iron mobilization genes in Arabidopsis thaliana. FEBS Lett. 2004;577(3):528-34.

[81] Bauer P, Ling HQ, Guerinot ML. FIT, the FER-LIKE IRON DEFICIENCY INDUCED TRANSCRIPTION FACTOR in Arabidopsis. Plant Physiol Biochem. 2007;45(5):260-1.

[82] Yuan Y, Wu H, Wang N, Li J, Zhao W, Du J, et al. FIT interacts with AtbHLH38 and AtbHLH39 in regulating iron uptake gene expression for iron homeostasis in Arabidopsis. Cell Res. 2008;18(3):385-97.

[83] Wang N, Cui Y, Liu Y, Fan H, Du J, Huang Z, et al. Requirement and functional redundancy of Ib subgroup bHLH proteins for iron deficiency responses and uptake in Arabidopsis thaliana. Mol Plant. 2012;6(2):503-13.

[84] Du J, Huang Z, Wang B, Sun H, Chen C, Ling HQ, et al. SlbHLH068 interacts with FER to regulate the iron-deficiency response in tomato. Ann Bot. 2015;116(1):23-34.

[85] Ogo Y, Itai RN, Nakanishi H, Kobayashi T, Takahashi M, Mori S, et al. The rice bHLH protein OsIRO2 is an essential regulator of the genes involved in Fe uptake under Fe-deficient conditions. Plant J. 2007;51(3):366-77.

[86] Wang HY, Klatte M, Jakoby M, Baumlein H, Weisshaar B, Bauer P. Iron deficiency-mediated stress regulation of four subgroup Ib BHLH genes in Arabidopsis thaliana. Planta. 2007;226(4):897-908.

[87] Schuler M, Keller A, Backes C, Philippar K, Lenhof HP, Bauer P. Transcriptome analysis by GeneTrail revealed regulation of functional categories in response to alterations of iron homeostasis in Arabidopsis thaliana. BMC Plant Biol. 2011;11:87.

[88] Bauer P, Blondet E. Transcriptome analysis of ein3 eil1 mutants in response to iron deficiency. Plant Signal Behav. 2011;6(11):1669-71.

[89] Maurer F, Naranjo Arcos MA, Bauer P. Responses of a triple mutant defective in three iron deficiency-induced Basic Helix-Loop-Helix genes of the subgroup Ib(2) to iron deficiency and salicylic acid. PLoS One. 2014;9(6):e99234.

[90] Ivanov R, Brumbarova T, Bauer P. Fitting into the harsh reality: regulation of iron-deficiency responses in dicotyledonous plants. Mol Plant. 2012;5(1):27-42.

[91] Yang TJ, Lin WD, Schmidt W. Transcriptional profiling of the Arabidopsis iron deficiency response reveals conserved transition metal homeostasis networks. Plant Physiol. 2010;152(4):2130-41.

[92] Buckhout TJ, Yang TJ, Schmidt W. Early iron-deficiency-induced transcriptional changes in Arabidopsis roots as revealed by microarray analyses. BMC Genomics. 2009;10:147.

[93] Long TA, Tsukagoshi H, Busch W, Lahner B, Salt DE, Benfey PN. The bHLH transcription factor POPEYE regulates response to iron deficiency in Arabidopsis roots. Plant Cell. 2010;22(7):2219-36.

[94] Selote D, Samira R, Matthiadis A, Gillikin JW, Long TA. Iron-binding E3 ligase mediates iron response in plants by targeting basic helix-loop-helix transcription factors. Plant Physiol. 2015;167(1):273-86.

[95] Matthiadis A, Long TA. Further insight into BRUTUS domain composition and functionality. Plant Signal Behav. 2016;11(8):e1204508.

[96] Kobayashi T, Nagasaka S, Senoura T, Itai RN, Nakanishi H, Nishizawa NK. Iron-binding haemerythrin RING ubiquitin ligases regulate plant iron responses and accumulation. Nat Commun. 2013;4:2792.

[97] McElver J, Tzafrir I, Aux G, Rogers R, Ashby C, Smith K, et al. Insertional mutagenesis of genes required for seed development in Arabidopsis thaliana. Genetics. 2001;159(4):1751-63.

[98] Tzafrir I, Pena-Muralla R, Dickerman A, Berg M, Rogers R, Hutchens S, et al. Identification of genes required for embryo development in Arabidopsis. Plant Physiol. 2004;135(3):1206-20.

[99] Zhang J, Liu B, Li M, Feng D, Jin H, Wang P, et al. The bHLH transcription factor bHLH104 interacts with IAA-LEUCINE RESISTANT3 and modulates iron homeostasis in Arabidopsis. Plant Cell. 2015;27(3):787-805.

[100] Li X, Zhang H, Ai Q, Liang G, Yu D. Two bHLH Transcription Factors, bHLH34 and bHLH104, Regulate Iron Homeostasis in Arabidopsis thaliana. Plant Physiol. 2016;170(4):2478-93.

[101] Palmer CM, Hindt MN, Schmidt H, Clemens S, Guerinot ML. MYB10 and MYB72 are required for growth under iron-limiting conditions. PLoS Genet. 2013;9(11):e1003953.

[102] Brumbarova T, Bauer P, Ivanov R. Molecular mechanisms governing Arabidopsis iron uptake. Trends Plant Sci. 2014.

[103] Lucena C, Waters BM, Romera FJ, Garcia MJ, Morales M, Alcantara E, et al. Ethylene could influence ferric reductase, iron transporter, and H+-ATPase gene expression by affecting FER (or FER-like) gene activity. J Exp Bot. 2006;57(15):4145-54.

[104] Garcia MJ, Suarez V, Romera FJ, Alcantara E, Perez-Vicente R. A new model involving ethylene, nitric oxide and Fe to explain the regulation of Fe-acquisition genes in Strategy I plants. Plant Physiol Biochem. 2011;49(5):537-44.

[105] Meiser J, Lingam S, Bauer P. Posttranslational regulation of the iron deficiency basic helix-loop-helix transcription factor FIT is affected by iron and nitric oxide. Plant Physiol. 2011;157(4):2154-66.

[106] Lingam S, Mohrbacher J, Brumbarova T, Potuschak T, Fink-Straube C, Blondet E, et al. Interaction between the bHLH transcription factor FIT and ETHYLENE INSENSITIVE3/ETHYLENE INSENSITIVE3-LIKE1 reveals molecular linkage between the regulation of iron acquisition and ethylene signaling in Arabidopsis. Plant Cell. 2011;23(5):1815-29.

[107] Yang JL, Chen WW, Chen LQ, Qin C, Jin CW, Shi YZ, et al. The 14-3-3 protein GENERAL REGULATORY FACTOR11 (GRF11) acts downstream of nitric oxide to regulate iron acquisition in Arabidopsis thaliana. New Phytol. 2013;197(3):815-24.

[108] Chen WW, Yang JL, Qin C, Jin CW, Mo JH, Ye T, et al. Nitric oxide acts downstream of auxin to trigger root ferric-chelate reductase activity in response to iron deficiency in Arabidopsis. Plant Physiol. 2010;154(2):810-9.

[109] Matsuoka K, Furukawa J, Bidadi H, Asahina M, Yamaguchi S, Satoh S. Gibberellin-induced expression of Fe uptake-related genes in Arabidopsis. Plant Cell Physiol. 2014;55(1):87-98.

[110] Wild M, Daviere JM, Regnault T, Sakvarelidze-Achard L, Carrera E, Lopez Diaz I, et al. Tissue-Specific Regulation of Gibberellin Signaling Fine-Tunes Arabidopsis Iron-Deficiency Responses. Dev Cell. 2016;37(2):190-200.

[111] Fan H, Zhang Z, Wang N, Cui Y, Sun H, Liu Y, et al. SKB1/PRMT5-mediated histone H4R3 dimethylation of Ib subgroup bHLH genes negatively regulates iron homeostasis in Arabidopsis thaliana. Plant J. 2014;77(2):209-21.

[112] Yang Y, Ou B, Zhang J, Si W, Gu H, Qin G, et al. The Arabidopsis Mediator subunit MED16 regulates iron homeostasis by associating with EIN3/EIL1 through subunit MED25. Plant J. 2014;77(6):838-51.

[113] Zhang Y, Wu H, Wang N, Fan H, Chen C, Cui Y, et al. Mediator subunit 16 functions in the regulation of iron uptake gene expression in Arabidopsis. New Phytol. 2014;203(3):770-83.

[114] Aksoy E, Jeong IS, Koiwa H. Loss of function of Arabidopsis C-terminal domain phosphatase-like1 activates iron deficiency responses at the transcriptional level. Plant Physiol. 2013;161(1):330-45.

[115] Jeong IS, Fukudome A, Aksoy E, Bang WY, Kim S, Guan Q, et al. Regulation of abiotic stress signalling by Arabidopsis C-terminal domain phosphatase-like 1 requires interaction with a k-homology domain-containing protein. PLoS One. 2013;8(11):e80509.

[116] Halliwell B, Gutteridge JM. Oxygen toxicity, oxygen radicals, transition metals and disease. Biochem J. 1984;219(1):1-14.

[117] Sies H, Oxidative stress, Academic Press. Michigan. 1985, p. 507. 9780126427608.

[118] Ahmad P, Sarwat M, Sharma S. Reactive Oxigen Species, Antioxidants and Signaling in Plants. Journal of Plant Biology. 2008;51(3):167-73.

[119] Schreck R, Rieber P, Baeuerle PA. Reactive oxygen intermediates as apparently widely used messengers in the activation of the NF-kappa B transcription factor and HIV-1. The EMBO journal. 1991;10(8):2247.

[120] Pahl HL, Baeuerle PA. Oxygen and the control of gene expression. Bioessays. 1994;16(7):497-502.

[121] Dalton TP, Shertzer HG, Puga A. Regulation of gene expression by reactive oxygen. Annual review of pharmacology and toxicology. 1999;39(1):67-101.

[122] Dat J, Vandenabeele S, Vranová E, Van Montagu M, Inzé D, Van Breusegem F. Dual action of the active oxygen species during plant stress responses. Cellular and Molecular Life Sciences CMLS. 2000;57(5):779-95.

[123] Low P, Merida J. The oxidative burst in plant defense: function and signal transduction. Physiologia Plantarum. 1996;96(3):533-42.

[124] Fenton H. LXXIII.—Oxidation of tartaric acid in presence of iron. Journal of the Chemical Society, Transactions. 1894;65:899-910.

[125] Haber F, Weiss J, editors. The catalytic decomposition of hydrogen peroxide by iron salts. Proceedings of the Royal Society of London A: Mathematical, Physical and Engineering Sciences; 1934: The Royal Society.

[126] Kehrer JP. The Haber–Weiss reaction and mechanisms of toxicity. Toxicology. 2000;149(1):43-50.

[127] Mittler R. Oxidative stress, antioxidants and stress tolerance. Trends Plant Sci. 2002;7(9):405-10.

[128] Schrader M, Fahimi HD. Mammalian peroxisomes and reactive oxygen species. Histochem Cell Biol. 2004;122(4):383-93.

[129] Tripathy BC, Oelmuller R. Reactive oxygen species generation and signaling in plants. Plant Signal Behav. 2012;7(12):1621-33.

[130] Noctor G, Mhamdi A, Chaouch S, Han Y, Neukermans J, Marquez-Garcia B, et al. Glutathione in plants: an integrated overview. Plant Cell Environ. 2012;35(2):454-84.

[131] Eshdat Y, Holland D, Faltin Z, Ben-Hayyim G. Plant glutathione peroxidases. Physiologia Plantarum. 1997;100(2):234-40.

[132] Menden B, Kohlhoff M, Moerschbacher BM. Wheat cells accumulate a syringyl-rich lignin during the hypersensitive resistance response. Phytochemistry. 2007;68(4):513-20.

[133] Lange BM, Lapierre C, Sandermann Jr H. Elicitor-induced spruce stress lignin (structural similarity to early developmental lignins). Plant Physiology. 1995;108(3):1277-87.

[134] Smit F, Dubery IA. Cell wall reinforcement in cotton hypocotyls in response to a Verticillium dahliae elicitor. Phytochemistry. 1997;44(5):811-5.

[135] Sattler SE, Funnell-Harris DL. Modifying lignin to improve bioenergy feedstocks: strengthening the barrier against pathogens? Frontiers in plant science. 2013;4.

[136] Monaghan J, Zipfel C. Plant pattern recognition receptor complexes at the plasma membrane. Curr Opin Plant Biol. 2012;15(4):349-57.

[137] Boller T, Felix G. A renaissance of elicitors: perception of microbe-associated molecular patterns and danger signals by pattern-recognition receptors. Annu Rev Plant Biol. 2009;60:379-406.

[138] Heath MC. Hypersensitive response-related death; Programmed Cell Death in Higher Plants 2000, ed, 9401037973

[139] Mishina TE, Zeier J. Pathogen-associated molecular pattern recognition rather than development of tissue necrosis contributes to bacterial induction of systemic acquired resistance in Arabidopsis. Plant J. 2007;50(3):500-13.

[140] Shah J, Zeier J. Long-distance communication and signal amplification in systemic acquired resistance. Frontiers in Plant Science. 2013;4.

[141] Eichhorn H, Lessing F, Winterberg B, Schirawski J, Kamper J, Muller P, et al. A ferroxidation/permeation iron uptake system is required for virulence in Ustilago maydis. Plant Cell. 2006;18(11):3332-45.

[142] Oide S, Moeder W, Krasnoff S, Gibson D, Haas H, Yoshioka K, et al. NPS6, encoding a nonribosomal peptide synthetase involved in siderophore-mediated iron metabolism, is a conserved virulence determinant of plant pathogenic ascomycetes. Plant Cell. 2006;18(10):2836-53.

[143] Hwang LH, Seth E, Gilmore SA, Sil A. SRE1 regulates iron-dependent and -independent pathways in the fungal pathogen Histoplasma capsulatum. Eukaryot Cell. 2012;11(1):16-25.

[144] Dellagi A, Rigault M, Segond D, Roux C, Kraepiel Y, Cellier F, et al. Siderophore-mediated upregulation of Arabidopsis ferritin expression in response to Erwinia chrysanthemi infection. Plant J. 2005;43(2):262-72.

[145] Liu G, Greenshields DL, Sammynaiken R, Hirji RN, Selvaraj G, Wei Y. Targeted alterations in iron homeostasis underlie plant defense responses. J Cell Sci. 2007;120(4):596-605.

[146] Ratledge C, Dover LG. Iron metabolism in pathogenic bacteria. Annual reviews in microbiology. 2000;54(1):881-941.

[147] Chet I, Ordentlich A, Shapira R, Oppenheim A. Mechanisms of biocontrol of soil-borne plant pathogens by rhizobacteria. Plant and Soil. 1990;129(1):85-92.

[148] Masalha J, Kosegarten H, Elmaci Ö, Mengel K. The central role of microbial activity for iron acquisition in maize and sunflower. Biology and Fertility of Soils. 2000;30(5-6):433-9.

[149] Pii Y, Borruso L, Brusetti L, Crecchio C, Cesco S, Mimmo T. The interaction between iron nutrition, plant species and soil type shapes the rhizosphere microbiome. Plant Physiol Biochem. 2016;99:39-48.

[150] Iavicoli A, Boutet E, Buchala A, Metraux JP. Induced systemic resistance in Arabidopsis thaliana in response to root inoculation with Pseudomonas fluorescens CHA0. Molecular plant-microbe interactions : MPMI. 2003;16(10):851-8.

[151] Bakker PA, Pieterse CM, van Loon LC. Induced Systemic Resistance by Fluorescent Pseudomonas spp. Phytopathology. 2007;97(2):239-43.

[152] Zamioudis C, Korteland J, Van Pelt JA, van Hamersveld M, Dombrowski N, Bai Y, et al. Rhizobacterial volatiles and photosynthesis-related signals coordinate MYB72 expression in Arabidopsis roots during onset of induced systemic resistance and iron-deficiency responses. Plant J. 2015;84(2):309-22.

[153] Aznar A, Chen NW, Rigault M, Riache N, Joseph D, Desmaele D, et al. Scavenging iron: a novel mechanism of plant immunity activation by microbial siderophores. Plant Physiol. 2014;164(4):2167-83.

[154] Zamioudis C, Hanson J, Pieterse CM. beta-Glucosidase BGLU42 is a MYB72-dependent key regulator of rhizobacteria-induced systemic resistance and modulates iron deficiency responses in Arabidopsis roots. New Phytol. 2014;204(2):368-79.

[155] Sivitz AB, Hermand V, Curie C, Vert G. Arabidopsis bHLH100 and bHLH101 Control Iron Homeostasis via a FIT-Independent Pathway. PLoS ONE. 2012;7(9):e44843.

[156] Maurer F. Eisenmangelinduzierbare bHLH Transkriptionsfaktoren der Untergruppe Ib(2) in der Eisenhomöostase von Arabidopsis thaliana und im Kontext hormoneller Signale. PhD Degree. Saarbruecken, Germany: Saarland University; 2012.

[157] Liu YG, Mitsukawa N, Oosumi T, Whittier RF. Efficient isolation and mapping of Arabidopsis thaliana T-DNA insert junctions by thermal asymmetric interlaced PCR. Plant J. 1995;8(3):457-63.

[158] Klatte M, Bauer P. Accurate real-time reverse transcription quantitative PCR. Plant Signal Transduction: Methods and Protocols. 2009:61-77.

[159] Abdallah HB, Bauer P. Quantitative Reverse Transcription-qPCR-Based Gene Expression Analysis in Plants. Plant Signal Transduction: Methods and Protocols. 2016:9-24.

[160] Brumbarova T, Le CTT, Bauer P. Hydrogen Peroxide Measurement in Arabidopsis Root Tissue Using Amplex Red. Bio-Protocols. 2016;6(21).

[161] Rodrıguez-Delgado M, Malovaná S, Perez J, Borges T, Montelongo FG. Separation of phenolic compounds by high-performance liquid chromatography with absorbance and fluorimetric detection. Journal of chromatography A. 2001;912(2):249-57.

[162] Mai H-J, Pateyron S, Bauer P. Iron homeostasis in Arabidopsis thaliana: transcriptomic analyses reveal novel FIT-regulated genes, iron deficiency marker genes and functional gene networks. BMC Plant Biology. 2016;16(1):211.

[163] Supek F, Bosnjak M, Skunca N, Smuc T. REVIGO summarizes and visualizes long lists of gene ontology terms. PLoS One. 2011;6(7):e21800.

[164] Mittler R, Vanderauwera S, Gollery M, Van Breusegem F. Reactive oxygen gene network of plants. Trends Plant Sci. 2004;9(10):490-8.

[165] Kuo M-H, Allis CD. In vivo cross-linking and immunoprecipitation for studying dynamic protein: DNA associations in a chromatin environment. Methods. 1999;19(3):425-33.

[166] Kaufmann K, Muino JM, Østerås M, Farinelli L, Krajewski P, Angenent GC. Chromatin immunoprecipitation (ChIP) of plant transcription factors followed by sequencing (ChIP-SEQ) or hybridization to whole genome arrays (ChIP-CHIP). Nature protocols. 2010;5(3):457-72.

[167] Fan J, Crooks C, Lamb C. High-throughput quantitative luminescence assay of the growth in planta of Pseudomonas syringae chromosomally tagged with Photorhabdus luminescens luxCDABE. Plant J. 2008;53(2):393-9.

[168] Janski N, Masoud K, Batzenschlager M, Herzog E, Evrard JL, Houlne G, et al. The GCP3-interacting proteins GIP1 and GIP2 are required for gamma-tubulin complex protein localization, spindle integrity, and chromosomal stability. Plant Cell. 2012;24(3):1171-87.

[169] Meiser J. Iron dependent post-translational regulation of the bHLH transcription factor FIT in Arabidopsis thaliana. PhD Degree. Saarbrücken, Germany: Saarland University; 2011.

[170] Vert G, Grotz N, Dedaldechamp F, Gaymard F, Guerinot ML, Briat JF, et al. IRT1, an Arabidopsis transporter essential for iron uptake from the soil and for plant growth. Plant Cell. 2002;14(6):1223-33.

[171] Mizoguchi T, Wheatley K, Hanzawa Y, Wright L, Mizoguchi M, Song H-R, et al. LHY and CCA1 are partially redundant genes required to maintain circadian rhythms in Arabidopsis. Developmental cell. 2002;2(5):629-41.

[172] Alabadí D, Yanovsky MJ, Más P, Harmer SL, Kay SA. Critical role for CCA1 and LHY in maintaining circadian rhythmicity in Arabidopsis. Current Biology. 2002;12(9):757-61.

[173] Alabadí D, Oyama T, Yanovsky MJ, Harmon FG, Más P, Kay SA. Reciprocal regulation between TOC1 and LHY/CCA1 within the Arabidopsis circadian clock. Science (New York, NY). 2001;293(5531):880-3.

[174] Salome PA, Oliva M, Weigel D, Kramer U. Circadian clock adjustment to plant iron status depends on chloroplast and phytochrome function. EMBO J. 2013;32(4):511-23.

[175] Hong S, Kim SA, Guerinot ML, McClung CR. Reciprocal interaction of the circadian clock with the iron homeostasis network in Arabidopsis. Plant Physiol. 2013;161(2):893-903.

[176] Khanna R, Kronmiller B, Maszle DR, Coupland G, Holm M, Mizuno T, et al. The Arabidopsis B-box zinc finger family. The Plant Cell. 2009;21(11):3416-20.

[177] Wang CQ, Guthrie C, Sarmast MK, Dehesh K. BBX19 interacts with CONSTANS to repress FLOWERING LOCUS T transcription, defining a flowering time checkpoint in Arabidopsis. Plant Cell. 2014;26(9):3589-602.

[178] Sakai T, Wada T, Ishiguro S, Okada K. RPT2: a signal transducer of the phototropic response in Arabidopsis. The Plant Cell. 2000;12(2):225-36.

[179] Motchoulski A, Liscum E. Arabidopsis NPH3: a NPH1 photoreceptor-interacting protein essential for phototropism. Science (New York, NY). 1999;286(5441):961-4.

[180] Haga K, Tsuchida-Mayama T, Yamada M, Sakai T. Arabidopsis ROOT PHOTOTROPISM2 Contributes to the Adaptation to High-Intensity Light in Phototropic Responses. Plant Cell. 2015;27(4):1098-112.

[181] Kai K, Shimizu B, Mizutani M, Watanabe K, Sakata K. Accumulation of coumarins in Arabidopsis thaliana. Phytochemistry. 2006;67(4):379-86.

[182] Kai K, Mizutani M, Kawamura N, Yamamoto R, Tamai M, Yamaguchi H, et al. Scopoletin is biosynthesized via ortho-hydroxylation of feruloyl CoA by a 2-oxoglutarate-dependent dioxygenase in Arabidopsis thaliana. Plant J. 2008;55(6):989-99.

[183] Hayat S, Hayat Q, Alyemeni MN, Wani AS, Pichtel J, Ahmad A. Role of proline under changing environments: a review. Plant Signal Behav. 2012;7(11):1456-66.

[184] Wu H, Li L, Du J, Yuan Y, Cheng X, Ling HQ. Molecular and biochemical characterization of the Fe(III) chelate reductase gene family in Arabidopsis thaliana. Plant Cell Physiol. 2005;46(9):1505-14.

[185] Raven JA, Evans MC, Korb RE. The role of trace metals in photosynthetic electron transport in O2-evolving organisms. Photosynthesis Research. 1999;60(2-3):111-50.

[186] Demmig-Adams B, Gilmore AM, Adams W. Carotenoids 3: in vivo function of carotenoids in higher plants. The FASEB Journal. 1996;10(4):403-12.

[187] Niyogi KK, Björkman O, Grossman AR. The roles of specific xanthophylls in photoprotection. Proceedings of the National Academy of Sciences. 1997;94(25):14162-7.

[188] Von Wettstein D, Gough S, Kannangara CG. Chlorophyll biosynthesis. The Plant Cell. 1995;7(7):1039.

[189] Bonfig KB, Schreiber U, Gabler A, Roitsch T, Berger S. Infection with virulent and avirulent P. syringae strains differentially affects photosynthesis and sink metabolism in Arabidopsis leaves. Planta. 2006;225(1):1-12.

[190] Bowling SA, Clarke JD, Liu Y, Klessig DF, Dong X. The cpr5 mutant of Arabidopsis expresses both NPR1-dependent and NPR1-independent resistance. The Plant Cell. 1997;9(9):1573-84.

[191] Pieterse CM, Zamioudis C, Berendsen RL, Weller DM, Van Wees SC, Bakker PA. Induced systemic resistance by beneficial microbes. Annu Rev Phytopathol. 2014;52:347-75.

[192] Zhang Y, Tessaro MJ, Lassner M, Li X. Knockout analysis of Arabidopsis transcription factors TGA2, TGA5, and TGA6 reveals their redundant and essential roles in systemic acquired resistance. Plant Cell. 2003;15(11):2647-53.

[193] Spoel SH, Mou Z, Tada Y, Spivey NW, Genschik P, Dong X. Proteasome-mediated turnover of the transcription coactivator NPR1 plays dual roles in regulating plant immunity. Cell. 2009;137(5):860-72.

[194] Wu H, Chen C, Du J, Liu H, Cui Y, Zhang Y, et al. Co-overexpression FIT with AtbHLH38 or AtbHLH39 in Arabidopsis-enhanced cadmium tolerance via increased cadmium sequestration in roots and improved iron homeostasis of shoots. Plant Physiol. 2012;158(2):790-800.

[195] Connolly EL, Guerinot M. Iron stress in plants. Genome Biol. 2002;3(8):REVIEWS1024.

[196] Sivitz A, Grinvalds C, Barberon M, Curie C, Vert G. Proteasome-mediated turnover of the transcriptional activator FIT is required for plant iron-deficiency responses. Plant J. 2011;66(6):1044-52.

[197] Fagard M, Vaucheret H. (TRANS)GENE SILENCING IN PLANTS: How Many Mechanisms? Annu Rev Plant Physiol Plant Mol Biol. 2000;51:167-94.

[198] Yan JY, Li CX, Sun L, Ren JY, Li GX, Ding ZJ, et al. A WRKY transcription factor regulates Fe translocation under Fe deficiency in Arabidopsi. Plant Physiol. 2016.

[199] Hu Y, Dong Q, Yu D. Arabidopsis WRKY46 coordinates with WRKY70 and WRKY53 in basal resistance against pathogen Pseudomonas syringae. Plant Sci. 2012;185-186:288-97.

[200] Ding ZJ, Yan JY, Xu XY, Yu DQ, Li GX, Zhang SQ, et al. Transcription factor WRKY46 regulates osmotic stress responses and stomatal movement independently in Arabidopsis. Plant J. 2014;79(1):13-27.

[201] Klatte M, Schuler M, Wirtz M, Fink-Straube C, Hell R, Bauer P. The analysis of Arabidopsis nicotianamine synthase mutants reveals functions for nicotianamine in seed iron loading and iron deficiency responses. Plant Physiol. 2009;150(1):257-71.

[202] Schuler M. The role of nicotianamine in the metal homeostasis of Arabidopsis thaliana. PhD Degree. Saarbruecken, Germany: Saarland University; 2011.

[203] Foyer C, Descourvieres P, Kunert K. Protection against oxygen radicals: an important defence mechanism studied in transgenic plants. Plant, Cell & Environment. 1994;17(5):507-23.

[204] Fridovich I. Superoxide radical and superoxide dismutases. Annual review of biochemistry. 1995;64(1):97-112.

[205] Alscher RG, Erturk N, Heath LS. Role of superoxide dismutases (SODs) in controlling oxidative stress in plants. Journal of experimental botany. 2002;53(372):1331-41.

[206] Asada K. THE WATER-WATER CYCLE IN CHLOROPLASTS: Scavenging of Active Oxygens and Dissipation of Excess Photons. Annu Rev Plant Physiol Plant Mol Biol. 1999;50:601-39.

[207] Briat J-F, Lobréaux S, Grignon N, Vansuyt G. Regulation of plant ferritin synthesis: how and why. Cellular and Molecular Life Sciences CMLS. 1999;56(1-2):155-66.

[208] Beckers GJ, Jaskiewicz M, Liu Y, Underwood WR, He SY, Zhang S, et al. Mitogen-activated protein kinases 3 and 6 are required for full priming of stress responses in Arabidopsis thaliana. Plant Cell. 2009;21(3):944-53.

[209] Tornero P, Dangl J. A high-throughput method for quantifying growth of phytopathogenic bacteria in Arabidopsis thaliana. Plant journal. 2001;28(4):475-81.

[210] Weinmann AS, Farnham PJ. Identification of unknown target genes of human transcription factors using chromatin immunoprecipitation. Methods. 2002;26(1):37-47.

[211] Blanc G, Barakat A, Guyot R, Cooke R, Delseny M. Extensive duplication and reshuffling in the Arabidopsis genome. Plant Cell. 2000;12(7):1093-101.

[212] Lynch M, Conery JS. The evolutionary fate and consequences of duplicate genes. Science (New York, NY). 2000;290(5494):1151-5.

[213] Heim MA, Jakoby M, Werber M, Martin C, Weisshaar B, Bailey PC. The basic helix-loop-helix transcription factor family in plants: a genome-wide study of protein structure and functional diversity. Mol Biol Evol. 2003;20(5):735-47.

[214] Jansen R, Embden J, Gaastra W, Schouls L. Identification of genes that are associated with DNA repeats in prokaryotes. Molecular microbiology. 2002;43(6):1565-75.

9. Appendix

Table 22: Differentially regulated genes in 39Ox vs. WT at +Fe and –Fe. List sorted alphabetically of all genes with mean ratios and p-values regulated in the microarray analysis in roots of 6 days-old Arabidopsis seedlings 39Ox vs. Col-0 plants grown directly on iron sufficiency or deficiency Hoagland medium. The mean ratios are the log2 fold change values of the pairwise comparison.

		Ratio				Ratio				Ratio	
D CATMAv6	AGI	+Fe	-Fe	D CATMAv6	AGI	+Fe	-Fe	D CATMAv6	AGI	+Fe	-Fe
CATMA1OA00010R1	AT1G01010	3.43	2.02	CATMA1OA04290F1	AT1G05385	-2.08	-1.20	CATMA1OA08620F1	AT1G09780	1.65	1.17
CATMA1OA00045F1	AT1G01060	-1.71	-2.65	CATMA1OA04350R1	AT1G05450	1.40	2.07	CATMA1OA08630F1	AT1G09790	6.53	7.13
CATMA1OA00050F1	AT1G01070	-1.51	-1.33	CATMA1ON95262F1	AT1G05530	4.11	4.18	CATMA1OA08730F1	AT1G09880	1.50	-1.07
CATMA1OA00060F1	AT1G01080	-1.82	-1.40	CATMA1OC71052F1	AT1G05575	2.38	1.38	CATMA1OC71132F1	AT1G09932	3.82	1.26
CATMA1OA00110F1	AT1G01120	-1.61	-1.49	CATMA1ON94903F1	AT1G05650	-6.79	-2.34	CATMA1OA08840R1	AT1G09970	2.05	1.28
CATMA1ON92421F1	AT1G01170	-1.50	-1.20	CATMA1ON94904F1	AT1G05660	-5.54	-1.67	CATMA1OA08916R1	AT1G10070	1.34	1.65
CATMA1OA00180F1	AT1G01190	-1.49	3.73	CATMA1OF00023F1	AT1G05680	1.07	1.75	CATMA1OA09000F1	AT1G10140	1.71	1.35
CATMA1OA00190F1	AT1G01200	-1.64	-1.25	CATMA1ON102005R1	AT1G05700	6.50	1.82	CATMA1OA09040F1	AT1G10170	1.62	1.64
CATMA1OA00320F1	AT1G01340	1.68	1.54	CATMA1OA04710R1	AT1G05710	1.93	-1.13	CATMA1OA09190F1	AT1G10340	1.77	-1.26
CATMA1OA00370R1	AT1G01380	2.24	2.20	CATMA1OA04820R1	AT1G05820	-1.66	-1.04	CATMA1OC71140F1	AT1G10360	-1.83	-1.09
CATMA1OC71005F1	AT1G01390	-1.83	1.46	CATMA1OA04900R1	AT1G05880	1.18	1.62	CATMA1OC71141F1	AT1G10370	-1.80	-1.33
CATMA1OA00460F1	AT1G01470	1.76	1.99	CATMA1OA05065F1	AT1G06040	-1.59	-1.42	CATMA1OA09230R1	AT1G10380	-2.47	-1.01
CATMA1OA00465R1	AT1G01480	4.27	3.45	CATMA1ON92342R1	AT1G06090	-1.80	1.07	CATMA1OA09322F1	AT1G10470	-1.80	1.03
CATMA1OA00470F1	AT1G01490	1.51	1.10	CATMA1ON92349R1	AT1G06100	-1.33	-1.80	CATMA1OA09340R1	AT1G10510	-1.77	-1.37
CATMA1OA00550R1	AT1G01570	2.07	1.84	CATMA1OF00028R1	AT1G06120	-5.08	-1.51	CATMA1OC71143F1	AT1G10640	-1.50	-1.58
CATMA1OA00560R1	AT1G01580	14.50	1.35	CATMA1OA05200R1	AT1G06160	2.15	1.43	CATMA1OA09640F1	AT1G10760	1.88	1.57
CATMA1ON101947F1	AT1G01620	-1.56	-1.18	CATMA1ON102012R1	AT1G06240	-1.53	-1.44	CATMA1OA09650F1	AT1G10770	1.13	2.27
CATMA1OA00640F1	AT1G01660	1.60	2.25	CATMA1OA05490F1	AT1G06460	1.38	1.53	CATMA1OA09670R1	AT1G10790	-1.51	1.07
CATMA1OA00650F1	AT1G01670	1.75	1.35	CATMA1OA05510F1	AT1G06475	1.08	-1.63	CATMA1OA09850R1	AT1G10960	-1.59	-1.36
CATMA1OA00660F1	AT1G01680	2.25	3.51	CATMA1OA05520R1	AT1G06490	1.52	1.14	CATMA1OA09880F1	AT1G10990	1.98	-1.02
CATMA1OA00725R1	AT1G01720	1.73	-1.03	CATMA1OA05540R1	AT1G06510	-1.82	-1.08	CATMA1OA09920R1	AT1G11050	1.86	1.14
CATMA1OC71012F1	AT1G01860	-1.79	-1.11	CATMA1OA05580F1	AT1G06550	1.53	-1.13	CATMA1OA09940F1	AT1G11070	-1.58	-1.17
CATMA1OA01160R1	AT1G02150	-1.57	-1.22	CATMA1OA05650R1	AT1G06620	1.64	-1.12	CATMA1OA09950F1	AT1G11080	-4.10	-2.11
CATMA1OA01186R1	AT1G02205	-1.36	-1.76	CATMA1OC71070R1	AT1G06640	-1.54	-1.11	CATMA1OA10070R1	AT1G11170	1.54	1.39
CATMA1OA01200F1	AT1G02220	5.04	1.93	CATMA1OA05730F1	AT1G06690	-1.66	-1.34	CATMA1OA10110F1	AT1G11190	-1.12	2.63
CATMA1OC71016F1	AT1G02230	1.36	1.72	CATMA1OA05880F1	AT1G06800	1.51	1.08	CATMA1OA10130F1	AT1G11210	2.31	1.78
CATMA1OA01250F1	AT1G02280	-1.76	-1.14	CATMA1OC71073R1	AT1G06830	1.03	-1.57	CATMA1OA10175R1	AT1G11260	-1.65	1.40
CATMA1OD06013R1	AT1G02320	-1.64	-1.45	CATMA1OA05910F1	AT1G06840	1.55	1.03	CATMA1OA10240F1	AT1G11310	1.60	1.10
CATMA1OA01350F1	AT1G02360	1.96	1.43	CATMA1OA06040F1	AT1G06980	-1.59	1.11	CATMA1OA10260R1	AT1G11330	1.86	1.02
CATMA1OA01380R1	AT1G02390	1.84	1.54	CATMA1OA06060F1	AT1G07000	2.12	1.50	CATMA1OA10390R1	AT1G11450	-2.74	-1.18
CATMA1OA01420R1	AT1G02410	1.22	1.52	CATMA1OA06070R1	AT1G07010	-1.59	-1.13	CATMA1OF02512R1	AT1G11460	-3.71	1.15
CATMA1OC71018F1	AT1G02470	1.45	1.69	CATMA1OA06120F1	AT1G07050	2.08	1.18	CATMA1OA10510F1	AT1G11545	-1.85	-1.34
CATMA1OA01500R1	AT1G02520	1.45	1.86	CATMA1OA06190F1	AT1G07135	2.42	-1.01	CATMA1OC71158F1	AT1G11820	-1.63	-1.21
CATMA1OC71021R1	AT1G02570	-1.05	-1.56	CATMA1ON92574R1	AT1G07175	-2.24	1.76	CATMA1OA10870R1	AT1G11860	-1.56	-1.16
CATMA1OA01590R1	AT1G02640	-1.66	1.14	CATMA1OA06310F1	AT1G07260	1.74	1.03	CATMA1OC71160R1	AT1G11870	-1.57	-1.25
CATMA1OA01730R1	AT1G02810	1.89	1.04	CATMA1OA06385R1	AT1G07320	-1.76	-1.18	CATMA1OA11060R1	AT1G12010	3.01	-1.12
CATMA1OA01755F1	AT1G02820	-2.23	-1.74	CATMA1OA06500F1	AT1G07430	1.07	1.65	CATMA1OA11080F1	AT1G12030	-1.01	-8.46
CATMA1ON101965R1	AT1G02850	5.63	1.40	CATMA1OC71081F1	AT1G07440	-1.65	-1.25	CATMA1OA11090R1	AT1G12040	1.42	1.56
CATMA1OA01820F1	AT1G02900	-1.67	1.17	CATMA1OC71082F1	AT1G07450	-2.70	-1.57	CATMA1ON94924R1	AT1G12080	-1.71	-1.12
CATMA1OA01825F1	AT1G02910	-1.57	-1.17	CATMA1ON92174F1	AT1G07490	-1.09	-1.91	CATMA1OA11140R1	AT1G12100	-1.58	-1.22
CATMA1ON92561F1	AT1G02920	5.69	1.54	CATMA1OA06580F1	AT1G07500	1.05	-1.92	CATMA1OA11145R1	AT1G12110	-1.06	-1.69
CATMA1OF00011F1	AT1G02930	5.74	1.32	CATMA1OA06650R1	AT1G07560	1.83	1.19	CATMA1OA11170R1	AT1G12140	1.60	1.08
CATMA1OA01880F1	AT1G03020	-1.42	-1.83	CATMA1OA06680F1	AT1G07590	1.54	1.01	CATMA1OC71165R1	AT1G12200	3.73	1.23
CATMA1OC71028F1	AT1G03106	-1.28	2.28	CATMA1OC71085R1	AT1G07610	2.00	1.00	CATMA1OA11240R1	AT1G12220	1.54	-1.06
CATMA1OA02160R1	AT1G03290	1.61	1.41	CATMA1ON92670F1	AT1G07620	2.22	1.79	CATMA1OA11270R1	AT1G12244	-1.55	-1.34
CATMA1OA02220R1	AT1G03340	1.65	1.17	CATMA1OA06872F1	AT1G07880	1.82	-1.55	CATMA1OA11280R1	AT1G12250	-1.64	-1.17
CATMA1OA02340F1	AT1G03470	-1.18	-2.13	CATMA1OA06874R1	AT1G07890	2.18	1.54	CATMA1OA11290F1	AT1G12260	-1.58	1.14
CATMA1ON92344R1	AT1G03495	2.02	-2.61	CATMA1ON95260R1	AT1G07900	1.77	1.65	CATMA1OA11350R1	AT1G12320	1.57	-1.06
CATMA1OA02490R1	AT1G03600	-2.48	-1.17	CATMA1OA07030F1	AT1G08050	2.10	1.41	CATMA1OA11470R1	AT1G12460	-1.54	-1.63
CATMA1OA02535F1	AT1G03660	1.12	1.66	CATMA1OC71095F1	AT1G08080	5.01	-1.05	CATMA1OA11720R1	AT1G12740	-1.52	-1.02
CATMA1OA02595R1	AT1G03740	1.72	1.31	CATMA1OA07063R1	AT1G08090	-1.67	-1.15	CATMA1OA11780F1	AT1G12800	-1.56	-1.23
CATMA1OA02650R1	AT1G03790	2.65	1.55	CATMA1OA07066F1	AT1G08100	-1.63	-3.09	CATMA1OA11800R1	AT1G12805	-1.34	-2.14
CATMA1OA02710F1	AT1G03850	1.66	1.67	CATMA1OA07130F1	AT1G08150	-1.60	-1.63	CATMA1OA11900F1	AT1G12900	-1.72	-1.08
CATMA1OA02730R1	AT1G03880	-11.53	-6.22	CATMA1OA07220F1	AT1G08230	2.61	1.12	CATMA1OA11930R1	AT1G12940	3.64	1.35
CATMA1OA02740R1	AT1G03890	-2.99	-1.45	CATMA1OA07280F1	AT1G08290	1.72	-1.05	CATMA1OF00063R1	AT1G13080	-2.52	-1.51
CATMA1OD05001F1	AT1G03940	1.38	-1.97	CATMA1OA07320F1	AT1G08320	1.59	1.44	CATMA1OC71181R1	AT1G13110	1.53	-1.06
CATMA1OA03102F1	AT1G04240	-1.59	-1.18	CATMA1ON102039R1	AT1G08430	2.32	-1.11	CATMA1OC71182F1	AT1G13195	1.52	1.45
CATMA1OA03160F1	AT1G04330	-1.93	-1.52	CATMA1OA07465R1	AT1G08500	-1.63	-1.46	CATMA1OA12220F1	AT1G13210	2.43	1.50
CATMA1OA03200R1	AT1G04370	3.65	1.04	CATMA1OA07796R1	AT1G08930	1.75	1.27	CATMA1OA12230R1	AT1G13220	-1.01	1.59
CATMA1OA03235F1	AT1G04400	1.53	1.33	CATMA1OA07800R1	AT1G08940	2.28	1.40	CATMA1OA12310F1	AT1G13310	1.49	1.51
CATMA1OA03250R1	AT1G04420	-2.75	-1.22	CATMA1OA07910R1	AT1G09090	1.98	1.36	CATMA1ON92429F1	AT1G13340	2.26	1.83
CATMA1OA03360R1	AT1G04520	-1.43	-1.56	CATMA1OC71113F1	AT1G09210	2.16	1.14	CATMA1OA12420R1	AT1G13420	1.60	-1.89
CATMA1OA03410R1	AT1G04560	-2.91	-1.27	CATMA1OA08070F1	AT1G09230	1.16	1.65	CATMA1OA12430R1	AT1G13430	1.21	-1.60
CATMA1ON101983F1	AT1G04620	-1.65	-1.03	CATMA1OA08080R1	AT1G09240	2.44	5.33	CATMA1OC71186F1	AT1G13470	2.62	2.83
CATMA1OA03500F1	AT1G04660	-1.76	-1.31	CATMA1OC71117R1	AT1G09310	-1.09	-1.77	CATMA1OA12480F1	AT1G13480	3.29	1.33
CATMA1OA03840R1	AT1G05000	1.76	-1.09	CATMA1OC71120R1	AT1G09340	-2.19	-1.12	CATMA1ON92067F1	AT1G13490	2.26	1.22
CATMA1OA03900F1	AT1G05060	1.84	1.44	CATMA1ON92609R1	AT1G09390	-2.07	-1.32	CATMA1OC71187F1	AT1G13510	1.50	1.26
CATMA1OA04000R1	AT1G05140	-1.68	-1.11	CATMA1OA08310R1	AT1G09460	2.39	1.49	CATMA1OC71188F1	AT1G13520	1.98	1.61
CATMA1OA04040F1	AT1G05190	-1.78	-1.39	CATMA1OC71125R1	AT1G09500	1.60	1.70	CATMA1OD05008R1	AT1G13609	-1.11	-2.14
CATMA1OA04170F1	AT1G05300	1.02	1.97	CATMA1OA08400R1	AT1G09540	-1.07	1.68	CATMA1OA12590F1	AT1G13610	-1.31	-3.36
CATMA1OC71047F1	AT1G05340	3.46	2.43	CATMA1OA08413R1	AT1G09560	2.97	1.45	CATMA1OA12640F1	AT1G13650	-6.03	-1.57

Table 22: Continued

		Ratio				Ratio				Ratio	
D CATMAv6	AGI	+Fe	-Fe	D CATMAv6	AGI	+Fe	-Fe	D CATMAv6	AGI	+Fe	-Fe
CATMA1OA12650R1	AT1G13670	-1.74	-1.31	CATMA1OA17400R1	AT1G18380	1.59	1.36	CATMA1OA21880F1	AT1G22850	-1.61	-1.13
CATMA1OC71192R1	AT1G13820	-1.71	-1.18	CATMA1OC71277R1	AT1G18390	1.59	1.21	CATMA1OA21980R1	AT1G22930	2.05	1.89
CATMA1OA12940R1	AT1G13990	1.72	1.48	CATMA1ON94952F1	AT1G18470	1.29	1.65	CATMA1OC71361F1	AT1G23020	1.49	-1.92
CATMA1OA12980F1	AT1G14030	-1.56	-1.13	CATMA1OA17615R1	AT1G18570	4.74	1.79	CATMA1OA22110R1	AT1G23040	1.65	1.61
CATMA1OA13090F1	AT1G14120	-2.88	-2.20	CATMA1OA17630R1	AT1G18590	-1.05	-1.50	CATMA1OA22130F1	AT1G23060	1.75	1.30
CATMA1OA13120R1	AT1G14150	-2.03	-1.26	CATMA1OA17680F1	AT1G18650	-1.34	-1.66	CATMA1OA22170F1	AT1G23110	2.20	-1.28
CATMA1OA13130F1	AT1G14160	-2.02	-1.01	CATMA1OA17780R1	AT1G18730	-2.25	-1.08	CATMA1OA22180R1	AT1G23120	2.41	-1.13
CATMA1ON92590F1	AT1G14182	1.89	3.35	CATMA1OC72289R1	AT1G18773	-2.70	-1.34	CATMA1OC71363F1	AT1G23140	1.93	-1.01
CATMA1OA13170R1	AT1G14185	3.72	2.42	CATMA1OA17860F1	AT1G18810	-1.51	-1.51	CATMA1OA22290F1	AT1G23205	-2.32	-1.53
CATMA1OA13280F1	AT1G14270	-1.95	-1.23	CATMA1OC71281R1	AT1G18880	-1.56	1.13	CATMA1OA22460F1	AT1G23390	-1.59	-1.63
CATMA1OA13290R1	AT1G14280	-1.83	-1.53	CATMA1OA17960F1	AT1G18910	1.20	1.26	CATMA1OA22534F1	AT1G23560	1.66	1.37
CATMA1OA13300F1	AT1G14290	-1.73	-1.42	CATMA1OF02520F1	AT1G18970	1.61	-1.01	CATMA1OA22610R1	AT1G23720	-1.07	1.66
CATMA1OA13350R1	AT1G14345	-2.01	-1.23	CATMA1OA18010F1	AT1G18980	2.15	-1.30	CATMA1OA22630F1	AT1G23740	-1.70	-1.37
CATMA1OC71203R1	AT1G14370	3.65	1.37	CATMA1OA18050R1	AT1G19020	4.61	1.30	CATMA1OA22680F1	AT1G23800	1.86	1.09
CATMA1OA13430R1	AT1G14430	-1.67	-1.34	CATMA1OA18090F1	AT1G19050	-2.69	1.04	CATMA1OA22700F1	AT1G23830	2.10	1.34
CATMA1OA13490R1	AT1G14480	2.29	1.09	CATMA1OA18195R1	AT1G19150	-2.20	-1.28	CATMA1OA22710F1	AT1G23840	2.44	1.55
CATMA1OA13550F1	AT1G14540	1.27	-1.90	CATMA1OA18220R1	AT1G19180	3.19	1.59	CATMA1OA22720F1	AT1G23850	1.54	-1.01
CATMA1OC71207R1	AT1G14780	2.16	1.00	CATMA1OA18290F1	AT1G19250	1.37	2.40	CATMA1OA22730R1	AT1G23870	1.66	1.55
CATMA1OA13890R1	AT1G14860	3.58	1.93	CATMA1OA18340F1	AT1G19310	1.62	1.33	CATMA1OA22870F1	AT1G24020	-1.13	-1.87
CATMA1OC71209F1	AT1G14870	3.36	1.41	CATMA1OA18400R1	AT1G19380	1.86	1.09	CATMA1OA22950R1	AT1G24090	1.70	1.11
CATMA1OA13910F1	AT1G14880	1.26	3.69	CATMA1OA18530F1	AT1G19510	-1.32	1.61	CATMA1OA23010R1	AT1G24145	3.88	1.75
CATMA1OA13920R1	AT1G14890	1.80	-1.12	CATMA1OA18560R1	AT1G19530	1.50	1.53	CATMA1ON92336R1	AT1G24147	1.82	1.89
CATMA1OC71210F1	AT1G14930	-1.43	-1.51	CATMA1OA18630F1	AT1G19610	2.06	1.10	CATMA1OA23165F1	AT1G24260	-2.31	-1.61
CATMA1OA14030F1	AT1G15040	23.19	-1.07	CATMA1OA18650F1	AT1G19630	2.08	-1.22	CATMA1OC71389F1	AT1G24320	1.77	1.53
CATMA1OA14110R1	AT1G15125	3.44	2.03	CATMA1OA18695F1	AT1G19670	-1.33	-1.61	CATMA1OA23520F1	AT1G24575	1.71	1.06
CATMA1OF00073R1	AT1G15150	-1.76	-1.42	CATMA1ON102189F1	AT1G19720	-1.97	1.11	CATMA1OA23510R1	AT1G24580	-1.38	-7.84
CATMA1OC71216R1	AT1G15170	1.59	1.12	CATMA1OA18780R1	AT1G19770	1.53	1.09	CATMA1OA23570F1	AT1G24620	-1.55	-1.34
CATMA1OC71217R1	AT1G15180	-1.61	-1.23	CATMA1OA18865R1	AT1G19850	2.23	1.10	CATMA1OA23880F1	AT1G25230	-1.65	1.02
CATMA1OA14260R1	AT1G15260	-1.95	-1.94	CATMA1OA18910F1	AT1G19900	-3.64	1.30	CATMA1OC71392R1	AT1G25275	1.97	1.01
CATMA1OA14400R1	AT1G15380	1.15	-2.12	CATMA1OA18950R1	AT1G19960	8.30	3.48	CATMA1OA24050F1	AT1G25390	1.66	1.15
CATMA1OA14420R1	AT1G15390	-1.55	-1.06	CATMA1OA19170F1	AT1G20160	-1.78	-3.23	CATMA1OA24060F1	AT1G25400	1.61	1.23
CATMA1OA14440R1	AT1G15410	1.48	-1.65	CATMA1OA19190F1	AT1G20190	-1.50	-1.45	CATMA1OA24170R1	AT1G25480	1.97	2.17
CATMA1OA14470R1	AT1G15430	1.59	1.06	CATMA1OA19333F1	AT1G20340	-1.73	-1.13	CATMA1OA24220F1	AT1G25530	2.46	1.02
CATMA1OA14680R1	AT1G15670	2.32	1.29	CATMA1OA19470R1	AT1G20470	-1.50	-1.35	CATMA1OA24430R1	AT1G26210	-1.67	-1.80
CATMA1OA14740F1	AT1G15730	-1.75	-1.05	CATMA1OA19510F1	AT1G20510	1.90	1.10	CATMA1OA24440R1	AT1G26220	-2.47	-1.30
CATMA1OA14830F1	AT1G15790	3.59	1.51	CATMA1OA19640R1	AT1G20620	2.08	2.20	CATMA1OA24480R1	AT1G26250	2.82	-1.06
CATMA1OA14840F1	AT1G15800	1.53	1.23	CATMA1OA19645R1	AT1G20630	1.40	2.19	CATMA1OC71401F1	AT1G26380	4.86	2.39
CATMA1ON92423R1	AT1G15885	-1.58	-1.16	CATMA1OC71308R1	AT1G20700	1.56	1.25	CATMA1ON92133F1	AT1G26390	24.65	2.82
CATMA1OA15010R1	AT1G15980	-1.88	-1.10	CATMA1OA19840R1	AT1G20780	1.50	1.17	CATMA1OF00148F1	AT1G26400	4.36	1.99
CATMA1OA15080R1	AT1G16080	-1.70	-1.09	CATMA1OA19890R1	AT1G20810	-1.67	-1.26	CATMA1OA24650F1	AT1G26410	6.78	2.12
CATMA1ON94939R1	AT1G16120	2.11	1.60	CATMA1OC71311R1	AT1G20816	-1.55	-1.20	CATMA1ON92357F1	AT1G26420	5.91	1.86
CATMA1ON94940R1	AT1G16140	2.21	1.38	CATMA1OA19910R1	AT1G20830	-1.61	-1.03	CATMA1OA24680F1	AT1G26450	1.81	-1.18
CATMA1ON94941R1	AT1G16150	1.58	1.81	CATMA1OA19913F1	AT1G20840	1.75	1.16	CATMA1OA24790R1	AT1G26560	-1.51	-1.59
CATMA1OA15310R1	AT1G16320	-1.69	1.19	CATMA1OA19916R1	AT1G20850	-1.63	1.01	CATMA1OA24930R1	AT1G26700	-1.61	1.16
CATMA1OA15360R1	AT1G16370	-1.58	-1.63	CATMA1ON92705F1	AT1G21100	2.12	1.47	CATMA1ON94982R1	AT1G26730	1.92	1.02
CATMA1OA15380R1	AT1G16390	-1.73	-1.26	CATMA1ON92460F1	AT1G21110	2.10	1.47	CATMA1OA24990F1	AT1G26761	-1.82	-1.51
CATMA1OA15390R1	AT1G16400	-1.47	-1.54	CATMA1ON92153F1	AT1G21120	3.41	1.71	CATMA1ON92479R1	AT1G26762	2.61	1.34
CATMA1OA15400R1	AT1G16410	1.00	-1.96	CATMA1ON92537F1	AT1G21130	2.76	1.55	CATMA1OA25130R1	AT1G26920	-1.58	1.00
CATMA1OA15430R1	AT1G16445	-1.92	-1.19	CATMA1OC71317R1	AT1G21140	4.00	2.13	CATMA1OA25160R1	AT1G26945	1.05	-1.53
CATMA1OC71245F1	AT1G16515	-1.89	-1.16	CATMA1OA20200F1	AT1G21150	-1.53	-1.01	CATMA1OC71410R1	AT1G27020	3.43	-1.09
CATMA1OA15630R1	AT1G16670	1.80	1.32	CATMA1ON92691R1	AT1G21245	1.89	1.93	CATMA1OC71411R1	AT1G27030	1.63	1.52
CATMA1OA15690R1	AT1G16720	-2.08	-1.17	CATMA1OC71318R1	AT1G21250	1.32	1.77	CATMA1OA25330F1	AT1G27100	4.29	1.90
CATMA1OA15700F1	AT1G16730	-1.45	-1.53	CATMA1OB20325R1	AT1G21270	2.27	1.45	CATMA1OA25700F1	AT1G27461	-1.91	-1.39
CATMA1OA15870R1	AT1G16880	-1.58	-1.08	CATMA1OF02529F1	AT1G21326	1.67	1.14	CATMA1OA25720R1	AT1G27480	-1.63	-1.20
CATMA1ON102147R1	AT1G17020	2.73	1.61	CATMA1ON102218F1	AT1G21350	-1.78	-1.22	CATMA1OA25965F1	AT1G27730	2.65	1.39
CATMA1ON102148R1	AT1G17050	-1.82	-1.27	CATMA1ON102219R1	AT1G21360	1.58	1.47	CATMA1OA25970R1	AT1G27740	3.71	2.08
CATMA1OA16085F1	AT1G17090	-1.92	-1.19	CATMA1OA20450F1	AT1G21390	1.72	1.26	CATMA1OA26010F1	AT1G27770	1.69	1.43
CATMA1OA16090R1	AT1G17100	-1.57	-1.43	CATMA1OA20470R1	AT1G21400	1.54	1.23	CATMA1OA26160R1	AT1G27980	1.97	1.07
CATMA1OC71256F1	AT1G17140	-1.34	-1.62	CATMA1OA20505R1	AT1G21450	1.74	1.31	CATMA1OA26240F1	AT1G28050	1.96	1.45
CATMA1OA16150F1	AT1G17147	1.76	2.01	CATMA1OA20550F1	AT1G21500	-1.89	-1.09	CATMA1OA26390F1	AT1G28190	1.57	1.58
CATMA1OC71257R1	AT1G17170	2.11	1.69	CATMA1ON94964F1	AT1G21520	10.48	1.41	CATMA1OA26405F1	AT1G28230	4.58	1.52
CATMA1OC71258R1	AT1G17180	1.70	1.36	CATMA1OA20580F1	AT1G21525	7.33	3.45	CATMA1OA26430F1	AT1G28260	1.91	1.51
CATMA1OA16240R1	AT1G17230	-1.04	-1.56	CATMA1OA20610F1	AT1G21540	-1.54	1.06	CATMA1OA26515F1	AT1G28330	1.45	1.78
CATMA1OA16280F1	AT1G17250	2.62	-1.07	CATMA1OA20760R1	AT1G21670	2.42	1.68	CATMA1OA26550F1	AT1G28370	2.76	1.26
CATMA1OA16330R1	AT1G17300	-2.83	-1.28	CATMA1OA20770R1	AT1G21680	1.29	1.55	CATMA1OA26570R1	AT1G28380	1.91	1.18
CATMA1OC71260F1	AT1G17380	1.56	1.09	CATMA1OA20840R1	AT1G21750	1.59	1.17	CATMA1OA26690F1	AT1G28480	2.44	1.57
CATMA1OC71263R1	AT1G17430	-1.27	1.86	CATMA1OA20890F1	AT1G21810	-1.53	-1.22	CATMA1OC71438F1	AT1G28570	1.51	1.01
CATMA1OA16510R1	AT1G17460	1.55	1.14	CATMA1OA20920F1	AT1G21850	1.43	2.18	CATMA1OA26790F1	AT1G28580	1.71	1.03
CATMA1ON102159F1	AT1G17650	-2.03	-1.44	CATMA1ON94967F1	AT1G21860	1.27	1.78	CATMA1OC71439F1	AT1G28600	1.61	-1.11
CATMA1OA16700F1	AT1G17665	1.71	1.37	CATMA1OA21215R1	AT1G22070	1.61	1.27	CATMA1OC71442R1	AT1G28680	1.62	1.03
CATMA1OA16740R1	AT1G17700	-1.68	-1.82	CATMA1OA21280R1	AT1G22150	1.98	-1.18	CATMA1OF02557F1	AT1G28700	-2.07	-1.38
CATMA1ON102162R1	AT1G17745	2.29	1.34	CATMA1OA21290R1	AT1G22160	2.36	-1.19	CATMA1OA27050R1	AT1G29070	-2.29	-1.47
CATMA1OC71265R1	AT1G17810	-1.58	-1.28	CATMA1OC71330F1	AT1G22180	1.75	1.13	CATMA1OA27080R1	AT1G29100	2.56	4.62
CATMA1OA16955R1	AT1G17950	1.14	1.59	CATMA1OA21460R1	AT1G22330	-1.52	-1.09	CATMA1OA27250R1	AT1G29270	1.61	1.23
CATMA1OA16960F1	AT1G17960	2.29	-1.26	CATMA1OC71338F1	AT1G22360	1.77	1.04	CATMA1OA27260R1	AT1G29280	2.14	1.46
CATMA1OA17070F1	AT1G18060	-2.14	-1.23	CATMA1OF00114F1	AT1G22370	2.55	1.13	CATMA1OA27270R1	AT1G29290	2.16	1.70
CATMA1OA17095F1	AT1G18100	2.86	-1.15	CATMA1OC71341R1	AT1G22440	1.62	1.14	CATMA1OA27305F1	AT1G29330	1.52	1.30
CATMA1OA17150R1	AT1G18170	-1.64	-1.36	CATMA1ON92265F1	AT1G22510	1.60	1.13	CATMA1ON102303F1	AT1G29395	3.15	1.38
CATMA1ON92402F1	AT1G18200	4.18	1.56	CATMA1OA21680F1	AT1G22570	1.28	1.71	CATMA1OF00201F1	AT1G29420	-1.25	-1.54
CATMA1OA17200F1	AT1G18210	1.71	1.22	CATMA1OA21690R1	AT1G22590	-1.94	-1.34	CATMA1ON92540F1	AT1G29430	-1.51	-1.64
CATMA1OC71274F1	AT1G18330	-1.82	-1.16	CATMA1OA21823R1	AT1G22770	1.49	1.72	CATMA1ON92689F1	AT1G29440	-1.45	-1.80

Table 22: Continued

		Ratio	
D CATMAv6	AGI	+Fe	-Fe
CATMA1ON102304F1	AT1G29450	-1.35	-1.89
CATMA1ON92113F1	AT1G29460	-1.39	-2.15
CATMA1ON92279R1	AT1G29490	-1.44	-2.24
CATMA1ON92388R1	AT1G29500	-1.38	-1.85
CATMA1ON92052R1	AT1G29510	-1.52	-1.73
CATMA1OA27485F1	AT1G29530	-1.54	-1.22
CATMA1OA27610F1	AT1G29690	1.65	1.13
CATMA1OA27620F1	AT1G29700	-1.70	-1.09
CATMA1OC71461F1	AT1G29720	-1.75	-2.13
CATMA1OF00212R1	AT1G29830	1.54	-1.02
CATMA1OA28065R1	AT1G30040	3.15	1.23
CATMA1OA28100F1	AT1G30080	1.75	1.30
CATMA1OA28190R1	AT1G30160	1.82	1.05
CATMA1OA28250F1	AT1G30220	1.59	1.09
CATMA1OA28393R1	AT1G30400	1.53	1.17
CATMA1OA28540R1	AT1G30520	-1.72	-1.10
CATMA1OA28550R1	AT1G30530	-1.01	-1.68
CATMA1OA28670R1	AT1G30620	1.75	-1.00
CATMA1OA28700R1	AT1G30650	1.90	1.17
CATMA1OA28740R1	AT1G30690	-1.59	-1.41
CATMA1OA28780R1	AT1G30730	3.52	1.18
CATMA1OA28800F1	AT1G30750	-1.62	-1.14
CATMA1OA28830R1	AT1G30760	5.59	-1.15
CATMA1OA28940F1	AT1G30820	1.57	1.43
CATMA1OA28980R1	AT1G30840	-8.30	1.08
CATMA1OA29020R1	AT1G30870	1.62	1.61
CATMA1OC71482F1	AT1G31050	-3.04	1.08
CATMA1OA29240F1	AT1G31060	-2.04	1.18
CATMA1OC71486F1	AT1G31130	1.57	1.10
CATMA1OA29555F1	AT1G31330	-1.36	1.84
CATMA1OA29810R1	AT1G31580	1.62	1.78
CATMA1OC71500R1	AT1G31710	-1.68	-1.33
CATMA1OA29980F1	AT1G31770	1.04	-1.52
CATMA1OA30010R1	AT1G31800	-1.83	-1.51
CATMA1OA30080F1	AT1G31820	2.25	1.15
CATMA1ON102339F1	AT1G31835	-1.97	-1.31
CATMA1OA30190F1	AT1G31920	-2.38	-1.86
CATMA1OA30400R1	AT1G32060	-1.62	-1.13
CATMA1OC71504F1	AT1G32100	-1.89	1.00
CATMA1ON92166F1	AT1G32110	-1.67	1.04
CATMA1OA30550F1	AT1G32200	-1.55	1.10
CATMA1OA30570R1	AT1G32220	-1.61	-1.14
CATMA1ON95020R1	AT1G32300	3.01	3.36
CATMA1OA30720F1	AT1G32350	1.22	1.75
CATMA1OA30770R1	AT1G32380	1.59	1.32
CATMA1OA30870F1	AT1G32470	-1.78	-1.40
CATMA1OA30910R1	AT1G32510	2.25	1.21
CATMA1OA30940R1	AT1G32540	-1.25	2.27
CATMA1OA30942F1	AT1G32550	-1.60	-1.15
CATMA1OC71516R1	AT1G32700	1.50	1.30
CATMA1ON102349R1	AT1G32740	1.08	2.04
CATMA1OC71521R1	AT1G32940	1.80	1.47
CATMA1OC71522R1	AT1G32960	2.50	1.26
CATMA1OA31300R1	AT1G32990	-1.55	-1.23
CATMA1OA31330F1	AT1G33030	2.65	1.16
CATMA1OA31520F1	AT1G33240	-1.53	-1.09
CATMA1OA31580R1	AT1G33290	-1.63	-1.20
CATMA1OA31710F1	AT1G33440	-2.75	-2.46
CATMA1OA31830R1	AT1G33560	2.09	1.19
CATMA1OF02569F1	AT1G33720	1.76	1.31
CATMA1OA31990R1	AT1G33760	1.60	1.24
CATMA1OC71542R1	AT1G33790	1.42	1.69
CATMA1OA32040R1	AT1G33810	-1.65	-1.17
CATMA1OA32195R1	AT1G33960	1.52	1.86
CATMA1OA32200F1	AT1G33970	1.67	1.34
CATMA1OA32230F1	AT1G34000	-1.51	-1.19
CATMA1OA32340R1	AT1G34050	1.83	3.69
CATMA1OA32360F1	AT1G34060	8.60	2.06
CATMA1OA32490R1	AT1G34180	3.43	1.00
CATMA1OA32560R1	AT1G34260	1.68	1.63
CATMA1OA32740R1	AT1G34420	1.62	1.35
CATMA1OC71559F1	AT1G34510	1.04	-1.85
CATMA1ON95044R1	AT1G34520	-1.71	-1.54
CATMA1OA33035R1	AT1G34680	-2.25	1.18
CATMA1OA33060F1	AT1G34760	2.38	1.45
CATMA1OA33270R1	AT1G35140	-1.21	-1.55
CATMA1ON92141F1	AT1G35170	-2.01	-1.41
CATMA1OF00254F1	AT1G35180	-2.46	-1.72
CATMA1OA33330R1	AT1G35190	1.64	1.12
CATMA1OA33350F1	AT1G35210	2.87	2.00
CATMA1OA33365R1	AT1G35230	3.32	1.85
CATMA1OC71566F1	AT1G35250	-1.99	1.14
CATMA1OA33420F1	AT1G35290	1.36	-2.05
CATMA1OA33430F1	AT1G35310	2.89	-1.01
CATMA1ON95048F1	AT1G35350	1.72	1.00
CATMA1ON102393F1	AT1G35580	1.51	1.48
CATMA1OA33890R1	AT1G35710	3.65	1.82
CATMA1OA34270R1	AT1G36180	2.24	1.08
CATMA1OA34520F1	AT1G36390	-1.60	-1.10
CATMA1OD02597F1	AT1G36950	1.69	1.44
CATMA1ON92582F1	AT1G42490	1.61	1.01
CATMA1OA36040R1	AT1G42550	-1.81	-1.42
CATMA1OA36300R1	AT1G42970	-2.28	-1.33
CATMA1OA36330F1	AT1G42990	1.93	1.22
CATMA1OA36370R1	AT1G43020	-1.62	-1.26
CATMA1OA36590R1	AT1G43160	-1.88	-1.28
CATMA1OA36890F1	AT1G43560	-1.67	-1.06
CATMA1OA37010F1	AT1G43650	-2.83	1.05
CATMA1OA37020R1	AT1G43670	-1.59	1.12
CATMA1OA37240R1	AT1G43790	-1.96	1.00
CATMA1OA37250R1	AT1G43800	-3.78	-5.13
CATMA1OA37400F1	AT1G43910	8.08	2.62
CATMA1OA37510F1	AT1G44000	-2.58	-1.51
CATMA1ON95070R1	AT1G44050	-1.56	1.06
CATMA1OA37610F1	AT1G44110	-1.51	-1.43
CATMA1OA37630F1	AT1G44130	1.78	1.45
CATMA1OC71613F1	AT1G44350	-1.40	-1.55
CATMA1OC71615F1	AT1G44446	-1.72	-1.09
CATMA1OC71618R1	AT1G44575	-1.59	-1.29
CATMA1OA37780F1	AT1G44800	-1.51	-1.31
CATMA1OA37880F1	AT1G44920	-1.57	1.12
CATMA1OA37930R1	AT1G45000	1.57	1.18
CATMA1OC71627F1	AT1G45010	-1.31	-1.71
CATMA1OA37950R1	AT1G45015	-1.67	-1.58
CATMA1OA38000F1	AT1G45145	1.68	1.48
CATMA1OA38050R1	AT1G45180	1.60	-1.07
CATMA1OC71631R1	AT1G45191	1.08	-3.34
CATMA1OC71632R1	AT1G45201	-1.15	-1.70
CATMA1OC71634F1	AT1G45230	-1.73	-1.12
CATMA1OC71663R1	AT1G47395	-1.90	-6.60
CATMA1OC71664R1	AT1G47400	-4.27	-4.25
CATMA1OD02628F1	AT1G47540	-18.1	-6.79
CATMA1OA38560R1	AT1G47580	-1.97	-1.43
CATMA1ON92104F1	AT1G47590	-1.62	1.10
CATMA1OA38970R1	AT1G47890	1.60	1.56
CATMA1OA39055F1	AT1G47960	2.16	-1.03
CATMA1OA39070F1	AT1G47980	1.07	-1.51
CATMA1OA39090F1	AT1G48000	4.27	1.02
CATMA1OA39150F1	AT1G48090	1.50	1.19
CATMA1OA39180R1	AT1G48100	-1.76	1.03
CATMA1OA39210R1	AT1G48130	-3.12	-2.22
CATMA1ON92232R1	AT1G48210	1.79	1.35
CATMA1OF02632_NR1	AT1G48220	1.69	1.37
CATMA1OA39330F1	AT1G48260	1.63	2.03
CATMA1OA39430R1	AT1G48350	-1.89	-1.26
CATMA1OA39460R1	AT1G48370	1.57	1.16
CATMA1OA39570R1	AT1G48470	-1.54	-1.24
CATMA1ON102535R1	AT1G48480	-1.69	-1.19
CATMA1OA39610R1	AT1G48510	1.52	-1.18
CATMA1OA39620R1	AT1G48520	-1.69	-1.48
CATMA1ON92604F1	AT1G48605	1.64	1.20
CATMA1OA39780R1	AT1G48640	1.62	1.33
CATMA1OC72379R1	AT1G48745	-2.56	-1.09
CATMA1ON92486R1	AT1G48750	-3.21	-1.66
CATMA1OA40070F1	AT1G48930	2.01	1.46
CATMA1OA40120R1	AT1G48990	-1.64	-1.15
CATMA1OA40130F1	AT1G49000	2.08	1.33
CATMA1OA40140R1	AT1G49010	-1.73	1.09
CATMA1OA40190R1	AT1G49050	1.85	1.30
CATMA1OC71712R1	AT1G49200	-2.64	-2.06
CATMA1OC71713R1	AT1G49210	-1.53	-1.07
CATMA1OF02635R1	AT1G49220	-2.54	-2.01
CATMA1OA40480F1	AT1G49360	1.70	1.10
CATMA1OA40500R1	AT1G49380	-1.74	-1.43
CATMA1OC71715R1	AT1G49390	1.70	1.18
CATMA1OA40560R1	AT1G49450	-1.60	1.04
CATMA1OA40570R1	AT1G49470	-1.66	-1.12
CATMA1OA40610F1	AT1G49500	-2.94	-1.54
CATMA1OA40620R1	AT1G49510	-1.57	-1.13
CATMA1OA40675R1	AT1G49570	4.63	-1.16
CATMA1OC71720R1	AT1G49720	1.84	1.69
CATMA1OC71721F1	AT1G49730	-1.75	1.16
	AT1G49820	2.62	1.61
CATMA1OA40940R1	AT1G49860	1.99	-1.46
CATMA1OC71726R1	AT1G49975	-1.68	-1.07
CATMA1OA41150R1	AT1G50040	-1.52	1.03
CATMA1OA41270R1	AT1G50180	-1.08	-1.76
CATMA1OA41325F1	AT1G50250	-1.79	-1.08
CATMA1OA41355F1	AT1G50290	-2.14	-1.13
CATMA1OA41375F1	AT1G50320	-1.95	1.10
CATMA1OA41480F1	AT1G50420	1.78	1.23
CATMA1OA41510F1	AT1G50450	-1.86	-1.38
CATMA1OA41630F1	AT1G50590	-2.04	-1.07
CATMA1OA41770R1	AT1G50730	-2.95	-1.43
CATMA1OA41790R1	AT1G50740	1.90	1.31
CATMA1OC71743R1	AT1G50900	-1.72	-1.02
CATMA1OA42150F1	AT1G51080	-1.82	-1.19
CATMA1OA42160R1	AT1G51090	1.55	1.11
CATMA1OA42170R1	AT1G51100	-1.94	-1.16
CATMA1OA42180R1	AT1G51110	-1.68	-1.45
CATMA1OA42340F1	AT1G51260	-1.55	1.40
CATMA1OA42350R1	AT1G51270	1.55	1.23
CATMA1OA42420R1	AT1G51340	1.05	-1.62
CATMA1OC71753F1	AT1G51420	2.27	1.33
CATMA1ON92136R1	AT1G51470	-1.30	1.54
CATMA1OC71754R1	AT1G51490	-1.33	1.55
CATMA1OA42740R1	AT1G51610	1.26	1.54
CATMA1OA42750R1	AT1G51620	1.51	-1.23
CATMA1OA42782F1	AT1G51680	1.58	1.07
CATMA1OC71758R1	AT1G51760	1.59	1.12
CATMA1OA42900F1	AT1G51805	1.52	-1.15
CATMA1ON95101F1	AT1G51820	1.45	-1.98
CATMA1ON95102F1	AT1G51830	1.99	-1.09
CATMA1OC71760F1	AT1G51840	2.47	-1.06
CATMA1ON92310F1	AT1G51850	1.62	-1.12
CATMA1OF00378_NF1	AT1G51860	2.04	1.17
CATMA1OB43120F1	AT1G52000	2.72	1.29
CATMA1OA43130F1	AT1G52050	-2.30	1.22
CATMA1OA43140F1	AT1G52060	-2.78	1.09
CATMA1OC71765F1	AT1G52070	-1.59	1.12
CATMA1OA43160F1	AT1G52100	-2.46	-1.79
CATMA1OA43190F1	AT1G52120	34.46	13.14
CATMA1OA43200F1	AT1G52130	5.81	3.20
CATMA1OA43260R1	AT1G52190	-1.78	-1.68
CATMA1OA43273F1	AT1G52220	-1.58	-1.04
CATMA1OA43455R1	AT1G52400	1.17	-1.52
CATMA1ON102614R1	AT1G52410	1.40	-1.66
CATMA1OA43550F1	AT1G52510	-1.77	-1.12
CATMA1OA43640F1	AT1G52590	-1.53	1.00
CATMA1OA43745R1	AT1G52690	1.52	-1.24
CATMA1ON95109F1	AT1G52700	1.66	-1.76
CATMA1OA43820R1	AT1G52760	1.58	1.08
CATMA1OC71784F1	AT1G52855	2.13	2.10
CATMA1OB43915F1	AT1G52880	1.52	1.32
CATMA1OA43920F1	AT1G52890	2.31	1.05
CATMA1OC71786F1	AT1G53035	1.50	1.75
CATMA1OA44160F1	AT1G53130	1.72	-1.02
CATMA1OA44260R1	AT1G53250	-1.62	-1.11
CATMA1OA44280R1	AT1G53270	-1.13	1.72
CATMA1OF00393F1	AT1G53340	1.58	1.24
CATMA1OC71791R1	AT1G53430	1.58	1.14
CATMA1OA44560F1	AT1G53520	-2.05	-1.50
CATMA1OA44590F1	AT1G53560	-1.88	-1.40
CATMA1OA44680F1	AT1G53635	1.87	1.34
CATMA1OA44750R1	AT1G53670	-1.95	-1.24
CATMA1OA44760R1	AT1G53680	-1.58	1.05
CATMA1OA44880F1	AT1G53790	2.85	1.41
CATMA1OA44930R1	AT1G53830	-3.29	-1.14
CATMA1OA45020R1	AT1G53910	1.59	1.69
CATMA1OA45100F1	AT1G54000	1.51	-1.34
CATMA1OF02651F1	AT1G54010	-1.19	-1.62
CATMA1OA45150F1	AT1G54050	-1.68	-1.21
CATMA1OA45210F1	AT1G54100	2.69	1.04
CATMA1OA45320R1	AT1G54200	1.80	1.00
CATMA1OC71811R1	AT1G54300	2.13	1.10
CATMA1OA45430R1	AT1G54310	-1.78	-1.06
CATMA1OA45460R1	AT1G54350	-1.40	-1.54
CATMA1OA45640F1	AT1G54500	-1.55	1.26
CATMA1OA45660R1	AT1G54520	-1.52	-1.01
CATMA1OA45720R1	AT1G54575	2.26	-1.47
CATMA1OA45760F1	AT1G54660	-4.55	1.30
CATMA1OA45820R1	AT1G54740	-2.12	-1.57
CATMA1OC71824R1	AT1G54780	-1.64	-1.04

Table 22: Continued

		Ratio	
D CATMAv6	AGI	+Fe	-Fe
CATMA1OA45873F1	AT1G54790	-2.18	-1.16
CATMA1OA45930F1	AT1G54860	-1.51	-1.13
CATMA1OA45940R1	AT1G54870	-1.21	-1.52
CATMA1OA45950R1	AT1G54890	1.25	1.78
CATMA1OA46000R1	AT1G54940	1.20	1.54
CATMA1OC71828R1	AT1G54970	1.84	1.55
CATMA1OA46052R1	AT1G55010	-1.35	-2.89
CATMA1OA46055R1	AT1G55020	3.40	-1.02
CATMA1OC71829R1	AT1G55090	-1.59	-1.18
CATMA1OA46140F1	AT1G55110	1.58	1.13
CATMA1OA46290R1	AT1G55240	-2.16	-1.01
CATMA1OA46460F1	AT1G55360	-1.02	-2.38
CATMA1OA46480R1	AT1G55370	-1.63	-1.38
CATMA1OA46560F1	AT1G55450	1.95	1.13
CATMA1OA46580R1	AT1G55480	-2.27	-1.31
CATMA1OA46590F1	AT1G55490	-1.96	-1.18
CATMA1OA46840F1	AT1G55760	1.86	1.59
CATMA1OC71844F1	AT1G55780	1.55	1.87
CATMA1OC71847F1	AT1G55805	-1.51	1.15
CATMA1OA47044R1	AT1G55850	1.90	-1.03
CATMA1OC71852R1	AT1G55910	-1.65	-1.18
CATMA1ON102668F1	AT1G55960	-2.17	-1.33
CATMA1OC71855F1	AT1G56010	1.87	1.31
CATMA1OA47120R1	AT1G56050	-2.40	-1.10
CATMA1OC71857F1	AT1G56060	2.16	1.44
CATMA1OA47150F1	AT1G56080	1.63	1.22
CATMA1OC71859F1	AT1G56120	1.77	1.69
CATMA1OA47240F1	AT1G56145	1.78	1.33
CATMA1OA47250R1	AT1G56150	-1.34	-1.63
CATMA1OA47260R1	AT1G56160	2.03	1.73
CATMA1OA47270R1	AT1G56170	-1.09	-1.72
CATMA1OA47290R1	AT1G56190	-1.51	-1.27
CATMA1OD02660F1	AT1G56240	4.12	2.06
CATMA1OC71861F1	AT1G56250	4.48	2.56
CATMA1OA47390F1	AT1G56300	1.65	2.08
CATMA1OA47520R1	AT1G56430	-4.05	-3.39
CATMA1OA47590R1	AT1G56510	2.33	-1.06
CATMA1OA47670F1	AT1G56580	-1.03	-1.53
CATMA1OA47745F1	AT1G56650	1.80	-1.17
CATMA1OA47890F1	AT1G57590	1.62	-1.10
CATMA1OD00438R1	AT1G57630	2.75	2.11
CATMA1OA48060R1	AT1G57770	-1.98	-1.63
CATMA1OF00443F1	AT1G57990	2.18	1.36
CATMA1OA48228R1	AT1G58070	-1.82	-1.14
CATMA1OA48310R1	AT1G58190	1.70	-1.09
CATMA1OC71874R1	AT1G58225	4.64	1.54
CATMA1OA48460F1	AT1G58290	-1.52	2.21
CATMA1OA48485F1	AT1G58320	2.98	1.18
CATMA1OA48493R1	AT1G58340	1.71	2.20
CATMA1OA48540F1	AT1G58410	1.76	1.15
CATMA1OC71877R1	AT1G58520	-1.51	-1.40
CATMA1ON102693R1	AT1G58602	2.09	1.15
CATMA1OA48657R1	AT1G59620	1.81	1.31
CATMA1ON95141F1	AT1G59640	1.54	-1.13
CATMA1OA48770R1	AT1G59740	2.06	1.01
CATMA1OA48900R1	AT1G59840	-1.84	-1.81
CATMA1OA48930R1	AT1G59870	2.64	1.37
CATMA1OA49050F1	AT1G60000	-1.67	-1.12
CATMA1OA49070F1	AT1G60030	2.19	1.01
CATMA1OA49090F1	AT1G60050	1.58	-1.12
CATMA1ON92681F1	AT1G60270	-1.63	-1.71
CATMA1OC71889F1	AT1G60470	-2.65	1.37
CATMA1OA49570F1	AT1G60550	-1.74	-1.39
CATMA1OA49600F1	AT1G60590	-1.52	-1.96
CATMA1OA49610F1	AT1G60600	-1.86	-1.11
CATMA1OA49620F1	AT1G60610	2.14	1.28
CATMA1OC71894F1	AT1G60730	3.49	1.73
CATMA1OF00476R1	AT1G60740	2.08	2.01
CATMA1OC72405F1	AT1G60750	1.48	1.97
CATMA1OA49900F1	AT1G60890	1.89	1.13
CATMA1OC71897R1	AT1G60950	-1.57	1.51
CATMA1OA49950F1	AT1G60960	-1.62	2.06
CATMA1OA50180F1	AT1G61130	-1.76	-1.62
CATMA1OA50310F1	AT1G61260	1.75	1.72
CATMA1OA50390R1	AT1G61340	2.05	1.29
CATMA1OA50410F1	AT1G61360	2.27	1.11
CATMA1OA50420F1	AT1G61370	1.62	1.09
CATMA1ON92491R1	AT1G61415	1.21	1.56
CATMA1ON92491F1	AT1G61420	2.07	1.31
CATMA1ON102713F1	AT1G61460	1.95	1.31
CATMA1OA50640F1	AT1G61560	2.92	1.10
CATMA1OA50710R1	AT1G61610	1.55	-1.06
CATMA1OA50760R1	AT1G61667	-1.67	-1.19
CATMA1OC72411R1	AT1G61795	-1.54	1.45
CATMA1OA50880R1	AT1G61800	1.87	-1.44
CATMA1OA50890R1	AT1G61810	1.73	1.17
CATMA1OC71919R1	AT1G61820	1.72	1.55
CATMA1ON95163R1	AT1G62181	2.45	1.22
CATMA1OA51340F1	AT1G62262	1.62	1.01
CATMA1OA51380F1	AT1G62290	-1.68	-1.18
CATMA1OA51390F1	AT1G62300	2.17	1.27
CATMA1ON102724F1	AT1G62305	1.51	1.11
CATMA1OA51570F1	AT1G62420	1.46	-7.88
CATMA1ON102726R1	AT1G62500	-1.84	-1.42
CATMA1OA51630F1	AT1G62510	-3.23	-1.23
CATMA1OA51660R1	AT1G62540	2.83	-1.38
CATMA1OA51680R1	AT1G62560	-1.32	-2.77
CATMA1OA51770R1	AT1G62660	1.60	1.10
CATMA1OC71938F1	AT1G62750	-1.73	-1.12
CATMA1OA51915F1	AT1G62780	-1.83	-1.16
CATMA1OA51930F1	AT1G62810	2.19	1.15
CATMA1ON92177R1	AT1G62840	2.19	1.34
CATMA1OC71945F1	AT1G62935	-1.56	-1.01
CATMA1OA52120F1	AT1G62960	-1.91	-1.28
CATMA1OC71946R1	AT1G62975	-3.13	-2.30
CATMA1OA52180F1	AT1G63010	1.61	1.05
CATMA1OA52660R1	AT1G63440	2.38	1.64
CATMA1OA52770R1	AT1G63560	1.07	1.92
CATMA1OA52940F1	AT1G63710	-1.39	-1.89
CATMA1OA52950F1	AT1G63720	2.54	1.51
CATMA1OC71963R1	AT1G63750	2.88	1.02
CATMA1OA53090F1	AT1G63860	1.19	-1.03
CATMA1ON92455F1	AT1G63990	1.02	1.57
CATMA1OA53240R1	AT1G64000	1.59	1.10
CATMA1OA53300R1	AT1G64065	2.24	1.18
CATMA1OA53400F1	AT1G64150	-1.73	-1.23
CATMA1OA53410R1	AT1G64160	30.24	1.19
CATMA1OC71969F1	AT1G64200	-2.35	-1.52
CATMA1OA53640R1	AT1G64355	-1.61	-1.24
CATMA1OA53670F1	AT1G64380	-2.21	-1.28
CATMA1OA53730R1	AT1G64430	-1.56	-1.32
CATMA1ON95180F1	AT1G64480	1.25	-1.50
CATMA1OA53790R1	AT1G64500	-3.46	-2.27
CATMA1OA53800F1	AT1G64510	-2.12	-1.36
CATMA1OA53820R1	AT1G64530	-1.52	-1.12
CATMA1OA53900R1	AT1G64590	-2.77	2.13
CATMA1OA53940R1	AT1G64625	1.84	-1.03
CATMA1OC71976F1	AT1G64640	-1.81	-1.57
CATMA1OA53980R1	AT1G64660	2.83	1.34
CATMA1OA54000R1	AT1G64680	-1.84	-1.24
CATMA1OA54020F1	AT1G64700	1.69	-1.08
CATMA1OA54030R1	AT1G64710	2.43	1.49
CATMA1OA54040F1	AT1G64720	-1.61	-1.28
CATMA1OA54080R1	AT1G64770	-1.66	-1.43
CATMA1OA54205R1	AT1G64900	-1.16	1.68
CATMA1OA54210F1	AT1G64910	-1.25	1.75
CATMA1ON92380R1	AT1G64940	1.51	1.44
CATMA1OC71982R1	AT1G64950	1.51	1.25
CATMA1OA54270F1	AT1G64980	-1.28	-3.17
CATMA1OA54370F1	AT1G65090	-4.49	-2.30
CATMA1ON102762F1	AT1G65150	-1.03	-1.61
CATMA1OA54520R1	AT1G65230	-1.66	-1.24
CATMA1ON92238R1	AT1G65310	-1.76	-1.22
CATMA1OA54690F1	AT1G65370	1.57	-1.01
CATMA1OA54790R1	AT1G65450	-1.29	-1.68
CATMA1OC71995R1	AT1G65500	4.70	-1.65
CATMA1OC71996R1	AT1G65510	2.00	1.15
CATMA1OA54840F1	AT1G65520	1.57	1.10
CATMA1OA54870F1	AT1G65570	-2.65	1.43
CATMA1OA54970F1	AT1G65690	5.07	1.31
CATMA1ON95196R1	AT1G65790	1.72	1.50
CATMA1OA55080R1	AT1G65800	1.59	1.46
CATMA1OA55110R1	AT1G65820	1.67	1.33
CATMA1OC72001F1	AT1G65845	1.13	-1.53
CATMA1OC72002F1	AT1G65860	-1.33	-3.21
CATMA1OF00535R1	AT1G65870	-1.73	-1.46
CATMA1OA55190F1	AT1G65900	-1.76	-1.51
CATMA1ON92496F1	AT1G65970	2.83	1.41
CATMA1OA55350R1	AT1G66090	3.54	1.15
CATMA1OA55360F1	AT1G66100	-2.70	-4.70
CATMA1OA55390R1	AT1G66130	-1.58	-1.26
CATMA1OA55410R1	AT1G66160	2.01	-1.08
CATMA1OA55490R1	AT1G66230	-3.37	-2.15
CATMA1ON95199F1	AT1G66280	1.61	-1.02
CATMA1OA55600F1	AT1G66330	-1.58	-1.19
CATMA1OF02692_NR1	AT1G66380	1.75	-1.03
CATMA1OA55685R1	AT1G66390	2.86	1.05
CATMA1OA55740F1	AT1G66460	-1.83	1.01
CATMA1OA55770F1	AT1G66480	1.85	1.12
CATMA1OA55820R1	AT1G66540	-2.20	-1.33
CATMA1OF00552F1	AT1G66690	6.91	2.19
CATMA1OD02694F1	AT1G66700	21.24	4.75
CATMA1OD00555R1	AT1G66725	-2.51	-1.93
CATMA1OA56100R1	AT1G66820	-1.68	-1.19
CATMA1OA56120F1	AT1G66840	-1.82	-1.67
CATMA1OA56170R1	AT1G66880	1.96	1.15
CATMA1OA56210F1	AT1G66920	2.22	-1.58
CATMA1OA56230F1	AT1G66940	-2.03	-2.62
CATMA1OA56290F1	AT1G67000	3.31	-1.07
CATMA1OA56390F1	AT1G67090	-1.52	-1.12
CATMA1OC72425R1	AT1G67148	5.17	1.16
CATMA1OA56480R1	AT1G67150	1.74	1.35
CATMA1OA56620F1	AT1G67310	1.53	1.14
CATMA1OA56690F1	AT1G67370	1.10	1.94
CATMA1OA56910R1	AT1G67560	1.66	-1.04
CATMA1OA57080R1	AT1G67700	-1.85	-1.34
CATMA1OA57105F1	AT1G67740	-1.54	1.07
CATMA1ON102790R1	AT1G67750	1.33	-1.60
CATMA1OA57120F1	AT1G67760	3.31	1.02
CATMA1OA57200F1	AT1G67800	2.38	1.29
CATMA1OA57210R1	AT1G67810	3.67	2.32
CATMA1OA57290F1	AT1G67865	-2.06	1.23
CATMA1OC72047F1	AT1G67970	2.52	2.17
CATMA1OA57396R1	AT1G67980	4.08	1.82
CATMA1OC72051R1	AT1G68010	-2.13	-1.26
CATMA1OA57435R1	AT1G68050	2.56	2.26
CATMA1OA57480R1	AT1G68110	-1.60	-1.15
CATMA1OA57610R1	AT1G68238	-3.97	-1.72
CATMA1OC72054F1	AT1G68260	-1.55	-1.07
CATMA1ON95210F1	AT1G68280	-1.61	-1.03
CATMA1OA57680R1	AT1G68290	2.89	1.15
CATMA1OA57710R1	AT1G68320	1.18	2.42
CATMA1OA57770R1	AT1G68390	1.03	1.58
CATMA1OA57830F1	AT1G68450	1.51	1.93
CATMA1OA57900F1	AT1G68520	1.75	-1.13
CATMA1OA57940R1	AT1G68570	1.41	-1.52
CATMA1OC72060F1	AT1G68590	-1.76	-1.04
CATMA1OA57980R1	AT1G68600	2.94	1.40
CATMA1OA58000R1	AT1G68620	1.80	1.24
CATMA1OA58030R1	AT1G68650	1.34	2.01
CATMA1OA58110R1	AT1G68725	-1.53	-1.25
CATMA1OA58130F1	AT1G68740	-2.60	-1.89
CATMA1OA58170F1	AT1G68780	-1.63	-1.54
CATMA1OA58210R1	AT1G68810	-1.62	-1.07
CATMA1OA58250F1	AT1G68850	-1.12	1.90
CATMA1ON92586F1	AT1G68862	-1.78	-1.47
CATMA1OA58260R1	AT1G68870	-1.76	-1.64
CATMA1OA58290F1	AT1G68880	3.60	2.15
CATMA1OA58420R1	AT1G69050	2.07	2.55
CATMA1OA58490R1	AT1G69160	-1.35	-1.51
CATMA1OA58510R1	AT1G69200	-1.52	-1.10
CATMA1OA58530F1	AT1G69230	-2.13	-1.04
CATMA1OC72069F1	AT1G69270	1.69	1.03
CATMA1OC72070R1	AT1G69325	1.88	1.13
CATMA1OA58690R1	AT1G69410	1.54	-1.07
CATMA1OA58740F1	AT1G69450	1.79	1.21
CATMA1OA58770F1	AT1G69480	1.65	1.09
CATMA1OA58800R1	AT1G69490	9.38	2.29
CATMA1OC72074R1	AT1G69520	1.59	-1.26
CATMA1OA58905F1	AT1G69570	-1.73	-2.27
CATMA1OA59050R1	AT1G69740	-1.66	-1.10
CATMA1OA59100R1	AT1G69790	2.73	1.61
CATMA1OA59160F1	AT1G69840	1.69	1.12
CATMA1OA59180R1	AT1G69870	2.59	1.01
CATMA1OA59190R1	AT1G69880	11.05	1.08
CATMA1OA59200F1	AT1G69890	1.96	1.70
CATMA1OA59230F1	AT1G69920	3.27	1.44
CATMA1OA59240F1	AT1G69930	4.63	1.51
CATMA1ON95217F1	AT1G70140	2.03	-1.18
CATMA1OA59500F1	AT1G70200	-1.57	-1.01
CATMA1OA59540F1	AT1G70260	4.64	1.35
CATMA1OA59550R1	AT1G70270	2.94	-2.20
CATMA1OA59570F1	AT1G70290	1.65	-1.09

Table 22: Continued

		Ratio	
D CATMAv6	AGI	+Fe	-Fe
CATMA1OA59635F1	AT1G70370	-1.77	-1.26
CATMA1OA59710F1	AT1G70440	1.88	1.23
CATMA1OA59780F1	AT1G70520	2.02	1.10
CATMA1OA59790F1	AT1G70530	1.72	1.24
CATMA1OA59830R1	AT1G70560	1.00	1.55
CATMA1OC72090R1	AT1G70760	-1.57	-1.21
CATMA1OC72092R1	AT1G70810	2.17	1.27
CATMA1OA60100R1	AT1G70820	1.25	1.57
CATMA1OA60110F1	AT1G70830	1.33	-1.92
CATMA1OA60130F1	AT1G70850	-3.07	-1.53
CATMA1OC72438F1	AT1G70860	-2.43	-1.55
CATMA1OA60160F1	AT1G70880	-1.15	-1.54
CATMA1ON92300F1	AT1G70885	-1.66	-1.41
CATMA1OA60230R1	AT1G70950	1.52	-1.11
CATMA1OA60270F1	AT1G70985	-2.98	-1.80
CATMA1OA60280F1	AT1G70990	-1.54	-1.11
CATMA1OA60300R1	AT1G71010	1.74	1.27
CATMA1OA60310F1	AT1G71015	-1.38	-1.68
CATMA1OA60325F1	AT1G71030	-1.83	-1.31
CATMA1OA60330F1	AT1G71040	1.92	1.31
CATMA1OA60390R1	AT1G71100	1.97	1.01
CATMA1OA60400R1	AT1G71110	1.68	1.22
CATMA1OA60430R1	AT1G71140	5.10	2.42
CATMA1OA60700F1	AT1G71380	2.04	1.19
CATMA1OA60720R1	AT1G71400	2.06	1.42
CATMA1OA60820R1	AT1G71500	-1.98	-1.04
CATMA1OA60840R1	AT1G71530	1.43	1.77
CATMA1OA60870F1	AT1G71691	-1.13	-1.58
CATMA1OA60940R1	AT1G71740	-1.55	-1.25
CATMA1OA61020F1	AT1G71810	-1.86	-1.29
CATMA1OA61090F1	AT1G71870	-1.51	-1.41
CATMA1OA61250R1	AT1G72030	-1.80	-1.66
CATMA1OA61460R1	AT1G72230	-1.91	-1.08
CATMA1OA61530F1	AT1G72280	2.18	1.36
CATMA1OA61650F1	AT1G72430	-2.28	-1.69
CATMA1OA61750R1	AT1G72520	3.17	1.61
CATMA1OA61860F1	AT1G72640	-1.89	-1.44
CATMA1ON102843R1	AT1G72645	-1.89	-1.80
CATMA1OA61890F1	AT1G72670	-1.59	-1.26
CATMA1OA61900F1	AT1G72680	1.97	1.15
CATMA1OA62020R1	AT1G72790	1.05	1.55
CATMA1OA62055F1	AT1G72830	1.99	1.34
CATMA1OA62090R1	AT1G72870	1.67	1.33
CATMA1ON95224R1	AT1G72900	4.35	1.53
CATMA1ON102847R1	AT1G72910	1.70	1.28
CATMA1OC72124R1	AT1G72920	2.15	-1.19
CATMA1OA62155R1	AT1G72930	1.56	1.40
CATMA1OA62185R1	AT1G72970	-1.25	-1.61
CATMA1OA62270F1	AT1G73040	2.19	-1.32
CATMA1OA62290R1	AT1G73060	-1.79	-1.26
CATMA1OA62340F1	AT1G73110	-1.64	-1.23
CATMA1OA62360F1	AT1G73120	14.68	3.38
CATMA1OA62410F1	AT1G73165	-2.26	-1.21
CATMA1OC72132R1	AT1G73190	-4.90	-3.41
CATMA1OA62540F1	AT1G73260	9.97	-1.24
CATMA1ON95226F1	AT1G73290	-1.60	-1.14
CATMA1ON95227F1	AT1G73310	-1.68	-1.18
CATMA1OA62630F1	AT1G73330	-8.61	1.37
CATMA1ON102851F1	AT1G73500	1.89	1.12
CATMA1OA62850F1	AT1G73550	1.51	-1.08
CATMA1OA62950R1	AT1G73630	-1.62	-1.33
CATMA1OA62980F1	AT1G73655	-1.80	1.10
CATMA1OA63030F1	AT1G73700	1.66	1.74
CATMA1OC72137F1	AT1G73805	1.39	2.16
CATMA1OA63140F1	AT1G73810	1.68	1.76
CATMA1OA63200R1	AT1G73870	-4.56	-2.62
CATMA1OA63240R1	AT1G73885	-1.56	-1.21
CATMA1OA63356F1	AT1G74000	2.22	2.19
CATMA1OA63360F1	AT1G74010	4.25	1.92
CATMA1OB63370F1	AT1G74020	1.59	1.16
CATMA1OA63440F1	AT1G74070	-2.18	-1.39
CATMA1OA63470R1	AT1G74090	-1.59	-1.69
CATMA1OA63750R1	AT1G74360	1.78	1.49
CATMA1OA63760F1	AT1G74370	-1.66	-1.21
CATMA1OC72150F1	AT1G74440	1.07	1.16
CATMA1OA63870F1	AT1G74460	-2.33	1.17
CATMA1OA63980F1	AT1G74590	8.27	1.64
CATMA1OA64020R1	AT1G74650	1.88	1.31
CATMA1OA64030F1	AT1G74660	-1.51	1.06
CATMA1OA64040R1	AT1G74670	-1.75	-1.27
CATMA1OA64075R1	AT1G74710	1.69	1.34
CATMA1OC72154R1	AT1G74730	-1.73	1.08
CATMA1OA64120F1	AT1G74770	2.27	-1.25
CATMA1ON95231R1	AT1G74810	3.23	-1.25
CATMA1ON95232F1	AT1G74880	-1.58	-1.40
CATMA1ON95233F1	AT1G74890	-1.76	-1.31
CATMA1OA64335F1	AT1G74970	-1.91	-1.35
CATMA1OA64350R1	AT1G75000	1.84	1.20
CATMA1OC72158R1	AT1G75030	-1.56	-1.02
CATMA1OA64430F1	AT1G75100	-2.46	-1.28
CATMA1OC72159F1	AT1G75120	-1.19	-1.74
CATMA1OA64590F1	AT1G75250	-3.77	1.68
CATMA1OD02716R1	AT1G75290	1.54	-1.06
CATMA1OA64680R1	AT1G75350	-2.02	-1.32
CATMA1OA64720F1	AT1G75380	1.54	1.20
CATMA1OA64800R1	AT1G75460	-1.69	1.17
CATMA1OA64980F1	AT1G75680	-1.50	-1.23
CATMA1OA64990F1	AT1G75690	-2.65	-1.30
CATMA1OC72165F1	AT1G75750	-1.58	1.05
CATMA1OA65113R1	AT1G75830	-1.33	-2.27
CATMA1OA65180R1	AT1G75910	1.33	3.39
CATMA1ON92286R1	AT1G76040	1.90	1.00
CATMA1OA65330F1	AT1G76110	-1.68	-1.11
CATMA1OA65440F1	AT1G76240	-2.03	-1.11
CATMA1OC72178R1	AT1G76410	2.78	1.74
CATMA1OC72179R1	AT1G76450	-2.57	-1.36
CATMA1OC72180F1	AT1G76460	-1.52	-1.02
CATMA1OA65690F1	AT1G76470	2.26	1.32
CATMA1OA65720R1	AT1G76520	2.31	1.36
CATMA1OA65770R1	AT1G76570	-1.82	-1.31
CATMA1OA65790R1	AT1G76590	2.25	1.88
CATMA1OA65800R1	AT1G76600	1.86	1.13
CATMA1OA65860F1	AT1G76650	2.22	1.45
CATMA1OF02719R1	AT1G76705	-1.63	-1.19
CATMA1OA66020R1	AT1G76800	2.58	1.18
CATMA1OC72188F1	AT1G76930	1.88	-1.05
CATMA1ON92048F1	AT1G76952	-3.16	1.06
CATMA1OA66190F1	AT1G76960	7.07	2.58
CATMA1OA66210F1	AT1G76970	2.06	1.28
CATMA1OA66220F1	AT1G76980	2.11	1.36
CATMA1OA66250R1	AT1G77000	1.90	1.49
CATMA1OA66290F1	AT1G77060	-1.52	1.11
CATMA1OA66300F1	AT1G77090	-1.73	-1.18
CATMA1OA66500F1	AT1G77280	2.08	1.50
CATMA1OA66550F1	AT1G77330	-1.85	1.02
CATMA1OA66600F1	AT1G77380	7.65	1.10
CATMA1OA66671R1	AT1G77490	-2.07	-1.16
CATMA1OC72199R1	AT1G77510	1.89	1.21
CATMA1OC72201R1	AT1G77530	-2.80	-1.06
CATMA1OA66840F1	AT1G77690	-1.60	-1.32
CATMA1OA66910F1	AT1G77760	-1.83	-1.18
CATMA1OA67050R1	AT1G77890	1.92	1.46
CATMA1OA67060R1	AT1G77920	2.72	1.12
CATMA1ON102937F1	AT1G77990	1.54	-1.61
CATMA1OA67190R1	AT1G78080	1.63	-1.06
CATMA1OA67195R1	AT1G78090	-2.36	-1.22
CATMA1OA67240F1	AT1G78120	-1.86	-1.02
CATMA1OA67260F1	AT1G78140	-1.55	1.02
CATMA1OA67310R1	AT1G78180	-1.61	-1.09
CATMA1OA67350R1	AT1G78230	-2.41	-1.30
CATMA1OA67370R1	AT1G78260	-1.64	-1.64
CATMA1OA67410F1	AT1G78290	1.71	1.35
CATMA1OA67430F1	AT1G78320	-3.39	1.05
CATMA1OC72216F1	AT1G78340	-1.15	1.72
CATMA1OC72217F1	AT1G78360	2.50	1.01
CATMA1OA67470F1	AT1G78370	-1.13	-1.77
CATMA1OA67500R1	AT1G78410	3.43	1.95
CATMA1OA67530F1	AT1G78450	-2.81	-1.34
CATMA1OA67540F1	AT1G78460	1.77	1.13
CATMA1OA67590F1	AT1G78510	-1.83	-1.35
CATMA1OA67690R1	AT1G78630	-1.73	-1.28
CATMA1OA67860F1	AT1G78780	1.64	1.40
CATMA1OC72226F1	AT1G78820	-1.71	-1.32
CATMA1OA67930F1	AT1G78830	1.60	1.02
CATMA1OA68030F1	AT1G78915	-1.94	-1.34
CATMA1OA68060F1	AT1G78950	-1.63	1.28
CATMA1ON92515R1	AT1G78970	1.79	-1.16
CATMA1OA68100F1	AT1G78990	-1.74	1.33
CATMA1OA68110F1	AT1G78995	-1.51	1.23
CATMA1OA68310R1	AT1G79180	3.27	1.14
CATMA1OA68420R1	AT1G79320	-1.28	2.17
CATMA1OA68430R1	AT1G79330	-1.08	1.70
CATMA1OB68460F1	AT1G79360	1.72	1.04
CATMA1ON102953F1	AT1G79440	1.52	1.26
CATMA1OA68540R1	AT1G79450	2.28	1.16
CATMA1OA68590F1	AT1G79510	-1.57	-1.03
CATMA1OA68620F1	AT1G79530	1.57	1.13
CATMA1OA68830F1	AT1G79700	-1.19	1.73
CATMA1OA68900R1	AT1G79760	-1.81	1.37
CATMA1OA68910R1	AT1G79770	-1.39	-1.52
CATMA1OA68930F1	AT1G79790	-1.83	-1.24
CATMA1OA68980F1	AT1G79830	1.04	1.52
CATMA1OA69000F1	AT1G79850	-1.97	-1.31
CATMA1OA69010F1	AT1G79860	1.24	1.66
CATMA1OA69210F1	AT1G80030	-1.72	-1.22
CATMA1OA69290R1	AT1G80110	2.15	1.32
CATMA1OA69310F1	AT1G80130	8.04	-1.26
CATMA1ON92544F1	AT1G80133	1.13	1.61
CATMA1OA69340R1	AT1G80160	15.12	1.17
CATMA1OA69430F1	AT1G80240	1.72	1.48
CATMA1OA69533F1	AT1G80340	-8.82	-1.59
CATMA1OA69540F1	AT1G80360	2.90	3.36
CATMA1OA69550R1	AT1G80380	-1.95	-1.02
CATMA1OA69620R1	AT1G80440	2.12	-1.03
CATMA1OA69770R1	AT1G80570	1.98	1.24
CATMA1OA69790F1	AT1G80590	1.60	1.03
CATMA1OA70050R1	AT1G80820	1.96	1.21
CATMA1OB70055F1	AT1G80830	2.92	1.21
CATMA1ON92243R1	AT1G80840	2.54	1.09
CATMA2OA00260F1	AT2G01180	2.37	1.15
CATMA2ON90732F1	AT2G01290	-1.54	-1.23
CATMA2OA00410R1	AT2G01340	2.25	1.04
CATMA2OA00475F1	AT2G01420	1.56	-1.22
CATMA2OA00510R1	AT2G01460	1.08	1.65
CATMA2ON90698R1	AT2G01464	-1.04	1.66
CATMA2OA00550F1	AT2G01505	1.16	1.57
CATMA2OC47009R1	AT2G01520	-6.57	-1.20
CATMA2ON90609R1	AT2G01530	-4.14	-1.82
CATMA2OA00720F1	AT2G01670	2.00	1.22
CATMA2OA00810F1	AT2G01755	-1.80	-1.36
CATMA2ON90853F1	AT2G01818	-1.61	1.19
CATMA2OA00910R1	AT2G01860	-2.05	-1.07
CATMA2OC47010F1	AT2G01880	2.61	2.21
CATMA2OA00940F1	AT2G01890	1.82	1.59
CATMA2OA00970F1	AT2G01918	-2.66	-1.58
CATMA2OA01040R1	AT2G01980	1.51	1.13
CATMA2OC47012F1	AT2G02010	3.55	-1.03
CATMA2OA01080R1	AT2G02020	-1.89	-1.12
CATMA2OA01180R1	AT2G02120	4.02	1.74
CATMA2OD00616R1	AT2G02130	-1.79	-1.11
CATMA2OC47015F1	AT2G02250	2.51	1.48
CATMA2OA01287F1	AT2G02310	6.01	2.76
CATMA2OA01304R1	AT2G02370	1.53	1.39
CATMA2OD02731R1	AT2G02390	2.15	1.35
CATMA2OC47022F1	AT2G02500	-1.52	-1.36
CATMA2ON90850R1	AT2G02610	-2.11	-1.35
CATMA2ON90463R1	AT2G02640	-1.88	-1.36
CATMA2OA01720F1	AT2G02820	-1.83	-1.02
CATMA2OA01770F1	AT2G02850	1.80	1.29
CATMA2ON90433F1	AT2G02930	4.80	1.22
CATMA2OA01885R1	AT2G02990	2.40	1.07
CATMA2ON101345F1	AT2G03090	-2.63	-1.87
CATMA2OA02230F1	AT2G03310	-1.21	1.58
CATMA2ON90713F1	AT2G03420	-1.57	-1.01
CATMA2OC47040R1	AT2G03530	2.11	1.08
CATMA2OA02510R1	AT2G03590	2.10	-1.03
CATMA2OA02595R1	AT2G03710	-1.97	-1.53
CATMA2OA02660F1	AT2G03750	-2.06	-1.96
CATMA2OA02665F1	AT2G03760	1.52	1.46
CATMA2OA02970R1	AT2G04032	1.29	-1.63
CATMA2ON101347R1	AT2G04039	-1.63	-1.20
CATMA2ON90412F1	AT2G04070	1.55	1.39
CATMA2ON90696F1	AT2G04080	1.37	1.51
CATMA2OA03130F1	AT2G04160	1.70	1.01
CATMA2ON94717R1	AT2G04260	3.17	1.79
CATMA2OA03395R1	AT2G04400	1.54	1.08
CATMA2OC47061R1	AT2G04495	2.20	1.83
CATMA2OC47063R1	AT2G04515	1.24	-1.52
CATMA2OA03700R1	AT2G04790	-2.77	-1.61
CATMA2OA03720F1	AT2G04800	-1.90	1.13
CATMA2OA04040F1	AT2G05160	-2.22	1.09
CATMA2OA04160F1	AT2G05310	-1.72	-1.16
CATMA2OC47084R1	AT2G05440	2.05	1.03

Table 22: Continued

		Ratio	
D CATMAv6	AGI	+Fe	-Fe
CATMA2ON94725R1	AT2G05441	3.20	1.55
CATMA2OC47085R1	AT2G05510	4.69	1.69
CATMA2OA04310R1	AT2G05540	-3.69	-1.23
CATMA2OA04320R1	AT2G05580	-3.88	-2.32
CATMA2OA04350F1	AT2G05620	-2.02	-1.23
CATMA2ON101367F1	AT2G05630	1.51	1.52
CATMA2OA04450R1	AT2G05710	1.35	1.87
CATMA2OC47092F1	AT2G05715	-1.87	-1.42
CATMA2OA04620R1	AT2G05830	2.05	1.90
CATMA2OA04670F1	AT2G05910	1.94	1.42
CATMA2OA04740F1	AT2G05940	1.69	1.26
CATMA2OA04825F1	AT2G06050	1.77	-1.07
CATMA2OA05200F1	AT2G06530	1.68	1.16
CATMA2OA05540R1	AT2G06850	-1.34	-1.69
CATMA2ON94730F1	AT2G07440	-1.91	-1.17
CATMA2OA06230F1	AT2G07600	-2.01	-1.01
CATMA2OA06250R1	AT2G07640	1.77	1.42
CATMA2ON101449F1	AT2G07723	1.53	1.06
CATMA2OA07380R1	AT2G07727	1.26	1.62
CATMA2OA07560F1	AT2G07739	-1.92	1.00
CATMA2OA06380F1	AT2G07777	1.05	-1.65
CATMA2ON90714F1	AT2G10557	-1.50	-1.02
CATMA2OA09080F1	AT2G10920	1.66	1.12
CATMA2OA09920R1	AT2G11810	3.26	1.11
CATMA2OA10000R1	AT2G11930	-1.76	-1.01
CATMA2OF00745F1	AT2G12190	1.64	1.33
CATMA2OA10610F1	AT2G12462	-1.90	-1.24
CATMA2ON90680F1	AT2G12660	-2.44	-1.36
CATMA2OD05059R1	AT2G12905	-2.00	1.36
CATMA2OA12410R1	AT2G13790	2.16	1.21
CATMA2OA12420R1	AT2G13800	1.93	1.35
CATMA2OA12430R1	AT2G13810	-1.38	3.37
CATMA2ON94747R1	AT2G14080	1.68	-1.03
CATMA2OA12670F1	AT2G14095	-1.62	2.19
CATMA2OA12750R1	AT2G14247	-3.18	-5.47
CATMA2OC47174R1	AT2G14560	4.33	4.06
CATMA2OC47176F1	AT2G14610	2.96	1.49
CATMA2OA13400R1	AT2G14660	-1.68	-1.12
CATMA2ON101541R1	AT2G14840	1.66	-1.24
CATMA2OA13640F1	AT2G14880	-1.81	-1.17
CATMA2OA13810R1	AT2G15010	-4.76	-1.54
CATMA2OA13820F1	AT2G15020	-12.61	-4.83
CATMA2OC47913R1	AT2G15040	1.67	1.38
CATMA2OC47187R1	AT2G15050	-1.10	-1.57
CATMA2OD02807R1	AT2G15220	2.27	1.16
CATMA2ON90476F1	AT2G15350	-2.16	-1.42
CATMA2ON94756F1	AT2G15370	-1.94	-1.34
CATMA2OF00788F1	AT2G15390	1.96	1.12
CATMA2OC47194R1	AT2G15480	1.86	1.27
CATMA2OA14420R1	AT2G15490	2.23	1.38
CATMA2OA14670F1	AT2G15760	1.51	1.15
CATMA2OA14690F1	AT2G15780	14.94	1.10
CATMA2OA14730R1	AT2G15830	1.12	2.13
CATMA2OA14770F1	AT2G15890	2.15	2.28
CATMA2ON101563F1	AT2G16005	3.58	-2.99
CATMA2OC47210F1	AT2G16060	1.01	-2.78
CATMA2OA15130F1	AT2G16310	1.58	-1.06
CATMA2OA15380F1	AT2G16660	1.97	1.49
CATMA2OC47231R1	AT2G16700	1.96	1.19
CATMA2ON90595R1	AT2G16835	-1.60	-1.40
CATMA2OC47235R1	AT2G16850	-1.17	-1.58
CATMA2OC47239R1	AT2G16980	-2.18	1.04
CATMA2OA15760R1	AT2G17040	6.52	1.22
CATMA2OA16010R1	AT2G17280	1.76	1.33
CATMA2OB16020F1	AT2G17300	-2.00	-1.37
CATMA2OA16160F1	AT2G17470	1.56	-1.00
CATMA2OA16360F1	AT2G17695	-1.70	-1.29
CATMA2OA16390R1	AT2G17710	1.48	1.62
CATMA2OA16420F1	AT2G17740	-1.85	-1.82
CATMA2OA16486F1	AT2G17820	1.77	-1.05
CATMA2OA16520F1	AT2G17850	1.01	-1.67
CATMA2ON90788R1	AT2G17972	-2.66	-1.38
CATMA2OA16680R1	AT2G18000	1.52	1.19
CATMA2OA16790F1	AT2G18120	-1.01	-1.53
CATMA2OA16820F1	AT2G18150	5.37	1.49
CATMA2ON94772F1	AT2G18190	1.00	1.52
CATMA2OA16860F1	AT2G18193	2.29	1.24
CATMA2OC47917R1	AT2G18328	-2.47	-1.21
CATMA2OA17010F1	AT2G18350	1.54	1.32
CATMA2OC47266F1	AT2G18360	2.15	1.12
CATMA2OA17040F1	AT2G18380	-1.55	-1.23
CATMA2OA17220R1	AT2G18560	-2.12	1.00
CATMA2OC47271R1	AT2G18570	-1.79	-1.19
CATMA2OA17260F1	AT2G18600	2.67	1.07
CATMA2OC47273F1	AT2G18660	11.96	2.58
CATMA2OA17340R1	AT2G18690	3.47	1.78
CATMA2OA17350R1	AT2G18700	1.29	1.63
CATMA2OA17355F1	AT2G18710	-1.54	-1.53
CATMA2OA17420R1	AT2G18800	-2.66	-1.43
CATMA2OA17490R1	AT2G18890	-2.05	-1.55
CATMA2ON90448F1	AT2G18969	-1.81	-1.34
CATMA2OA17670R1	AT2G19060	-3.00	-1.22
CATMA2OC47292R1	AT2G19200	-1.99	1.35
CATMA2OA18025R1	AT2G19450	1.59	1.35
CATMA2OA18070F1	AT2G19500	1.58	-1.06
CATMA2OA18190F1	AT2G19650	-1.55	-1.72
CATMA2OC47312F1	AT2G19800	-1.16	1.68
CATMA2OA18340R1	AT2G19810	1.64	1.32
CATMA2OA18410F1	AT2G19900	2.34	1.17
CATMA2OA18460F1	AT2G19970	1.55	-2.53
CATMA2OA18480F1	AT2G19990	1.76	-1.77
CATMA2OA18500F1	AT2G20010	1.51	1.16
CATMA2OA18520R1	AT2G20030	3.02	2.30
CATMA2OF00812R1	AT2G20142	5.50	1.44
CATMA2OA18740F1	AT2G20270	-1.54	-1.02
CATMA2OA18790R1	AT2G20320	1.57	1.34
CATMA2OA19210F1	AT2G20670	-3.46	-1.50
CATMA2OA19260F1	AT2G20720	-1.08	2.67
CATMA2OA19280F1	AT2G20724	-1.71	-1.14
CATMA2OA19310R1	AT2G20750	-1.70	-1.25
CATMA2OA19410F1	AT2G20825	2.71	1.55
CATMA2OA19440F1	AT2G20835	-1.25	-1.83
CATMA2OA19490R1	AT2G20890	-1.88	-1.33
CATMA2OA19595R1	AT2G20960	1.61	1.28
CATMA2OA19690R1	AT2G21045	-1.56	-1.04
CATMA2OA19750F1	AT2G21100	-1.87	1.04
CATMA2OA19780F1	AT2G21130	1.77	1.49
CATMA2OA19790F1	AT2G21140	-1.34	-1.59
CATMA2OA19870F1	AT2G21210	-4.45	-1.98
CATMA2OC47340R1	AT2G21220	-2.29	-1.30
CATMA2OA19980F1	AT2G21280	-1.71	-1.52
CATMA2OA20010R1	AT2G21320	-2.80	-2.52
CATMA2OA20020F1	AT2G21330	-1.62	-1.26
CATMA2OA20070R1	AT2G21385	-1.95	-1.32
CATMA2OA20175F1	AT2G21490	-1.58	-1.09
CATMA2OA20180F1	AT2G21500	1.88	1.15
CATMA2OA20210R1	AT2G21530	-1.55	-1.03
CATMA2OA20230R1	AT2G21550	1.68	1.11
CATMA2OA20240F1	AT2G21560	-1.74	1.11
CATMA2OA20260R1	AT2G21590	1.33	-2.86
CATMA2OA20300R1	AT2G21640	1.59	1.35
CATMA2OA20310R1	AT2G21650	-1.66	3.05
CATMA2OA20440F1	AT2G21840	1.67	1.05
CATMA2OA20450R1	AT2G21850	1.63	1.41
CATMA2OA20460F1	AT2G21860	-1.87	-1.26
CATMA2OA20480F1	AT2G21880	-1.61	-1.22
CATMA2ON90731F1	AT2G21895	3.23	1.48
CATMA2OA20500F1	AT2G21900	2.33	3.24
CATMA2OC47348R1	AT2G21960	-1.87	-1.24
CATMA2OA20740F1	AT2G22200	-1.71	-1.03
CATMA2OC47356F1	AT2G22240	1.83	-1.33
CATMA2OA20940R1	AT2G22420	1.56	-1.03
CATMA2OA20953F1	AT2G22430	1.90	1.28
CATMA2OA20970R1	AT2G22450	1.14	1.55
CATMA2OA21030F1	AT2G22510	-2.16	1.81
CATMA2OA21090R1	AT2G22590	-1.59	-1.19
CATMA2OF00825R1	AT2G22630	-3.06	1.07
CATMA2OA21150F1	AT2G22650	-1.52	-1.15
CATMA2OA21260R1	AT2G22770	-1.56	-1.56
CATMA2OA21340R1	AT2G22860	5.65	1.29
CATMA2ON90706F1	AT2G22880	2.38	1.48
CATMA2OC47366R1	AT2G22920	-2.11	-1.04
CATMA2ON94791R1	AT2G22960	-1.64	-1.16
CATMA2OA21470R1	AT2G22980	-2.32	1.17
CATMA2OC47370R1	AT2G22990	-1.68	-1.13
CATMA2OC47372R1	AT2G23010	2.51	1.22
CATMA2OC47373F1	AT2G23030	2.86	1.47
CATMA2OA21630R1	AT2G23130	-2.03	-1.30
CATMA2OA21655F1	AT2G23150	8.93	1.22
CATMA2OA21780R1	AT2G23270	1.32	1.63
CATMA2OA21820R1	AT2G23320	1.68	1.12
CATMA2ON94799F1	AT2G23400	-1.56	1.34
CATMA2OA21877F1	AT2G23410	-1.53	1.13
CATMA2OA21910F1	AT2G23450	1.62	1.24
CATMA2OA21940R1	AT2G23540	-1.96	1.41
CATMA2ON94800F1	AT2G23560	-2.10	1.08
CATMA2OF00834F1	AT2G23590	-1.51	-1.26
CATMA2ON94801F1	AT2G23620	1.13	-1.59
CATMA2OA22030F1	AT2G23630	1.51	1.26
CATMA2OA22040R1	AT2G23640	-1.80	-1.36
CATMA2OA22060F1	AT2G23670	-1.75	-1.13
CATMA2OA22070R1	AT2G23680	3.37	1.37
CATMA2OA22080R1	AT2G23690	-1.51	-1.58
CATMA2OA22170F1	AT2G23810	1.82	1.31
CATMA2OA22310R1	AT2G23970	1.31	1.51
CATMA2OC47400F1	AT2G24020	-1.70	-1.22
CATMA2OA22410R1	AT2G24060	-1.79	-1.17
CATMA2OA22440R1	AT2G24090	-2.18	-1.32
CATMA2OA22500F1	AT2G24160	1.69	-1.07
CATMA2OA22515R1	AT2G24180	2.97	1.39
CATMA2OA22560R1	AT2G24240	1.65	1.09
CATMA2OA22590F1	AT2G24260	1.88	1.16
CATMA2OA22720R1	AT2G24395	-1.70	-1.18
CATMA2OA22760F1	AT2G24430	1.31	1.54
CATMA2OA22870R1	AT2G24540	-2.83	-2.10
CATMA2ON94805F1	AT2G24600	3.49	1.04
CATMA2OA23050F1	AT2G24710	3.89	1.84
CATMA2OA23060F1	AT2G24720	1.70	2.01
CATMA2OA23140R1	AT2G24762	-2.98	-1.83
CATMA2OA23220F1	AT2G24850	2.76	2.28
CATMA2OA23280F1	AT2G24970	-1.28	-1.52
CATMA2ON90591R1	AT2G24980	1.71	1.60
CATMA2OA23405R1	AT2G25080	-2.23	1.01
CATMA2OA23430R1	AT2G25110	1.83	1.03
CATMA2ON90481R1	AT2G25410	-1.04	1.54
CATMA2OA23790F1	AT2G25450	1.58	1.19
CATMA2OB23810R1	AT2G25470	-1.20	-2.30
CATMA2OA23850R1	AT2G25510	1.49	1.64
CATMA2OA23980R1	AT2G25625	2.65	2.46
CATMA2OA24060F1	AT2G25680	-2.68	-1.82
CATMA2OA24110F1	AT2G25730	1.30	1.50
CATMA2OA24120F1	AT2G25735	2.04	1.27
CATMA2OA24230F1	AT2G25830	-1.69	-1.20
CATMA2OA24240R1	AT2G25840	-1.63	-1.16
CATMA2OA24320F1	AT2G25940	1.84	1.23
CATMA2OA24450F1	AT2G26080	-1.58	-1.08
CATMA2OA24670R1	AT2G26310	1.74	1.26
CATMA2OA24680R1	AT2G26340	-1.74	-1.30
CATMA2OA24700R1	AT2G26370	2.78	-1.02
CATMA2OA24710F1	AT2G26380	2.34	1.04
CATMA2OA24760R1	AT2G26440	1.76	1.24
CATMA2OA24810R1	AT2G26480	1.89	1.36
CATMA2OA24825R1	AT2G26500	-1.77	1.76
CATMA2OA24850R1	AT2G26520	-1.67	-1.06
CATMA2OA24855F1	AT2G26530	2.29	1.31
CATMA2OA24880F1	AT2G26560	5.97	2.60
CATMA2OA24970R1	AT2G26640	-1.59	-1.15
CATMA2OA25010R1	AT2G26695	2.13	1.03
CATMA2OA25030R1	AT2G26710	1.69	1.54
CATMA2OC47440F1	AT2G26740	1.62	1.04
CATMA2OF02846F1	AT2G26750	1.75	1.08
CATMA2OA25140R1	AT2G26820	-3.72	-2.39
CATMA2OA25270F1	AT2G26930	-1.54	-1.37
CATMA2OA25400R1	AT2G27035	-1.59	1.07
CATMA2OA25440R1	AT2G27080	2.11	1.35
CATMA2OA25510R1	AT2G27130	-1.56	-1.33
CATMA2OA25525R1	AT2G27150	1.91	1.12
CATMA2OB25570R1	AT2G27200	1.62	1.34
CATMA2OA25680F1	AT2G27290	-1.78	-1.03
CATMA2OA25770F1	AT2G27370	-1.98	-1.15
CATMA2OC47452R1	AT2G27380	-1.28	-1.86
CATMA2OF02848F1	AT2G27395	-7.29	-3.56
CATMA2OC47453R1	AT2G27402	-2.78	-2.59
CATMA2OA25830F1	AT2G27420	-4.27	-2.77
CATMA2OA25980F1	AT2G27535	1.70	-1.01
CATMA2OA25985R1	AT2G27550	3.03	-1.14
CATMA2OA26090F1	AT2G27680	-1.52	-1.12
CATMA2OC47461R1	AT2G27740	-1.56	1.00
CATMA2OA26310F1	AT2G27920	1.16	1.54
CATMA2OA26390R1	AT2G28000	-1.51	-1.15
CATMA2OA26510F1	AT2G28110	1.57	1.04
CATMA2OA26520R1	AT2G28120	1.57	1.41
CATMA2OA26560R1	AT2G28160	1.52	1.46

Table 22: Continued

		Ratio	
D CATMAv6	AGI	+Fe	-Fe
CATMA2OA26583R1	AT2G28190	-1.79	-1.16
CATMA2OA26640R1	AT2G28250	-1.73	-1.04
CATMA2OA26660R1	AT2G28270	1.61	-1.06
CATMA2OA26840F1	AT2G28400	1.76	1.28
CATMA2ON101726R1	AT2G28410	-1.70	-1.07
CATMA2OA26900F1	AT2G28470	-1.81	-1.49
CATMA2OA26920F1	AT2G28490	-6.27	-3.24
CATMA2OA26930F1	AT2G28500	2.63	1.35
CATMA2OA26990R1	AT2G28570	3.04	-1.25
CATMA2OA27030R1	AT2G28605	-1.93	-1.29
CATMA2OA27045F1	AT2G28630	-1.56	-2.17
CATMA2OA27070R1	AT2G28660	1.95	1.15
CATMA2ON90485F1	AT2G28670	-1.64	-1.01
CATMA2OA27100F1	AT2G28690	3.05	1.12
CATMA2OA27110F1	AT2G28700	2.28	-1.18
CATMA2OA27190F1	AT2G28780	-1.62	-1.27
CATMA2ON101728F1	AT2G28800	-1.57	-1.09
CATMA2OA27220F1	AT2G28820	-1.82	1.27
CATMA2OA27290F1	AT2G28900	1.75	1.04
CATMA2OA27330F1	AT2G28940	1.60	1.19
CATMA2OB27340F1	AT2G28950	-1.57	-1.76
CATMA2OA27360R1	AT2G28970	-1.68	1.07
CATMA2OA27480R1	AT2G29070	1.59	1.07
CATMA2OC47481F1	AT2G29170	-1.86	1.13
CATMA2OA27610R1	AT2G29180	-1.89	-1.72
CATMA2ON90827R1	AT2G29280	-1.51	-1.60
CATMA2OC47483R1	AT2G29300	-1.06	-1.84
CATMA2OA27730R1	AT2G29330	2.08	-1.26
CATMA2OA27740R1	AT2G29340	1.83	1.11
CATMA2OA27750R1	AT2G29350	4.49	2.16
CATMA2OC47485R1	AT2G29360	-1.74	-1.21
CATMA2OC47486F1	AT2G29440	1.83	1.48
CATMA2OD02856F1	AT2G29460	9.64	2.51
CATMA2OC47487F1	AT2G29470	2.02	1.19
CATMA2OA28050R1	AT2G29660	-1.56	1.13
CATMA2OA28065R1	AT2G29680	-1.53	-1.06
CATMA2OA28085F1	AT2G29720	2.28	1.51
CATMA2OA28230R1	AT2G29870	-1.14	1.77
CATMA2OC47499F1	AT2G29995	1.97	1.27
CATMA2OA28340R1	AT2G30010	-1.13	-1.61
CATMA2OA28376R1	AT2G30070	-1.23	-1.55
CATMA2OA28440R1	AT2G30140	2.83	1.56
CATMA2OA28490F1	AT2G30210	-1.53	1.03
CATMA2OA28530F1	AT2G30250	1.76	1.34
CATMA2OA28765F1	AT2G30520	-1.96	-1.73
CATMA2OC47507F1	AT2G30540	-1.63	-1.96
CATMA2OA28860R1	AT2G30600	-1.52	1.32
CATMA2OC47511F1	AT2G30660	13.60	2.77
CATMA2OC47512F1	AT2G30670	6.56	-1.18
CATMA2OA28940F1	AT2G30695	-1.52	-1.29
CATMA2ON90691F1	AT2G30750	26.56	2.27
CATMA2ON90626R1	AT2G30766	-5.07	-4.68
CATMA2ON90522F1	AT2G30770	15.76	2.63
CATMA2OB29040F1	AT2G30790	-1.93	-1.10
CATMA2OA29070F1	AT2G30840	2.09	1.08
CATMA2OC47519R1	AT2G30942	1.68	1.10
CATMA2OA29145R1	AT2G30950	-1.52	-1.11
CATMA2OC47523R1	AT2G31083	-1.91	-1.15
CATMA2OC47524R1	AT2G31085	-3.50	1.63
CATMA2OA29340F1	AT2G31110	1.55	-1.25
CATMA2OA29390F1	AT2G31170	-1.59	-1.25
CATMA2OC47528F1	AT2G31180	5.50	-1.15
CATMA2OA29570F1	AT2G31345	2.47	1.47
CATMA2OC47531R1	AT2G31380	-2.84	-2.88
CATMA2OA29950F1	AT2G31730	-1.27	-1.70
CATMA2OC47539R1	AT2G31790	-1.69	-1.64
CATMA2OA30110F1	AT2G31865	5.06	1.59
CATMA2OC47541R1	AT2G31880	2.20	1.26
CATMA2OA30220R1	AT2G31945	2.34	2.02
CATMA2OA30260F1	AT2G31990	-1.79	1.23
CATMA2OC47543F1	AT2G32020	1.65	1.31
CATMA2OA30460F1	AT2G32180	-1.66	-1.33
CATMA2OC47548R1	AT2G32190	2.20	1.40
CATMA2OD02863R1	AT2G32200	2.64	1.69
CATMA2OC47550R1	AT2G32270	-3.82	-1.45
CATMA2OA30590R1	AT2G32280	2.05	1.14
CATMA2OA30615R1	AT2G32300	-1.63	-1.35
CATMA2OC47951R1	AT2G32487	1.52	1.21
CATMA2OA30820R1	AT2G32550	-3.02	-1.08
CATMA2OM00181R1	AT2G32610	-1.22	1.55
CATMA2OA30880F1	AT2G32640	-1.56	-1.38
CATMA2ON90712R1	AT2G32650	-1.65	-1.33
CATMA2OA30920F1	AT2G32660	5.50	1.15
CATMA2OA30940F1	AT2G32680	1.81	1.45
CATMA2ON101779F1	AT2G32880	-3.03	-1.30
CATMA2OC47562R1	AT2G32960	2.29	-1.01
CATMA2OA31180R1	AT2G32990	-2.59	1.04
CATMA2ON94833F1	AT2G33020	2.12	1.85
CATMA2OC47565F1	AT2G33070	-1.80	-1.39
CATMA2OA31330R1	AT2G33180	-2.09	-1.15
CATMA2OA31410R1	AT2G33250	-1.53	-1.20
CATMA2OC47569F1	AT2G33330	-1.84	-1.35
CATMA2OA31540F1	AT2G33380	2.03	1.01
CATMA2OA31610R1	AT2G33450	-1.88	-1.26
CATMA2OA31650R1	AT2G33490	1.62	1.35
CATMA2OA31740R1	AT2G33570	-1.57	-1.31
CATMA2OA32000F1	AT2G33800	-1.73	-1.25
CATMA2OA32020F1	AT2G33830	1.19	2.48
CATMA2OA32070F1	AT2G33850	-1.37	-2.43
CATMA2OA32080F1	AT2G33855	-1.61	-1.18
CATMA2OA32190R1	AT2G34060	-1.64	-1.12
CATMA2OB32300F1	AT2G34180	2.27	1.09
CATMA2OC47593F1	AT2G34450	-1.50	-1.19
CATMA2OA32630F1	AT2G34490	1.10	-1.95
CATMA2OA32640F1	AT2G34500	1.96	-1.45
CATMA2OA32710F1	AT2G34580	-1.09	1.51
CATMA2OA32740R1	AT2G34610	7.03	1.35
CATMA2OC47595R1	AT2G34620	-1.57	-1.16
CATMA2OA32773F1	AT2G34650	2.52	1.32
CATMA2OD05077R1	AT2G34655	1.49	1.88
CATMA2OA32820F1	AT2G34700	-3.85	-1.74
CATMA2OA32930R1	AT2G34810	-1.72	-1.41
CATMA2OB32950F1	AT2G34830	2.83	2.50
CATMA2OA32960R1	AT2G34840	1.21	1.50
CATMA2OA32980R1	AT2G34860	-1.81	-1.33
CATMA2OA32990R1	AT2G34870	-5.58	-2.81
CATMA2OA33010F1	AT2G34890	1.36	1.95
CATMA2OA33030R1	AT2G34910	1.94	2.60
CATMA2OA33070F1	AT2G34960	1.69	-1.28
CATMA2OC47600R1	AT2G35070	1.10	1.79
CATMA2ON101807R1	AT2G35090	1.01	1.81
CATMA2OA33270F1	AT2G35130	-1.66	-1.38
CATMA2OA33400R1	AT2G35270	1.76	1.26
CATMA2OA33490F1	AT2G35350	1.64	1.21
CATMA2OC47603R1	AT2G35370	-1.58	-1.16
CATMA2OA33510R1	AT2G35380	-1.77	1.36
CATMA2OA33520R1	AT2G35410	-1.59	-1.21
CATMA2OA33590R1	AT2G35500	-1.84	-1.30
CATMA2OA33850F1	AT2G35680	1.24	1.29
CATMA2OC47609F1	AT2G35730	2.63	1.34
CATMA2OA33940F1	AT2G35770	-2.10	-1.02
CATMA2OB34000R1	AT2G35820	-1.51	-1.23
CATMA2OD02870R1	AT2G35830	-1.51	-1.11
CATMA2OA34030R1	AT2G35850	2.99	1.99
CATMA2OA34120F1	AT2G35930	2.08	1.38
CATMA2OA34130F1	AT2G35940	1.78	1.20
CATMA2ON90783R1	AT2G35960	-1.72	-1.24
CATMA2OA34180R1	AT2G35980	9.30	1.80
CATMA2OC47613R1	AT2G35990	1.31	-1.54
CATMA2OA34280F1	AT2G36080	1.52	1.16
CATMA2OA34300F1	AT2G36100	-1.84	-1.02
CATMA2OA34450F1	AT2G36261	2.01	1.16
CATMA2OA34460F1	AT2G36270	1.94	1.07
CATMA2OA34480R1	AT2G36295	-1.82	1.52
CATMA2OA34690R1	AT2G36430	-1.52	-1.23
CATMA2OA34750F1	AT2G36490	-1.13	-1.57
CATMA2OA34770F1	AT2G36530	1.53	1.22
CATMA2OA34810R1	AT2G36570	-1.60	-1.30
CATMA2OA34860F1	AT2G36630	-2.15	-1.28
CATMA2OA34865F1	AT2G36640	-2.22	-1.26
CATMA2OB34910R1	AT2G36690	-1.60	-1.71
CATMA2OA34980F1	AT2G36750	1.06	2.67
CATMA2ON90646F1	AT2G36760	1.03	2.14
CATMA2OF02874F1	AT2G36770	1.61	1.80
CATMA2OA35085R1	AT2G36830	-2.48	-1.62
CATMA2OA35140F1	AT2G36870	-2.13	-1.91
CATMA2OA35230R1	AT2G36950	1.72	1.33
CATMA2OA35250R1	AT2G36970	2.88	1.27
CATMA2OA35265F1	AT2G36990	-1.72	-1.08
CATMA2OA35300R1	AT2G37025	-2.55	-1.57
CATMA2ON90837R1	AT2G37030	-1.55	-1.22
CATMA2OA35330F1	AT2G37040	1.59	1.12
CATMA2OA35370R1	AT2G37070	-1.03	1.52
CATMA2OA35385F1	AT2G37090	-1.79	1.05
CATMA2OA35400R1	AT2G37110	1.77	1.24
CATMA2OC47630F1	AT2G37170	-2.02	-1.31
CATMA2OA35456R1	AT2G37180	-2.56	-1.39
CATMA2OA35650R1	AT2G37380	-1.91	-1.23
CATMA2OA35720R1	AT2G37440	-1.96	-1.01
CATMA2OC47636F1	AT2G37450	-1.84	-1.40
CATMA2OA35740F1	AT2G37460	-1.87	-1.04
CATMA2OA35920F1	AT2G37640	-1.66	-1.36
CATMA2OA35940F1	AT2G37660	-1.96	-1.18
CATMA2OB35995F1	AT2G37710	2.03	1.04
CATMA2ON101845R1	AT2G37720	-1.84	-2.06
CATMA2OA36020F1	AT2G37740	1.64	1.04
CATMA2OA36040R1	AT2G37760	1.97	1.11
CATMA2OA36240R1	AT2G37940	1.58	1.22
CATMA2ON94852F1	AT2G38025	-1.61	-1.09
CATMA2OA36370R1	AT2G38080	-1.59	1.11
CATMA2OA36435R1	AT2G38140	-1.86	-1.24
CATMA2OA36520R1	AT2G38210	-2.26	-1.07
CATMA2OA36550F1	AT2G38240	2.16	1.46
CATMA2OA36560R1	AT2G38250	1.78	1.11
CATMA2OA36595F1	AT2G38290	2.02	1.22
CATMA2OA36620R1	AT2G38320	-2.10	1.02
CATMA2OA36640F1	AT2G38340	1.25	1.51
CATMA2OC47649R1	AT2G38380	1.67	1.05
CATMA2OA36690R1	AT2G38390	-1.84	-1.05
CATMA2OC47650F1	AT2G38465	1.87	1.76
CATMA2OC47651R1	AT2G38470	3.45	1.09
CATMA2OA36770F1	AT2G38480	-1.53	-1.10
CATMA2OA36780F1	AT2G38490	1.36	1.52
CATMA2OA36890R1	AT2G38600	-2.16	-1.32
CATMA2OA36920F1	AT2G38640	-1.64	-1.90
CATMA2OC47655R1	AT2G38695	-1.66	-1.22
CATMA2OA37000R1	AT2G38720	-1.58	-1.18
CATMA2OA37026F1	AT2G38750	-1.48	-2.21
CATMA2OA37033R1	AT2G38760	-1.48	-1.72
CATMA2OA37050R1	AT2G38780	-1.91	-1.34
CATMA2OA37060F1	AT2G38790	1.65	1.75
CATMA2OC47656R1	AT2G38823	2.42	4.85
CATMA2OA37120F1	AT2G38860	2.81	1.12
CATMA2OC47658F1	AT2G38905	-1.71	-1.13
CATMA2OA37175R1	AT2G38940	-1.22	-1.68
CATMA2OA37280F1	AT2G39040	-4.94	-1.24
CATMA2OA37430F1	AT2G39200	-2.12	-1.27
CATMA2OA37440F1	AT2G39210	1.62	1.18
CATMA2OA37480F1	AT2G39250	-2.15	1.02
CATMA2OA37500R1	AT2G39270	1.47	1.70
CATMA2OA37550F1	AT2G39310	-1.25	-2.51
CATMA2OA37610F1	AT2G39360	1.52	-1.09
CATMA2ON101862F1	AT2G39380	2.09	-1.14
CATMA2OC47663R1	AT2G39400	1.94	1.29
CATMA2OA37680R1	AT2G39420	-1.53	1.28
CATMA2OC47664R1	AT2G39430	-1.55	-1.05
CATMA2ON90423R1	AT2G39470	-2.40	-1.49
CATMA2OA37780F1	AT2G39510	1.77	-2.51
CATMA2OA37830F1	AT2G39560	-1.74	-1.11
CATMA2OA37900F1	AT2G39650	1.84	1.39
CATMA2OA37910R1	AT2G39660	1.78	1.09
CATMA2OK00018R1	AT2G39725	1.54	1.10
CATMA2OA37967F1	AT2G39730	-1.79	-1.14
CATMA2OA38140F1	AT2G39920	2.07	3.82
CATMA2OA38300F1	AT2G40080	1.37	1.56
CATMA2ON101864R1	AT2G40095	2.01	1.59
CATMA2OA38335R1	AT2G40100	-1.55	1.48
CATMA2ON101865R1	AT2G40110	-1.02	1.64
CATMA2ON101866R1	AT2G40140	2.25	1.26
CATMA2OA38400R1	AT2G40150	-2.48	-1.42
CATMA2OA38420R1	AT2G40160	-1.78	1.10
CATMA2OA38430F1	AT2G40170	1.90	1.43
CATMA2ON101867R1	AT2G40180	1.40	1.59
CATMA2OA38460R1	AT2G40200	2.07	1.06
CATMA2OB38570F1	AT2G40300	1.69	2.70
CATMA2OA38620F1	AT2G40340	2.30	2.49
CATMA2ON90504F1	AT2G40350	1.48	2.34
CATMA2OA38650F1	AT2G40370	1.19	1.76
CATMA2OA38680R1	AT2G40400	-3.61	-1.31
CATMA2OA38810R1	AT2G40490	-1.62	-1.26
CATMA2OA38880R1	AT2G40570	-1.53	-1.04
CATMA2OA38930F1	AT2G40610	-1.76	-1.64
CATMA2OA38980R1	AT2G40670	-1.59	-1.33

Table 22: Continued

		Ratio	
D CATMAv6	AGI	+Fe	-Fe
CATMA2OA38990R1	AT2G40690	-1.62	-1.40
CATMA2OA39060F1	AT2G40750	-1.21	1.78
CATMA2OA39080R1	AT2G40760	-1.56	-1.20
CATMA2OA39180R1	AT2G40840	1.75	1.23
CATMA2OA39230F1	AT2G40900	-2.72	-1.49
CATMA2OA39280F1	AT2G40940	1.79	1.05
CATMA2OA39310R1	AT2G40960	-2.21	-1.70
CATMA2OA39400F1	AT2G41050	-1.52	-1.42
CATMA2OA39435R1	AT2G41090	1.64	1.21
CATMA2OC47695R1	AT2G41100	2.94	1.37
CATMA2OA39530R1	AT2G41180	1.74	1.19
CATMA2OA39540F1	AT2G41190	-1.35	-1.52
CATMA2OA39590F1	AT2G41240	-1.19	-13.94
CATMA2OA39600F1	AT2G41250	-1.46	-1.52
CATMA2OA39655R1	AT2G41310	-1.62	-1.10
CATMA2OA39750R1	AT2G41380	7.42	-1.12
CATMA2OA39780F1	AT2G41410	2.38	1.05
CATMA2OA39890F1	AT2G41480	-1.38	-1.53
CATMA2OA40020R1	AT2G41640	1.85	1.26
CATMA2OA40060F1	AT2G41680	-1.71	-1.04
CATMA2OA40080F1	AT2G41700	1.68	1.04
CATMA2OA40110F1	AT2G41720	-1.58	-1.04
CATMA2OF02886R1	AT2G41730	2.25	1.61
CATMA2OA40160R1	AT2G41780	1.58	1.08
CATMA2OD02887F1	AT2G41810	-3.26	-1.02
CATMA2OA40400R1	AT2G41990	-2.04	-1.26
CATMA2ON90529R1	AT2G42060	-2.12	-1.44
CATMA2OA40520R1	AT2G42130	-1.62	-1.35
CATMA2OA40560R1	AT2G42170	-2.16	1.00
CATMA2OA40585R1	AT2G42200	-1.62	-1.35
CATMA2OA40600R1	AT2G42220	-2.32	-1.63
CATMA2OA40730F1	AT2G42340	1.08	2.06
CATMA2OA40820R1	AT2G42430	1.58	1.01
CATMA2OA40960F1	AT2G42530	6.90	2.42
CATMA2OC47720F1	AT2G42540	1.76	1.05
CATMA2OA41060F1	AT2G42660	1.51	2.09
CATMA2OA41180R1	AT2G42750	-1.15	-2.10
CATMA2OA41220F1	AT2G42790	1.10	1.27
CATMA2OA41290F1	AT2G42870	-1.76	1.33
CATMA2OA41305R1	AT2G42890	1.46	1.58
CATMA2OA41310R1	AT2G42900	-1.90	-1.45
CATMA2OA41370R1	AT2G42975	-1.95	-1.19
CATMA2OA41400F1	AT2G43000	4.67	2.80
CATMA2OA41410R1	AT2G43010	-1.51	-1.19
CATMA2OA41450R1	AT2G43050	2.15	1.09
CATMA2OA41460R1	AT2G43060	1.73	-1.01
CATMA2OA41790F1	AT2G43390	-2.17	1.93
CATMA2OA41890R1	AT2G43480	1.81	1.08
CATMA2OA41910R1	AT2G43500	2.42	1.22
CATMA2OA41920R1	AT2G43510	4.97	1.23
CATMA2OC47737R1	AT2G43535	-1.05	-2.24
CATMA2OC47738R1	AT2G43550	-1.55	-1.23
CATMA2OA41980F1	AT2G43560	-1.76	-1.27
CATMA2OA41990F1	AT2G43570	8.49	1.26
CATMA2OA42020F1	AT2G43600	-1.59	1.06
CATMA2OA42030F1	AT2G43610	1.51	1.75
CATMA2OA42040F1	AT2G43620	-1.75	-2.20
CATMA2OA42070R1	AT2G43670	-1.68	1.35
CATMA2OA42220R1	AT2G43820	2.23	1.45
CATMA2OA42300R1	AT2G43890	-3.25	1.09
CATMA2OA42340F1	AT2G43920	1.53	-1.12
CATMA2OA42380F1	AT2G43945	-1.56	-1.19
CATMA2OA42450R1	AT2G44010	1.58	1.13
CATMA2OA42510R1	AT2G44080	1.67	1.02
CATMA2OC47752F1	AT2G44290	1.88	1.61
CATMA2OA42750R1	AT2G44340	-1.64	-1.39
CATMA2OA42820F1	AT2G44390	-1.60	-1.01
CATMA2OA42920R1	AT2G44480	3.51	1.15
CATMA2OA42930R1	AT2G44490	1.73	1.14
CATMA2ON94877R1	AT2G44640	-1.52	-1.18
CATMA2OC47760R1	AT2G44690	-1.20	-1.57
CATMA2OA43190F1	AT2G44740	-1.58	-1.15
CATMA2OA43260R1	AT2G44800	-1.44	-1.63
CATMA2OC47764R1	AT2G44920	-1.84	-1.28
CATMA2OA43420R1	AT2G44940	-2.84	1.03
CATMA2OA43610F1	AT2G45220	-1.19	-2.03
CATMA2OA43690R1	AT2G45290	1.68	1.96
CATMA2OA43780F1	AT2G45400	1.57	1.53
CATMA2OA43840R1	AT2G45430	1.58	1.22
CATMA2OA43870F1	AT2G45470	-1.84	-1.28
CATMA2OA43910R1	AT2G45510	1.68	1.33
CATMA2OA44000R1	AT2G45600	-1.01	-1.69
CATMA2OA44050F1	AT2G45660	-1.98	-1.06
CATMA2OA44160F1	AT2G45760	3.93	2.42
CATMA2OA44165R1	AT2G45770	-1.52	1.00
CATMA2OA44210F1	AT2G45820	-1.59	1.00
CATMA2OA44320R1	AT2G45920	2.72	2.02
CATMA2OA44490R1	AT2G46090	-1.53	-1.20
CATMA2OA44650R1	AT2G46250	-1.88	-1.40
CATMA2OA44770F1	AT2G46400	8.31	3.17
CATMA2OC47792F1	AT2G46410	1.93	1.28
CATMA2OA44785R1	AT2G46430	2.08	1.46
CATMA2ON101923R1	AT2G46440	3.32	1.38
CATMA2OA44950R1	AT2G46535	-1.67	-1.10
CATMA2OA45030R1	AT2G46600	1.96	1.24
CATMA2OA45100F1	AT2G46670	-3.34	-1.62
CATMA2OA45105F1	AT2G46680	2.29	1.14
CATMA2OA45110R1	AT2G46690	-2.26	-1.14
CATMA2OA45190R1	AT2G46735	-1.97	-1.31
CATMA2OC47798F1	AT2G46750	6.86	2.52
CATMA2OA45250R1	AT2G46790	-3.36	-1.47
CATMA2OA45270R1	AT2G46820	-1.61	-1.07
CATMA2OA45275R1	AT2G46830	-2.29	-2.25
CATMA2OA45350R1	AT2G46910	-2.36	-1.72
CATMA2OA45400F1	AT2G46940	1.37	1.63
CATMA2OA45470F1	AT2G47000	1.43	1.66
CATMA2OA45580F1	AT2G47130	1.65	1.35
CATMA2ON90753F1	AT2G47180	-2.26	1.12
CATMA2OA45630R1	AT2G47190	1.63	1.13
CATMA2OA45640F1	AT2G47200	-1.87	1.81
CATMA2OA45730F1	AT2G47260	1.96	1.04
CATMA2OA45830F1	AT2G47370	-1.87	-1.33
CATMA2OA45910R1	AT2G47450	-1.50	-1.15
CATMA2OA45915R1	AT2G47460	-2.19	-1.25
CATMA2ON90811R1	AT2G47470	1.57	1.14
CATMA2OC47808R1	AT2G47485	1.42	1.52
CATMA2OA46010R1	AT2G47550	2.47	1.40
CATMA2OA46260F1	AT2G47840	-1.55	1.00
CATMA2OA46300R1	AT2G47880	2.16	-1.57
CATMA2OA46310R1	AT2G47890	-1.34	1.56
CATMA2OA46340R1	AT2G47910	-1.79	-1.18
CATMA2OA46360F1	AT2G47930	-1.88	-1.56
CATMA2OA46390R1	AT2G47950	6.71	1.09
CATMA2OA46445R1	AT2G48010	1.63	1.11
CATMA2OA46480R1	AT2G48070	-1.52	-1.18
CATMA2OA46490F1	AT2G48080	-1.21	-1.87
CATMA2OA46500F1	AT2G48090	2.52	2.05
CATMA2OA46540F1	AT2G48130	-1.80	1.09
CATMA2OA46550R1	AT2G48140	-1.74	1.26
CATMA3OA00100F1	AT3G01060	-1.90	1.02
CATMA3OA00185F1	AT3G01190	-2.22	1.12
CATMA3OA00250F1	AT3G01260	-1.84	1.94
CATMA3OA00270F1	AT3G01290	4.11	1.37
CATMA3OC57007R1	AT3G01350	-1.69	-2.14
CATMA3OA00390F1	AT3G01420	3.88	-1.06
CATMA3OA00420R1	AT3G01440	-1.77	-1.44
CATMA3OA00470R1	AT3G01480	-1.89	-1.18
CATMA3OA00490F1	AT3G01500	-3.35	-1.19
CATMA3OA00500F1	AT3G01510	-1.72	-1.06
CATMA3OA00555F1	AT3G01550	-2.39	-1.96
CATMA3OA00570F1	AT3G01570	-8.82	-4.54
CATMA3OA00600R1	AT3G01600	1.58	-1.12
CATMA3ON94378R1	AT3G01760	-1.62	-1.32
CATMA3OA00833R1	AT3G01830	1.48	1.50
CATMA3ON100560R1	AT3G01860	1.42	1.50
CATMA3OA00955F1	AT3G01970	7.08	1.44
CATMA3OA00970R1	AT3G01990	1.67	1.08
CATMA3OA01170F1	AT3G02170	1.51	-1.04
CATMA3OA01355F1	AT3G02380	-4.12	-5.15
CATMA3OA01360R1	AT3G02400	1.12	1.52
CATMA3OA01430R1	AT3G02480	1.22	-2.35
CATMA3ON90975F1	AT3G02493	-1.94	1.10
CATMA3OA01510F1	AT3G02550	2.21	-1.88
CATMA3OA01540F1	AT3G02570	-1.11	-1.53
CATMA3OA01570R1	AT3G02610	-1.75	-1.04
CATMA3OF02894_NR1	AT3G02620	-1.51	-1.30
CATMA3OA01740F1	AT3G02800	2.05	1.34
CATMA3OA01765R1	AT3G02830	-1.76	-1.39
CATMA3OA01800R1	AT3G02875	1.92	-1.02
CATMA3OA01815F1	AT3G02885	-2.52	-2.26
CATMA3OA01926R1	AT3G03020	2.01	1.25
CATMA3OA02085R1	AT3G03190	-1.99	-1.94
CATMA3OA02160F1	AT3G03270	1.09	-1.66
CATMA3OA02430R1	AT3G03500	-1.96	1.24
CATMA3OA02553F1	AT3G03630	-1.68	-1.04
CATMA3OF00966F1	AT3G03820	-1.44	-1.71
CATMA3OC57065F1	AT3G03830	-1.41	-1.77
CATMA3OA02840R1	AT3G03870	1.77	1.42
CATMA3OA02960R1	AT3G03990	1.73	-1.07
CATMA3OA03000F1	AT3G04030	-2.64	-1.32
CATMA3OA03040F1	AT3G04070	12.85	2.39
CATMA3OA03090R1	AT3G04140	-2.19	-1.57
CATMA3OA03160F1	AT3G04210	2.22	1.56
CATMA3OA03170F1	AT3G04220	1.75	-1.03
CATMA3OA03340R1	AT3G04370	-1.69	1.89
CATMA3OF02898R1	AT3G04410	5.32	2.14
CATMA3OC57072R1	AT3G04420	2.42	1.58
CATMA3OA03520R1	AT3G04530	2.16	-1.03
CATMA3OA03743F1	AT3G04720	4.15	-1.05
CATMA3OA03770F1	AT3G04760	-1.73	-1.01
CATMA3OA03800R1	AT3G04790	-1.70	1.00
CATMA3OA04215R1	AT3G05200	1.52	1.16
CATMA3ON100595F1	AT3G05360	1.98	1.18
CATMA3OC57084R1	AT3G05400	2.04	-1.07
CATMA3OA04440R1	AT3G05410	-1.68	-1.23
CATMA3OA04650R1	AT3G05625	-1.72	-1.61
CATMA3OD02902R1	AT3G05727	-1.25	-4.96
CATMA3OA04770R1	AT3G05730	-1.63	-1.57
CATMA3OD02903F1	AT3G05770	2.68	1.19
CATMA3OA04910R1	AT3G05858	2.06	1.22
CATMA3OB04930F1	AT3G05900	-1.85	-1.22
CATMA3OA04970F1	AT3G05937	1.79	1.44
CATMA3OA05130F1	AT3G06070	-1.18	-1.55
CATMA3OA05210F1	AT3G06145	-2.91	-1.43
CATMA3OA05440R1	AT3G06360	1.55	1.17
CATMA3OA05470F1	AT3G06390	-2.11	1.34
CATMA3OA05540F1	AT3G06435	1.04	-1.70
CATMA3OA05640R1	AT3G06500	1.55	1.22
CATMA3OC57105F1	AT3G06750	-1.36	-1.63
CATMA3OA05990F1	AT3G06770	-1.57	-1.27
CATMA3OA06020R1	AT3G06810	1.52	1.11
CATMA3OA06050R1	AT3G06840	-1.71	-1.29
CATMA3OA06056R1	AT3G06860	1.80	1.06
CATMA3OA06080R1	AT3G06890	4.83	2.15
CATMA3ON91370R1	AT3G06950	-1.64	-1.53
CATMA3OA06180R1	AT3G06980	-1.57	-1.22
CATMA3OA06230F1	AT3G07040	1.57	-1.21
CATMA3OA06350F1	AT3G07160	1.52	1.35
CATMA3OA06750F1	AT3G07520	1.59	-1.02
CATMA3OA06910R1	AT3G07650	2.69	1.93
CATMA3OA06970F1	AT3G07710	1.04	3.40
CATMA3OA06980R1	AT3G07720	5.82	2.33
CATMA3OF00991R1	AT3G07730	1.59	1.19
CATMA3OA07310F1	AT3G08040	8.42	1.25
CATMA3OA07350F1	AT3G08505	-1.90	-1.31
CATMA3OA07410F1	AT3G08590	1.87	1.53
CATMA3ON94405F1	AT3G08720	2.08	1.38
CATMA3OA07540F1	AT3G08740	-1.63	-1.10
CATMA3OA07570F1	AT3G08770	-1.03	-1.84
CATMA3OA07660F1	AT3G08860	1.95	-1.03
CATMA3OA07670F1	AT3G08870	1.29	1.51
CATMA3OA07740R1	AT3G08920	-1.71	-1.24
CATMA3OA07810R1	AT3G08970	4.43	1.25
CATMA3OA07850R1	AT3G09010	2.53	1.52
CATMA3OA07860R1	AT3G09020	1.64	1.63
CATMA3OA07910R1	AT3G09050	-1.52	-1.02
CATMA3OC57129F1	AT3G09162	-2.71	-1.32
CATMA3OA08060F1	AT3G09190	-1.54	-1.15
CATMA3OA08080F1	AT3G09210	-1.82	-1.23
CATMA3ON94406F1	AT3G09240	-2.06	1.41
CATMA3ON91048F1	AT3G09260	-1.33	-1.55
CATMA3OA08275F1	AT3G09390	2.10	1.21
CATMA3OA08320R1	AT3G09450	-2.25	-2.03
CATMA3OA08450F1	AT3G09580	-1.82	1.09
CATMA3OA08470R1	AT3G09600	-1.11	-1.84
CATMA3OA08700R1	AT3G09830	2.38	1.20
CATMA3OA08760F1	AT3G09910	1.51	1.04
CATMA3OA08785R1	AT3G09922	1.94	1.17
CATMA3OA08790F1	AT3G09925	1.65	2.12
CATMA3OA08820F1	AT3G09940	2.32	1.81
CATMA3OA08910F1	AT3G10020	1.55	1.91
CATMA3OA08930F1	AT3G10040	1.87	-1.59
CATMA3OA08940R1	AT3G10060	-2.15	-1.27

Table 22: Continued

		Ratio	
D CATMAv6	AGI	+Fe	-Fe
CATMA3OA09080R1	AT3G10120	2.28	1.07
CATMA3OA09195F1	AT3G10230	-1.53	-1.11
CATMA3OA09320F1	AT3G10320	2.12	1.76
CATMA3OC57145F1	AT3G10405	-1.86	-1.29
CATMA3OA09400F1	AT3G10410	1.60	1.32
CATMA3OA09450R1	AT3G10450	1.54	-1.11
CATMA3OA09500R1	AT3G10500	2.13	1.80
CATMA3OA09980F1	AT3G10930	4.27	1.20
CATMA3OA10060F1	AT3G10986	2.31	1.75
CATMA3OF01002F1	AT3G11010	2.82	2.29
CATMA3OA10110R1	AT3G11050	1.12	1.57
CATMA3ON94416R1	AT3G11080	2.04	2.36
CATMA3OA10150R1	AT3G11090	-1.94	-1.23
CATMA3OA10160R1	AT3G11110	-1.56	-1.18
CATMA3OA10360R1	AT3G11340	2.09	-1.01
CATMA3OA10403F1	AT3G11410	1.63	1.40
CATMA3OA10410R1	AT3G11420	2.16	2.21
CATMA3OA10420R1	AT3G11430	-1.56	1.81
CATMA3OA10540F1	AT3G11580	2.86	1.20
CATMA3OA10585R1	AT3G11630	-1.98	-1.19
CATMA3OA10755F1	AT3G11820	1.76	1.13
CATMA3OA10770F1	AT3G11840	2.47	1.67
CATMA3OA10850R1	AT3G11930	-1.99	-1.32
CATMA3OA10870F1	AT3G11945	-1.62	-1.24
CATMA3OA10980F1	AT3G12070	1.58	1.03
CATMA3OA11050R1	AT3G12110	-1.73	-1.16
CATMA3ON94420F1	AT3G12203	-2.82	-1.30
CATMA3OF01008F1	AT3G12240	1.01	1.83
CATMA3OA11270R1	AT3G12320	-2.48	-2.24
CATMA3OA11290F1	AT3G12345	-1.75	-1.18
CATMA3OA11440F1	AT3G12500	14.93	3.05
CATMA3OA11450R1	AT3G12510	1.71	1.13
CATMA3OA11460F1	AT3G12520	1.88	-1.23
CATMA3OA11535F1	AT3G12580	-2.04	-1.32
CATMA3OC57173F1	AT3G12685	-1.65	-1.08
CATMA3OA11680R1	AT3G12700	2.56	1.13
CATMA3OC57177F1	AT3G12780	-1.98	-1.17
CATMA3OA11780F1	AT3G12820	4.20	-1.13
CATMA3OA11860R1	AT3G12900	7.79	-2.55
CATMA3OA11870R1	AT3G12910	2.49	1.91
CATMA3OA11910R1	AT3G12930	-1.50	-1.18
CATMA3OA12115F1	AT3G13080	3.03	1.82
CATMA3ON94428F1	AT3G13090	2.82	1.15
CATMA3OA12140F1	AT3G13120	-1.78	-1.29
CATMA3OA12440F1	AT3G13330	1.78	1.40
CATMA3OA12510R1	AT3G13380	1.70	1.26
CATMA3OD05086F1	AT3G13403	-1.77	-1.50
CATMA3ON91348R1	AT3G13432	1.42	2.71
CATMA3OA12580R1	AT3G13435	1.24	1.88
CATMA3OA12620R1	AT3G13470	-1.51	-1.23
CATMA3OA12630F1	AT3G13480	-1.55	-1.08
CATMA3OA12760R1	AT3G13610	3.77	1.60
CATMA3OC57195F1	AT3G13672	2.12	-1.06
CATMA3OA12930R1	AT3G13740	-1.54	-1.03
CATMA3OA12935R1	AT3G13750	-1.82	1.47
CATMA3OA13170R1	AT3G13950	1.90	2.06
CATMA3ON100712F1	AT3G14050	1.55	-1.03
CATMA3OA13280F1	AT3G14060	2.22	-1.14
CATMA3OA13350F1	AT3G14110	-1.51	-1.35
CATMA3ON91236F1	AT3G14130	1.70	1.10
CATMA3OA13460F1	AT3G14200	-1.73	-1.10
CATMA3OA13510F1	AT3G14230	1.63	-1.01
CATMA3OA13540F1	AT3G14260	2.43	2.32
CATMA3ON91331F1	AT3G14362	1.68	1.05
CATMA3OA13640F1	AT3G14370	2.33	-1.19
CATMA3OA13700R1	AT3G14420	-1.52	-1.12
CATMA3ON94433R1	AT3G14452	-1.59	-1.58
CATMA3OA13740F1	AT3G14460	1.58	1.02
CATMA3OA13750R1	AT3G14470	2.39	1.37
CATMA3OA13900F1	AT3G14590	1.66	1.39
CATMA3OA13930R1	AT3G14610	1.64	1.09
CATMA3OA13940R1	AT3G14620	6.63	1.59
CATMA3ON94435R1	AT3G14630	1.71	1.23
CATMA3OA14030R1	AT3G14680	3.51	1.41
CATMA3OA14050R1	AT3G14700	3.43	1.44
CATMA3OA14110R1	AT3G14760	-2.04	-1.42
CATMA3OA14120F1	AT3G14770	-1.65	-1.05
CATMA3OA14130F1	AT3G14780	2.00	1.54
CATMA3OA14210R1	AT3G14850	-1.60	-1.24
CATMA3OA14260F1	AT3G14900	-1.51	-1.04
CATMA3OA14290R1	AT3G14930	-1.74	-1.10
CATMA3OA14295R1	AT3G14940	2.87	1.60
CATMA3OA14340R1	AT3G14990	1.77	1.30
CATMA3OA14470F1	AT3G15115	-1.58	-1.35
CATMA3OA14490F1	AT3G15130	-1.42	-1.52
CATMA3OA14510F1	AT3G15150	-1.83	-1.22
CATMA3OC57216R1	AT3G15190	-1.72	-1.38
CATMA3OA14660F1	AT3G15300	1.88	1.43
CATMA3OA14720F1	AT3G15354	-1.75	-1.57
CATMA3OA14725F1	AT3G15356	1.56	1.33
CATMA3OA14790R1	AT3G15370	1.15	1.89
CATMA3OA14870R1	AT3G15450	1.17	2.51
CATMA3OA14910R1	AT3G15500	2.75	1.68
CATMA3OA14920R1	AT3G15510	1.67	1.68
CATMA3OA14930R1	AT3G15518	1.87	1.30
CATMA3OA14940F1	AT3G15520	-2.38	-1.37
CATMA3OA14950F1	AT3G15530	1.59	-1.04
CATMA3OA15030F1	AT3G15630	1.20	1.61
CATMA3OA15070R1	AT3G15680	-1.30	-1.52
CATMA3OC57229R1	AT3G15770	-1.05	1.78
CATMA3OA15240R1	AT3G15850	-3.31	-1.29
CATMA3OA15300F1	AT3G15900	-1.71	-1.31
CATMA3OA15410R1	AT3G15990	1.80	-1.16
CATMA3OA15420F1	AT3G16000	-1.53	-1.10
CATMA3OA15450R1	AT3G16030	1.69	1.18
CATMA3OA15560R1	AT3G16150	1.85	1.04
CATMA3OA15590R1	AT3G16175	-1.61	-1.35
CATMA3OA15645R1	AT3G16240	-3.48	-1.77
CATMA3OA15650F1	AT3G16250	-1.60	1.09
CATMA3OC57235R1	AT3G16360	-1.31	-2.89
CATMA3OA15780R1	AT3G16370	-1.72	-2.03
CATMA3OC57239R1	AT3G16430	-1.23	-1.61
CATMA3OA15870R1	AT3G16450	-1.25	-1.67
CATMA3OA15890F1	AT3G16470	-1.69	-1.21
CATMA3OA15930F1	AT3G16520	1.55	1.74
CATMA3OD02932F1	AT3G16530	2.08	1.44
CATMA3ON94444F1	AT3G16565	1.70	1.28
CATMA3OA16100R1	AT3G16670	-3.37	-2.20
CATMA3OA16130R1	AT3G16720	2.13	1.24
CATMA3OA16200R1	AT3G16800	-1.92	-1.81
CATMA3OA16260F1	AT3G16860	2.40	1.11
CATMA3OA16340R1	AT3G16940	1.51	1.08
CATMA3OA16390R1	AT3G17000	1.51	1.26
CATMA3OA16410F1	AT3G17020	1.52	1.20
CATMA3OA16430F1	AT3G17040	-1.76	-1.52
CATMA3OA16510R1	AT3G17110	2.79	-1.22
CATMA3OA16840R1	AT3G17410	1.59	1.23
CATMA3OA16940F1	AT3G17510	-1.75	-1.14
CATMA3OA17030R1	AT3G17609	-2.23	-1.58
CATMA3OA17130F1	AT3G17680	-1.46	-1.53
CATMA3OA17140R1	AT3G17690	2.83	1.27
CATMA3ON94451R1	AT3G17720	1.78	1.24
CATMA3OA17290R1	AT3G17790	1.41	-1.71
CATMA3OC57263R1	AT3G17820	1.56	1.06
CATMA3OA17380R1	AT3G17890	-1.65	-1.22
CATMA3OA17470F1	AT3G18010	-1.41	-1.59
CATMA3OA17550R1	AT3G18080	1.52	1.20
CATMA3OC57266R1	AT3G18170	-1.79	-1.91
CATMA3ON94457R1	AT3G18180	-1.48	-1.68
CATMA3OA17720F1	AT3G18200	-1.68	-1.04
CATMA3OA17790F1	AT3G18250	2.69	1.82
CATMA3OA17840R1	AT3G18290	-1.27	-2.72
CATMA3ON91308F1	AT3G18320	-1.77	-1.14
CATMA3OA17940R1	AT3G18370	1.59	1.13
CATMA3OC57271F1	AT3G18450	-3.57	-1.19
CATMA3OA18270F1	AT3G18660	-1.51	-1.00
CATMA3OA18390R1	AT3G18773	-2.52	-1.84
CATMA3OA18400R1	AT3G18777	-1.68	-1.13
CATMA3OA18460F1	AT3G18830	2.25	1.29
CATMA3OA18530R1	AT3G18890	-2.07	-1.05
CATMA3OA18540R1	AT3G18900	-1.61	-1.19
CATMA3OA18660F1	AT3G19010	1.62	1.29
CATMA3OA18680F1	AT3G19030	-2.23	-1.50
CATMA3OA18785F1	AT3G19150	1.64	1.06
CATMA3OA18840F1	AT3G19200	3.45	1.13
CATMA3OA19000R1	AT3G19390	1.96	1.14
CATMA3OA19030F1	AT3G19430	-1.91	1.20
CATMA3OA19070R1	AT3G19480	-2.05	-1.48
CATMA3OA19200F1	AT3G19580	2.30	1.56
CATMA3OA19250F1	AT3G19615	4.08	1.13
CATMA3OA19295F1	AT3G19660	2.28	1.32
CATMA3OC57282F1	AT3G19710	-1.08	-1.63
CATMA3OA19400R1	AT3G19800	-1.55	-1.20
CATMA3OA19600R1	AT3G19990	1.53	1.00
CATMA3OA19930F1	AT3G20250	1.63	1.49
CATMA3OA19950R1	AT3G20270	-1.54	-1.43
CATMA3OA20020F1	AT3G20340	5.73	1.58
CATMA3OA20050R1	AT3G20370	-1.15	-1.60
CATMA3OC57288R1	AT3G20380	3.27	-1.18
CATMA3OA20080F1	AT3G20395	1.63	-1.03
CATMA3OA20130F1	AT3G20450	-1.79	1.02
CATMA3OA20150F1	AT3G20470	1.86	-2.14
CATMA3OC57293R1	AT3G20590	1.59	1.45
CATMA3OD02940R1	AT3G20600	-1.04	1.50
CATMA3OA20370F1	AT3G20640	-1.72	-1.07
CATMA3OA20390F1	AT3G20660	2.47	1.12
CATMA3OA20690R1	AT3G20930	-1.51	-1.28
CATMA3ON91119R1	AT3G20940	-1.48	-1.58
CATMA3OC57301R1	AT3G20960	2.31	1.34
CATMA3OA20880F1	AT3G21055	-1.76	-1.11
CATMA3OC57304F1	AT3G21070	2.21	1.34
CATMA3OA20920F1	AT3G21080	1.77	1.32
CATMA3OA21086F1	AT3G21240	2.14	1.17
CATMA3OC57307F1	AT3G21260	1.51	1.20
CATMA3OC57309F1	AT3G21340	1.10	1.82
CATMA3ON94469R1	AT3G21352	1.53	-1.09
CATMA3OC57310F1	AT3G21370	-1.04	-1.57
CATMA3OA21270R1	AT3G21390	-1.64	-1.47
CATMA3OA21290R1	AT3G21420	3.45	1.36
CATMA3OA21320F1	AT3G21460	-1.56	1.22
CATMA3ON91024F1	AT3G21500	3.86	1.06
CATMA3OA21385F1	AT3G21510	3.21	1.14
CATMA3OA21390R1	AT3G21520	4.40	1.39
CATMA3OA21420F1	AT3G21550	-2.22	-1.06
CATMA3OA21540F1	AT3G21670	-3.14	-1.40
CATMA3OA21550F1	AT3G21680	-1.53	-1.30
CATMA3OA21560R1	AT3G21690	1.63	1.35
CATMA3OA21620R1	AT3G21760	-2.00	-1.51
CATMA3OA21635R1	AT3G21770	1.86	-1.15
CATMA3ON91087F1	AT3G21850	1.08	1.73
CATMA3OA21735F1	AT3G21870	-1.78	-1.53
CATMA3OA21750F1	AT3G21890	-3.25	-2.22
CATMA3ON94471R1	AT3G22040	1.51	-1.31
CATMA3OA22000F1	AT3G22070	-1.53	-1.04
CATMA3OA22070F1	AT3G22142	-1.03	1.53
CATMA3OA22090F1	AT3G22160	2.05	1.62
CATMA3OC57318R1	AT3G22200	1.96	1.28
CATMA3OC57319F1	AT3G22210	-1.55	-1.24
CATMA3OC57320F1	AT3G22231	-1.75	1.55
CATMA3ON91413R1	AT3G22232	-1.94	1.16
CATMA3ON91231R1	AT3G22237	-1.77	1.19
CATMA3OA22365R1	AT3G22370	1.62	1.44
CATMA3OC57321R1	AT3G22415	-1.70	1.35
CATMA3OA22410R1	AT3G22420	-1.78	-1.41
CATMA3OC57324R1	AT3G22460	1.84	1.35
CATMA3OA22530F1	AT3G22540	-1.51	-1.29
CATMA3OA22560F1	AT3G22570	-1.07	1.59
CATMA3OA22590R1	AT3G22620	-1.65	-1.01
CATMA3OA22600F1	AT3G22640	-14.13	-4.23
CATMA3OA22715R1	AT3G22760	-1.54	-1.09
CATMA3OA22775F1	AT3G22840	-1.75	-2.45
CATMA3OA22820F1	AT3G22880	-1.21	1.83
CATMA3OA22850F1	AT3G22920	-1.11	1.71
CATMA3OA22955R1	AT3G23000	-1.52	-1.57
CATMA3OA23020F1	AT3G23080	-1.65	1.05
CATMA3OA23040F1	AT3G23090	-1.76	1.03
CATMA3OA23060F1	AT3G23110	2.71	1.31
CATMA3OA23080F1	AT3G23120	10.53	1.86
CATMA3OA23210F1	AT3G23210	-2.02	-1.55
CATMA3OA23230F1	AT3G23230	1.33	1.65
CATMA3OA23245R1	AT3G23250	5.55	-1.59
CATMA3OA23280R1	AT3G23280	1.54	1.37
CATMA3OA23380R1	AT3G23450	-1.30	-1.83
CATMA3OA23460F1	AT3G23550	3.61	2.83
CATMA3OA23470F1	AT3G23560	1.70	1.48
CATMA3ON91412F1	AT3G23635	1.58	1.31
CATMA3OA23650F1	AT3G23700	-1.72	-1.10
CATMA3OA23680F1	AT3G23740	-1.55	-1.38
CATMA3OA23700F1	AT3G23760	-1.74	-1.21
CATMA3OA23750R1	AT3G23800	-2.43	-1.26
CATMA3ON100824R1	AT3G23805	-1.73	-1.54
CATMA3OC57358R1	AT3G24020	-2.06	-1.09
CATMA3OA24080F1	AT3G24140	-1.57	-1.12

Table 22: Continued

		Ratio	
D CATMAv6	AGI	+Fe	-Fe
CATMA3OA24233F1	AT3G24300	-1.80	1.00
CATMA3OA24320F1	AT3G24420	-1.72	-1.48
CATMA3OA24330F1	AT3G24430	-1.54	-1.19
CATMA3OA24470R1	AT3G24520	1.08	1.04
CATMA3OA24550R1	AT3G24590	-1.58	-1.24
CATMA3OA24620F1	AT3G24670	1.22	2.05
CATMA3ON91238F1	AT3G24900	1.83	1.65
CATMA3ON91385F1	AT3G24982	3.67	2.00
CATMA3OF01084F1	AT3G25010	1.96	2.01
CATMA3ON91075F1	AT3G25020	3.76	2.02
CATMA3OA25040R1	AT3G25190	2.48	1.39
CATMA3OA25100R1	AT3G25250	2.01	1.83
CATMA3OA25220F1	AT3G25480	-1.63	-1.03
CATMA3OA25310F1	AT3G25560	-1.75	1.01
CATMA3OD05090R1	AT3G25597	2.77	1.24
CATMA3ON94499F1	AT3G25610	2.83	1.53
CATMA3OC57383F1	AT3G25655	-1.85	1.06
CATMA3OA25440F1	AT3G25660	-1.58	-1.27
CATMA3OA25490R1	AT3G25710	-1.62	-1.27
CATMA3OC57384F1	AT3G25717	1.51	1.08
CATMA3OA25530R1	AT3G25730	2.56	1.25
CATMA3OC57387R1	AT3G25760	2.87	1.35
CATMA3OC57388R1	AT3G25770	1.96	2.01
CATMA3OC57389R1	AT3G25780	1.87	-1.10
CATMA3OA25590R1	AT3G25790	-4.15	-1.41
CATMA3OA25600F1	AT3G25805	-1.57	-1.11
CATMA3ON94501R1	AT3G25810	-2.97	-1.21
CATMA3OA25670F1	AT3G25840	1.08	1.66
CATMA3OA25700F1	AT3G25882	1.79	1.97
CATMA3OA25720R1	AT3G25900	2.50	1.44
CATMA3OA25740F1	AT3G25920	-1.90	-1.39
CATMA3ON100867F1	AT3G25930	1.40	1.78
CATMA3OA25760R1	AT3G25950	1.37	1.80
CATMA3OA25800F1	AT3G25990	1.58	1.04
CATMA3OA25860R1	AT3G26060	-1.73	-1.12
CATMA3OA25900R1	AT3G26090	1.65	1.09
CATMA3OA25960F1	AT3G26130	1.55	1.18
CATMA3ON94504F1	AT3G26150	1.60	1.76
CATMA3OF01092F1	AT3G26160	1.34	1.71
CATMA3ON91016F1	AT3G26180	1.25	1.86
CATMA3OA26060F1	AT3G26210	1.84	1.07
CATMA3OC57399F1	AT3G26220	1.92	1.03
CATMA3OC57401F1	AT3G26280	1.64	-1.21
CATMA3ON91120F1	AT3G26310	-1.83	-1.30
CATMA3ON90993F1	AT3G26330	-3.98	-1.06
CATMA3OA26280R1	AT3G26440	1.76	1.28
CATMA3OF01102F1	AT3G26450	1.25	-1.51
CATMA3OC57405F1	AT3G26460	-2.01	-1.62
CATMA3OA26310R1	AT3G26470	1.79	1.43
CATMA3OA26340F1	AT3G26500	1.96	1.28
CATMA3OA26362R1	AT3G26570	-1.66	-1.27
CATMA3OC57406F1	AT3G26590	1.98	1.05
CATMA3OA26368R1	AT3G26600	1.63	1.50
CATMA3ON100872F1	AT3G26630	-1.62	-1.04
CATMA3OA26440F1	AT3G26690	1.79	1.21
CATMA3OA26460R1	AT3G26710	-2.01	-1.20
CATMA3OC57411R1	AT3G26740	1.75	1.71
CATMA3OA26510R1	AT3G26770	2.08	1.11
CATMA3OA26545F1	AT3G26790	-1.54	-1.19
CATMA3OF01108R1	AT3G26830	5.18	1.32
CATMA3ON100877F1	AT3G26900	-1.85	-1.23
CATMA3OA26752F1	AT3G26960	-1.13	-2.30
CATMA3OA26850F1	AT3G27050	-2.27	-1.17
CATMA3OA26960R1	AT3G27160	-1.71	-1.21
CATMA3OA26965R1	AT3G27170	-1.67	-1.11
CATMA3OA27020F1	AT3G27210	1.49	1.52
CATMA3OA27110F1	AT3G27290	1.51	1.13
CATMA3OA27260R1	AT3G27400	2.23	-1.09
CATMA3OA27410R1	AT3G27540	-1.62	-1.19
CATMA3OA27510F1	AT3G27630	1.55	1.03
CATMA3OC57426R1	AT3G27660	-7.87	-4.11
CATMA3OC57427R1	AT3G27690	-1.79	-1.20
CATMA3OA27600R1	AT3G27750	-1.63	1.01
CATMA3OD02963R1	AT3G27830	-1.55	-1.09
CATMA3OF01121R1	AT3G27850	-1.71	-1.24
CATMA3OA27720F1	AT3G27920	-1.87	-1.23
CATMA3OA27760F1	AT3G27960	-1.54	-1.24
CATMA3OA27840R1	AT3G28050	3.04	2.42
CATMA3OC57429R1	AT3G28070	1.66	-1.05
CATMA3OA27920F1	AT3G28150	1.87	1.02
CATMA3OA28035R1	AT3G28210	1.82	1.98
CATMA3ON100910R1	AT3G28220	-1.95	-1.46
CATMA3OA28100R1	AT3G28270	-2.74	-2.02
CATMA3OA28190F1	AT3G28340	1.56	1.16
CATMA3OA28200F1	AT3G28345	3.51	4.22
CATMA3OA28350F1	AT3G28460	-1.77	-1.23
CATMA3OA28420R1	AT3G28540	2.51	1.64
CATMA3OA28430F1	AT3G28550	1.28	1.55
CATMA3OA28460R1	AT3G28580	8.55	1.74
CATMA3OA28470R1	AT3G28600	2.08	1.06
CATMA3OA28945F1	AT3G28930	2.00	1.22
CATMA3ON100918F1	AT3G28940	1.74	1.15
CATMA3ON94536F1	AT3G28990	1.77	1.15
CATMA3OA29010R1	AT3G29000	3.10	1.97
CATMA3OA29035F1	AT3G29030	-1.80	-2.52
CATMA3OA29070R1	AT3G29035	1.57	1.16
CATMA3OA29300F1	AT3G29185	-1.94	-1.32
CATMA3OA29370R1	AT3G29230	-1.65	1.16
CATMA3OA29380R1	AT3G29240	-1.56	1.17
CATMA3OA29470R1	AT3G29290	-1.53	-1.18
CATMA3OA29610F1	AT3G29410	-1.59	-1.23
CATMA3OA29750F1	AT3G29590	1.77	-1.69
CATMA3ON100935F1	AT3G29630	-3.71	-1.20
CATMA3OA29930R1	AT3G29670	1.92	2.09
CATMA3ON91353F1	AT3G29762	-2.08	1.05
CATMA3OA30170R1	AT3G29780	-1.51	-1.12
CATMA3OA30250R1	AT3G29810	1.83	-1.58
CATMA3OC57473R1	AT3G29970	-1.52	-2.52
CATMA3OA30610R1	AT3G30340	-1.32	-1.90
CATMA3OA30650F1	AT3G30390	1.77	1.10
CATMA3OA31045R1	AT3G30720	-5.19	-4.64
CATMA3OA31275F1	AT3G30775	2.10	1.55
CATMA3OA31550F1	AT3G30875	-1.52	1.08
CATMA3OA33370F1	AT3G32990	-1.35	1.55
CATMA3OA33372F1	AT3G33000	-1.85	1.38
CATMA3OA33374F1	AT3G33002	-1.70	1.14
CATMA3OA33376F1	AT3G33004	-1.90	1.17
CATMA3OA34200F1	AT3G42180	-1.55	-1.32
CATMA3OF06005F1	AT3G42628	-1.65	-1.01
CATMA3OA35130F1	AT3G42860	1.75	1.21
CATMA3OA35850F1	AT3G43430	2.79	1.11
CATMA3OA36080R1	AT3G43540	-1.54	-1.19
CATMA3ON94573R1	AT3G43630	2.23	1.45
CATMA3OA36410R1	AT3G43670	1.70	1.98
CATMA3ON91063F1	AT3G43820	1.83	3.12
CATMA3OA36740F1	AT3G43850	-3.38	1.05
CATMA3OA36850R1	AT3G44020	-1.73	-1.38
CATMA3OA37212R1	AT3G44300	4.43	1.06
CATMA3OA37270F1	AT3G44350	1.20	1.96
CATMA3OA37380F1	AT3G44450	-2.34	1.10
CATMA3ON91323F1	AT3G44480	1.57	1.03
CATMA3OC57549R1	AT3G44550	-1.44	1.53
CATMA3ON101090R1	AT3G44560	-1.59	1.80
CATMA3ON91082R1	AT3G44670	1.91	1.06
CATMA3OA37710R1	AT3G44720	1.80	1.42
CATMA3OC57553R1	AT3G44770	-1.04	1.66
CATMA3OC57558R1	AT3G44860	1.44	2.28
CATMA3OA37910R1	AT3G44890	-1.76	-1.31
CATMA3OA37960F1	AT3G44940	-2.22	-1.20
CATMA3OA37990R1	AT3G44970	1.71	1.17
CATMA3OA38015F1	AT3G44990	-3.45	-1.78
CATMA3OA38070R1	AT3G45050	-1.80	-1.31
CATMA3OA38080F1	AT3G45060	-2.38	1.77
CATMA3OA38160F1	AT3G45130	20.17	1.79
CATMA3OA38175R1	AT3G45140	1.84	-1.16
CATMA3OA38190F1	AT3G45160	-2.22	-1.18
CATMA3OA38240F1	AT3G45210	-2.07	-1.25
CATMA3OA38310F1	AT3G45260	1.49	1.53
CATMA3ON91352R1	AT3G45290	1.79	-1.29
CATMA3OA38430F1	AT3G45430	-1.82	-1.54
CATMA3OC57567F1	AT3G45443	-1.57	-1.17
CATMA3OC57577R1	AT3G45640	2.50	1.14
CATMA3OA38680R1	AT3G45680	-3.66	-1.93
CATMA3OC57579R1	AT3G45700	-2.35	-1.78
CATMA3OC57580R1	AT3G45710	-3.03	-2.09
CATMA3OC57581R1	AT3G45730	4.65	-1.03
CATMA3OA38870F1	AT3G45860	2.32	1.65
CATMA3ON91116R1	AT3G45920	1.93	1.21
CATMA3OF01304F1	AT3G46080	2.73	1.58
CATMA3ON90987F1	AT3G46090	3.91	1.71
CATMA3OA39110R1	AT3G46130	-1.68	1.35
CATMA3OC57593F1	AT3G46270	9.86	1.52
CATMA3OA39300F1	AT3G46280	-1.33	-1.81
CATMA3OC57594F1	AT3G46330	2.15	1.03
CATMA3OF01308R1	AT3G46370	-2.00	1.00
CATMA3ON94603R1	AT3G46480	1.07	1.66
CATMA3OC57596R1	AT3G46490	-2.68	-1.71
CATMA3OA39570R1	AT3G46500	1.78	1.19
CATMA3OA39680R1	AT3G46600	2.07	-1.12
CATMA3OC57600F1	AT3G46690	2.10	1.12
CATMA3OA39790F1	AT3G46700	-1.23	-1.96
CATMA3OA39870R1	AT3G46780	-1.56	1.05
CATMA3OA39980R1	AT3G46900	5.03	2.19
CATMA3OA40050F1	AT3G46970	1.85	1.53
CATMA3OA40110R1	AT3G47030	-1.33	-1.54
CATMA3OC57611F1	AT3G47040	4.18	1.84
CATMA3OA40130F1	AT3G47050	2.78	1.22
CATMA3OA40150F1	AT3G47070	-1.71	1.55
CATMA3ON91379F1	AT3G47090	2.21	1.41
CATMA3OA40350F1	AT3G47340	1.74	1.58
CATMA3OA40420F1	AT3G47420	-1.19	-1.85
CATMA3OA40440R1	AT3G47430	-3.03	-1.67
CATMA3OA40460F1	AT3G47450	-1.69	-1.13
CATMA3OC57618F1	AT3G47470	-1.58	-1.20
CATMA3OA40490F1	AT3G47480	2.94	1.54
CATMA3OC57619F1	AT3G47500	-2.58	-1.40
CATMA3OA40540R1	AT3G47540	1.63	1.33
CATMA3OA40630R1	AT3G47640	1.48	-1.66
CATMA3OA40640R1	AT3G47650	-2.05	-1.12
CATMA3OA40790R1	AT3G47780	1.22	1.62
CATMA3OA40820R1	AT3G47800	1.79	1.41
CATMA3OA40900F1	AT3G47860	-1.41	1.60
CATMA3OA40990R1	AT3G47980	-1.56	1.19
CATMA3OA41110F1	AT3G48080	2.90	1.38
CATMA3OA41120F1	AT3G48090	1.59	1.14
CATMA3ON101137F1	AT3G48100	-1.73	-1.16
CATMA3OA41153F1	AT3G48180	1.91	1.30
CATMA3OA41320R1	AT3G48340	-1.20	2.13
CATMA3ON91416R1	AT3G48346	-1.03	2.62
CATMA3OA41330R1	AT3G48350	-1.53	1.28
CATMA3OA41360R1	AT3G48390	-1.81	1.53
CATMA3OA41390R1	AT3G48420	-1.81	-1.34
CATMA3OA41430F1	AT3G48450	2.15	1.81
CATMA3OA41440R1	AT3G48460	-2.05	-1.59
CATMA3OA41520F1	AT3G48560	-1.55	-1.08
CATMA3OA41540R1	AT3G48580	4.19	-1.14
CATMA3OA41600F1	AT3G48640	1.54	2.01
CATMA3OA41610R1	AT3G48650	2.02	1.86
CATMA3OA41710R1	AT3G48720	1.00	-1.66
CATMA3OA41720R1	AT3G48730	-1.59	-1.32
CATMA3OA41730F1	AT3G48740	-1.59	-1.16
CATMA3OA41885R1	AT3G48890	1.56	1.11
CATMA3ON94621F1	AT3G48940	-2.26	1.18
CATMA3OA41950F1	AT3G48970	-1.62	-1.21
CATMA3OA42080F1	AT3G49070	-1.79	1.12
CATMA3ON91365R1	AT3G49120	3.86	2.04
CATMA3OA42120R1	AT3G49130	1.72	1.05
CATMA3OA42160F1	AT3G49160	2.07	3.36
CATMA3OA42360R1	AT3G49330	-1.83	1.48
CATMA3OA42380F1	AT3G49350	1.56	1.15
CATMA3OC57657F1	AT3G49370	1.51	1.35
CATMA3OA42560F1	AT3G49530	1.72	1.08
CATMA3OC57669R1	AT3G49620	3.40	-1.03
CATMA3OA42716R1	AT3G49690	1.38	1.64
CATMA3OA42800F1	AT3G49760	-1.89	-1.07
CATMA3OA42820R1	AT3G49780	4.08	-1.02
CATMA3OA42890R1	AT3G49845	-1.55	1.08
CATMA3OA43010F1	AT3G49960	1.89	1.79
CATMA3OA43300R1	AT3G50260	2.35	1.61
CATMA3ON94632R1	AT3G50280	1.42	1.73
CATMA3OA43470R1	AT3G50400	-1.55	1.54
CATMA3OA43510F1	AT3G50440	-1.25	-1.85
CATMA3OA43550R1	AT3G50480	1.66	-1.01
CATMA3OA43600F1	AT3G50560	-5.26	-1.42
CATMA3OA43620F1	AT3G50580	-1.67	1.57
CATMA3OA43660F1	AT3G50610	1.99	-2.11
CATMA3OA43687F1	AT3G50685	-1.54	-1.27
CATMA3OA43750F1	AT3G50740	2.95	1.34
CATMA3OA43775R1	AT3G50770	2.61	1.64
CATMA3OC57692F1	AT3G50820	-1.97	-1.23
CATMA3OA43910R1	AT3G50900	1.73	1.08
CATMA3OA43920R1	AT3G50910	1.62	1.16
CATMA3OA43940R1	AT3G50930	5.40	1.65

Table 22: Continued

		Ratio	
D CATMAv6	AGI	+Fe	-Fe
CATMA3OC57695R1	AT3G50950	2.02	1.33
CATMA3OA43980R1	AT3G50970	1.05	1.64
CATMA3OA44010F1	AT3G51000	1.97	1.23
CATMA3OA44200F1	AT3G51200	1.58	3.00
CATMA3OA44410F1	AT3G51400	1.51	1.69
CATMA3OC57703R1	AT3G51430	2.03	1.26
CATMA3OA44550R1	AT3G51540	4.43	2.17
CATMA3OA44603F1	AT3G51600	-1.09	-1.67
CATMA3OA44650R1	AT3G51670	1.08	-1.59
CATMA3OA44710F1	AT3G51750	-1.58	1.18
CATMA3OA44760F1	AT3G51820	-1.60	-1.20
CATMA3OA44780R1	AT3G51860	2.60	1.56
CATMA3OA44790R1	AT3G51870	-1.86	1.15
CATMA3OA44800F1	AT3G51890	1.91	1.45
CATMA3OA45070R1	AT3G52150	-1.91	-1.39
CATMA3OA45100F1	AT3G52170	-1.51	-1.26
CATMA3OA45110F1	AT3G52180	2.13	1.25
CATMA3OA45320R1	AT3G52380	-2.00	-1.05
CATMA3OA45345R1	AT3G52430	1.75	1.44
CATMA3OA45400F1	AT3G52490	1.61	1.24
CATMA3OA45460F1	AT3G52530	1.10	1.68
CATMA3OA45480F1	AT3G52550	-1.46	-1.61
CATMA3OC57723F1	AT3G52720	-1.76	-3.38
CATMA3OA45670F1	AT3G52740	-1.63	-1.13
CATMA3OA45680F1	AT3G52750	-1.70	-1.32
CATMA3OA45720F1	AT3G52790	-1.68	1.15
CATMA3OA45760F1	AT3G52820	-1.07	1.66
CATMA3OF03047R1	AT3G52830	-1.69	1.23
CATMA3ON101186F1	AT3G52880	1.53	1.13
CATMA3OC57728R1	AT3G52900	-1.57	-1.13
CATMA3OA45990F1	AT3G53040	1.05	2.32
CATMA3OA46063F1	AT3G53100	-2.67	-1.43
CATMA3OC57735R1	AT3G53130	-1.52	-1.34
CATMA3OC57736F1	AT3G53150	2.83	1.11
CATMA3OC57737F1	AT3G53160	1.63	1.30
CATMA3OC57741F1	AT3G53200	3.17	1.26
CATMA3OA46140R1	AT3G53230	1.91	2.03
CATMA3ON90971F1	AT3G53235	-4.56	-1.02
CATMA3OA46170R1	AT3G53250	-2.11	-1.45
CATMA3OA46195R1	AT3G53280	1.11	-1.90
CATMA3OC57764F1	AT3G53420	-1.62	-1.37
CATMA3OA46410F1	AT3G53460	1.05	1.69
CATMA3OC57769R1	AT3G53480	3.73	2.78
CATMA3OC57775F1	AT3G53540	1.90	1.11
CATMA3OA46750R1	AT3G53800	1.15	1.72
CATMA3OA46850F1	AT3G53900	-1.56	-1.33
CATMA3OA46940F1	AT3G53980	-5.12	-2.29
CATMA3OA46950F1	AT3G53990	1.41	1.60
CATMA3OA46990F1	AT3G54040	4.78	1.33
CATMA3OA47000R1	AT3G54050	-1.59	-1.12
CATMA3OA47070F1	AT3G54100	1.53	1.16
CATMA3OA47110F1	AT3G54150	10.17	1.98
CATMA3OA47150F1	AT3G54210	-1.94	-1.30
CATMA3OC57788F1	AT3G54390	-1.74	-1.39
CATMA3OA47350R1	AT3G54420	1.86	1.10
CATMA3OA47440F1	AT3G54500	-1.80	-1.61
CATMA3OA47480F1	AT3G54530	1.13	1.85
CATMA3ON94652R1	AT3G54590	1.71	1.88
CATMA3OA47540R1	AT3G54600	-1.57	-1.74
CATMA3OA47550F1	AT3G54620	1.53	1.19
CATMA3OA47570F1	AT3G54640	1.74	1.05
CATMA3OA47630F1	AT3G54720	-1.54	1.07
CATMA3OA47740R1	AT3G54820	1.94	-1.04
CATMA3OA47770F1	AT3G54830	-2.18	-1.17
CATMA3OA47840F1	AT3G54880	2.92	1.75
CATMA3OA47850F1	AT3G54900	-1.94	-1.16
CATMA3OA48090F1	AT3G55080	-1.62	-1.11
CATMA3OA48140F1	AT3G55130	1.83	-1.11
CATMA3OA48230R1	AT3G55230	-1.67	-1.01
CATMA3OA48240F1	AT3G55240	1.14	1.53
CATMA3OA48250R1	AT3G55250	-1.56	-1.28
CATMA3OA48280R1	AT3G55270	1.71	1.17
CATMA3OA48330F1	AT3G55330	-1.60	-1.00
CATMA3OA48390R1	AT3G55420	-1.63	-1.14
CATMA3OA48410R1	AT3G55450	1.50	1.29
CATMA3OA48450F1	AT3G55500	-2.37	-1.55
CATMA3OA48480R1	AT3G55515	2.07	-1.31
CATMA3OA48610R1	AT3G55630	-1.65	-1.18
CATMA3OA48680R1	AT3G55700	2.50	1.42
CATMA3OA48700R1	AT3G55720	1.62	1.03
CATMA3OA48770R1	AT3G55800	-2.04	-1.24
CATMA3OA48860R1	AT3G55880	1.60	1.36
CATMA3OC57814R1	AT3G55890	1.65	1.44
CATMA3OA48880R1	AT3G55910	1.81	1.82
CATMA3ON94657R1	AT3G55940	-2.16	1.02
CATMA3OA48940F1	AT3G55970	4.72	1.52
CATMA3ON101217R1	AT3G55980	2.21	-1.09
CATMA3OA48980R1	AT3G56010	-1.68	-1.09
CATMA3OA49050F1	AT3G56090	3.19	1.36
CATMA3OA49125R1	AT3G56170	1.59	1.11
CATMA3OA49150R1	AT3G56200	1.61	-1.11
CATMA3OA49180F1	AT3G56230	-2.09	-1.09
CATMA3ON101220F1	AT3G56240	-1.63	-1.18
CATMA3OA49200F1	AT3G56260	1.58	1.01
CATMA3OA49230F1	AT3G56290	-2.16	-1.46
CATMA3OA49300R1	AT3G56330	-1.55	-1.10
CATMA3OA49340R1	AT3G56360	-6.02	-1.83
CATMA3OC57822F1	AT3G56400	2.03	1.51
CATMA3OA49590F1	AT3G56620	1.74	1.39
CATMA3OA49620R1	AT3G56650	-2.01	-1.16
CATMA3OA49680F1	AT3G56710	3.36	1.92
CATMA3OA49900F1	AT3G56910	-1.78	-1.18
CATMA3OC57834R1	AT3G56940	-1.98	-1.29
CATMA3OA49950F1	AT3G56970	-1.47	-5.19
CATMA3OA49960F1	AT3G56980	28.92	10.70
CATMA3OA50010F1	AT3G57020	-1.76	-1.28
CATMA3OA50023R1	AT3G57040	-1.87	-1.12
CATMA3OA50160F1	AT3G57160	1.57	1.55
CATMA3OA50260F1	AT3G57240	1.41	2.28
CATMA3OA50275F1	AT3G57260	4.36	1.71
CATMA3OA50330F1	AT3G57330	2.06	1.34
CATMA3OA50380R1	AT3G57380	1.92	1.08
CATMA3OA50430R1	AT3G57440	-1.09	1.91
CATMA3ON94663F1	AT3G57460	2.61	1.31
CATMA3OA50520F1	AT3G57520	2.99	2.08
CATMA3OA50700R1	AT3G57680	2.27	1.33
CATMA3OA50770R1	AT3G57740	1.79	-1.06
CATMA3OA50890F1	AT3G57880	1.60	-1.05
CATMA3OA51070F1	AT3G58060	12.52	2.99
CATMA3OA51270F1	AT3G58270	2.34	1.11
CATMA3OA51810R1	AT3G58810	15.43	1.96
CATMA3OA51840F1	AT3G58830	-1.52	-1.13
CATMA3OA52080F1	AT3G59040	-1.51	-1.03
CATMA3OA52130R1	AT3G59080	1.81	-1.11
CATMA3OA52190F1	AT3G59140	1.83	1.09
CATMA3OA52260R1	AT3G59210	1.59	1.26
CATMA3OA52270R1	AT3G59220	2.69	-1.34
CATMA3OA52300F1	AT3G59250	-2.08	-1.52
CATMA3OA52380F1	AT3G59340	-1.64	-1.30
CATMA3OC57876F1	AT3G59370	-1.61	-1.05
CATMA3OA52440F1	AT3G59400	-1.92	-1.34
CATMA3OA52725R1	AT3G59700	2.28	1.22
CATMA3OA52730F1	AT3G59710	3.69	3.29
CATMA3ON90978F1	AT3G59740	2.01	1.06
CATMA3ON91054F1	AT3G59930	-2.46	1.21
CATMA3OA52950R1	AT3G59940	-1.19	-1.84
CATMA3OA52980F1	AT3G59980	-2.08	-1.21
CATMA3OA53130R1	AT3G60120	8.78	1.13
CATMA3OA53150R1	AT3G60140	18.18	2.81
CATMA3ON91339F1	AT3G60160	1.68	1.44
CATMA3ON101272F1	AT3G60210	-1.79	-1.20
CATMA3OA53290R1	AT3G60260	1.38	1.67
CATMA3OA53310R1	AT3G60290	-1.49	-1.71
CATMA3OA53340R1	AT3G60330	3.59	1.75
CATMA3OA53380F1	AT3G60370	-1.63	-1.20
CATMA3OA53430R1	AT3G60420	2.50	1.84
CATMA3OA53522F1	AT3G60520	-1.58	1.11
CATMA3OC57890F1	AT3G60540	1.66	1.50
CATMA3ON91310R1	AT3G60647	1.64	-1.10
CATMA3OA53650R1	AT3G60650	1.76	-1.11
CATMA3OA53700R1	AT3G60700	-2.05	-1.03
CATMA3OA53790F1	AT3G60800	1.52	1.04
CATMA3OD03059R1	AT3G60966	1.56	1.05
CATMA3OF03060R1	AT3G60970	1.58	1.43
CATMA3OA54230R1	AT3G61060	-1.58	1.64
CATMA3OC57896R1	AT3G61080	-1.66	1.01
CATMA3OA54270F1	AT3G61100	-1.63	-1.22
CATMA3OC57901R1	AT3G61220	-1.53	-1.06
CATMA3OA54400F1	AT3G61260	-1.85	1.05
CATMA3OA54520F1	AT3G61380	-1.61	-1.15
CATMA3ON101292R1	AT3G61410	3.30	2.60
CATMA3ON94693F1	AT3G61730	-1.13	1.70
CATMA3OA54910F1	AT3G61750	-2.61	-1.52
CATMA3OA54930R1	AT3G61770	-1.58	-1.06
CATMA3OA55020R1	AT3G61870	-1.51	1.79
CATMA3OA55060R1	AT3G61930	5.94	1.00
CATMA3OA55120F1	AT3G61990	1.80	1.28
CATMA3OA55150F1	AT3G62020	-1.77	-1.06
CATMA3OA55155R1	AT3G62030	-2.47	-1.30
CATMA3ON91212F1	AT3G62040	-2.78	-1.06
CATMA3OA55250F1	AT3G62110	-1.89	-1.48
CATMA3OA55290F1	AT3G62150	2.01	-1.04
CATMA3OA55410F1	AT3G62260	1.85	1.64
CATMA3OA55420F1	AT3G62270	2.05	1.04
CATMA3OA55430F1	AT3G62280	1.84	1.05
CATMA3OA55720R1	AT3G62550	2.69	1.96
CATMA3OA55760F1	AT3G62590	1.29	1.69
CATMA3OC57916R1	AT3G62680	1.81	1.76
CATMA3OA55860F1	AT3G62700	1.51	1.11
CATMA3ON101306R1	AT3G62740	-4.92	-1.08
CATMA3OA55940F1	AT3G62770	1.53	1.77
CATMA3OA55990R1	AT3G62820	-1.66	-1.21
CATMA3OA56080F1	AT3G62910	-1.59	-1.30
CATMA3OA56110F1	AT3G62930	-2.07	1.25
CATMA3OC57918R1	AT3G62950	-4.76	1.13
CATMA3OC57919R1	AT3G62960	1.64	-1.20
CATMA3OA56160R1	AT3G62990	1.94	1.20
CATMA3OA56180R1	AT3G63010	2.36	1.49
CATMA3OA56200R1	AT3G63030	1.55	1.19
CATMA3OA56210F1	AT3G63040	-2.46	-1.44
CATMA3OA56310F1	AT3G63120	-1.51	-1.17
CATMA3OA56380F1	AT3G63190	-1.65	-1.16
CATMA3OA56390R1	AT3G63200	-1.93	-1.14
CATMA3OA56460R1	AT3G63280	-1.75	1.40
CATMA3OA56550F1	AT3G63360	-1.15	1.58
CATMA3OA56610F1	AT3G63410	-1.51	-1.16
CATMA3OC57928R1	AT3G63470	-1.54	-1.02
CATMA3OC57930R1	AT3G63490	-1.63	-1.14
CATMA4OA00070R1	AT4G00050	-1.37	-1.67
CATMA4OF01409F1	AT4G00070	1.81	1.67
CATMA4OA00190F1	AT4G00165	-1.58	-1.06
CATMA4OA00360R1	AT4G00305	1.08	1.76
CATMA4OB00440F1	AT4G00370	-1.64	-1.30
CATMA4OA00460F1	AT4G00390	1.50	1.50
CATMA4ON90137F1	AT4G00670	-2.11	1.14
CATMA4OA00860R1	AT4G00780	-1.39	-1.55
CATMA4OA00960F1	AT4G00880	-1.85	1.16
CATMA4OA01020F1	AT4G00910	1.72	1.61
CATMA4OA01110R1	AT4G00970	1.92	1.33
CATMA4OA01180F1	AT4G01010	4.69	1.40
CATMA4OA01230R1	AT4G01050	-1.83	-1.37
CATMA4OA01300R1	AT4G01130	1.58	1.02
CATMA4OA01310F1	AT4G01140	-1.92	-1.30
CATMA4OA01510F1	AT4G01310	-1.84	-1.40
CATMA4OA01530R1	AT4G01330	-1.50	-1.39
CATMA4OA01560R1	AT4G01360	2.04	1.10
CATMA4OC42029F1	AT4G01380	1.75	1.00
CATMA4ON94158F1	AT4G01390	4.46	2.51
CATMA4OA01630R1	AT4G01430	1.66	-1.80
CATMA4OA01640R1	AT4G01440	-1.72	1.10
CATMA4OA01750F1	AT4G01540	1.74	1.30
CATMA4OA01760F1	AT4G01550	1.71	1.15
CATMA4OA01820R1	AT4G01600	-1.91	-1.53
CATMA4OA01840R1	AT4G01630	-3.12	-1.94
CATMA4OA01880F1	AT4G01680	-1.41	-1.52
CATMA4OA01890F1	AT4G01700	1.92	1.10
CATMA4OA01920R1	AT4G01720	1.59	1.34
CATMA4OC42043F1	AT4G01800	-1.55	1.01
CATMA4OA02090F1	AT4G01870	7.12	1.19
CATMA4OA02110R1	AT4G01883	-2.74	-1.04
CATMA4ON90194F1	AT4G01910	1.64	1.12
CATMA4OC42046F1	AT4G01920	1.83	1.12
CATMA4OA02410F1	AT4G02130	-1.60	-1.11
CATMA4OA02550R1	AT4G02280	4.49	1.46
CATMA4OA02630R1	AT4G02330	7.16	1.94
CATMA4OA02835F1	AT4G02520	3.38	1.17
CATMA4OA02840F1	AT4G02530	-2.23	-1.28
CATMA4OC42060R1	AT4G02725	-1.51	-1.16
CATMA4OA03200F1	AT4G02850	-2.14	-1.46
CATMA4OA03280R1	AT4G02940	1.74	1.76
CATMA4OA03380F1	AT4G03060	-1.58	-1.91
CATMA4OA03586R1	AT4G03280	-1.76	-1.04
CATMA4OA03630R1	AT4G03320	1.85	1.65

Table 22: Continued

		Ratio	
D CATMAv6	AGI	+Fe	-Fe
CATMA4OA03800F1	AT4G03450	1.81	3.44
CATMA4OA03850R1	AT4G03500	-3.27	1.03
CATMA4OC42092R1	AT4G03540	1.03	1.63
CATMA4OA04200F1	AT4G03820	1.78	1.22
CATMA4OA04390R1	AT4G03960	1.88	-1.21
CATMA4OC42104F1	AT4G04330	1.28	2.65
CATMA4ON90114F1	AT4G04408	-1.56	1.05
CATMA4OA05070F1	AT4G04490	3.32	1.71
CATMA4OA05080R1	AT4G04500	2.28	1.60
CATMA4ON94181R1	AT4G04540	2.05	1.19
CATMA4OA05150F1	AT4G04620	2.51	1.37
CATMA4OA05180F1	AT4G04640	-1.74	1.09
CATMA4OC42113F1	AT4G04745	1.51	1.68
CATMA4ON94184R1	AT4G04750	1.78	1.84
CATMA4OF03087R1	AT4G04760	1.60	1.75
CATMA4OA05320F1	AT4G04770	1.11	2.65
CATMA4OA05410R1	AT4G04840	-4.50	-2.83
CATMA4OA05550F1	AT4G04955	1.65	1.48
CATMA4OA05600R1	AT4G04990	-1.82	1.10
CATMA4OA05830F1	AT4G05170	-1.32	2.16
CATMA4ON90261R1	AT4G05320	1.61	1.21
CATMA4OA06220R1	AT4G05530	1.56	1.09
CATMA4OC42139R1	AT4G06534	2.01	1.68
CATMA4OC42140R1	AT4G06536	1.69	1.56
CATMA4OC42144F1	AT4G06744	1.53	1.18
CATMA4OC42145F1	AT4G06746	3.01	1.49
CATMA4OA07190F1	AT4G07820	5.62	-1.25
CATMA4OA07550R1	AT4G08040	1.75	-1.75
CATMA4ON94204F1	AT4G08230	1.56	1.09
CATMA4OA08050R1	AT4G08300	-2.30	1.57
CATMA4OF01525F1	AT4G08370	1.65	1.40
CATMA4OA08153R1	AT4G08390	1.19	1.76
CATMA4ON90331F1	AT4G08400	1.57	1.74
CATMA4OF01527F1	AT4G08410	1.67	2.11
CATMA4OA08290F1	AT4G08470	1.71	1.36
CATMA4OA08380F1	AT4G08570	-2.19	1.01
CATMA4ON90319F1	AT4G08770	6.08	1.10
CATMA4OF01535R1	AT4G08780	6.06	1.20
CATMA4OA08740F1	AT4G08850	1.53	-1.05
CATMA4OA08780R1	AT4G08867	1.11	-1.74
CATMA4ON90356F1	AT4G08869	-1.07	-1.58
CATMA4OA08760F1	AT4G08870	1.16	-1.55
CATMA4OA08890R1	AT4G08950	1.55	1.19
CATMA4OA08970F1	AT4G09010	-1.79	-1.33
CATMA4OA09000R1	AT4G09020	3.03	1.13
CATMA4OA09020F1	AT4G09040	-1.77	-1.20
CATMA4OC42178R1	AT4G09110	9.64	2.02
CATMA4OA09130R1	AT4G09160	-1.26	-1.56
CATMA4OA09280R1	AT4G09300	1.79	1.23
CATMA4OA09340F1	AT4G09350	-1.82	-1.21
CATMA4OA09520R1	AT4G09500	1.92	1.10
CATMA4OA09550F1	AT4G09530	2.79	2.55
CATMA4OA09560R1	AT4G09550	-13.33	-9.91
CATMA4OA09580R1	AT4G09570	1.73	1.36
CATMA4OA09680R1	AT4G09650	-1.66	-1.12
CATMA4OC42186R1	AT4G09820	3.48	-1.56
CATMA4OC42195R1	AT4G10020	-1.58	-1.10
CATMA4ON90336F1	AT4G10030	-1.52	-1.19
CATMA4OA10120R1	AT4G10060	-1.76	-1.37
CATMA4OA10170R1	AT4G10120	1.50	1.09
CATMA4OA10310F1	AT4G10265	1.46	-2.87
CATMA4OA10320R1	AT4G10270	1.41	-2.04
CATMA4OA10340R1	AT4G10300	-1.78	-1.14
CATMA4OA10345R1	AT4G10310	-2.49	-1.24
CATMA4OA10540R1	AT4G10500	7.79	1.31
CATMA4ON94220R1	AT4G10510	9.72	1.97
CATMA4ON94221F1	AT4G10540	2.82	1.32
CATMA4OF01568F1	AT4G10550	3.69	1.18
CATMA4OA10760R1	AT4G10720	2.62	-1.23
CATMA4OF03124F1	AT4G10860	1.54	1.11
CATMA4OA11010R1	AT4G10910	-1.26	-1.60
CATMA4OC42217R1	AT4G11000	2.12	1.34
CATMA4OC42218F1	AT4G11020	-1.63	-1.59
CATMA4OA11180R1	AT4G11100	-1.60	-1.29
CATMA4OA11240R1	AT4G11170	1.10	1.62
CATMA4OA11260R1	AT4G11175	-1.72	-1.12
CATMA4OF01577R1	AT4G11190	-1.35	-2.45
CATMA4OC42220R1	AT4G11211	-1.31	-2.16
CATMA4OC42222R1	AT4G11310	-6.74	1.42
CATMA4OC42223R1	AT4G11320	-4.42	1.19
CATMA4OA11510R1	AT4G11393	3.69	1.50
CATMA4OA11590R1	AT4G11460	-1.40	-1.58
CATMA4OA11610R1	AT4G11480	2.12	1.06
CATMA4OA11745F1	AT4G11600	2.65	1.48
CATMA4ON90267F1	AT4G11642	3.19	-1.12
CATMA4OA11780F1	AT4G11650	22.10	1.05
CATMA4OA11790R1	AT4G11655	1.69	1.23
CATMA4OA11810F1	AT4G11670	1.13	1.10
CATMA4OF03131F1	AT4G11840	1.52	1.22
CATMA4OC42235F1	AT4G11850	1.65	1.19
CATMA4OA12000R1	AT4G11890	3.39	1.71
CATMA4OA12020R1	AT4G11910	1.95	1.31
CATMA4OA12160R1	AT4G12030	-1.54	-1.33
CATMA4OA12180F1	AT4G12050	1.35	1.61
CATMA4OA12210R1	AT4G12080	1.44	1.50
CATMA4OA12240F1	AT4G12120	1.96	1.58
CATMA4OA12400R1	AT4G12290	5.99	2.33
CATMA4OA12440F1	AT4G12330	2.39	-1.42
CATMA4OA12530F1	AT4G12420	-1.56	-1.39
CATMA4ON94232R1	AT4G12440	-1.79	-1.60
CATMA4OC42251F1	AT4G12480	2.34	-1.32
CATMA4OC42252F1	AT4G12490	2.36	-1.34
CATMA4ON90216F1	AT4G12510	-2.01	-1.35
CATMA4ON90124F1	AT4G12520	-1.73	-1.26
CATMA4OD03132R1	AT4G12545	-7.50	-2.21
CATMA4OD01600R1	AT4G12550	-8.38	-2.88
CATMA4ON100199R1	AT4G12720	2.12	1.32
CATMA4OC42256F1	AT4G12735	2.19	1.63
CATMA4OA12960R1	AT4G12830	-1.87	-1.20
CATMA4ON100202F1	AT4G12910	2.07	1.97
CATMA4OA13100F1	AT4G12970	-1.85	-1.78
CATMA4OA13140R1	AT4G13030	1.58	1.22
CATMA4OA13280F1	AT4G13180	1.68	1.24
CATMA4OA13300F1	AT4G13195	1.81	1.12
CATMA4ON98283R1	AT4G13245	1.60	1.24
CATMA4OA13370F1	AT4G13250	1.47	6.16
CATMA4OC42272R1	AT4G13310	2.39	-1.03
CATMA4OA13550R1	AT4G13390	1.15	2.03
CATMA4OA13595F1	AT4G13420	-1.06	2.28
CATMA4OA13610R1	AT4G13440	-1.71	1.23
CATMA4OM00079R1	AT4G13493	-2.50	-1.37
CATMA4OM00028R1	AT4G13494	-1.84	-1.05
CATMA4ON100211F1	AT4G13500	-1.75	-1.05
CATMA4OC42278F1	AT4G13560	-1.62	-1.04
CATMA4OA13740F1	AT4G13575	-3.58	-1.25
CATMA4OA13800R1	AT4G13620	-2.02	-1.91
CATMA4OA13850R1	AT4G13670	-1.59	-1.27
CATMA4OA13955F1	AT4G13770	-1.24	-1.58
CATMA4OA13980F1	AT4G13800	-2.44	-1.53
CATMA4OF01608F1	AT4G13810	2.45	1.39
CATMA4ON100216F1	AT4G13820	1.95	1.15
CATMA4OC42284F1	AT4G13890	1.26	1.56
CATMA4ON90251R1	AT4G13920	1.95	1.22
CATMA4OA14220F1	AT4G14010	-1.74	1.08
CATMA4OA14230F1	AT4G14020	1.32	-1.61
CATMA4OA14330F1	AT4G14090	1.87	-1.89
CATMA4OA14375F1	AT4G14130	-2.65	1.29
CATMA4OA14480R1	AT4G14220	1.59	1.28
CATMA4OA14700F1	AT4G14365	3.56	1.46
CATMA4OA14720F1	AT4G14370	1.69	1.14
CATMA4OA14770R1	AT4G14400	3.17	1.99
CATMA4OA14840R1	AT4G14465	1.52	-1.10
CATMA4OA14850F1	AT4G14480	-1.65	1.08
CATMA4OC42296R1	AT4G14560	1.60	1.29
CATMA4OA14950F1	AT4G14580	1.53	1.48
CATMA4OA15020R1	AT4G14630	2.62	-1.13
CATMA4OA15030F1	AT4G14650	-1.52	-1.02
CATMA4OA15086R1	AT4G14690	-5.03	-2.68
CATMA4OC42301F1	AT4G14710	2.18	1.28
CATMA4OC42304R1	AT4G14780	-2.51	1.17
CATMA4OA15340R1	AT4G14870	-1.80	-1.16
CATMA4OA15350R1	AT4G14890	-1.78	-1.22
CATMA4OA15630R1	AT4G15093	1.71	1.20
CATMA4OA15660R1	AT4G15120	1.52	1.17
CATMA4OA15700R1	AT4G15160	-2.05	1.18
CATMA4ON94252R1	AT4G15233	2.19	1.13
CATMA4ON94253R1	AT4G15236	2.11	1.16
CATMA4OA15850R1	AT4G15248	-3.96	-1.88
CATMA4OC42313R1	AT4G15260	1.90	1.43
CATMA4OC42314F1	AT4G15270	2.95	1.36
CATMA4ON94254R1	AT4G15280	3.69	1.42
CATMA4OF01619F1	AT4G15290	-2.02	1.07
CATMA4OA15960F1	AT4G15330	1.84	2.02
CATMA4OA15970F1	AT4G15340	1.93	-1.30
CATMA4ON94259F1	AT4G15370	1.46	-3.73
CATMA4ON100247R1	AT4G15393	1.39	-6.47
CATMA4OF03143R1	AT4G15396	1.52	-1.26
CATMA4ON94260R1	AT4G15398	1.05	-2.12
CATMA4OA16120R1	AT4G15417	-1.69	-1.55
CATMA4OA16150R1	AT4G15430	-1.69	-1.79
CATMA4OC42318F1	AT4G15480	-1.62	-1.52
CATMA4OA16220F1	AT4G15490	1.71	1.56
CATMA4OA16240R1	AT4G15510	-1.64	-1.17
CATMA4OA16270F1	AT4G15530	3.57	1.03
CATMA4OC42319R1	AT4G15540	1.92	1.00
CATMA4ON100252R1	AT4G15610	2.08	1.26
CATMA4OC42321R1	AT4G15620	1.74	-1.15
CATMA4OF01621R1	AT4G15660	-3.31	-1.43
CATMA4ON90046R1	AT4G15670	-2.35	-1.85
CATMA4OC42322R1	AT4G15680	-3.00	-1.54
CATMA4OC42323R1	AT4G15690	-2.78	-1.21
CATMA4ON90142R1	AT4G15700	-3.14	-1.29
CATMA4OA16570F1	AT4G15780	-1.57	-1.20
CATMA4OA16650F1	AT4G15830	-1.66	-1.49
CATMA4OA16790F1	AT4G15960	-1.72	1.05
CATMA4OD03145F1	AT4G15990	-1.47	1.72
CATMA4OC42796R1	AT4G16008	1.52	1.24
CATMA4OC42335F1	AT4G16146	2.13	1.71
CATMA4OC42336F1	AT4G16155	-1.59	-1.03
CATMA4OA16930R1	AT4G16160	-1.79	-1.25
CATMA4OA16980R1	AT4G16190	1.89	1.58
CATMA4OA17000F1	AT4G16210	1.75	1.22
CATMA4ON94265F1	AT4G16240	1.62	-1.06
CATMA4OA17080F1	AT4G16260	14.21	-1.23
CATMA4OA17180F1	AT4G16370	-2.47	-2.82
CATMA4OA17210R1	AT4G16400	1.15	1.53
CATMA4ON90023F1	AT4G16410	-1.75	-1.24
CATMA4OA17380F1	AT4G16515	-1.21	-1.93
CATMA4OA17500F1	AT4G16563	1.43	1.81
CATMA4OA17550R1	AT4G16600	1.09	1.99
CATMA4OA17570F1	AT4G16620	1.19	3.62
CATMA4OA17600R1	AT4G16660	1.66	1.18
CATMA4OA17630F1	AT4G16690	-2.30	-1.15
CATMA4OA17710R1	AT4G16745	1.75	-1.01
CATMA4OC42352F1	AT4G16880	-2.15	-1.47
CATMA4ON94267F1	AT4G16960	1.92	1.08
CATMA4OA18000R1	AT4G16980	-1.74	-1.29
CATMA4OA18050F1	AT4G17030	2.98	-1.89
CATMA4OA18230R1	AT4G17215	-1.75	1.63
CATMA4OA18240F1	AT4G17220	-1.90	1.05
CATMA4ON100279F1	AT4G17230	2.11	1.39
CATMA4OA18290R1	AT4G17250	1.85	-1.12
CATMA4OA18330F1	AT4G17280	-1.65	1.28
CATMA4OA18370R1	AT4G17340	-4.01	-2.39
CATMA4OA18490F1	AT4G17470	2.85	1.05
CATMA4OA18523F1	AT4G17490	1.83	1.18
CATMA4OA18526R1	AT4G17500	2.05	1.23
CATMA4OA18580R1	AT4G17560	-1.89	-1.32
CATMA4OA18680R1	AT4G17660	3.19	1.44
CATMA4OA18700F1	AT4G17680	2.25	1.17
CATMA4OA18710R1	AT4G17690	2.08	2.41
CATMA4OA18790R1	AT4G17760	-1.63	-1.10
CATMA4OA18850R1	AT4G17810	-1.93	-1.21
CATMA4OA18930R1	AT4G17900	1.82	1.30
CATMA4OC42374F1	AT4G17980	2.27	1.09
CATMA4OC42378R1	AT4G18120	1.73	1.20
CATMA4OA19190R1	AT4G18170	3.89	1.33
CATMA4OF01640R1	AT4G18197	2.83	1.04
CATMA4OA19240R1	AT4G18205	2.30	1.10
CATMA4OA19250R1	AT4G18210	2.06	1.18
CATMA4OF03153R1	AT4G18220	1.66	-1.03
CATMA4OA19290F1	AT4G18250	3.10	2.28
CATMA4OA19330R1	AT4G18280	-1.54	-1.10
CATMA4OA19420F1	AT4G18360	2.28	1.20
CATMA4OA19425R1	AT4G18370	-1.95	-1.26
CATMA4OA19570F1	AT4G18480	-1.75	-1.22
CATMA4OA19650F1	AT4G18550	-1.76	2.26
CATMA4OA19730R1	AT4G18610	-1.51	-1.13
CATMA4OA19860F1	AT4G18740	-2.42	-1.59
CATMA4ON94277F1	AT4G18760	-1.74	-1.43
CATMA4OA19990F1	AT4G18880	2.25	1.39
CATMA4OA20000R1	AT4G18890	1.78	-1.10
CATMA4OA20030R1	AT4G18910	2.14	1.07

Table 22: Continued

		Ratio	
D CATMAv6	AGI	+Fe	-Fe
CATMA4OA20110F1	AT4G18990	1.60	1.22
CATMA4OC42392R1	AT4G19100	-1.73	-1.20
CATMA4OA20330R1	AT4G19160	1.48	1.55
CATMA4OA20400R1	AT4G19200	1.66	1.41
CATMA4OA20540F1	AT4G19370	4.67	1.99
CATMA4ON100294F1	AT4G19420	1.81	1.25
CATMA4OA20720F1	AT4G19512	-2.58	-1.05
CATMA4OA20740R1	AT4G19530	-1.57	-1.26
CATMA4OA20900F1	AT4G19660	1.60	1.29
CATMA4OA20920R1	AT4G19680	12.10	2.18
CATMA4OA20925R1	AT4G19690	16.32	1.95
CATMA4OA20930F1	AT4G19700	2.20	1.26
CATMA4OA21020F1	AT4G19810	2.36	1.56
CATMA4OA21035F1	AT4G19830	-2.15	-1.27
CATMA4OC42406F1	AT4G19880	1.52	1.20
CATMA4OA21200R1	AT4G19970	-1.57	1.32
CATMA4OA21220F1	AT4G19980	1.81	-1.15
CATMA4OA21230F1	AT4G19985	-1.67	-1.35
CATMA4OA21380R1	AT4G20110	1.56	1.25
CATMA4OA21390R1	AT4G20130	-1.53	-1.42
CATMA4ON100304R1	AT4G20170	-1.15	-1.53
CATMA4OC42415F1	AT4G20230	-2.71	-1.80
CATMA4OA21500F1	AT4G20240	-1.64	-1.42
CATMA4OA21570R1	AT4G20320	1.84	-1.38
CATMA4OA21620R1	AT4G20360	-1.70	-1.16
CATMA4OC42419R1	AT4G20380	1.56	1.27
CATMA4OA21640R1	AT4G20390	-2.62	1.26
CATMA4OA22250R1	AT4G20760	-1.54	-1.40
CATMA4OA22370R1	AT4G20860	1.76	1.07
CATMA4OA22560R1	AT4G21020	-2.60	-1.55
CATMA4OA22700R1	AT4G21120	1.72	1.21
CATMA4OA22780F1	AT4G21190	-1.66	-1.20
CATMA4OA22810F1	AT4G21215	1.98	1.51
CATMA4OD03168R1	AT4G21250	-2.04	-1.07
CATMA4OA22880R1	AT4G21280	-1.88	-1.06
CATMA4OA22910R1	AT4G21320	-1.66	-1.25
CATMA4OA23010F1	AT4G21400	1.58	1.16
CATMA4OC42435R1	AT4G21445	-1.88	-1.13
CATMA4OA23210F1	AT4G21560	1.51	1.23
CATMA4OA23230R1	AT4G21580	1.81	1.17
CATMA4OA23250R1	AT4G21590	1.34	-1.51
CATMA4OA23340F1	AT4G21680	4.86	1.58
CATMA4OA23420R1	AT4G21760	-1.88	-2.73
CATMA4OC42443F1	AT4G21840	6.02	2.18
CATMA4OA23520F1	AT4G21860	-1.54	-1.21
CATMA4OA23540F1	AT4G21870	-1.51	-1.78
CATMA4OA23750F1	AT4G22070	2.38	1.05
CATMA4ON90111F1	AT4G22080	1.72	1.20
CATMA4OA23840R1	AT4G22160	-1.89	1.05
CATMA4OA23885F1	AT4G22200	-1.62	-1.24
CATMA4OD03173R1	AT4G22212	-1.71	-1.12
CATMA4OA23900R1	AT4G22214	1.94	1.04
CATMA4OC42449R1	AT4G22230	-1.18	1.79
CATMA4OA24180F1	AT4G22460	-1.93	-1.26
CATMA4OA24200F1	AT4G22485	-1.03	-3.33
CATMA4OA24210F1	AT4G22490	-1.07	-3.49
CATMA4OA24220F1	AT4G22505	-1.04	-3.38
CATMA4ON90155R1	AT4G22513	-1.31	-3.73
CATMA4ON90116R1	AT4G22517	-1.23	-4.13
CATMA4OA24250R1	AT4G22520	-1.47	-3.39
CATMA4OA24260F1	AT4G22530	1.84	1.37
CATMA4OA24300F1	AT4G22570	-1.50	-1.53
CATMA4OA24340F1	AT4G22610	7.73	-1.20
CATMA4OA24370R1	AT4G22640	-1.83	1.07
CATMA4OA24390R1	AT4G22666	-1.97	-1.12
CATMA4OF01696R1	AT4G22710	2.91	1.44
CATMA4OC42454R1	AT4G22730	-1.21	-1.57
CATMA4OA24570F1	AT4G22790	-1.57	-1.10
CATMA4OA24580R1	AT4G22810	1.98	1.77
CATMA4OA24590F1	AT4G22820	1.72	1.25
CATMA4OA24600F1	AT4G22830	-2.02	-1.15
CATMA4OF03177F1	AT4G22870	1.54	-3.03
CATMA4OA24645F1	AT4G22880	2.47	-3.34
CATMA4ON100352R1	AT4G22890	-1.61	-1.45
CATMA4OA24770F1	AT4G23020	-1.40	-1.54
CATMA4OA24880F1	AT4G23130	1.92	1.20
CATMA4OF03179R1	AT4G23140	6.09	1.42
CATMA4OA24900R1	AT4G23150	2.18	1.72
CATMA4ON90360R1	AT4G23160	4.56	1.47
CATMA4OA24930R1	AT4G23170	1.87	1.67
CATMA4OA24940R1	AT4G23180	2.40	1.44
CATMA4OA24945F1	AT4G23190	2.51	1.01
CATMA4ON100356F1	AT4G23210	-1.41	-1.62
CATMA4OA24980F1	AT4G23220	2.01	-1.02
CATMA4OA25030F1	AT4G23260	1.98	1.12
CATMA4ON94299R1	AT4G23280	2.02	1.65
CATMA4OA25060F1	AT4G23290	-1.50	-1.70
CATMA4OA25210R1	AT4G23400	-1.77	-1.43
CATMA4ON94300R1	AT4G23410	1.62	1.21
CATMA4OA25290R1	AT4G23470	1.59	1.21
CATMA4OA25320F1	AT4G23496	-3.12	-1.27
CATMA4OA25330R1	AT4G23500	-1.72	-1.18
CATMA4OA25340F1	AT4G23510	4.11	1.58
CATMA4OA25450R1	AT4G23600	3.59	1.34
CATMA4OA25460R1	AT4G23610	1.57	1.24
CATMA4OA25510F1	AT4G23670	-1.03	-2.16
CATMA4OA25520F1	AT4G23690	1.80	-1.08
CATMA4OA25530F1	AT4G23700	1.71	1.02
CATMA4OA25590F1	AT4G23770	-1.85	-1.62
CATMA4OC42475F1	AT4G23810	2.18	-1.31
CATMA4OA25654R1	AT4G23870	-1.74	-1.50
CATMA4ON100371R1	AT4G23990	2.66	1.49
CATMA4OC42480F1	AT4G24015	-1.52	1.27
CATMA4OA25810R1	AT4G24090	-1.64	-1.16
CATMA4OA25830F1	AT4G24110	1.91	2.02
CATMA4OA25840R1	AT4G24120	1.91	2.54
CATMA4OA25860F1	AT4G24140	-1.65	1.32
CATMA4OA25920F1	AT4G24190	1.68	1.11
CATMA4OC42484R1	AT4G24380	1.82	1.07
CATMA4OA26180R1	AT4G24450	2.98	-1.82
CATMA4OA26210R1	AT4G24480	2.28	1.18
CATMA4OA26240R1	AT4G24510	-1.30	-1.63
CATMA4OC42486R1	AT4G24570	1.87	1.19
CATMA4OA26380F1	AT4G24670	-1.90	-1.17
CATMA4OA26400R1	AT4G24690	2.91	2.18
CATMA4OA26410F1	AT4G24700	-5.38	-2.91
CATMA4ON100379F1	AT4G24750	-2.03	-1.35
CATMA4OA26465F1	AT4G24770	-1.82	-1.14
CATMA4OA26470F1	AT4G24780	-1.08	-1.60
CATMA4OA26620F1	AT4G24930	-2.26	-1.31
CATMA4OA26710F1	AT4G25010	3.18	-1.09
CATMA4OA26730R1	AT4G25030	2.18	2.00
CATMA4OA26750R1	AT4G25050	-1.81	-1.16
CATMA4OA26770R1	AT4G25080	-1.65	-1.26
CATMA4OA26790F1	AT4G25100	-3.01	1.55
CATMA4OA26830R1	AT4G25140	-8.50	-5.57
CATMA4OC42489R1	AT4G25220	1.51	-1.40
CATMA4OA26940R1	AT4G25250	-1.50	-1.27
CATMA4OA26980F1	AT4G25290	-2.09	-1.31
CATMA4OC42490R1	AT4G25310	3.08	-1.04
CATMA4OA27200F1	AT4G25450	-1.51	-1.09
CATMA4OA27390F1	AT4G25700	-1.75	-1.49
CATMA4OA27450R1	AT4G25760	-1.61	-1.21
CATMA4OA27470R1	AT4G25780	-2.13	-1.79
CATMA4OC42498R1	AT4G25810	2.13	-1.40
CATMA4OA27496R1	AT4G25820	1.57	1.25
CATMA4OC42499R1	AT4G25860	1.66	-1.16
CATMA4OA27600R1	AT4G25900	2.26	1.29
CATMA4OA27602R1	AT4G25910	-1.84	-1.26
CATMA4OA27610R1	AT4G25930	1.10	1.76
CATMA4OA27612F1	AT4G25940	1.83	1.67
CATMA4OC42500R1	AT4G25960	-1.12	-1.52
CATMA4OA27647R1	AT4G26050	-3.39	-1.56
CATMA4OC42502F1	AT4G26060	1.53	1.46
CATMA4ON100393R1	AT4G26070	1.83	1.32
CATMA4ON100394F1	AT4G26080	1.54	1.17
CATMA4ON90076R1	AT4G26090	1.91	1.32
CATMA4OA27675R1	AT4G26120	1.54	1.30
CATMA4OA27685R1	AT4G26150	-3.11	-1.87
CATMA4OA27720R1	AT4G26200	2.27	-1.11
CATMA4OA27740R1	AT4G26220	-1.77	-1.49
CATMA4OA27800F1	AT4G26270	2.18	1.46
CATMA4ON90145R1	AT4G26288	-1.69	-1.18
CATMA4OC42507F1	AT4G26320	-2.35	-1.21
CATMA4OA28030R1	AT4G26470	2.62	1.51
CATMA4OA28090R1	AT4G26520	-1.75	-1.57
CATMA4OA28100R1	AT4G26530	-1.15	1.76
CATMA4OA28130F1	AT4G26555	-1.91	-1.08
CATMA4OA28330F1	AT4G26740	-10.00	-4.11
CATMA4OA28370R1	AT4G26790	-1.38	1.52
CATMA4OA28430F1	AT4G26850	-1.25	-1.67
CATMA4OA28450F1	AT4G26860	-1.69	-1.26
CATMA4OA28490F1	AT4G26910	1.54	1.11
CATMA4OA28530F1	AT4G26950	2.66	1.30
CATMA4OA28560R1	AT4G26970	1.28	1.69
CATMA4OD03185R1	AT4G27030	-2.69	-1.22
CATMA4OC42518R1	AT4G27140	-12.83	-5.30
CATMA4OF01721R1	AT4G27150	-17.94	-13.30
CATMA4ON90121R1	AT4G27160	-4.46	-2.32
CATMA4ON90334R1	AT4G27170	-11.05	-4.00
CATMA4OA28860F1	AT4G27280	1.63	1.07
CATMA4OA28880F1	AT4G27300	2.20	1.51
CATMA4OA28890R1	AT4G27310	-1.82	-1.48
CATMA4OA28930R1	AT4G27360	-1.51	-2.36
CATMA4OA28940F1	AT4G27370	-1.63	-1.01
CATMA4OA28990F1	AT4G27410	-1.61	-1.62
CATMA4OA29005R1	AT4G27430	-1.54	-1.06
CATMA4OA29020F1	AT4G27450	-1.72	-1.38
CATMA4OA29090F1	AT4G27520	-1.93	-1.26
CATMA4OA29170R1	AT4G27590	2.36	1.15
CATMA4OA29340F1	AT4G27700	-1.91	-1.28
CATMA4OA29500R1	AT4G27860	-1.23	-1.60
CATMA4OA29540R1	AT4G27900	1.65	-1.15
CATMA4OA29590F1	AT4G27970	1.84	-1.03
CATMA4OA29670F1	AT4G28025	-1.68	-1.11
CATMA4OA29690R1	AT4G28040	4.35	-1.37
CATMA4OC42530F1	AT4G28050	-1.54	-1.37
CATMA4OC42532F1	AT4G28080	-1.88	-1.11
CATMA4OC42533R1	AT4G28085	1.69	1.13
CATMA4OA29890F1	AT4G28250	-1.77	-1.32
CATMA4OA29930F1	AT4G28290	-1.53	-2.34
CATMA4OA29940R1	AT4G28300	1.55	1.27
CATMA4OA29990R1	AT4G28350	1.64	1.16
CATMA4OA30120R1	AT4G28460	1.56	2.23
CATMA4OA30155R1	AT4G28490	3.18	1.19
CATMA4OA30170R1	AT4G28520	-8.40	-2.78
CATMA4OA30180F1	AT4G28530	-1.12	2.76
CATMA4OA30310R1	AT4G28660	-2.54	-1.39
CATMA4OA30360R1	AT4G28703	1.67	-1.11
CATMA4OA30420R1	AT4G28730	-1.84	-1.07
CATMA4ON100422R1	AT4G28780	-2.05	-2.01
CATMA4OA30570R1	AT4G28850	1.56	1.03
CATMA4OA30650R1	AT4G28940	-2.57	-1.02
CATMA4OA30720R1	AT4G29060	-1.59	-1.36
CATMA4OA30770R1	AT4G29110	1.80	1.52
CATMA4ON100428F1	AT4G29190	2.34	1.53
CATMA4OC42545R1	AT4G29210	1.61	1.32
CATMA4OA30900R1	AT4G29240	-1.29	-1.62
CATMA4OC42546F1	AT4G29270	-1.83	-1.71
CATMA4OA30980R1	AT4G29340	-1.56	-1.56
CATMA4OA31030R1	AT4G29400	-1.85	-1.58
CATMA4OA31220F1	AT4G29590	-1.52	-1.19
CATMA4OA31410R1	AT4G29780	1.58	1.59
CATMA4OA31540F1	AT4G29900	2.14	1.50
CATMA4OC42556F1	AT4G29905	-2.37	-1.40
CATMA4OA31590R1	AT4G29930	-2.03	-1.01
CATMA4ON100437F1	AT4G30120	3.17	3.20
CATMA4OA31790F1	AT4G30140	-1.01	-2.51
CATMA4OA31835R1	AT4G30210	1.64	1.15
CATMA4OA32040F1	AT4G30430	1.51	-1.04
CATMA4OA32060F1	AT4G30450	-3.31	-1.49
CATMA4ON90064F1	AT4G30490	1.68	1.03
CATMA4OC42565R1	AT4G30610	-1.56	-1.41
CATMA4OC42565F1	AT4G30620	-1.61	-1.18
CATMA4ON100442F1	AT4G30670	3.63	1.23
CATMA4OA32470R1	AT4G30845	-1.65	-1.09
CATMA4OA32615F1	AT4G30950	-1.91	-1.20
CATMA4OA32620R1	AT4G30960	1.62	-1.01
CATMA4OA32650R1	AT4G30993	-1.54	-1.42
CATMA4OA32920F1	AT4G31240	1.55	1.57
CATMA4OA33000F1	AT4G31320	-1.72	-1.12
CATMA4OA33010R1	AT4G31330	-1.75	-1.10
CATMA4ON90384R1	AT4G31351	1.67	-1.25
CATMA4ON90122R1	AT4G31354	1.79	-1.20
CATMA4OA33066R1	AT4G31380	1.95	1.02
CATMA4OA33123F1	AT4G31470	-1.60	-1.05
CATMA4OA33170R1	AT4G31530	-1.57	-1.18
CATMA4OA33370R1	AT4G31730	-2.04	1.08
CATMA4OA33440R1	AT4G31800	3.46	1.71
CATMA4OA33520R1	AT4G31870	-2.81	-1.36
CATMA4OA33530F1	AT4G31875	-1.75	1.35
CATMA4ON100455R1	AT4G31940	12.34	2.87
CATMA4ON90125R1	AT4G31950	24.07	3.57

Table 22: Continued

		Ratio	
D CATMAv6	AGI	+Fe	-Fe
CATMA4OF03195R1	AT4G31970	23.10	2.72
CATMA4OA33850R1	AT4G32190	-1.62	-1.28
CATMA4OA33990R1	AT4G32280	-2.06	-1.38
CATMA4OA34220R1	AT4G32480	1.56	-1.37
CATMA4OC42598R1	AT4G32590	-1.65	-1.14
CATMA4OA34386F1	AT4G32650	1.53	1.21
CATMA4OA34500R1	AT4G32770	-1.53	-1.10
CATMA4OC42601R1	AT4G32785	-2.41	1.05
CATMA4OA34540R1	AT4G32810	2.75	2.02
CATMA4OA34610R1	AT4G32870	1.76	1.39
CATMA4OA34660R1	AT4G32915	-1.67	-1.19
CATMA4OA34690F1	AT4G32940	3.54	2.11
CATMA4OA34770F1	AT4G33020	1.23	1.61
CATMA4OA34780F1	AT4G33040	2.48	1.18
CATMA4OA34790F1	AT4G33050	3.52	1.30
CATMA4OF03201F1	AT4G33110	-1.51	-1.46
CATMA4ON90335F1	AT4G33120	-1.59	-1.36
CATMA4OA34905F1	AT4G33150	2.39	-1.14
CATMA4OA35030F1	AT4G33300	2.22	1.38
CATMA4OA35050F1	AT4G33330	-1.52	-1.45
CATMA4OA35200F1	AT4G33470	-1.50	-1.29
CATMA4OA35220F1	AT4G33490	1.65	1.03
CATMA4OA35246R1	AT4G33520	-1.50	-1.31
CATMA4OA35250F1	AT4G33530	-1.58	-1.16
CATMA4OA35280R1	AT4G33550	-2.92	-1.51
CATMA4OF01764R1	AT4G33610	-1.74	1.34
CATMA4OC42608F1	AT4G33660	-1.65	-1.06
CATMA4OA35420R1	AT4G33666	-1.60	1.05
CATMA4ON100474R1	AT4G33720	71.60	-2.92
CATMA4OA35490R1	AT4G33730	1.58	2.27
CATMA4OA35530F1	AT4G33770	-1.83	1.26
CATMA4OA35550F1	AT4G33790	-3.14	-1.04
CATMA4OA35660F1	AT4G33880	-1.77	-1.30
CATMA4OA35780R1	AT4G33960	-1.84	1.19
CATMA4OA35800F1	AT4G33980	3.59	2.97
CATMA4OA35845R1	AT4G34050	1.91	-1.03
CATMA4ON90203F1	AT4G34131	1.81	1.39
CATMA4OA35980R1	AT4G34150	1.68	1.54
CATMA4OA36000F1	AT4G34180	1.91	1.23
CATMA4OA36005F1	AT4G34190	-1.84	-1.17
CATMA4OA36040F1	AT4G34220	-1.04	-1.53
CATMA4OC42615F1	AT4G34230	2.05	-1.03
CATMA4OA36150R1	AT4G34320	1.96	2.03
CATMA4OA36180F1	AT4G34350	-1.65	-1.09
CATMA4OA36210R1	AT4G34380	1.63	1.17
CATMA4OA36220R1	AT4G34390	1.63	1.36
CATMA4OA36260R1	AT4G34420	3.10	1.51
CATMA4OA36390R1	AT4G34550	-2.51	-1.76
CATMA4OA36450F1	AT4G34610	-2.16	-1.44
CATMA4OA36460F1	AT4G34620	-2.06	-1.40
CATMA4OA36470F1	AT4G34630	1.54	-1.16
CATMA4OA36503F1	AT4G34710	1.64	-1.68
CATMA4OA36510F1	AT4G34730	-1.98	-1.21
CATMA4OA36550F1	AT4G34760	-2.09	-1.47
CATMA4OA36560R1	AT4G34770	-1.29	-2.40
CATMA4OA36570R1	AT4G34790	-1.47	-1.80
CATMA4OC42624R1	AT4G34800	-1.46	-1.55
CATMA4OC42625R1	AT4G34810	-1.16	-1.71
CATMA4OA36600F1	AT4G34830	-2.19	-1.04
CATMA4OC42630R1	AT4G35030	-1.81	-1.26
CATMA4OA36800F1	AT4G35060	-1.73	-1.13
CATMA4OA36830F1	AT4G35110	1.51	1.12
CATMA4ON94350F1	AT4G35150	-4.00	-1.73
CATMA4OA36890F1	AT4G35160	-2.96	-1.48
CATMA4OA36980F1	AT4G35250	-2.42	-1.04
CATMA4OA37055R1	AT4G35350	-1.64	-1.02
CATMA4OA37110F1	AT4G35420	-1.42	1.66
CATMA4OA37130F1	AT4G35440	-1.79	1.58
CATMA4OA37145F1	AT4G35480	1.52	1.28
CATMA4ON100497R1	AT4G35770	-8.32	-1.22
CATMA4OC42843R1	AT4G35783	-1.51	-1.13
CATMA4OA37620F1	AT4G35985	-1.15	1.58
CATMA4OA37660F1	AT4G36010	1.54	1.37
CATMA4OA37680F1	AT4G36030	1.89	1.34
CATMA4OA37700F1	AT4G36050	1.03	1.63
CATMA4OA37710R1	AT4G36060	-1.58	1.18
CATMA4OA37770R1	AT4G36110	1.77	1.07
CATMA4OA37810R1	AT4G36150	1.75	1.15
CATMA4OA37973F1	AT4G36360	-1.46	-1.53
CATMA4OA37980F1	AT4G36390	-1.75	-1.22
CATMA4OA38005F1	AT4G36430	14.73	1.45
CATMA4OA38060F1	AT4G36500	1.57	1.01
CATMA4OA38070F1	AT4G36520	1.53	1.83
CATMA4OA38090F1	AT4G36530	-1.57	-1.21
CATMA4OA38150F1	AT4G36610	-1.57	1.82
CATMA4OA38220F1	AT4G36670	1.49	1.67
CATMA4OA38260F1	AT4G36700	-3.78	-11.35
CATMA4OA38300F1	AT4G36740	-1.03	-1.62
CATMA4OA38440F1	AT4G36850	-2.52	-1.26
CATMA4OA38590R1	AT4G37010	1.16	1.50
CATMA4OA38610R1	AT4G37030	3.10	2.23
CATMA4OC42666R1	AT4G37040	-1.55	-1.24
CATMA4ON94362F1	AT4G37060	2.24	-1.02
CATMA4OF03207F1	AT4G37070	1.53	-1.15
CATMA4OA38660R1	AT4G37080	-1.99	-1.54
CATMA4OA38690F1	AT4G37110	-1.75	-1.20
CATMA4OC42669F1	AT4G37150	-2.29	-1.21
CATMA4OA38740F1	AT4G37160	-1.61	1.15
CATMA4OA38790R1	AT4G37220	-2.99	-1.49
CATMA4OA38820R1	AT4G37240	-1.71	-1.06
CATMA4OA38880R1	AT4G37300	-1.68	-1.07
CATMA4OA38900F1	AT4G37320	1.76	1.06
CATMA4OC42674F1	AT4G37370	5.62	1.36
CATMA4ON90271F1	AT4G37409	-2.11	-1.03
CATMA4ON90271R1	AT4G37410	-3.12	-1.33
CATMA4OA39085R1	AT4G37520	2.32	1.33
CATMA4OA39100F1	AT4G37540	-1.81	-1.30
CATMA4OA39140F1	AT4G37610	-1.55	-1.06
CATMA4OA39220F1	AT4G37700	-7.58	-2.36
CATMA4OA39270R1	AT4G37760	-1.52	1.07
CATMA4OA39350F1	AT4G37850	-1.08	-2.08
CATMA4OA39370F1	AT4G37870	1.69	-1.19
CATMA4OA39430F1	AT4G37920	-1.74	-1.32
CATMA4OA39470R1	AT4G37950	-1.69	-1.37
CATMA4OA39560F1	AT4G38060	1.04	1.53
CATMA4OA39600R1	AT4G38080	-1.88	1.52
CATMA4OA39680R1	AT4G38160	-1.71	-1.33
CATMA4OA39720F1	AT4G38210	1.61	-1.15
CATMA4OA39840R1	AT4G38340	2.62	1.33
CATMA4OA39920F1	AT4G38400	-1.40	-1.94
CATMA4OA39930R1	AT4G38410	1.73	-1.08
CATMA4OA39970R1	AT4G38470	1.63	1.21
CATMA4OA39990R1	AT4G38490	-1.50	-1.22
CATMA4OA40036R1	AT4G38540	2.97	1.36
CATMA4ON100531R1	AT4G38550	1.76	1.18
CATMA4OA40140F1	AT4G38690	-1.71	-1.34
CATMA4ON90019R1	AT4G38825	-1.49	-2.80
CATMA4OA40270F1	AT4G38840	-1.56	-1.43
CATMA4OA40280R1	AT4G38850	-1.69	-1.40
CATMA4OA40290R1	AT4G38860	-1.69	-1.29
CATMA4OA40400R1	AT4G38960	-1.57	-1.65
CATMA4OA40410F1	AT4G38970	-1.89	-1.20
CATMA4OA40580F1	AT4G39090	1.68	1.37
CATMA4OA40640R1	AT4G39210	2.02	-1.03
CATMA4OA40650F1	AT4G39230	2.42	-1.28
CATMA4OC42699F1	AT4G39250	-2.62	-2.50
CATMA4OA40735R1	AT4G39330	-1.20	-1.83
CATMA4OA40840F1	AT4G39460	-1.76	-1.33
CATMA4OC42706R1	AT4G39480	-1.02	-2.15
CATMA4OA40890F1	AT4G39510	-1.10	-2.12
CATMA4ON94372F1	AT4G39580	3.36	1.54
CATMA4OA41020R1	AT4G39670	1.61	1.26
CATMA4OA41030R1	AT4G39675	-4.87	-1.31
CATMA4OA41060R1	AT4G39700	1.76	1.12
CATMA4OA41065F1	AT4G39710	-1.93	-1.41
CATMA4OC42710F1	AT4G39770	-1.86	-1.33
CATMA4OA41190R1	AT4G39795	-1.36	1.59
CATMA4OA41220R1	AT4G39830	2.03	1.12
CATMA4OA41335R1	AT4G39940	-1.04	-1.52
CATMA4OA41360R1	AT4G39955	1.97	-1.06
CATMA4OA41390F1	AT4G39970	-1.62	-1.06
CATMA4OA41393R1	AT4G39980	1.81	1.23
CATMA5OA00030F1	AT5G01015	-2.16	-2.27
CATMA5OA00080R1	AT5G01060	1.51	1.32
CATMA5OA00100F1	AT5G01075	-1.67	-1.37
CATMA5OC64011F1	AT5G01330	-1.67	-1.18
CATMA5OA00430F1	AT5G01360	-2.29	1.27
CATMA5OA00550R1	AT5G01490	1.76	1.53
CATMA5OA00580R1	AT5G01520	1.20	2.02
CATMA5OA00590R1	AT5G01530	-1.52	-1.01
CATMA5OA00655F1	AT5G01600	-1.07	3.73
CATMA5OA00750F1	AT5G01700	1.12	1.77
CATMA5ON91770F1	AT5G01720	1.93	1.05
CATMA5OA00790R1	AT5G01740	-2.59	-2.25
CATMA5OA00900R1	AT5G01850	1.87	1.26
CATMA5OA00930R1	AT5G01870	2.71	-1.99
CATMA5OA01030F1	AT5G01950	1.70	1.25
CATMA5OA01080F1	AT5G02000	-1.74	-1.21
CATMA5OC64020F1	AT5G02020	1.74	-1.01
CATMA5ON91500R1	AT5G02120	-2.48	-1.21
CATMA5OA01230R1	AT5G02160	-2.49	1.12
CATMA5OA01270R1	AT5G02200	1.76	-1.12
CATMA5OC64024F1	AT5G02290	2.10	1.16
CATMA5OA01570F1	AT5G02490	1.60	-1.04
CATMA4OA01580R1	AT5G02540	-1.78	-1.48
CATMA5OA01660R1	AT5G02580	3.79	1.38
CATMA5OA01730F1	AT5G02640	-1.60	-1.03
CATMA5OA01790R1	AT5G02710	-1.59	-1.26
CATMA5OA01860R1	AT5G02780	19.26	2.48
CATMA5OC64034F1	AT5G02830	-2.15	-1.33
CATMA5OA01970R1	AT5G02880	1.57	1.33
CATMA5OA01990F1	AT5G02890	-1.25	-1.70
CATMA5OF03218_NF1	AT5G02940	-1.51	-1.40
CATMA5OA02240R1	AT5G03120	-2.11	-1.37
CATMA5OA02270R1	AT5G03160	1.81	1.18
CATMA5OA02340R1	AT5G03230	1.17	-1.77
CATMA5ON92030F1	AT5G03260	-2.08	1.00
CATMA5OA02420F1	AT5G03310	-1.40	1.50
CATMA5OA02440R1	AT5G03330	1.85	1.08
CATMA5OA02460F1	AT5G03350	1.28	2.20
CATMA5OA02510F1	AT5G03380	1.62	1.18
CATMA5OA02660R1	AT5G03490	1.79	1.46
CATMA5OA02720R1	AT5G03545	1.66	2.18
CATMA5OA02740F1	AT5G03555	-1.63	-1.29
CATMA5OA02760R1	AT5G03570	8.11	2.74
CATMA5OA02810F1	AT5G03630	2.09	1.05
CATMA5OA02940F1	AT5G03760	-1.56	-1.88
CATMA5OA02970F1	AT5G03780	1.62	-1.07
CATMA5OA03050F1	AT5G03860	-2.48	-1.46
CATMA5OA03135F1	AT5G03940	-1.81	-1.13
CATMA5OA03150F1	AT5G03960	-1.52	-1.18
CATMA5ON91435F1	AT5G03995	-4.02	1.01
CATMA5OA03190F1	AT5G04000	-2.00	1.08
CATMA5OA03210F1	AT5G04020	1.50	1.19
CATMA5OA03300R1	AT5G04120	1.78	-2.50
CATMA5OC64053F1	AT5G04150	-1.09	-3.40
CATMA5OA03380R1	AT5G04200	-1.83	1.13
CATMA5OA03420R1	AT5G04230	-1.30	-1.58
CATMA5OC64054F1	AT5G04340	1.92	1.40
CATMA5OA03600R1	AT5G04370	-2.13	1.00
CATMA5OC64063R1	AT5G04720	1.97	1.28
CATMA5OA03935F1	AT5G04730	3.15	1.22
CATMA5OA04010R1	AT5G04840	-1.69	-1.30
CATMA5OA04100R1	AT5G04930	1.72	1.37
CATMA5OC64068F1	AT5G04950	2.28	1.08
CATMA5OA04140R1	AT5G04960	1.64	1.31
CATMA5OA04450F1	AT5G05250	-1.54	-2.46
CATMA5OA04500F1	AT5G05320	3.53	1.53
CATMA5OA04520F1	AT5G05340	9.74	1.06
CATMA5ON91469R1	AT5G05365	2.50	-1.20
CATMA5OA04585R1	AT5G05410	-1.10	1.80
CATMA5OA04630R1	AT5G05460	1.54	1.18
CATMA5OA04670R1	AT5G05500	1.61	1.59
CATMA5ON91980R1	AT5G05580	-1.51	-1.27
CATMA5OA04790R1	AT5G05600	1.36	-1.66
CATMA5OA04882F1	AT5G05690	-1.90	-1.25
CATMA5OA04910F1	AT5G05730	1.89	1.06
CATMA5OA04920F1	AT5G05740	-1.47	-1.52
CATMA5ON91691R1	AT5G05880	1.54	1.07
CATMA5OA05150R1	AT5G05960	-1.35	-1.71
CATMA5OC64086R1	AT5G06090	1.12	1.60
CATMA5ON93849R1	AT5G06200	-1.64	-1.11
CATMA5OA05500R1	AT5G06290	-1.71	-1.05
CATMA5OA05530F1	AT5G06320	2.48	1.15
CATMA5OA05540F1	AT5G06330	2.69	1.26
CATMA5OA05580F1	AT5G06370	1.58	1.38
CATMA5OA05700F1	AT5G06490	1.61	2.03
CATMA5OA05740F1	AT5G06530	-1.08	-1.78
CATMA5ON91633F1	AT5G06630	1.55	1.95
CATMA5ON91477F1	AT5G06640	1.66	1.55
CATMA5OA05885F1	AT5G06690	-1.22	2.15
CATMA5OA05910F1	AT5G06730	14.26	1.14
CATMA5OA05920R1	AT5G06740	3.59	-1.15

Table 22: Continued

		Ratio	
D CATMAv6	AGI	+Fe	-Fe
CATMA5OA05930F1	AT5G06750	1.91	1.20
CATMA5OA06060R1	AT5G06839	1.79	1.33
CATMA5OC64099R1	AT5G06860	4.35	1.20
CATMA5ON99249R1	AT5G06980	-2.23	-2.12
CATMA5ON99250F1	AT5G07000	1.65	-1.43
CATMA5OD03227F1	AT5G07010	2.69	-1.32
CATMA5OA06200F1	AT5G07020	-1.84	-1.25
CATMA5OA06210F1	AT5G07030	-2.06	-1.13
CATMA5OA06280R1	AT5G07100	3.36	1.87
CATMA5OA06310R1	AT5G07130	-1.44	1.74
CATMA5OA06530R1	AT5G07310	2.49	1.03
CATMA5OA06655R1	AT5G07440	5.27	1.20
CATMA5OC64114F1	AT5G07450	1.60	2.01
CATMA5ON99254F1	AT5G07530	1.92	10.22
CATMA5OA06760F1	AT5G07550	1.10	1.82
CATMA5OD01840F1	AT5G07650	1.55	1.23
CATMA5OA06920R1	AT5G07680	-1.68	-1.37
CATMA5OA06925R1	AT5G07690	-2.32	-2.51
CATMA5OA07070F1	AT5G07820	1.64	1.30
CATMA5OA07080R1	AT5G07830	1.78	-1.06
CATMA5OA07150R1	AT5G07900	-1.74	-1.15
CATMA5OA07300R1	AT5G08050	-2.50	-1.03
CATMA5OA07320R1	AT5G08070	-1.55	-1.47
CATMA5OA07500F1	AT5G08240	1.82	1.40
CATMA5OA07540F1	AT5G08280	-1.52	-1.13
CATMA5OA07630F1	AT5G08350	1.64	1.31
CATMA5OA07660F1	AT5G08380	1.85	1.46
CATMA5OA07710F1	AT5G08410	-1.32	1.55
CATMA5ON91488R1	AT5G08540	-1.54	-1.23
CATMA5OA07970R1	AT5G08610	-1.54	-1.12
CATMA5OC64129R1	AT5G08660	1.59	1.10
CATMA5OC64133F1	AT5G08720	-1.61	-1.27
CATMA5OC64139F1	AT5G08790	2.18	1.27
CATMA5OA08100R1	AT5G09290	3.62	2.23
CATMA5OA08350F1	AT5G09520	-2.95	1.71
CATMA5OA08360F1	AT5G09530	-1.70	1.39
CATMA5OA08400R1	AT5G09570	3.71	-1.94
CATMA5ON99279R1	AT5G09640	-1.52	-1.21
CATMA5OA08480F1	AT5G09650	-1.62	-1.35
CATMA5OA08570R1	AT5G09760	-1.65	-1.31
CATMA5ON91583R1	AT5G09978	-2.38	-1.04
CATMA5OA08860R1	AT5G10100	-1.28	-1.59
CATMA5ON99289F1	AT5G10140	-1.51	-1.24
CATMA5OA08900F1	AT5G10150	-2.10	-1.69
CATMA5OA08950R1	AT5G10210	-2.48	1.07
CATMA5OA08970F1	AT5G10230	-3.34	-1.50
CATMA5OA08990F1	AT5G10250	-2.26	-1.66
CATMA5OA09140R1	AT5G10380	3.15	1.17
CATMA5OA09170R1	AT5G10410	-2.44	-1.29
CATMA5OA09183F1	AT5G10430	-1.62	-1.19
CATMA5OA09240R1	AT5G10510	1.78	-1.03
CATMA5OA09250F1	AT5G10520	2.22	-1.06
CATMA5OA09350F1	AT5G10620	-1.51	-1.27
CATMA4OA06830R1	AT5G10625	-1.67	-1.33
CATMA5OA09420F1	AT5G10690	-1.74	-1.53
CATMA5OA09500F1	AT5G10760	10.59	2.35
CATMA5OA09510F1	AT5G10770	1.50	1.16
CATMA5OA09830F1	AT5G11070	-1.55	-1.22
CATMA5OA09920R1	AT5G11160	-1.59	-1.26
CATMA5OA09970F1	AT5G11210	2.43	1.89
CATMA5OA10010F1	AT5G11250	1.51	-1.13
CATMA5OA10030F1	AT5G11270	-1.70	-1.07
CATMA5OA10220R1	AT5G11450	-1.83	-1.23
CATMA5OA10285F1	AT5G11520	1.58	1.37
CATMA5OA10290R1	AT5G11530	1.52	1.22
CATMA5OA10300F1	AT5G11540	-1.52	-1.36
CATMA5OA10380F1	AT5G11610	2.04	1.11
CATMA5OA10420R1	AT5G11650	1.69	1.16
CATMA5OA10440R1	AT5G11670	1.90	1.31
CATMA5OA10580R1	AT5G11790	-1.63	-1.26
CATMA5OA10710R1	AT5G11920	2.87	1.20
CATMA5OA10820F1	AT5G12010	1.66	1.25
CATMA5OC64181R1	AT5G12110	-3.01	-1.52
CATMA5OC64192F1	AT5G12330	2.99	-1.05
CATMA5OC64193F1	AT5G12340	2.11	-1.21
CATMA5OA11090F1	AT5G12860	-1.78	-1.08
CATMA5OA11110F1	AT5G12880	2.03	1.12
CATMA5OA11120F1	AT5G12890	1.87	-1.09
CATMA5OC64208R1	AT5G12950	-1.57	-1.02
CATMA5OA11290F1	AT5G13080	5.27	1.78
CATMA5OA11350F1	AT5G13140	-1.32	-1.52
CATMA5OA11380F1	AT5G13170	1.21	-2.54
CATMA5OA11520R1	AT5G13320	3.36	1.72
CATMA5OA11530R1	AT5G13330	4.93	1.29
CATMA5OA11600F1	AT5G13400	-1.08	-1.65
CATMA5OC64220R1	AT5G13510	-1.88	-1.12
CATMA5OA11770F1	AT5G13550	1.54	1.14
CATMA5OA11860F1	AT5G13630	-1.63	1.05
CATMA5OA11955F1	AT5G13730	-1.33	-1.55
CATMA5OA11970R1	AT5G13740	1.34	-3.50
CATMA5OA11990R1	AT5G13750	2.83	1.05
CATMA5OC64225R1	AT5G13770	-2.20	-1.68
CATMA5OA12030F1	AT5G13790	1.88	-1.10
CATMA5OA12055R1	AT5G13820	1.73	1.18
CATMA5OA12110F1	AT5G13880	1.62	1.00
CATMA5OC64228F1	AT5G13900	-2.44	1.77
CATMA5OA12130F1	AT5G13910	4.91	4.98
CATMA5OA12230R1	AT5G14000	1.65	1.03
CATMA5OA12285R1	AT5G14060	-1.60	-1.50
CATMA5OA12290R1	AT5G14070	-1.55	1.05
CATMA5OA12310R1	AT5G14090	-1.03	-1.78
CATMA5OA12320F1	AT5G14100	-1.57	-1.19
CATMA5OA12355F1	AT5G14130	-1.86	1.36
CATMA5OA12400F1	AT5G14180	2.32	-1.13
CATMA5OA12555F1	AT5G14320	-2.00	-1.26
CATMA5OA12560F1	AT5G14330	1.84	1.55
CATMA5OA12570R1	AT5G14340	1.67	1.28
CATMA5ON91718F1	AT5G14350	-1.55	-1.34
CATMA5OA12650F1	AT5G14410	-1.63	-1.32
CATMA5ON91885R1	AT5G14450	-1.27	-1.62
CATMA5OA12700F1	AT5G14460	-1.53	-1.25
CATMA5OA12860R1	AT5G14650	-1.80	-1.12
CATMA5OA12870F1	AT5G14660	-1.87	1.01
CATMA5OA12950R1	AT5G14730	2.18	1.51
CATMA5OC64237R1	AT5G14740	-2.01	-1.17
CATMA5OA12980R1	AT5G14760	-1.02	-1.88
CATMA5OA13000R1	AT5G14780	1.93	1.28
CATMA5OA13190R1	AT5G14920	1.08	1.59
CATMA5OA13200R1	AT5G14930	2.20	2.02
CATMA5OA13210F1	AT5G14940	1.57	1.66
CATMA5OA13400R1	AT5G15120	-1.06	-1.98
CATMA5OA13410R1	AT5G15130	1.56	1.46
CATMA5OA13470R1	AT5G15180	-4.76	-1.58
CATMA5OA13520R1	AT5G15240	-1.96	-1.19
CATMA5OA13570R1	AT5G15290	-1.88	-1.51
CATMA5OA13675F1	AT5G15410	-1.54	1.01
CATMA5OA13880R1	AT5G15630	-1.95	-1.06
CATMA5OA14010F1	AT5G15740	-1.50	-1.29
CATMA5OA14110R1	AT5G15830	-2.00	-1.04
CATMA5OD03243R1	AT5G15960	-3.51	-1.98
CATMA5OC64254R1	AT5G15970	-1.39	-1.63
CATMA5ON99372R1	AT5G16000	-1.63	-1.13
CATMA5OA14310R1	AT5G16030	-2.03	-1.41
CATMA5OA14370F1	AT5G16080	1.26	-1.68
CATMA5OC64262R1	AT5G16230	-1.02	1.50
CATMA5OC64267R1	AT5G16350	-1.63	-2.09
CATMA5OA14680F1	AT5G16360	1.93	1.55
CATMA5OA14706F1	AT5G16400	-1.65	-1.18
CATMA5OA14780F1	AT5G16480	-1.54	-1.11
CATMA5OA14865R1	AT5G16540	-1.88	-1.38
CATMA5OC64270F1	AT5G16570	3.80	1.72
CATMA5OA14910R1	AT5G16590	-1.56	-1.43
CATMA5OA14940R1	AT5G16620	-1.57	-1.10
CATMA5OA15050R1	AT5G16720	-1.53	-1.12
CATMA5OA15100R1	AT5G16770	-1.18	1.62
CATMA5OA15120F1	AT5G16790	-1.29	-1.60
CATMA5ON99384F1	AT5G16960	1.67	1.00
CATMA5OF01871F1	AT5G16970	1.89	-1.15
CATMA5ON91877F1	AT5G16980	1.70	-1.10
CATMA5ON91465F1	AT5G17165	2.07	2.10
CATMA5OA15460R1	AT5G17170	-1.78	4.13
CATMA5OA15500R1	AT5G17220	4.00	-1.70
CATMA5OA15570F1	AT5G17300	-2.72	-3.17
CATMA5OA15580F1	AT5G17310	-1.70	-1.22
CATMA5OA15595R1	AT5G17330	1.86	1.20
CATMA5OA15640F1	AT5G17380	1.59	1.12
CATMA5OA15720R1	AT5G17450	-1.19	-1.78
CATMA5OA15890F1	AT5G17600	-1.95	-1.42
CATMA5OA15960R1	AT5G17670	-1.73	-1.05
CATMA5OA16000F1	AT5G17710	-1.63	-1.12
CATMA5OA16060F1	AT5G17760	4.26	1.99
CATMA5OA16105F1	AT5G17820	1.95	1.88
CATMA5OA16130R1	AT5G17850	1.59	1.36
CATMA5OA16140F1	AT5G17860	8.60	1.56
CATMA5OA16150R1	AT5G17870	-1.62	-1.28
CATMA5ON91634F1	AT5G18010	-1.63	-2.22
CATMA5ON91879F1	AT5G18020	-1.70	-2.10
CATMA5ON91689R1	AT5G18030	-2.00	-2.14
CATMA5OF01881F1	AT5G18050	-1.69	-2.36
CATMA5OC64296R1	AT5G18060	-2.03	-1.75
CATMA5ON91724R1	AT5G18080	-1.71	-2.07
CATMA5OA16400R1	AT5G18130	3.99	2.02
CATMA5OA16510F1	AT5G18240	-1.86	-1.04
CATMA5OA16550F1	AT5G18270	1.50	1.32
CATMA5OA16580R1	AT5G18310	1.90	1.24
CATMA5ON93882F1	AT5G18350	1.31	1.96
CATMA5OA16630F1	AT5G18360	1.73	-1.08
CATMA5ON102990R1	AT5G18470	6.83	2.39
CATMA5OA16790F1	AT5G18490	1.87	1.37
CATMA5OA16910F1	AT5G18600	-3.85	-1.13
CATMA5OA16990F1	AT5G18660	-2.10	-1.54
CATMA5OA17020R1	AT5G18670	-1.43	-1.85
CATMA5OA17150R1	AT5G18780	1.51	1.72
CATMA5OA17210R1	AT5G18840	5.07	-1.00
CATMA5OA17220R1	AT5G18850	-1.61	-1.11
CATMA5OA17230R1	AT5G18860	-1.52	-1.19
CATMA5OA17440F1	AT5G19040	-2.73	-1.10
CATMA5OA17520F1	AT5G19110	2.52	1.10
CATMA5OA17550R1	AT5G19140	1.81	1.26
CATMA5OA17620R1	AT5G19190	-1.48	-1.94
CATMA5OA17840F1	AT5G19410	-1.35	1.61
CATMA5OA17870R1	AT5G19440	1.81	1.30
CATMA5OA17900R1	AT5G19470	3.33	1.01
CATMA5OA17930F1	AT5G19490	1.10	1.54
CATMA5OA17970F1	AT5G19530	-1.52	-1.10
CATMA5OC64312R1	AT5G19560	4.59	1.86
CATMA5OA18030F1	AT5G19600	-3.84	-1.40
CATMA5OA18130F1	AT5G19700	4.89	1.45
CATMA5OA18150R1	AT5G19730	-2.54	-1.30
CATMA5OA18270F1	AT5G19850	-2.06	-1.24
CATMA5OA18300F1	AT5G19870	-2.50	1.02
CATMA5OA18320F1	AT5G19880	4.33	1.31
CATMA5OA18330F1	AT5G19890	7.87	1.76
CATMA5OC64316R1	AT5G19940	-1.83	-1.33
CATMA5OA18480F1	AT5G20040	-1.72	-1.28
CATMA5OA18570F1	AT5G20140	-1.62	-1.05
CATMA5OA18590R1	AT5G20150	1.02	-1.79
CATMA5OA18660R1	AT5G20220	-1.57	-1.56
CATMA5OA18670R1	AT5G20230	2.09	1.55
CATMA5OA18710F1	AT5G20270	-1.71	-1.29
CATMA5OA18720F1	AT5G20280	1.46	1.51
CATMA5OC64324R1	AT5G20400	1.80	1.25
CATMA5OA19250R1	AT5G20720	-1.54	-1.15
CATMA5OA19330F1	AT5G20790	-1.12	-1.50
CATMA5OC64335R1	AT5G20810	1.66	1.06
CATMA5OA19350F1	AT5G20820	1.68	-1.14
CATMA5OA19710R1	AT5G21170	-1.53	1.16
CATMA5OC64341R1	AT5G21222	-1.59	-1.21
CATMA5OC64345R1	AT5G21430	-2.23	-1.26
CATMA5OC64346R1	AT5G21482	-1.73	-1.04
CATMA5OC64349F1	AT5G21920	-1.80	-1.34
CATMA5OC64352F1	AT5G21950	-1.13	1.64
CATMA5OC64380F1	AT5G22270	1.51	1.16
CATMA5OA19765R1	AT5G22300	2.45	2.14
CATMA5ON99435R1	AT5G22340	-2.08	-1.35
CATMA5OA19865R1	AT5G22410	1.57	-1.00
CATMA5OA19910F1	AT5G22450	1.52	1.28
CATMA5OA19920F1	AT5G22460	1.82	1.02
CATMA5OA19980R1	AT5G22520	1.90	2.45
CATMA5OA19990R1	AT5G22530	2.11	1.32
CATMA5OA20000F1	AT5G22540	1.36	1.51
CATMA5OC64387R1	AT5G22555	1.60	1.02
CATMA5OA20040F1	AT5G22570	1.97	1.50
CATMA5OA20090F1	AT5G22620	-1.61	-1.16
CATMA5OA20100R1	AT5G22630	1.56	1.18
CATMA5OA20160R1	AT5G22690	1.79	1.10
CATMA5OA20380F1	AT5G22890	6.97	2.43

Table 22: Continued

		Ratio	
D CATMAv6	AGI	+Fe	-Fe
CATMA5OA20550F1	AT5G23060	-1.75	-1.31
CATMA5OA20605R1	AT5G23120	-1.97	-1.42
CATMA5OA20670F1	AT5G23190	-1.59	1.86
CATMA5ON91914F1	AT5G23240	5.45	2.91
CATMA5OC64403R1	AT5G23510	1.86	1.10
CATMA5OA21090R1	AT5G23575	1.38	1.79
CATMA5OA21220R1	AT5G23730	-1.61	-1.42
CATMA5OA21230F1	AT5G23750	-1.71	-1.13
CATMA5OF01905R1	AT5G23820	-1.38	-1.69
CATMA5ON99455R1	AT5G23840	-2.35	-1.16
CATMA5OA21420F1	AT5G23940	-1.30	-1.89
CATMA5OA21530F1	AT5G24000	-1.65	-1.23
CATMA5OA21550F1	AT5G24030	1.63	1.37
CATMA5OA21560F1	AT5G24040	1.92	1.48
CATMA5OA21600F1	AT5G24070	-2.47	1.30
CATMA5OA21620F1	AT5G24090	1.66	1.18
CATMA5OA21630R1	AT5G24100	-1.79	-1.27
CATMA5OA21640R1	AT5G24105	-2.48	-1.47
CATMA5OA21650F1	AT5G24110	2.42	1.43
CATMA5OA21665F1	AT5G24120	-1.59	-1.28
CATMA5OA21675F1	AT5G24140	-1.65	-2.17
CATMA5OA21705F1	AT5G24160	2.02	1.36
CATMA5ON99466R1	AT5G24200	1.28	1.71
CATMA5OA21760R1	AT5G24210	2.71	1.76
CATMA5OA21800F1	AT5G24240	1.72	1.11
CATMA5ON93910F1	AT5G24270	2.45	1.16
CATMA5OA22020F1	AT5G24410	-2.28	-1.13
CATMA5OA22030F1	AT5G24420	-3.94	-2.21
CATMA5OA22070F1	AT5G24470	1.85	2.03
CATMA5OA22130R1	AT5G24530	1.62	1.45
CATMA5ON91688R1	AT5G24640	1.34	1.72
CATMA5OA22560F1	AT5G24870	1.63	1.61
CATMA5OA22640R1	AT5G24920	-1.43	1.94
CATMA5OA22820F1	AT5G25110	1.65	1.08
CATMA5OF01915R1	AT5G25130	-1.54	-1.15
CATMA5OA22900F1	AT5G25190	1.54	-1.38
CATMA5OA22930R1	AT5G25210	2.50	1.63
CATMA5OA22950F1	AT5G25240	1.79	1.31
CATMA5OA22960R1	AT5G25250	3.69	1.57
CATMA5OC64429F1	AT5G25350	1.51	1.30
CATMA5OC64434F1	AT5G25440	2.45	-1.16
CATMA5OA23200R1	AT5G25450	2.24	1.16
CATMA5OA23230F1	AT5G25470	2.19	-1.05
CATMA5OA23380F1	AT5G25610	1.21	-1.51
CATMA5OA23390F1	AT5G25620	-1.75	-1.06
CATMA5ON93922F1	AT5G25640	1.64	1.13
CATMA5ON91867F1	AT5G25770	1.95	1.48
CATMA5OA23485F1	AT5G25810	-6.12	-1.27
CATMA5OA23490F1	AT5G25820	1.73	1.27
CATMA5OA23500F1	AT5G25830	-1.19	-1.63
CATMA5ON93923R1	AT5G25910	1.64	1.16
CATMA5OA23590R1	AT5G25930	3.40	1.44
CATMA5OA23675R1	AT5G26030	1.80	1.25
CATMA5ON93926F1	AT5G26040	1.52	1.52
CATMA5ON93927R1	AT5G26080	1.05	1.54
CATMA5OA23790F1	AT5G26120	1.04	-1.71
CATMA5OA23850F1	AT5G26170	2.23	1.83
CATMA5OC64453R1	AT5G26200	-2.57	-1.59
CATMA5OA23890F1	AT5G26220	1.39	-1.64
CATMA5OA23940R1	AT5G26270	-1.59	1.18
CATMA5OF01923R1	AT5G26280	1.95	-1.33
CATMA5ON91982R1	AT5G26286	1.51	-1.33
CATMA5ON99490R1	AT5G26290	1.93	-1.03
CATMA5OA24040F1	AT5G26340	3.43	1.78
CATMA5OA24060R1	AT5G26570	1.75	1.25
CATMA5OA24115F1	AT5G26660	-1.73	-1.02
CATMA5OA24103R1	AT5G26690	1.50	1.90
CATMA5OA24083R1	AT5G26730	-2.11	-1.03
CATMA5OA24070F1	AT5G26742	-1.65	-1.08
CATMA5OA24340R1	AT5G26920	4.60	1.49
CATMA5OA24395R1	AT5G27000	-1.05	1.58
CATMA5ON91447F1	AT5G27060	1.35	1.77
CATMA5OC64479F1	AT5G27290	-2.35	-1.54
CATMA5OA24800F1	AT5G27390	-1.67	-1.32
CATMA5ON99501R1	AT5G27410	1.78	-1.19
CATMA5OA24850R1	AT5G27420	3.04	1.49
CATMA5OA24910F1	AT5G27520	1.51	1.10
CATMA5OA24950R1	AT5G27560	-1.58	-1.25
CATMA5OA24980R1	AT5G27600	1.77	1.18
CATMA5ON93941F1	AT5G27780	-1.45	-2.08
CATMA5OA25440F1	AT5G27920	2.58	1.28
CATMA5OA25670F1	AT5G28080	4.45	1.93
CATMA5OA26370R1	AT5G28500	-1.57	-1.15
CATMA5OF03288F1	AT5G28540	1.74	1.09
CATMA5OA26670R1	AT5G28646	2.22	1.22
CATMA5OA26680F1	AT5G28650	1.55	-1.13
CATMA5OC64509R1	AT5G28660	-1.72	-1.19
CATMA5OC64513F1	AT5G28750	-1.79	-1.22
CATMA5OA26910R1	AT5G28830	1.70	1.14
CATMA5ON91987F1	AT5G28996	1.54	-1.20
CATMA5OA28910R1	AT5G33290	1.88	1.37
CATMA5ON91631R1	AT5G33355	-1.63	1.24
CATMA5OA29040F1	AT5G33370	-1.38	-3.62
CATMA5OA30210F1	AT5G35100	-1.63	-1.02
CATMA5OF02011F1	AT5G35120	-1.72	1.07
CATMA5OA30360F1	AT5G35220	-1.53	-1.24
CATMA5OA30480F1	AT5G35370	1.67	1.19
CATMA5OC64549F1	AT5G35480	-1.89	2.07
CATMA5OC64550R1	AT5G35490	-1.66	1.28
CATMA5OC64551R1	AT5G35525	3.93	1.75
CATMA5OA30810R1	AT5G35580	1.91	1.72
CATMA5OA30906R1	AT5G35630	-1.99	-1.24
CATMA5ON99614F1	AT5G35660	-1.07	-1.60
CATMA5OA31080F1	AT5G35735	2.85	1.50
CATMA5OA31420R1	AT5G35940	-1.62	-1.79
CATMA5ON93964R1	AT5G35950	-1.65	-1.64
CATMA5ON93965R1	AT5G36000	1.06	1.79
CATMA5ON93966R1	AT5G36110	-1.58	-1.86
CATMA5OA31590F1	AT5G36120	-1.86	1.03
CATMA5OC64564F1	AT5G36130	-2.09	-4.10
CATMA5OF03312F1	AT5G36140	-1.62	-1.93
CATMA5OD03313F1	AT5G36150	1.60	-1.13
CATMA5OA31740F1	AT5G36220	2.51	-1.13
CATMA5OA32135F1	AT5G36910	-3.22	-2.72
CATMA5OD03321F1	AT5G36920	1.12	-2.08
CATMA5OC64570F1	AT5G36925	1.94	-1.19
CATMA5OA32770F1	AT5G37450	-1.01	1.57
CATMA5OA32890F1	AT5G37550	-2.33	-1.10
CATMA5OA32930F1	AT5G37600	1.80	1.35
CATMA5OA33040F1	AT5G37690	-1.74	1.35
CATMA5OA33080R1	AT5G37740	2.96	1.52
CATMA5OC64588R1	AT5G37750	1.62	1.10
CATMA5OA33200F1	AT5G37840	1.63	1.16
CATMA5ON91547R1	AT5G37940	1.67	-2.59
CATMA5ON91916R1	AT5G37950	-1.86	-1.52
CATMA5OF02072F1	AT5G37970	-2.91	-2.66
CATMA5ON92005F1	AT5G37990	-3.77	-3.46
CATMA5ON91628R1	AT5G38000	1.53	-3.29
CATMA5OC64594R1	AT5G38010	-1.73	-1.50
CATMA5OC64595F1	AT5G38020	-1.25	-5.96
CATMA5OF02076R1	AT5G38040	-1.67	-1.49
CATMA5OA33640R1	AT5G38200	2.05	1.01
CATMA5OA33660R1	AT5G38210	1.83	1.13
CATMA5OA33715F1	AT5G38280	1.86	1.57
CATMA5OA33780R1	AT5G38340	2.08	-1.11
CATMA5OA33800R1	AT5G38350	1.72	1.21
CATMA5OA33960F1	AT5G38410	-1.62	-1.07
CATMA5OC64608F1	AT5G38430	-1.75	-1.09
CATMA5OA33990F1	AT5G38450	-1.67	-1.51
CATMA5OA34040F1	AT5G38510	-1.73	-1.15
CATMA5OA34050R1	AT5G38520	-1.84	-1.49
CATMA5ON93988F1	AT5G38540	2.21	1.08
CATMA5OF02084F1	AT5G38550	2.83	1.85
CATMA5OA34210F1	AT5G38660	-1.58	-1.19
CATMA5OA34340R1	AT5G38750	1.08	1.53
CATMA5OC64616R1	AT5G38780	2.10	1.10
CATMA5OA34420R1	AT5G38820	16.88	4.07
CATMA5OA34450R1	AT5G38850	1.61	-1.09
CATMA5OA34500F1	AT5G38900	8.01	1.51
CATMA5OF02087R1	AT5G38930	-1.06	-2.55
CATMA5ON91973R1	AT5G38940	-1.20	-3.17
CATMA5OA34630R1	AT5G39020	1.82	-1.01
CATMA5OA34660R1	AT5G39050	3.07	1.81
CATMA5ON92031F1	AT5G39100	4.68	1.22
CATMA5ON91546F1	AT5G39110	2.80	-1.02
CATMA5ON91490F1	AT5G39120	26.55	1.98
CATMA5ON91726F1	AT5G39130	9.50	1.27
CATMA5ON91740F1	AT5G39160	18.73	1.32
CATMA5OF02096F1	AT5G39180	30.91	1.87
CATMA5OA34805F1	AT5G39190	12.03	1.05
CATMA5OA34820R1	AT5G39210	-1.57	-1.16
CATMA5OA35030R1	AT5G39450	1.69	1.39
CATMA5OA35090F1	AT5G39520	1.66	1.85
CATMA5OA35100F1	AT5G39530	-1.79	-1.30
CATMA5OA35160F1	AT5G39580	10.43	-1.26
CATMA5OA35200F1	AT5G39610	5.32	1.29
CATMA5OM00341F1	AT5G39635	1.18	2.74
CATMA5OA35240R1	AT5G39670	5.51	1.93
CATMA5OA35520R1	AT5G39860	-3.31	-1.84
CATMA5OA35660F1	AT5G40000	4.23	1.18
CATMA5OA35680F1	AT5G40010	3.24	2.11
CATMA5OA35770R1	AT5G40100	1.64	1.21
CATMA5OA35815F1	AT5G40160	-1.84	-1.09
CATMA5OA35820F1	AT5G40170	1.87	1.07
CATMA5OC64650F1	AT5G40240	1.87	1.15
CATMA5OA36010F1	AT5G40340	1.27	1.60
CATMA5OA36060R1	AT5G40390	-1.64	-1.57
CATMA5OA36085F1	AT5G40420	-5.87	-6.21
CATMA5OA36160R1	AT5G40510	1.70	1.71
CATMA5OA36240F1	AT5G40590	3.13	2.40
CATMA5OA36400R1	AT5G40690	1.03	1.62
CATMA5OA36420R1	AT5G40720	2.34	1.50
CATMA5OA36458R1	AT5G40780	2.48	1.37
CATMA5OA36535F1	AT5G40890	-1.90	-1.15
CATMA5OA36560R1	AT5G40910	1.61	1.07
CATMA5OA36620R1	AT5G40950	-1.73	-1.15
CATMA5ON91783R1	AT5G40990	11.22	2.42
CATMA5OA36760R1	AT5G41100	1.67	1.32
CATMA5OA36800R1	AT5G41140	-1.65	-1.01
CATMA5OC64677R1	AT5G41300	-1.62	-1.47
CATMA5OA37060F1	AT5G41460	1.03	-1.51
CATMA5OA37190F1	AT5G41590	-1.56	1.00
CATMA5OA37210F1	AT5G41610	2.93	1.07
CATMA5ON91692R1	AT5G41740	1.83	-1.08
CATMA5OF02124R1	AT5G41750	2.92	1.10
CATMA5OA37430R1	AT5G41761	1.64	1.65
CATMA5OA37480R1	AT5G41790	1.31	1.53
CATMA5OA37490R1	AT5G41800	1.54	1.14
CATMA5OA37620R1	AT5G41900	-1.32	-1.87
CATMA5OA37730R1	AT5G42010	2.41	1.00
CATMA5OA37770R1	AT5G42050	2.60	1.30
CATMA5OA37790F1	AT5G42070	-2.19	-1.34
CATMA5OD05179R1	AT5G42146	-1.75	-1.26
CATMA5OA37886R1	AT5G42180	-1.78	-1.17
CATMA5OA37910R1	AT5G42210	-1.29	1.96
CATMA5OA37990R1	AT5G42270	-1.86	-1.29
CATMA5OC64712F1	AT5G42530	1.57	1.55
CATMA5ON94020F1	AT5G42580	-2.49	-3.43
CATMA5OA38360F1	AT5G42590	-2.35	-2.15
CATMA5OA38390R1	AT5G42600	-1.58	-2.56
CATMA5OA38400R1	AT5G42610	-2.04	-1.10
CATMA5OA38470R1	AT5G42680	1.25	-1.73
CATMA5OA38480F1	AT5G42690	-1.57	1.03
CATMA5OA38550R1	AT5G42760	-1.82	-2.39
CATMA5OA38570F1	AT5G42765	-1.51	-1.01
CATMA5OA38610F1	AT5G42800	5.34	-2.32
CATMA5OA38640R1	AT5G42830	3.31	1.18
CATMA5OA38680F1	AT5G42870	1.61	1.22
CATMA5OA38710F1	AT5G42900	3.07	2.44
CATMA5OA39070F1	AT5G43180	-2.51	-1.05
CATMA5OA39150F1	AT5G43290	-2.17	-2.29
CATMA5OA39207F1	AT5G43380	1.63	-1.84
CATMA5OA39280R1	AT5G43420	1.55	1.04
CATMA5OA39310F1	AT5G43450	1.60	1.40
CATMA5OC64729F1	AT5G43520	-1.87	-1.07
CATMA5OC64731R1	AT5G43570	2.93	-1.05
CATMA5OA39400F1	AT5G43580	2.36	1.08
CATMA5OF03347R1	AT5G43620	1.62	1.04
CATMA5OA39450R1	AT5G43630	-1.60	-1.24
CATMA5OA39600F1	AT5G43750	-2.13	-1.42
CATMA5OA39635F1	AT5G43780	-1.05	1.76
CATMA5OA39767F1	AT5G43980	2.58	-1.06
CATMA5OA39790R1	AT5G44020	-1.86	-1.38
CATMA5OA39800R1	AT5G44030	-1.58	1.06
CATMA5OA39820R1	AT5G44050	-2.11	-1.53
CATMA5OA39835R1	AT5G44070	1.73	1.28
CATMA5OA39870F1	AT5G44120	-11.39	-12.92
CATMA5OA39880R1	AT5G44130	-1.92	-1.44
CATMA5OA39940R1	AT5G44190	-2.70	-1.79
CATMA5OA40010F1	AT5G44260	1.15	1.79
CATMA5OA40050F1	AT5G44310	-2.09	-1.63
CATMA5OF03349R1	AT5G44316	1.04	2.49
CATMA5OA40160F1	AT5G44390	-1.48	-1.50

Table 22: Continued

		Ratio	
D CATMAv6	AGI	+Fe	-Fe
CATMA5OA40170F1	AT5G44400	2.68	-1.30
CATMA5OF02158F1	AT5G44420	-1.08	1.64
CATMA5OA40310F1	AT5G44520	-1.74	-1.01
CATMA5OA40320R1	AT5G44530	-2.38	-1.21
CATMA5OC64755R1	AT5G44565	1.85	1.30
CATMA5ON91815R1	AT5G44574	-1.94	-1.43
CATMA5OA40400R1	AT5G44585	-1.98	1.26
CATMA5OA40480R1	AT5G44650	-1.58	-1.08
CATMA5OA40660F1	AT5G44820	1.79	1.34
CATMA5ON94033R1	AT5G44910	-1.55	-1.12
CATMA5ON91531R1	AT5G44920	2.00	1.28
CATMA5OC64763R1	AT5G44990	2.43	1.14
CATMA5OA40840R1	AT5G45000	1.94	1.30
CATMA5ON91594F1	AT5G45040	-1.60	-1.21
CATMA5OA40910F1	AT5G45070	13.02	2.36
CATMA5OA40920F1	AT5G45080	18.83	4.79
CATMA5OA40930F1	AT5G45090	2.05	1.51
CATMA5OA40940R1	AT5G45095	2.11	1.11
CATMA5OA40960F1	AT5G45105	18.50	6.29
CATMA5OA40970R1	AT5G45110	2.52	1.39
CATMA5OA41290F1	AT5G45340	-2.02	-2.05
CATMA5OA41350F1	AT5G45410	1.60	1.71
CATMA5OC64773F1	AT5G45460	-2.00	1.39
CATMA5OA41550F1	AT5G45580	1.88	1.57
CATMA5OA41610F1	AT5G45630	2.94	1.32
CATMA5OA41630F1	AT5G45650	1.36	1.72
CATMA5OA41670R1	AT5G45680	-2.73	-1.37
CATMA5OA41820F1	AT5G45820	-3.28	-1.10
CATMA5OA41840F1	AT5G45840	1.24	1.87
CATMA5ON91822F1	AT5G45940	-1.58	-1.36
CATMA5OA41950R1	AT5G45950	-1.37	-1.54
CATMA5OC64782F1	AT5G45960	-1.72	-1.39
CATMA5OA42040F1	AT5G46050	3.76	1.84
CATMA5OA42060R1	AT5G46060	1.29	1.53
CATMA5ON99745F1	AT5G46080	1.16	1.53
CATMA5OA42090R1	AT5G46090	-2.63	3.09
CATMA5OA42105R1	AT5G46110	-1.66	-1.07
CATMA5OA42180F1	AT5G46180	1.95	1.11
CATMA5OA42230R1	AT5G46220	-2.90	-1.46
CATMA5OA42245F1	AT5G46240	-1.53	-1.30
CATMA5OC64789F1	AT5G46260	1.62	-1.40
CATMA5OC64791F1	AT5G46295	1.12	-1.71
CATMA5OA42380R1	AT5G46390	-1.51	-1.20
CATMA5ON94041R1	AT5G46440	-1.81	-1.25
CATMA5OF03355R1	AT5G46500	1.67	-1.09
CATMA5OC64796R1	AT5G46520	1.76	1.13
CATMA5OA42580F1	AT5G46580	-1.52	-1.06
CATMA5OA42590R1	AT5G46590	3.50	1.54
CATMA5OA42790R1	AT5G46780	1.67	1.18
CATMA5OA42800F1	AT5G46790	-1.61	1.00
CATMA5OF03357R1	AT5G46871	-1.26	1.94
CATMA5ON91673F1	AT5G46890	-1.96	-1.08
CATMA5ON91627F1	AT5G46900	-2.10	-1.12
CATMA5OA43060R1	AT5G47050	2.06	1.81
CATMA5OA43080F1	AT5G47070	1.65	1.22
CATMA5OA43115R1	AT5G47120	1.84	1.52
CATMA5OA43120R1	AT5G47130	2.74	1.97
CATMA5OA43180F1	AT5G47190	-2.02	-1.39
CATMA5OA43205F1	AT5G47220	2.20	1.29
CATMA5OA43215R1	AT5G47230	1.50	1.23
CATMA5OA43220R1	AT5G47240	1.29	1.64
CATMA5OF03360R1	AT5G47330	2.11	-1.14
CATMA5OA43410F1	AT5G47450	-4.10	-2.11
CATMA5OA43550F1	AT5G47580	1.77	1.34
CATMA5OA43560F1	AT5G47590	-1.09	-1.87
CATMA5OA43780R1	AT5G47800	-1.39	-1.54
CATMA5ON92007R1	AT5G47900	-1.62	-1.23
CATMA5OA43885R1	AT5G47910	1.95	1.37
CATMA5OA43890F1	AT5G47920	1.87	-1.08
CATMA5OA43920F1	AT5G47950	-1.47	-1.52
CATMA5OA43930F1	AT5G47960	2.00	1.19
CATMA5OA43950R1	AT5G47980	1.14	-3.20
CATMA5OA43960R1	AT5G47990	-1.12	-3.49
CATMA5OA43970F1	AT5G48000	1.09	-6.55
CATMA5OC64823R1	AT5G48010	1.17	-3.96
CATMA5OA44050R1	AT5G48070	1.74	1.16
CATMA5OC64825R1	AT5G48175	2.60	1.14
CATMA5ON99764F1	AT5G48180	1.75	1.17
CATMA5OA44190R1	AT5G48220	-1.90	1.03
CATMA5OA44220F1	AT5G48250	1.53	1.80
CATMA5OA44340F1	AT5G48380	2.11	1.34
CATMA5OF02191R1	AT5G48400	3.15	1.21
CATMA5OA44380R1	AT5G48410	3.33	1.19
CATMA5OA44410F1	AT5G48430	-3.47	-1.34
CATMA5OA44435F1	AT5G48460	-1.75	-1.44
CATMA5OA44450R1	AT5G48480	-1.58	-1.26
CATMA5OA44460F1	AT5G48485	-1.54	-1.42
CATMA5OA44470F1	AT5G48490	-1.53	-1.71
CATMA5OA44616F1	AT5G48630	-1.68	-1.12
CATMA5OA44660F1	AT5G48657	4.52	1.61
CATMA5OA44680F1	AT5G48670	1.86	1.16
CATMA5OA44730F1	AT5G48790	-2.00	-1.23
CATMA5OA44770F1	AT5G48850	-1.57	1.23
CATMA5OA44830R1	AT5G48920	-1.81	1.06
CATMA5OA45100F1	AT5G49170	-1.25	-1.60
CATMA5OA45350F1	AT5G49360	-1.87	1.38
CATMA5ON99780R1	AT5G49520	5.13	-1.11
CATMA5OA45620F1	AT5G49620	7.80	1.32
CATMA5OA45625F1	AT5G49630	2.39	1.30
CATMA5OA45650F1	AT5G49665	3.28	1.08
CATMA5OA45660F1	AT5G49730	-1.54	1.37
CATMA5OC64851F1	AT5G49740	-1.65	-1.14
CATMA5OA45710R1	AT5G49770	1.73	1.01
CATMA5ON94058R1	AT5G49780	2.09	1.11
CATMA5OD03368F1	AT5G49850	3.04	-1.34
CATMA5OF03369F1	AT5G49860	2.81	-1.10
CATMA5OC64855F1	AT5G49890	1.53	1.30
CATMA5OA45825R1	AT5G49910	-1.75	-1.11
CATMA5OC64860R1	AT5G50130	1.92	1.31
CATMA5OA46120R1	AT5G50160	1.66	-1.17
CATMA5OC64869F1	AT5G50720	1.91	1.23
CATMA5OC64871R1	AT5G50760	4.36	1.65
CATMA5OA46770F1	AT5G50800	5.30	-1.40
CATMA5OC64875R1	AT5G50950	-2.26	1.57
CATMA5OC64878R1	AT5G51010	-1.57	1.92
CATMA5OC64879F1	AT5G51020	-1.81	-1.11
CATMA5OA46995R1	AT5G51070	1.56	1.40
CATMA5OA47040F1	AT5G51110	-2.01	-1.15
CATMA5OA47090R1	AT5G51160	2.96	1.98
CATMA5OA47120F1	AT5G51190	2.49	1.68
CATMA5OA47150R1	AT5G51210	-5.14	-2.58
CATMA5ON99806R1	AT5G51440	1.95	1.34
CATMA5ON94065F1	AT5G51500	-1.59	1.05
CATMA5OA47440R1	AT5G51520	-1.56	1.18
CATMA5OA47470R1	AT5G51545	-1.77	-1.16
CATMA5OC64885R1	AT5G51570	1.91	1.48
CATMA5OA47660R1	AT5G51720	-1.34	7.85
CATMA5ON99813R1	AT5G51830	1.94	1.69
CATMA5OA47850F1	AT5G51920	1.63	-1.05
CATMA5OA48040R1	AT5G52100	-1.92	-1.36
CATMA5OA48050F1	AT5G52110	-2.35	-1.24
CATMA5OC64896F1	AT5G52320	1.67	1.00
CATMA5OA48280F1	AT5G52390	7.06	1.25
CATMA5OA48310R1	AT5G52420	-1.61	-1.27
CATMA5OA48325R1	AT5G52440	-1.54	-1.15
CATMA5OC64901F1	AT5G52450	1.55	1.29
CATMA5OA48460F1	AT5G52570	-1.78	-1.30
CATMA5OA48600R1	AT5G52740	3.03	1.45
CATMA5OD03382R1	AT5G52750	5.26	1.64
CATMA5OC64907R1	AT5G52760	5.02	1.76
CATMA5OA48650F1	AT5G52790	-1.59	-1.45
CATMA5OA48800R1	AT5G52920	-1.51	-1.06
CATMA5OA48840R1	AT5G52960	-2.05	-1.18
CATMA5OA48860R1	AT5G52970	-2.28	-1.47
CATMA5OA49130F1	AT5G53210	-1.58	-1.37
CATMA5OA49170R1	AT5G53250	-2.12	-1.20
CATMA5OA49200R1	AT5G53280	-1.67	-1.14
CATMA5OA49230F1	AT5G53320	1.66	1.18
CATMA5ON99820R1	AT5G53420	1.85	-1.31
CATMA5OA49340R1	AT5G53450	-1.18	-4.28
CATMA5OA49380R1	AT5G53486	-2.20	-2.96
CATMA5OA49390F1	AT5G53490	-1.98	-1.13
CATMA5OA49450R1	AT5G53550	1.91	1.66
CATMA5OA49470F1	AT5G53580	-1.63	-1.20
CATMA5ON99826R1	AT5G53820	3.60	1.33
CATMA5OA49720R1	AT5G53830	1.96	1.00
CATMA5OA49750R1	AT5G53860	-1.59	-1.31
CATMA5OA49890R1	AT5G53980	1.58	-1.95
CATMA5OA49900F1	AT5G53990	3.68	1.24
CATMA5ON94084F1	AT5G54000	1.64	1.32
CATMA5OA49930F1	AT5G54020	-1.26	-1.13
CATMA5OC64927F1	AT5G54040	-1.89	-1.25
CATMA5OA49970F1	AT5G54060	1.48	-2.67
CATMA5OA50230R1	AT5G54370	-2.05	1.08
CATMA5OA50250R1	AT5G54400	3.17	-1.26
CATMA5OA50320F1	AT5G54470	-3.60	-2.36
CATMA5OA50340R1	AT5G54490	2.82	1.44
CATMA5OA50440R1	AT5G54585	-1.61	-1.09
CATMA5OA50455R1	AT5G54600	-1.65	-1.26
CATMA5OA50460F1	AT5G54610	1.10	2.51
CATMA5OC64944F1	AT5G54650	1.61	1.22
CATMA5OA50500R1	AT5G54660	1.69	1.10
CATMA5OA50505R1	AT5G54670	1.50	1.42
CATMA5ON99835F1	AT5G54700	-1.65	1.40
CATMA5OA50550F1	AT5G54710	2.09	1.03
CATMA5OC64947F1	AT5G54720	1.71	1.12
CATMA5OA50560F1	AT5G54730	1.61	1.59
CATMA5OC64949F1	AT5G54740	-14.88	-5.04
CATMA5OA50645F1	AT5G54840	1.50	1.31
CATMA5OA50670R1	AT5G54860	2.04	1.34
CATMA5OA50760F1	AT5G54960	2.17	1.62
CATMA5OA50780R1	AT5G54980	-1.55	-1.35
CATMA5OA50980R1	AT5G55220	-1.66	-1.54
CATMA5OA51000R1	AT5G55240	-1.95	-1.60
CATMA5OA51010F1	AT5G55250	-1.81	2.63
CATMA5ON94093F1	AT5G55370	2.08	1.01
CATMA5OA51090F1	AT5G55380	-1.54	-1.52
CATMA5ON99842R1	AT5G55450	2.15	1.22
CATMA5OA51190R1	AT5G55460	2.46	1.68
CATMA5OA51310F1	AT5G55560	1.59	1.09
CATMA5OA51320F1	AT5G55570	-1.98	-1.18
CATMA5OA51340R1	AT5G55590	-1.21	1.52
CATMA5OA51370R1	AT5G55620	-1.62	-1.19
CATMA5OA51375R1	AT5G55630	-1.61	-1.15
CATMA5OA51460R1	AT5G55720	-1.13	-1.64
CATMA5OC64977R1	AT5G55930	1.60	-1.10
CATMA5ON94096R1	AT5G56075	1.55	1.05
CATMA5ON94097F1	AT5G56080	6.42	2.01
CATMA5OA51860R1	AT5G56090	1.53	1.33
CATMA5OA51870R1	AT5G56100	-1.88	-1.31
CATMA5OA51990R1	AT5G56200	1.82	1.17
CATMA5OA52070R1	AT5G56270	1.71	-1.04
CATMA5OA52160F1	AT5G56350	1.51	1.11
CATMA5OC64987R1	AT5G56540	-1.91	-1.09
CATMA5OC64988F1	AT5G56550	-3.09	-1.54
CATMA5OA52440R1	AT5G56630	1.73	1.01
CATMA5ON91461F1	AT5G56795	1.69	1.03
CATMA5OA52600R1	AT5G56840	1.87	1.68
CATMA5OA52610F1	AT5G56850	-2.16	-1.55
CATMA5OA52620F1	AT5G56860	-2.29	-1.02
CATMA5ON99859R1	AT5G56870	-1.63	1.29
CATMA5OA52710F1	AT5G56960	1.39	1.51
CATMA5OA52730F1	AT5G56980	-1.51	-1.11
CATMA5OA52760R1	AT5G57010	1.61	1.79
CATMA5OC64995R1	AT5G57035	1.58	1.42
CATMA5OA52800R1	AT5G57070	-1.79	1.04
CATMA5OC64999F1	AT5G57123	1.13	1.60
CATMA5OA52970R1	AT5G57220	5.68	2.08
CATMA5OA53080R1	AT5G57340	1.68	1.29
CATMA5OA53090F1	AT5G57345	-1.54	1.45
CATMA5OA53230F1	AT5G57510	2.57	1.85
CATMA5OC65004F1	AT5G57530	1.55	1.01
CATMA5ON94105F1	AT5G57540	1.79	1.09
CATMA5OA53260F1	AT5G57550	1.01	1.74
CATMA5OC65008F1	AT5G57580	1.51	1.20
CATMA5OA53325R1	AT5G57620	1.47	1.51
CATMA5OA53400F1	AT5G57685	-1.55	1.06
CATMA5OA53440R1	AT5G57710	1.69	1.00
CATMA5OA53480R1	AT5G57760	-1.72	-1.74
CATMA5OA53490F1	AT5G57770	-2.42	-1.31
CATMA5OA53500F1	AT5G57780	-1.54	-1.51
CATMA5OA53510F1	AT5G57785	-1.36	-1.74
CATMA5OC65014R1	AT5G57887	1.63	1.10
CATMA5OC65015F1	AT5G57890	-1.53	-1.21
CATMA5OA53660F1	AT5G57900	1.82	1.27
CATMA5OA53780F1	AT5G58010	-1.30	1.68
CATMA5OA54010R1	AT5G58250	-1.57	-1.33
CATMA5OC65022F1	AT5G58310	-1.55	1.08
CATMA5OA54100R1	AT5G58350	2.28	1.30
CATMA5OA54150F1	AT5G58390	1.54	-1.50
CATMA5OA54240F1	AT5G58480	-1.51	-1.15
CATMA5OA54300R1	AT5G58540	1.43	1.67
CATMA5OA54370R1	AT5G58620	2.74	1.39

Table 22: Continued

		Ratio	
D CATMAv6	AGI	+Fe	-Fe
CATMA5OA54410R1	AT5G58660	1.52	1.34
CATMA5OD03392F1	AT5G58780	-1.31	-1.60
CATMA5OA54530R1	AT5G58787	1.53	1.36
CATMA5OA54840F1	AT5G59090	-1.58	-1.10
CATMA5OC65035F1	AT5G59310	5.01	1.02
CATMA5OC65036R1	AT5G59320	2.34	-2.47
CATMA5OC65037R1	AT5G59330	1.60	-2.83
CATMA5ON94115R1	AT5G59390	1.61	1.08
CATMA5OA55140R1	AT5G59400	-1.37	2.74
CATMA5OA55260F1	AT5G59520	-7.81	-1.22
CATMA5OA55270F1	AT5G59530	1.70	1.47
CATMA5OA55540R1	AT5G59750	-2.40	-1.36
CATMA5OA55595R1	AT5G59820	2.63	1.16
CATMA5OA55740F1	AT5G59990	-1.03	-1.54
CATMA5ON99018R1	AT5G60020	-1.77	-1.04
CATMA5OA55850F1	AT5G60100	1.79	1.63
CATMA5OA56010R1	AT5G60250	3.36	-1.11
CATMA5ON94122R1	AT5G60310	1.53	1.14
CATMA5OA56200F1	AT5G60490	-1.82	-1.09
CATMA5OA56240F1	AT5G60530	-1.97	1.36
CATMA5OA56390F1	AT5G60660	-4.38	-2.04
CATMA5OA56493R1	AT5G60770	2.18	1.24
CATMA5OA56496R1	AT5G60780	-1.83	1.22
CATMA5OA56510F1	AT5G60800	1.81	1.89
CATMA5OA56545R1	AT5G60850	-1.69	-1.22
CATMA5OC65062R1	AT5G60860	-1.61	-1.18
CATMA5OA56580R1	AT5G60890	-2.62	-1.35
CATMA5OA56650R1	AT5G61010	1.82	1.32
CATMA5OA56810R1	AT5G61160	3.09	4.01
CATMA5OA56865R1	AT5G61210	1.57	1.24
CATMA5OA56900F1	AT5G61250	1.23	1.69
CATMA5OA56910R1	AT5G61260	1.85	1.50
CATMA5ON91968R1	AT5G61290	1.63	-1.81
CATMA5OA56990F1	AT5G61340	-1.89	1.04
CATMA5ON99907R1	AT5G61380	1.73	1.61
CATMA5OA57030F1	AT5G61390	1.59	1.29
CATMA5OA57040F1	AT5G61410	-1.85	1.62
CATMA5ON99908F1	AT5G61420	-1.51	-1.41
CATMA5OA57100R1	AT5G61490	1.31	1.54
CATMA5OA57125F1	AT5G61520	2.51	1.05
CATMA5OA57170R1	AT5G61570	-1.64	-1.12
CATMA5OA57190F1	AT5G61590	1.63	1.10
CATMA5OA57200F1	AT5G61600	1.67	1.34
CATMA5OC65076R1	AT5G61610	1.03	1.60
CATMA5OA57250R1	AT5G61640	1.55	1.19
CATMA5OA57420F1	AT5G61820	1.89	1.23
CATMA5OA57480F1	AT5G61890	6.70	-1.09
CATMA5OA57700R1	AT5G62100	-1.53	-1.33
CATMA5OA57730F1	AT5G62140	-1.66	-1.48
CATMA5OA57860R1	AT5G62260	1.56	1.13
CATMA5OD03397R1	AT5G62340	-1.51	1.34
CATMA5OA57990F1	AT5G62390	1.65	1.24
CATMA5OA58020R1	AT5G62420	-2.45	1.37
CATMA5OA58030F1	AT5G62430	-3.20	-2.30
CATMA5OC65085F1	AT5G62480	-1.09	1.70
CATMA5OC65086R1	AT5G62520	1.69	1.01
CATMA5OC65087F1	AT5G62530	1.72	-1.11
CATMA5OA58140R1	AT5G62570	1.53	1.04
CATMA5OA58200R1	AT5G62620	1.56	1.10
CATMA5OA58220F1	AT5G62630	1.59	1.21
CATMA5ON92038R1	AT5G62670	-1.51	-1.24
CATMA5OA58310R1	AT5G62720	-1.83	1.14
CATMA5OA58380R1	AT5G62800	-1.60	-1.24
CATMA5OA58410F1	AT5G62840	-1.91	-1.09
CATMA5ON99924F1	AT5G62920	-2.17	-1.16
CATMA5OA58590R1	AT5G63030	1.65	1.09
CATMA5OC65101F1	AT5G63060	-1.62	-1.34
CATMA5OA58680F1	AT5G63100	-2.05	-1.12
CATMA5OA58760F1	AT5G63160	-4.58	-1.75
CATMA5OA58885F1	AT5G63310	-2.02	-1.37
CATMA5ON99931F1	AT5G63600	2.09	1.34
CATMA5OA59230R1	AT5G63680	1.54	1.01
CATMA5ON91606F1	AT5G63970	-1.17	1.61
CATMA5OA59490R1	AT5G63990	1.71	1.33
CATMA5ON91788R1	AT5G64000	2.30	1.47
CATMA5OA59535F1	AT5G64040	-1.68	1.18
CATMA5OA59550F1	AT5G64060	1.88	1.08
CATMA5OA59575F1	AT5G64100	1.96	1.24
CATMA5OA59580F1	AT5G64110	7.74	-3.77
CATMA5OA59590F1	AT5G64120	3.09	-1.19
CATMA5OC65119F1	AT5G64250	1.95	1.24
CATMA5OA59720R1	AT5G64260	1.67	1.28
CATMA5ON99934F1	AT5G64290	-1.51	1.00
CATMA5OA59800R1	AT5G64370	1.52	1.17
CATMA5OA59840F1	AT5G64410	1.58	1.30
CATMA5OA59860F1	AT5G64430	1.67	1.21
CATMA5OA59890F1	AT5G64460	-1.62	-1.19
CATMA5OA59910R1	AT5G64480	-1.61	-1.06
CATMA5OA59940R1	AT5G64510	2.04	-1.00
CATMA5OA60090F1	AT5G64660	1.96	1.23
CATMA5OA60150F1	AT5G64700	-2.02	1.14
CATMA5OA60235R1	AT5G64810	3.82	2.23
CATMA5OA60340R1	AT5G64905	2.08	1.04
CATMA5OA60370R1	AT5G64940	-2.48	-1.09
CATMA5OA60423R1	AT5G65010	-1.95	-1.55
CATMA5OA60485F1	AT5G65110	1.53	1.49
CATMA5OA60510F1	AT5G65140	1.97	1.00
CATMA5OA60560R1	AT5G65170	1.71	1.03
CATMA5OA60610R1	AT5G65220	-1.67	-1.24
CATMA5OA60620R1	AT5G65230	-1.67	-1.03
CATMA5OC65133F1	AT5G65300	1.81	1.48
CATMA5OA60830F1	AT5G65500	1.65	1.02
CATMA5OA60930F1	AT5G65600	2.43	1.17
CATMA5OA61040F1	AT5G65685	-1.68	-1.24
CATMA5OA61080R1	AT5G65730	-2.03	-2.00
CATMA5OA61085R1	AT5G65750	1.62	1.14
CATMA5OC65143R1	AT5G65870	2.78	-1.01
CATMA5OA61200R1	AT5G65890	-1.54	-1.32
CATMA5OA61320R1	AT5G65980	-1.26	-1.61
CATMA5OA61350F1	AT5G66005	-1.57	-1.44
CATMA5OA61460R1	AT5G66070	1.66	1.51
CATMA5OA61513R1	AT5G66130	2.04	1.09
CATMA5OC65148F1	AT5G66190	-1.69	-1.10
CATMA5OA61570F1	AT5G66210	2.12	1.13
CATMA5OA61730F1	AT5G66400	2.29	1.14
CATMA5OA61820F1	AT5G66470	-1.90	-1.34
CATMA5OA61830F1	AT5G66480	1.61	1.05
CATMA5OA61870R1	AT5G66520	-2.02	-1.42
CATMA5OC65153R1	AT5G66570	-1.92	-1.03
CATMA5OA61990R1	AT5G66620	1.22	1.58
CATMA5OA62030R1	AT5G66640	1.88	1.60
CATMA5OA62040F1	AT5G66650	1.54	1.19
CATMA5OA62080F1	AT5G66675	1.59	1.13
CATMA5ON91949R1	AT5G66690	1.24	-1.57
CATMA5OA62140R1	AT5G66740	-2.32	-1.63
CATMA5OA62155R1	AT5G66760	1.57	1.11
CATMA5OA62180R1	AT5G66790	1.83	1.37
CATMA5OA62190R1	AT5G66800	1.33	-1.59
CATMA5OA62210R1	AT5G66815	-1.07	-1.53
CATMA5OA62220R1	AT5G66816	2.43	-1.37
CATMA5OC65156R1	AT5G66880	1.25	1.52
CATMA5OA62360R1	AT5G66930	1.01	1.53
CATMA5OA62510R1	AT5G67060	1.52	1.93
CATMA5OA62600F1	AT5G67150	-1.88	-1.82
CATMA5OA62650F1	AT5G67200	-1.04	-1.58
CATMA5OA62660R1	AT5G67210	-2.00	-1.21
CATMA5OA62750F1	AT5G67280	-1.08	-1.51
CATMA5OA62765R1	AT5G67300	1.56	1.07
CATMA5OA62770F1	AT5G67310	1.56	1.09
CATMA5OA62785R1	AT5G67330	1.08	-2.01
CATMA5OA62790R1	AT5G67340	2.04	1.31
CATMA5OA62820F1	AT5G67370	-1.54	-2.88
CATMA5OA62830R1	AT5G67385	-1.72	-1.47
CATMA5OA62840F1	AT5G67390	-1.56	1.05
CATMA5OA62845R1	AT5G67400	1.76	1.53
CATMA5OA62930F1	AT5G67480	2.20	1.54
CATMACON93535F1	ATCG00020	-1.63	1.00
CATMACON93548F1	ATCG00050	-1.80	1.13
CATMACON93779R1	ATCG00100	-1.81	1.26
CATMACON98333R1	ATCG00110	-1.53	1.22
CATMACON93575F1	ATCG00120	-1.76	1.39
CATMACON93600F1	ATCG00130	-1.69	1.29
CATMACON93587F1	ATCG00140	-1.37	1.72
CATMACON93599F1	ATCG00150	-1.59	1.34
CATMACON93559F1	ATCG00160	-1.75	1.19
CATMACON93572F1	ATCG00170	-1.70	1.22
CATMACON93530F1	ATCG00180	-2.16	-1.02
CATMACON98334R1	ATCG00200	-1.89	1.40
CATMACON93808R1	ATCG00270	-1.53	1.78
CATMACON98338R1	ATCG00290	-1.63	1.66
CATMACON93565R1	ATCG00300	-1.60	1.49
CATMACON98339R1	ATCG00310	-1.57	1.09
CATMACON93555F1	ATCG00350	-1.51	1.10
CATMACON93581F1	ATCG00360	-1.91	1.42
CATMACON98341R1	ATCG00370	-1.57	1.32
CATMACON93563F1	ATCG00380	-2.06	-1.13
CATMACON98343R1	ATCG00410	-1.52	1.28
CATMACON93532F1	ATCG00420	-1.27	1.66
CATMACON93556F1	ATCG00430	-1.38	1.87
CATMACON93525R1	ATCG00500	-1.76	1.66
CATMACON93549R1	ATCG00520	-1.67	1.30
CATMACON93612R1	ATCG00530	-1.75	1.29
CATMACON93597R1	ATCG00540	-1.58	1.17
CATMACON93813R1	ATCG00590	-1.54	1.15
CATMACON98346F1	ATCG00620	-1.92	-1.07
CATMACON93611R1	ATCG00630	-2.13	1.05
CATMACON93539R1	ATCG00640	-2.02	1.05
CATMACON93608R1	ATCG00650	-2.23	-1.06
CATMACON93537F1	ATCG00660	-1.53	1.34
CATMACON93569R1	ATCG00680	-1.57	1.56
CATMACON93816R1	ATCG00690	-1.51	1.99
CATMACON93551F1	ATCG00700	-1.44	1.80
CATMACON93545R1	ATCG00710	-1.43	1.65
CATMACON93592R1	ATCG00720	-1.11	1.60
CATMACON93538F1	ATCG00740	-1.65	-1.15
CATMACON93604F1	ATCG00750	-1.60	-1.17
CATMACON93817F1	ATCG00760	-1.53	-1.20
CATMACON93561F1	ATCG00770	-1.65	-1.08
CATMACON93610F1	ATCG00780	-1.61	1.16
CATMACON93598F1	ATCG00790	-1.67	1.35
CATMACON93818F1	ATCG00800	-1.64	-1.16
CATMACON93577F1	ATCG01010	-1.58	1.19
CATMACON93579R1	ATCG01040	-1.90	1.03
CATMACON93547F1	ATCG01050	-1.57	1.39
CATMACON93542F1	ATCG01060	-1.56	1.37
CATMACON93584F1	ATCG01070	-1.75	1.33
CATMACON93574F1	ATCG01080	-1.75	1.16
CATMACON93576F1	ATCG01110	-1.68	-1.24
CATMACON93594F1	ATCG01120	-1.60	1.23
CATMACON93567F1	ATCG01130	-2.19	1.45
CATMAMON93652F1	ATMG00280	-1.57	1.24
CATMAMON93695R1	ATMG01090	1.05	-1.65

Table 23: GOs 39Ox vs. WT +Fe Upregulated. The differentially regulated genes and p-values (+Fe) of the gene list in Table were used to generate a GeneOnthology enrichment using the tool Virtual Plant.

GO ID	Term	Observed Frequency		Expected Frequency		p-value
GO:0050896	response to stimulus	568 out of 1767 genes	32.10%	3689 out of 24961 genes	14.80%	4.42E-66
GO:0006950	response to stress	364 out of 1767 genes	20.60%	2104 out of 24961 genes	8.40%	7.02E-49
GO:0065007	biological regulation	361 out of 1767 genes	20.40%	3661 out of 24961 genes	14.70%	9.24E-09
GO:0042221	response to chemical stimulus	325 out of 1767 genes	18.40%	1892 out of 24961 genes	7.60%	1.76E-42
GO:0050789	regulation of biological process	320 out of 1767 genes	18.10%	3434 out of 24961 genes	13.80%	1.62E-05
GO:0050794	regulation of cellular process	300 out of 1767 genes	17.00%	3050 out of 24961 genes	12.20%	4.79E-07
GO:0010033	response to organic substance	188 out of 1767 genes	10.60%	1148 out of 24961 genes	4.60%	2.86E-21
GO:0006952	defense response	178 out of 1767 genes	10.10%	747 out of 24961 genes	3.00%	8.31E-37
GO:0031323	regulation of cellular metabolic process	175 out of 1767 genes	9.90%	1859 out of 24961 genes	7.40%	2.75E-03
GO:0009628	response to abiotic stimulus	174 out of 1767 genes	9.80%	1360 out of 24961 genes	5.40%	8.02E-11
GO:0006810	transport	167 out of 1767 genes	9.50%	1732 out of 24961 genes	6.90%	1.43E-03
GO:0051234	establishment of localization	167 out of 1767 genes	9.50%	1745 out of 24961 genes	7.00%	2.00E-03
GO:0080090	regulation of primary metabolic process	167 out of 1767 genes	9.50%	1795 out of 24961 genes	7.20%	5.43E-03
GO:0031326	regulation of cellular biosynthetic process	162 out of 1767 genes	9.20%	1710 out of 24961 genes	6.90%	3.58E-03
GO:0009889	regulation of biosynthetic process	162 out of 1767 genes	9.20%	1715 out of 24961 genes	6.90%	3.93E-03
GO:0051171	regulation of nitrogen compound metabolic process	160 out of 1767 genes	9.10%	1717 out of 24961 genes	6.90%	6.56E-03
GO:0010556	regulation of macromolecule biosynthetic process	157 out of 1767 genes	8.90%	1667 out of 24961 genes	6.70%	5.08E-03
GO:2000112	regulation of cellular macromolecule biosynthetic process	157 out of 1767 genes	8.90%	1667 out of 24961 genes	6.70%	5.08E-03
GO:0019219	regulation of nucleotide and nucleic acid metabolic process	158 out of 1767 genes	8.90%	1696 out of 24961 genes	6.80%	6.89E-03
GO:0045449	regulation of transcription	155 out of 1767 genes	8.80%	1621 out of 24961 genes	6.50%	3.36E-03
GO:0009607	response to biotic stimulus	153 out of 1767 genes	8.70%	610 out of 24961 genes	2.40%	1.27E-33
GO:0051704	multi-organism process	148 out of 1767 genes	8.40%	589 out of 24961 genes	2.40%	1.34E-32
GO:0051707	response to other organism	147 out of 1767 genes	8.30%	558 out of 24961 genes	2.20%	3.72E-34
GO:0043412	macromolecule modification	145 out of 1767 genes	8.20%	1486 out of 24961 genes	6.00%	2.48E-03
GO:0006464	protein modification process	144 out of 1767 genes	8.10%	1322 out of 24961 genes	5.30%	3.12E-05
GO:0006793	phosphorus metabolic process	134 out of 1767 genes	7.60%	1002 out of 24961 genes	4.00%	2.08E-09
GO:0006796	phosphate metabolic process	133 out of 1767 genes	7.50%	1001 out of 24961 genes	4.00%	3.51E-09
GO:0007165	signal transduction	127 out of 1767 genes	7.20%	985 out of 24961 genes	3.90%	4.08E-08
GO:0009719	response to endogenous stimulus	125 out of 1767 genes	7.10%	920 out of 24961 genes	3.70%	3.69E-09
GO:0016310	phosphorylation	122 out of 1767 genes	6.90%	923 out of 24961 genes	3.70%	2.54E-08
GO:0006468	protein phosphorylation	120 out of 1767 genes	6.80%	907 out of 24961 genes	3.60%	3.16E-08
GO:0009725	response to hormone stimulus	106 out of 1767 genes	6.00%	849 out of 24961 genes	3.40%	3.73E-06
GO:0055114	oxidation-reduction process	99 out of 1767 genes	5.60%	793 out of 24961 genes	3.20%	9.27E-06
GO:0006355	regulation of transcription, DNA-dependent	92 out of 1767 genes	5.20%	883 out of 24961 genes	3.50%	5.15E-03
GO:0051252	regulation of RNA metabolic process	92 out of 1767 genes	5.20%	892 out of 24961 genes	3.60%	6.59E-03
GO:0051716	cellular response to stimulus	88 out of 1767 genes	5.00%	772 out of 24961 genes	3.10%	6.09E-04
GO:0010035	response to inorganic substance	86 out of 1767 genes	4.90%	507 out of 24961 genes	2.00%	3.34E-10
GO:0002376	immune system process	82 out of 1767 genes	4.60%	292 out of 24961 genes	1.20%	3.87E-20
GO:0009056	catabolic process	82 out of 1767 genes	4.60%	670 out of 24961 genes	2.70%	1.47E-04
GO:0010038	response to metal ion	74 out of 1767 genes	4.20%	417 out of 24961 genes	1.70%	1.60E-09
GO:0006955	immune response	72 out of 1767 genes	4.10%	260 out of 24961 genes	1.00%	2.28E-17
GO:0019748	secondary metabolic process	73 out of 1767 genes	4.10%	364 out of 24961 genes	1.50%	1.72E-11
GO:0019752	carboxylic acid metabolic process	73 out of 1767 genes	4.10%	672 out of 24961 genes	2.70%	6.62E-03
GO:0043436	oxoacid metabolic process	73 out of 1767 genes	4.10%	672 out of 24961 genes	2.70%	6.62E-03
GO:0006082	organic acid metabolic process	73 out of 1767 genes	4.10%	673 out of 24961 genes	2.70%	6.82E-03
GO:0042180	cellular ketone metabolic process	73 out of 1767 genes	4.10%	687 out of 24961 genes	2.80%	9.91E-03
GO:0045087	innate immune response	71 out of 1767 genes	4.00%	256 out of 24961 genes	1.00%	3.51E-17
GO:0006970	response to osmotic stress	71 out of 1767 genes	4.00%	425 out of 24961 genes	1.70%	2.94E-08
GO:0006979	response to oxidative stress	69 out of 1767 genes	3.90%	278 out of 24961 genes	1.10%	1.14E-14
GO:0009617	response to bacterium	68 out of 1767 genes	3.80%	256 out of 24961 genes	1.00%	1.15E-15
GO:0009651	response to salt stress	67 out of 1767 genes	3.80%	397 out of 24961 genes	1.60%	5.68E-08
GO:0009620	response to fungus	63 out of 1767 genes	3.60%	167 out of 24961 genes	0.70%	1.42E-20
GO:0055085	transmembrane transport	64 out of 1767 genes	3.60%	474 out of 24961 genes	1.90%	1.04E-04
GO:0009743	response to carbohydrate stimulus	62 out of 1767 genes	3.50%	203 out of 24961 genes	0.80%	1.23E-16
GO:0006811	ion transport	62 out of 1767 genes	3.50%	404 out of 24961 genes	1.60%	4.19E-06
GO:0044248	cellular catabolic process	62 out of 1767 genes	3.50%	520 out of 24961 genes	2.10%	2.48E-03
GO:0006725	cellular aromatic compound metabolic process	57 out of 1767 genes	3.20%	322 out of 24961 genes	1.30%	2.10E-07
GO:0065008	regulation of biological quality	57 out of 1767 genes	3.20%	426 out of 24961 genes	1.70%	3.56E-04
GO:0032501	multicellular organismal process	56 out of 1767 genes	3.20%	483 out of 24961 genes	1.90%	7.11E-03
GO:0010200	response to chitin	54 out of 1767 genes	3.10%	127 out of 24961 genes	0.50%	1.70E-19
GO:0008219	cell death	54 out of 1767 genes	3.10%	234 out of 24961 genes	0.90%	2.09E-10
GO:0016265	death	54 out of 1767 genes	3.10%	234 out of 24961 genes	0.90%	2.09E-10
GO:0042742	defense response to bacterium	53 out of 1767 genes	3.00%	201 out of 24961 genes	0.80%	4.81E-12
GO:0009266	response to temperature stimulus	53 out of 1767 genes	3.00%	399 out of 24961 genes	1.60%	7.14E-04
GO:0046686	response to cadmium ion	51 out of 1767 genes	2.90%	330 out of 24961 genes	1.30%	3.81E-05
GO:0070887	cellular response to chemical stimulus	51 out of 1767 genes	2.90%	374 out of 24961 genes	1.50%	5.82E-04
GO:0009737	response to abscisic acid stimulus	50 out of 1767 genes	2.80%	340 out of 24961 genes	1.40%	1.47E-04
GO:0050832	defense response to fungus	48 out of 1767 genes	2.70%	131 out of 24961 genes	0.50%	2.57E-15
GO:0012501	programmed cell death	47 out of 1767 genes	2.70%	197 out of 24961 genes	0.80%	1.77E-09
GO:0019438	aromatic compound biosynthetic process	44 out of 1767 genes	2.50%	218 out of 24961 genes	0.90%	4.13E-07
GO:0071310	cellular response to organic substance	45 out of 1767 genes	2.50%	337 out of 24961 genes	1.40%	2.17E-03
GO:0009415	response to water	42 out of 1767 genes	2.40%	211 out of 24961 genes	0.80%	1.16E-06
GO:0006812	cation transport	42 out of 1767 genes	2.40%	323 out of 24961 genes	1.30%	5.02E-03
GO:0009751	response to salicylic acid stimulus	40 out of 1767 genes	2.30%	147 out of 24961 genes	0.60%	1.78E-09
GO:0009414	response to water deprivation	41 out of 1767 genes	2.30%	202 out of 24961 genes	0.80%	1.08E-06
GO:0009409	response to cold	40 out of 1767 genes	2.30%	269 out of 24961 genes	1.10%	7.14E-04
GO:0009611	response to wounding	38 out of 1767 genes	2.20%	145 out of 24961 genes	0.60%	1.12E-08
GO:0007275	multicellular organismal development	37 out of 1767 genes	2.10%	281 out of 24961 genes	1.10%	7.57E-03
GO:0030001	metal ion transport	34 out of 1767 genes	1.90%	202 out of 24961 genes	0.80%	3.50E-04

Table 23: Continued

GO:0042592	homeostatic process	34 out of 1767 genes	1.90%	253 out of 24961 genes	1.00%	8.30E-03
GO:0009814	defense response, incompatible interaction	32 out of 1767 genes	1.80%	99 out of 24961 genes	0.40%	3.87E-09
GO:0006915	apoptosis	32 out of 1767 genes	1.80%	142 out of 24961 genes	0.60%	4.19E-06
GO:0009753	response to jasmonic acid stimulus	32 out of 1767 genes	1.80%	158 out of 24961 genes	0.60%	3.06E-05
GO:0009698	phenylpropanoid metabolic process	31 out of 1767 genes	1.80%	152 out of 24961 genes	0.60%	3.72E-05
GO:0048583	regulation of response to stimulus	32 out of 1767 genes	1.80%	182 out of 24961 genes	0.70%	2.95E-04
GO:0080167	response to karrikin	28 out of 1767 genes	1.60%	127 out of 24961 genes	0.50%	3.29E-05
GO:0019725	cellular homeostasis	28 out of 1767 genes	1.60%	191 out of 24961 genes	0.80%	7.71E-03
GO:0009699	phenylpropanoid biosynthetic process	26 out of 1767 genes	1.50%	121 out of 24961 genes	0.50%	1.04E-04
GO:0044282	small molecule catabolic process	26 out of 1767 genes	1.50%	162 out of 24961 genes	0.60%	4.32E-03
GO:0048878	chemical homeostasis	25 out of 1767 genes	1.40%	131 out of 24961 genes	0.50%	6.66E-04
GO:0006790	sulfur compound metabolic process	25 out of 1767 genes	1.40%	151 out of 24961 genes	0.60%	3.85E-03
GO:0009723	response to ethylene stimulus	23 out of 1767 genes	1.30%	134 out of 24961 genes	0.50%	4.17E-03
GO:0050801	ion homeostasis	22 out of 1767 genes	1.20%	97 out of 24961 genes	0.40%	2.49E-04
GO:0044264	cellular polysaccharide metabolic process	22 out of 1767 genes	1.20%	137 out of 24961 genes	0.50%	9.17E-03
GO:0055082	cellular chemical homeostasis	20 out of 1767 genes	1.10%	83 out of 24961 genes	0.30%	2.87E-04
GO:0006873	cellular ion homeostasis	19 out of 1767 genes	1.10%	77 out of 24961 genes	0.30%	3.33E-04
GO:0007568	aging	20 out of 1767 genes	1.10%	85 out of 24961 genes	0.30%	3.53E-04
GO:0016054	organic acid catabolic process	19 out of 1767 genes	1.10%	81 out of 24961 genes	0.30%	5.52E-04
GO:0046395	carboxylic acid catabolic process	19 out of 1767 genes	1.10%	81 out of 24961 genes	0.30%	5.52E-04
GO:0055080	cation homeostasis	19 out of 1767 genes	1.10%	81 out of 24961 genes	0.30%	5.52E-04
GO:0080134	regulation of response to stress	20 out of 1767 genes	1.10%	91 out of 24961 genes	0.40%	7.14E-04
GO:0006073	cellular glucan metabolic process	20 out of 1767 genes	1.10%	110 out of 24961 genes	0.40%	5.02E-03
GO:0044042	glucan metabolic process	20 out of 1767 genes	1.10%	113 out of 24961 genes	0.50%	6.38E-03
GO:0071705	nitrogen compound transport	19 out of 1767 genes	1.10%	107 out of 24961 genes	0.40%	7.69E-03
GO:0030003	cellular cation homeostasis	17 out of 1767 genes	1.00%	65 out of 24961 genes	0.30%	4.65E-04
GO:0031347	regulation of defense response	18 out of 1767 genes	1.00%	76 out of 24961 genes	0.30%	7.21E-04
GO:0009404	toxin metabolic process	16 out of 1767 genes	0.90%	46 out of 24961 genes	0.20%	5.27E-05
GO:0009407	toxin catabolic process	16 out of 1767 genes	0.90%	46 out of 24961 genes	0.20%	5.27E-05
GO:0006875	cellular metal ion homeostasis	16 out of 1767 genes	0.90%	52 out of 24961 genes	0.20%	1.72E-04
GO:0055065	metal ion homeostasis	16 out of 1767 genes	0.90%	55 out of 24961 genes	0.20%	2.91E-04
GO:0009817	defense response to fungus, incompatible interaction	15 out of 1767 genes	0.80%	41 out of 24961 genes	0.20%	6.50E-05
GO:0042430	indole-containing compound metabolic process	14 out of 1767 genes	0.80%	42 out of 24961 genes	0.20%	2.89E-04
GO:0000041	transition metal ion transport	15 out of 1767 genes	0.80%	53 out of 24961 genes	0.20%	6.06E-04
GO:0009624	response to nematode	15 out of 1767 genes	0.80%	61 out of 24961 genes	0.20%	2.03E-03
GO:0006820	anion transport	15 out of 1767 genes	0.80%	74 out of 24961 genes	0.30%	8.17E-03
GO:0000302	response to reactive oxygen species	14 out of 1767 genes	0.80%	67 out of 24961 genes	0.30%	9.17E-03
GO:0009816	defense response to bacterium. incompatible interaction	12 out of 1767 genes	0.70%	27 out of 24961 genes	0.10%	1.30E-04
GO:0010043	response to zinc ion	12 out of 1767 genes	0.70%	38 out of 24961 genes	0.20%	1.40E-03
GO:0009813	flavonoid biosynthetic process	12 out of 1767 genes	0.70%	49 out of 24961 genes	0.20%	7.11E-03
GO:0009873	ethylene mediated signaling pathway	12 out of 1767 genes	0.70%	49 out of 24961 genes	0.20%	7.11E-03
GO:0071369	cellular response to ethylene stimulus	12 out of 1767 genes	0.70%	50 out of 24961 genes	0.20%	8.00E-03
GO:0031407	oxylipin metabolic process	11 out of 1767 genes	0.60%	31 out of 24961 genes	0.10%	1.20E-03
GO:0009863	salicylic acid mediated signaling pathway	10 out of 1767 genes	0.60%	29 out of 24961 genes	0.10%	2.75E-03
GO:0071446	cellular response to salicylic acid stimulus	10 out of 1767 genes	0.60%	29 out of 24961 genes	0.10%	2.75E-03
GO:0042435	indole-containing compound biosynthetic process	11 out of 1767 genes	0.60%	37 out of 24961 genes	0.10%	3.75E-03
GO:0002252	immune effector process	10 out of 1767 genes	0.60%	32 out of 24961 genes	0.10%	4.84E-03
GO:0006826	iron ion transport	8 out of 1767 genes	0.50%	15 out of 24961 genes	0.10%	1.31E-03
GO:0009694	jasmonic acid metabolic process	9 out of 1767 genes	0.50%	26 out of 24961 genes	0.10%	5.02E-03
GO:0031408	oxylipin biosynthetic process	9 out of 1767 genes	0.50%	27 out of 24961 genes	0.10%	5.97E-03
GO:0006800	oxygen and reactive oxygen species metabolic process	9 out of 1767 genes	0.50%	29 out of 24961 genes	0.10%	8.00E-03
GO:0009695	jasmonic acid biosynthetic process	8 out of 1767 genes	0.50%	23 out of 24961 genes	0.10%	8.30E-03
GO:0006536	glutamate metabolic process	7 out of 1767 genes	0.40%	14 out of 24961 genes	0.10%	4.23E-03
GO:0055072	iron ion homeostasis	7 out of 1767 genes	0.40%	15 out of 24961 genes	0.10%	5.37E-03
GO:0009636	response to toxin	7 out of 1767 genes	0.40%	17 out of 24961 genes	0.10%	8.17E-03
GO:0009065	glutamine family amino acid catabolic process	5 out of 1767 genes	0.30%	7 out of 24961 genes	0.00%	8.00E-03
GO:0042343	indole glucosinolate metabolic process	5 out of 1767 genes	0.30%	7 out of 24961 genes	0.00%	8.00E-03

Table 24: GOs 39Ox vs. WT +Fe Downregulated. The Downregulated genes and p-values (+Fe) of the gene list in Table were used to generate a GeneOnthology enrichment using the tool Virtual Plant.

GO ID	Term	Observed Frequency		Expected Frequency		p-value
GO:0050896	response to stimulus	318 out of 1574 genes	20.20%	3689 out of 24961 genes	14.80%	1.76E-06
GO:0042221	response to chemical stimulus	160 out of 1574 genes	10.20%	1892 out of 24961 genes	7.60%	4.74E-03
GO:0009628	response to abiotic stimulus	153 out of 1574 genes	9.70%	1360 out of 24961 genes	5.40%	1.00E-08
GO:0071840	cellular component organization or biogenesis	116 out of 1574 genes	7.40%	1281 out of 24961 genes	5.10%	3.63E-03
GO:0055114	oxidation-reduction process	97 out of 1574 genes	6.20%	793 out of 24961 genes	3.20%	8.27E-07
GO:0071841	cellular component organization or biogenesis at cellular level	96 out of 1574 genes	6.10%	945 out of 24961 genes	3.80%	5.02E-04
GO:0009719	response to endogenous stimulus	93 out of 1574 genes	5.90%	920 out of 24961 genes	3.70%	7.03E-04
GO:0009725	response to hormone stimulus	87 out of 1574 genes	5.50%	849 out of 24961 genes	3.40%	8.06E-04
GO:0009416	response to light stimulus	78 out of 1574 genes	5.00%	477 out of 24961 genes	1.90%	5.31E-10
GO:0009314	response to radiation	78 out of 1574 genes	5.00%	493 out of 24961 genes	2.00%	1.36E-09
GO:0006412	translation	53 out of 1574 genes	3.40%	459 out of 24961 genes	1.80%	1.94E-03
GO:0009266	response to temperature stimulus	48 out of 1574 genes	3.00%	399 out of 24961 genes	1.60%	1.77E-03
GO:0006091	generation of precursor metabolites and energy	41 out of 1574 genes	2.60%	182 out of 24961 genes	0.70%	1.68E-08
GO:0071702	organic substance transport	37 out of 1574 genes	2.40%	261 out of 24961 genes	1.00%	6.90E-04
GO:0009409	response to cold	36 out of 1574 genes	2.30%	269 out of 24961 genes	1.10%	2.02E-03
GO:0009733	response to auxin stimulus	36 out of 1574 genes	2.30%	287 out of 24961 genes	1.10%	4.81E-03
GO:0051186	cofactor metabolic process	34 out of 1574 genes	2.20%	219 out of 24961 genes	0.90%	3.73E-04
GO:0006457	protein folding	31 out of 1574 genes	2.00%	237 out of 24961 genes	0.90%	6.30E-03
GO:0022900	electron transport chain	30 out of 1574 genes	1.90%	72 out of 24961 genes	0.30%	7.37E-11
GO:0015979	photosynthesis	30 out of 1574 genes	1.90%	83 out of 24961 genes	0.30%	7.03E-10
GO:0006461	protein complex assembly	28 out of 1574 genes	1.80%	121 out of 24961 genes	0.50%	5.62E-06
GO:0071822	protein complex subunit organization	29 out of 1574 genes	1.80%	137 out of 24961 genes	0.50%	1.46E-05
GO:0065003	macromolecular complex assembly	28 out of 1574 genes	1.80%	192 out of 24961 genes	0.80%	3.08E-03
GO:0043933	macromolecular complex subunit organization	29 out of 1574 genes	1.80%	210 out of 24961 genes	0.80%	4.77E-03
GO:0009767	photosynthetic electron transport chain	27 out of 1574 genes	1.70%	34 out of 24961 genes	0.10%	1.80E-14
GO:0043623	cellular protein complex assembly	26 out of 1574 genes	1.70%	106 out of 24961 genes	0.40%	5.74E-06
GO:0006869	lipid transport	27 out of 1574 genes	1.70%	146 out of 24961 genes	0.60%	2.25E-04
GO:0051188	cofactor biosynthetic process	27 out of 1574 genes	1.70%	147 out of 24961 genes	0.60%	2.41E-04
GO:0009639	response to red or far red light	26 out of 1574 genes	1.70%	151 out of 24961 genes	0.60%	6.90E-04
GO:0044085	cellular component biogenesis	27 out of 1574 genes	1.70%	176 out of 24961 genes	0.70%	2.07E-03
GO:0071843	cellular component biogenesis at cellular level	27 out of 1574 genes	1.70%	176 out of 24961 genes	0.70%	2.07E-03
GO:0034622	cellular macromolecular complex assembly	26 out of 1574 genes	1.70%	177 out of 24961 genes	0.70%	4.44E-03
GO:0034621	cellular macromolecular complex subunit organization	27 out of 1574 genes	1.70%	194 out of 24961 genes	0.80%	6.30E-03
GO:0046148	pigment biosynthetic process	23 out of 1574 genes	1.50%	77 out of 24961 genes	0.30%	1.88E-06
GO:0009657	plastid organization	23 out of 1574 genes	1.50%	93 out of 24961 genes	0.40%	2.36E-05
GO:0042440	pigment metabolic process	23 out of 1574 genes	1.50%	94 out of 24961 genes	0.40%	2.62E-05
GO:0070882	cellular cell wall organization or biogenesis	24 out of 1574 genes	1.50%	151 out of 24961 genes	0.60%	2.96E-03
GO:0009658	chloroplast organization	20 out of 1574 genes	1.30%	73 out of 24961 genes	0.30%	3.16E-05
GO:0080167	response to karrikin	20 out of 1574 genes	1.30%	127 out of 24961 genes	0.50%	8.98E-03
GO:0071669	plant-type cell wall organization or biogenesis	19 out of 1574 genes	1.20%	118 out of 24961 genes	0.50%	9.27E-03
GO:0009642	response to light intensity	17 out of 1574 genes	1.10%	78 out of 24961 genes	0.30%	1.33E-03
GO:0006779	porphyrin biosynthetic process	15 out of 1574 genes	1.00%	44 out of 24961 genes	0.20%	8.30E-05
GO:0010114	response to red light	16 out of 1574 genes	1.00%	55 out of 24961 genes	0.20%	1.90E-04
GO:0033014	tetrapyrrole biosynthetic process	15 out of 1574 genes	1.00%	48 out of 24961 genes	0.20%	1.90E-04
GO:0006778	porphyrin metabolic process	16 out of 1574 genes	1.00%	61 out of 24961 genes	0.20%	4.53E-04
GO:0033013	tetrapyrrole metabolic process	16 out of 1574 genes	1.00%	63 out of 24961 genes	0.30%	5.43E-04
GO:0009644	response to high light intensity	14 out of 1574 genes	0.90%	48 out of 24961 genes	0.20%	5.20E-04
GO:0009773	photosynthetic electron transport in photosystem I	12 out of 1574 genes	0.80%	15 out of 24961 genes	0.10%	1.84E-06
GO:0015995	chlorophyll biosynthetic process	12 out of 1574 genes	0.80%	26 out of 24961 genes	0.10%	8.19E-05
GO:0015994	chlorophyll metabolic process	13 out of 1574 genes	0.80%	39 out of 24961 genes	0.20%	3.83E-04
GO:0007623	circadian rhythm	12 out of 1574 genes	0.80%	49 out of 24961 genes	0.20%	4.77E-03
GO:0048511	rhythmic process	12 out of 1574 genes	0.80%	49 out of 24961 genes	0.20%	4.77E-03
GO:0009637	response to blue light	12 out of 1574 genes	0.80%	53 out of 24961 genes	0.20%	8.05E-03
GO:0010218	response to far red light	11 out of 1574 genes	0.70%	43 out of 24961 genes	0.20%	6.00E-03
GO:0010207	photosystem II assembly	10 out of 1574 genes	0.60%	12 out of 24961 genes	0.00%	1.57E-05
GO:0009668	plastid membrane organization	10 out of 1574 genes	0.60%	22 out of 24961 genes	0.10%	4.53E-04
GO:0010027	thylakoid membrane organization	10 out of 1574 genes	0.60%	22 out of 24961 genes	0.10%	4.53E-04
GO:0045036	protein targeting to chloroplast	10 out of 1574 genes	0.60%	26 out of 24961 genes	0.10%	1.10E-03
GO:0009828	plant-type cell wall loosening	10 out of 1574 genes	0.60%	35 out of 24961 genes	0.10%	5.43E-03
GO:0006733	oxidoreduction coenzyme metabolic process	10 out of 1574 genes	0.60%	39 out of 24961 genes	0.20%	9.83E-03
GO:0065002	intracellular protein transmembrane transport	8 out of 1574 genes	0.50%	17 out of 24961 genes	0.10%	1.99E-03
GO:0071806	protein transmembrane transport	8 out of 1574 genes	0.50%	17 out of 24961 genes	0.10%	1.99E-03
GO:0042375	quinone cofactor metabolic process	8 out of 1574 genes	0.50%	18 out of 24961 genes	0.10%	2.45E-03
GO:0045426	quinone cofactor biosynthetic process	8 out of 1574 genes	0.50%	18 out of 24961 genes	0.10%	2.45E-03
GO:0043155	negative regulation of photosynthesis, light reaction	6 out of 1574 genes	0.40%	9 out of 24961 genes	0.00%	3.43E-03
GO:0009772	photosynthetic electron transport in photosystem II	7 out of 1574 genes	0.40%	7 out of 24961 genes	0.00%	3.24E-04
GO:0045038	protein import into chloroplast thylakoid membrane	6 out of 1574 genes	0.40%	6 out of 24961 genes	0.00%	1.03E-03
GO:0010205	photoinhibition	6 out of 1574 genes	0.40%	9 out of 24961 genes	0.00%	3.43E-03
GO:0010876	lipid localization	7 out of 1574 genes	0.40%	18 out of 24961 genes	0.10%	9.27E-03
GO:0019915	lipid storage	7 out of 1574 genes	0.40%	18 out of 24961 genes	0.10%	9.27E-03